ABSTRACT

Title of Document:	REVIEW OF THERMAL ENERGY STORAGE TECHNOLOGIES AND EXPERIMENTAL INVESTIGATION OF ADSORPTION THERMAL ENERGY STORAGE FOR RESIDENTIAL APPLICATION
	Gang Li, Master of Science, 2013
Directed by:	Research Professor Yunho Hwang, Ph.D. Mechanical Engineering

Thermal energy storage (TES) technologies can reduce or eliminate the peak electric power loads in buildings, and utilize benefits of waste heat recovery and renewable energy. This thesis work consists of TES literature review and experimental investigation of adsorption TES. Review work includes cold storage technologies for air conditioning and subzero applications, and heat storage technologies for residential application. Different technologies involving sensible, latent and sorption TES were compared and resolutions of their issues were summarized. In addition, adsorption TES was experimentally investigated and its energy and exergy flows were analyzed to evaluate the effects of different operating parameters, such as temperature and heat transfer fluid mass flow rate for different chambers on the system performance. Finally, a computer model was developed for the adsorption heat TES system integrated with a vapor compression heat pump to assess its performance. Simulation results showed that overall coefficient of performance (COP) and exergy-based COP are approximately 3.11 and 0.20, respectively.

REVIEW OF THERMAL ENERGY STORAGE TECHNOLOGIES AND
EXPERIMENTAL INVESTIGATION OF ADSORPTION THERMAL ENERGY
STORAGE FOR RESIDENTIAL APPLICATION

By

Gang Li

Thesis submitted to the Faculty of the Graduated School of the
University of Maryland, College Park, in partial fulfillment
of the requirements for the degree of
Master of Science
2013

Advisory Committee:

      Research Professor Yunho Hwang, Chair
      Professor Jungho Kim
      Associate Professor Bao Yang

Dedication

To my parents

Acknowledgements

Table of Contents

List of Tables

Nomenclature

Abbreviations

CFC	chloroflourocarbon
CHP	combined heating and power
COP	coefficient of performance
DAQ	data acquisition
DHW	domestic hot water
DOE	Department of Energy
GWP	Global Warming Potential
HCFC	hydrochloroflourocarbon
HFC	hydroflourocarbon
HTC	heat transfer coefficient
HTF	heat transfer fluid
HX	heat exchanger
ODP	Ozone Depletion Potential
P	pressure [kPa *or* bar]
Q	accumulated energy [kJ]
Ex	accumulated exergy [kJ]
T	temperature [°C]
TES	thermal energy storage
Z01	Mitsubishi Plastics AQSOA FAM-Z01 zeolite

Greek Symbols

s	entropy [kJ/kg·K]
ρ	density [kg/m^3]
h	enthalpy [kJ/kg]
Δ	change *or* difference
ϵ	exergy efficiency
η	energy efficiency

Subscripts

abs	absorption
ads	adsorption
comp	compressor
cond	condenser
des	desorption
dest	destruction
eq	equilibrium
evap	evaporator
exp	expansion valve
in	inlet to a component
L	lift *or* low temperature *or* length
out	out of a system *or* the fluid outlet of a component

r	refrigerant
sat	saturation
w	water

1   Introduction

1.1   Motivation

The continuous increase in the level of energy consumption and depleting energy resources leads to serious energy and pollution issues nowadays. According to Energy Information Administration (EIA, 2011), total energy consumption for developed countries like the United States, was 9.36 trillion kWh in 1949. Then in 2011, total consumption increased to 28.5 trillion kWh (EIA, 2011), more than tripled during 62 years. Study from International Energy Agency (IEA) showed that fossil fuels, which causes harmful environmental issues, such as air pollution and climate change, still played the dominant role in the energy resources worldwide (IEA, 2009). This study showed that having already increased from 20.9 gigatonnes (Gt) in 1990 to 28.8 Gt in 2007, CO_2 emissions are projected to reach 34.5 Gt in 2020 and 40.2 Gt in 2030 with an average rate of annual growth of 1.5% over the full projection period.

Facing the challenge of energy crisis and pollution issues, it is necessary to develop and expand advanced technologies to reduce the energy demand, increase the energy supply while utilizing renewable energy effectively. In this context, the technology of thermal energy storage (TES) is proposed. TES is defined as the temporary holding of thermal energy in the form of hot or cold substances for later utilization. The application range can be from seasonal solar energy storage at high temperature level to heating, ventilation, and air conditioning, and refrigeration (HVAC&R) at low temperature level.

The integration of TES in HVAC&R applications is an attractive topic. With the adjustment of the time-discrepancy between power supply and demand, it can reduce or eliminate the peak electric power loads in buildings, has benefits of waste heat recovery and renewable energy utilization, etc. Regarding the HVAC&R applications, various TES technologies exist, such as sensible TES, latent TES and sorption TES. The selection and optimization of a TES system depends on many factors, including material thermal and physicochemical properties (density, specific heat, latent heat, etc.), storage capacity, heat loss and supply and utilization temperature requirements. In addition, different storage technologies have different issues, such as phase separation, corrosion, supercooling for latent thermal storage, low thermal conductivity in adsorption thermal storage, which deserve researchers' attention. Based on the literature review, there are still limited summary with detailed comparison and analysis work regarding TES in HVAC&R applications. Therefore necessary literature review work is conducted in this thesis.

For the types of TES, sensible and latent TES were already developed for many years for commercial implementation. While the sorption TES, especially the adsorption TES, is not yet commercialized due to poor heat and mass transfer of adsorbent beds, especially the low thermal conductivities and poor porosity characteristics of adsorbents. Therefore, more attention should be paid to the mechanism of adsorption storage for better understanding and design before its commercial implementation.

Regarding the adsorption TES, traditional assessment and evaluation of system performance is using the first law of thermodynamics, which states the equivalence

between heat and work, while it has the limitation of not showing the potential or quality of energy by the environmental state. Exergy analysis is a thermodynamic analysis technique, based on the combination of both first and second laws of thermodynamics, which provides an alternative means of assessing and comparing TES system performance. Exergy is defined as the work potential of a substance relative to a reference state. In particular, exergy analysis yields efficiencies which provide a true measure of how nearly actual performance approaches the ideal, and identifies more clearly the causes and locations of thermodynamic losses than energy analysis. Energy itself is not enough to understand all thermodynamic aspects. Therefore, exergy analysis is necessary to be considered. It has the potential for optimizing the energy demand and thermal storage system. Parametric studies are also necessary to be carried out for the adsorption TES process in order to investigate the storage efficiency and reveal potential performance improvements.

1.2 Objectives and thesis organization

The objective of this thesis is to improve understanding of different kinds of TES technologies and thereby support development and implementation of the adsorption TES technology. There are two main parts for this thesis: literature review work part (Part I), experimental work for adsorption TES part, and system evaluation part for adsorption TES with vapor compressor cycle system (Part II). Part I includes Chapter 1 through Chapter 5. Chapter 1, describes a brief background of this thesis. Chapter 2 through Chapter 5 show a comprehensive review of various types of TES technologies for air

conditioning, subzero and residential applications. It also summarizes the energy and exergy evaluation for TES technologies. Part II includes Chapter 6 through Chapter 8. Chapter 6 introduces the experimental apparatus and procedure for adsorption TES and Chapter 7 investigated thermal storage process in detail with energy analysis and exergy analysis. Chapter 8 evaluates adsorption storage system performance with heat pump integration, Chapter 9 shows the summary for conclusions and recommendations for future work.

2 Critical Literature Review of Cold TES Technologies for Air Conditioning Application

Cold storage, which primarily involves adding cold energy to a storage medium, and removing it from that medium for use at a later time, has wide applications for air conditioning use in buildings, vehicles, and other conditioned spaces. By separating the maximum cooling and power demands in time, it can offer cooling while reducing or eliminating the peak electric power load of the buildings, and has benefits such as waste heat recovery and renewable energy utilization. This section will mainly summarize the research work for air conditioning application.

Cold storage technologies can be classified according to the type of a storage medium and the manner in which the storage medium is used. Previous research has provided summaries and reasonable analyses for most of the common storage media such as water and ice. Saito (2002) suggested that water storage and static-type ice, which are based on established technologies, have little need for further study. More topics have surfaced in recent years for promising phase change material (PCM) storage. Moreover, utilizing sorption technologies for cold storage purpose has been developed recently. In this section, a brief introduction is provided for water storage and ice storage technologies, while more detailed description is provided for more promising cold storage materials.

2.1   Chilled water and ice slurries

Chilled water storage, which utilizes the sensible heat (4.184 kJ/kg K) to store cooling, needs a relatively large storage tank as compared to other storage systems that have a larger latent heat of fusion. However, it has wide application because of its suitable cold storage temperature (4~6°C). This characteristic enables it to be directly compatible with conventional water chillers and distribution systems, and provides good unit efficiency with a low investment. Ice storage uses the high fusion heat of water (335 kJ/kg), which can make storage tank much smaller. However, it stores cooling in the form of ice, which means that the refrigeration equipment must operate at temperatures well below its normal operating range for air conditioning application. Therefore, either special ice making equipment is used, or refrigeration chillers are selected for low temperature service.

2.1.1   Chilled water storage

Water is most dense at 4°C and becomes less dense at both higher and lower temperatures. Because of this density-temperature relationship, this type of storage system has the phenomenon of a stratified temperature distribution in a storage tank. Effective chilled water storage requires that some form of separation should be maintained between the stored cold water and the warmer return water. The mixing of two water streams at different temperatures, which is caused by the inlet diffuser during charge and discharge processes, significantly affects the temperature distribution in the tank. Here the two diffuser types most commonly used in today's commercial chilled

6

water storage tanks are shown in Figure 2.1 (Bahnfleth et al., 2003). Most studies related to this stratification tried to enhance the chilled water storage in terms of performance, simplicity, cost, and reliability. In a single stratified tank that stores both hot and cold water, diffusers are located at the top and bottom of the tank. Various physical methods, such as membranes, internal weirs, baffles, labyrinths, series tank, empty tanks, and thermally stratified systems, have been used to create the temperature stratification necessary for a high efficient storage (Mackie and Reeves, 1988; Dorgan and Elleson, 1993).

(a) With radial parallel plate diffusers   (b) With octagonal slotted-pipe diffusers
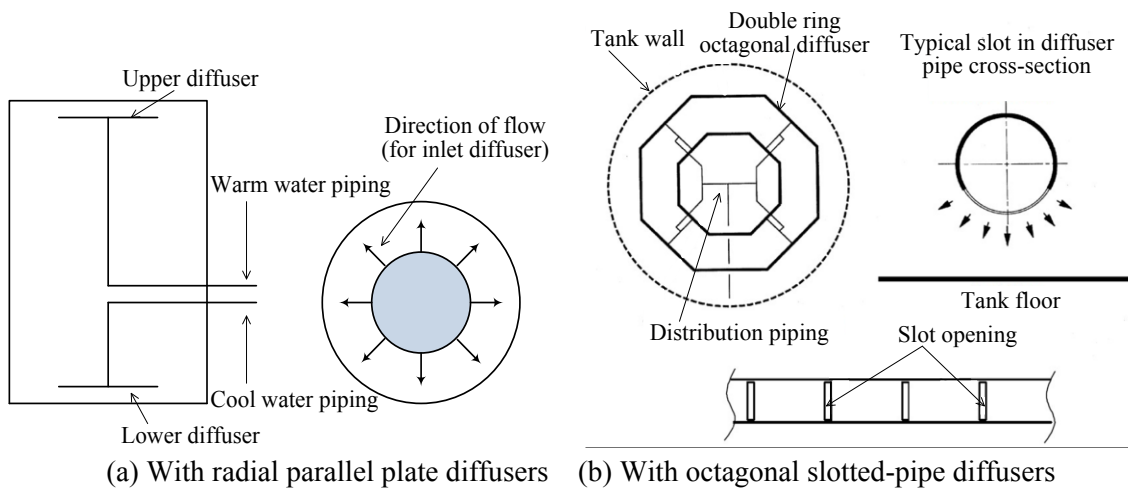
Figure 2.1: Stratified storage tank (Bahnfleth et al., 2003)

More attention has been paid to the numerical simulation for the transient behavior of the thermocline formation process in the thermal storage tank. Initially, one-dimensional simulation was developed. Cole and Bellinger (1982) developed a model based on tests performed in a scale model tank with a side inlet. Mixing was accounted for by a constant empirical mixing parameter, which is a function of the Fourier and Richardson numbers.

They reported that their simulation results agreed with their experimental results both in the interior of the tank and at the tank outlet. The primary deficiency observed in this model was that it under-predicted the temperature below the thermocline. Truman and Wildin (1989) developed a model, which was found to be reasonable in predicting the tank storage performance. Other models such as an effective diffusivity model to quantify the inlet mixing effect caused by various inlet geometries were also developed (Zurigat et al., 1991; Ghajar and Zurigat, 1991; Caldwell and Bahnfleth, 1998). Later, many two-dimensional studies have attempted to simulate the thermocline formation process and were able to predict it reasonably. A steady state model was developed by Stewart et al. (1992) to study the effects of a submerged, downward-impinging flow from a slot in a chilled water storage tank. The flow was modeled by a system of five nonlinear, coupled partial differential equations, and was solved using a successive substitution method. Another turbulent model was developed to simulate the mixing process of a cold flow into a two dimensional tank via a linear diffuser at a lower corner of the tank (Cai et al., 1993). Other related models are developed by Spall (1998), Musser and Bahnfleth (2001a, 2001b), and Bahnfleth et al. (2003).

2.1.2   Selection of depressant additives for ice slurry

As mentioned in the introduction, static ice storage will not be discussed in this chapter, because it has been well established (Saito, 2002). In a dynamic ice storage system, ice slurry can be directly transported through pipes, due to its high fluidity, heat transfer ability, and heat capacity with minute ice particles. The ice particles are in the range of

0.1 to 1 mm in diameter. It is made from aqueous solutions to avoid adhesion of ice particles to a cold surface. A dynamic ice-making system allows the use of cool air distribution as a result of a large temperature difference. Its benefits include the ability to use smaller fans and ducts, as well as for the introduction of less humid air into occupied spaces. In order to realize the ice slurry, the freezing point depressant additives are added. The most common freezing point depressant materials for water are glycols (Hirata et al., 2000; Inaba et al., 1998), alcohols (Ohkubo et al., 1999) and salts. Ice slurry can be made from harmless aqueous solutions such as an ethanol solution, a propylene glycol solution, and an economical aqueous solution such as ethylene glycol solution. The main purpose of using ice slurries is to take advantage of the latent heat of the ice crystals. Continuous ice slurry can usually be produced through buoyancy force (Hirata et al., 2000). Kumano et al. (2007) systemically studied the production of apparent latent heat from ice in aqueous solutions, which was defined as the effective latent heat, as shown in Figure 2.2 (combined from original figures by Kumano et al., 2007). It was found that the effective latent heat of fusion in an aqueous solution could be calculated by considering the effects of freezing point depression and dilution heat in each case. The relationship between the latent heat of fusion and the degree of freezing-point depression is also shown in Figure 2.2. Amount of heat generated by dilution was large in propylene glycol and ethanol solutions, and latent heat decreased in conjunction with a lowered freezing point. Moreover, the effect of dilution in NaCl solution was small, although latent heat of fusion decreased with the freezing point. The decrease in latent heat was very small in $NaNO_3$ solution due to the effect of the endothermic reaction.

(a) Latent heat vs. concentration (b) Latent heat vs. degree of freezing point depression
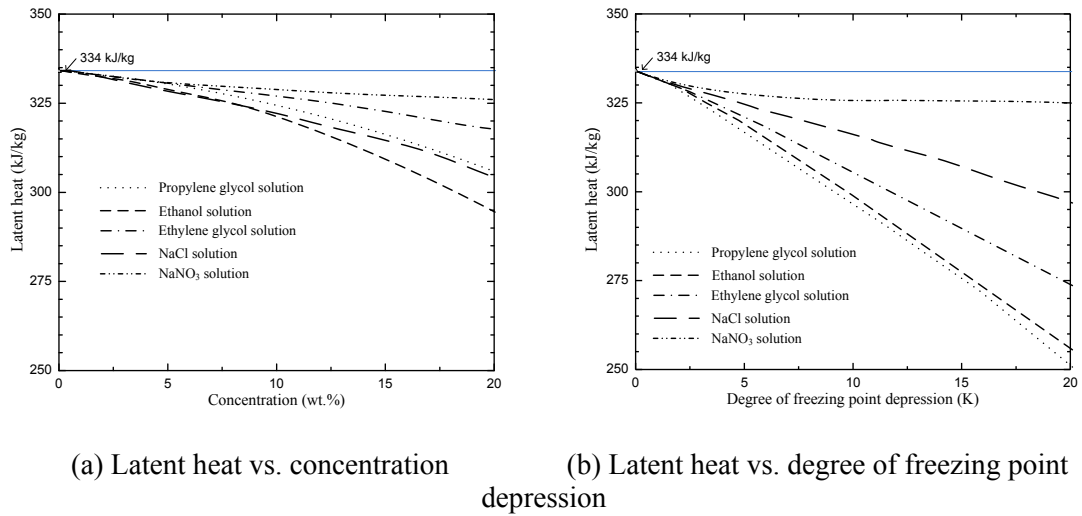
Figure 2.2: Latent heat of ice fusion in different aqueous solutions (Kumano et al., 2007)
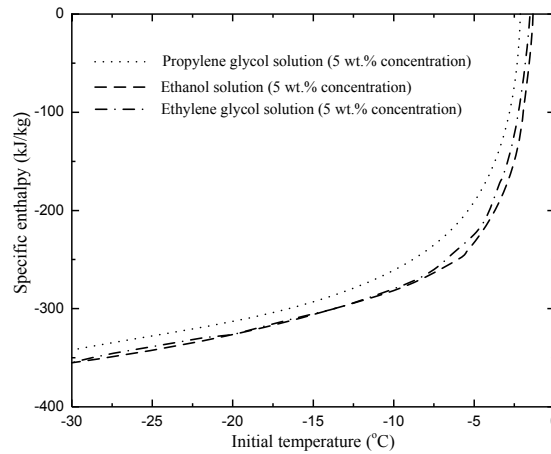
Figure 2.3: Relation between specific enthalpy and initial temperature of the sample (Kumano et al., 2010)

Kumano et al. (2010) also studied the specific enthalpy of different aqueous solutions, and show the relationship between the specific enthalpy and initial temperature of the sample, as shown in Figure 2.3 (combined from original figures by Kumano et al., 2010). For other materials, Lu et al. (2002) proposed using polyvinyl alcohol (PVOH) as an artificial additive in ice slurries. PVOH could be a substitute for antifreeze protein (AFP)

type I, which is an effective additive for making ice slurries resistant to recrystallization. Grandum and Nakagomi (1997) and Grandum et al. (1999) measured the properties of ice slurry produced by using an antifreeze protein, and discussed types of crystals produced under various conditions. Inada et al. (1999, 2000) examined the microscopic structure of these additives on ice crystals and discussed the mechanism of the antifreeze effect. Silane coupling agents (SCAs) were used as substitutes for AFPs and SCAs, which could form long-chain molecules in water, and were effective for crystallization control. As seen with scanning tunneling microscopy (STM) observation, long-chain SCA molecules are adsorbed onto ice crystal surfaces, thus preventing crystal growth at the site where the long-chain SCA molecules are adsorbed.

2.1.3　Dynamic ice-making system

The most important issues of the ice slurry application are its efficiency and reliability in conversion of water or an aqueous solution to ice crystals or ice slurry. Usually, there are two ways of making ice: the dynamic ice making method using supercooled water, and the vacuum ice slurry method.

2.1.3.1　Dynamic ice making method using supercooled water

A liquid can be cooled below its normal freezing point without being crystallized if a seed nucleus does not exist. This is called as "supercooled liquid." Ice crystals can be produced in a special supercool release device to eliminate the supercooled conditions from the water. A supercooler, which is a specially designed heat exchanger, is the core

component necessary to realize dynamic freezing of supercooled water. A dynamic-type ice storage system using supercooled water is shown in Figure 2.4 (Kozawa et al., 2005). Typically, the refrigeration system contains a supercooler, supercooler release device, and an ice-storage tank. Saito et al. (1992) studied the mechanical factors affecting the initiation of the freezing of supercooled water through experimenting the ice making methods using supercooled water. Okawa et al. (1997, 1999) and Okawa and Saito (1998) applied an electric charge on the freezing of supercooled water and reported its effects. They also studied the probability of ice-nucleation phenomena, and summarized possible solutions to control the initiation of crystallization. There are more scholars who have studied the fundamental issues related to ice making and heat transfer (Qu, 2000; Zhang et al., 2008; Li and Zhang, 2009). Usually the condition of supercooled water is unstable in dynamic-type ice storage systems. The water freezes easily with perturbation, and then can freeze inside the pipeline. In order to maintain stable high-quality ice slurry, it is necessary to control the degree of supercooling. This has been a popular topic of research.
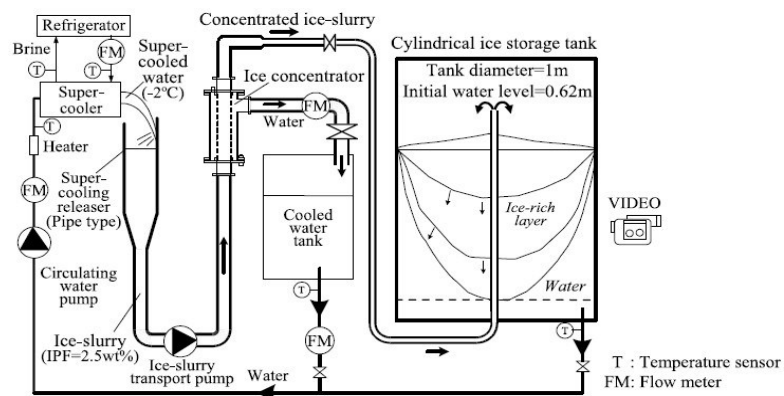
Figure 2.4: Schematic diagram of a dynamic-type ice storage system using subcooled water (Kozawa et al., 2005)

12

2.1.3.2 Vacuum ice slurry generation method

In this method, an aqueous solution used as the cold storage material is evaporated under a low-pressure condition, and the remaining solution is cooled and frozen as a consequence of the latent heat of evaporation. A circulating system to produce ice slurry is shown in Figure 2.5 (Asaoka et al., 2009). The system consists of an evaporator, a vacuum pump, and a condenser. Aqueous solution in the evaporator evaporates so that ice forms within. The vapor produced in the evaporator is transported to the condenser via a vacuum pump. Condensed liquid is diluted and returned to the evaporator for re-use. Since the external surface of the evaporator is warmer than the ice slurry in this system, the issue of ice sticking to the cooling surface has been eliminated. This improves the system efficiency because ice slurry production is continuous without any interruption. Kim et al. (2001) studied the consistency between theory and experiment for the dissipation rate of a liquid droplet and the change of surface temperature when using an ethylene glycol solution with a water spray method, which was based on the dissipation-control evaporation model. Lugo (2004) and Lugo et al. (2006) studied equilibrium condition using an ammonia solution and an ethanol solution with this method. Asaoka et al. (2009) further studied the vapor–liquid equilibrium data to estimate the coefficient of performance (COP) of the system with an ethanol solution. Further related studies were developed by Shin et al. (2000), Ge et al. (2007) and others. At present, most of the research interests related to the vacuum method are focused on heat and mass transfer inside the liquid, as well as the optimizing equipment and its components. In addition to ice-making system researches, numerous studies have focused on the storage tank. Egolf

et al. (2008) systemically summarized related research areas, such as ice particle fields, and showed a comparison of the usual method of storage with and without mixing in the tank, as shown in Figure 2.6. This method of storage without mixing allows saving the electrical energy. The inlets and outlets shown are parts of the secondary circuit.
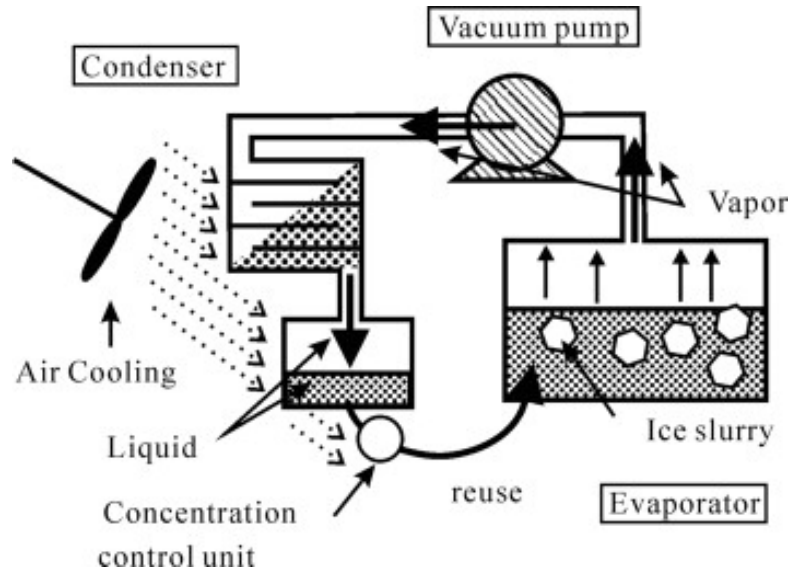
Figure 2.5: Schematic diagram of a vacuum ice slurry generation system (Asaoka et al., 2009)
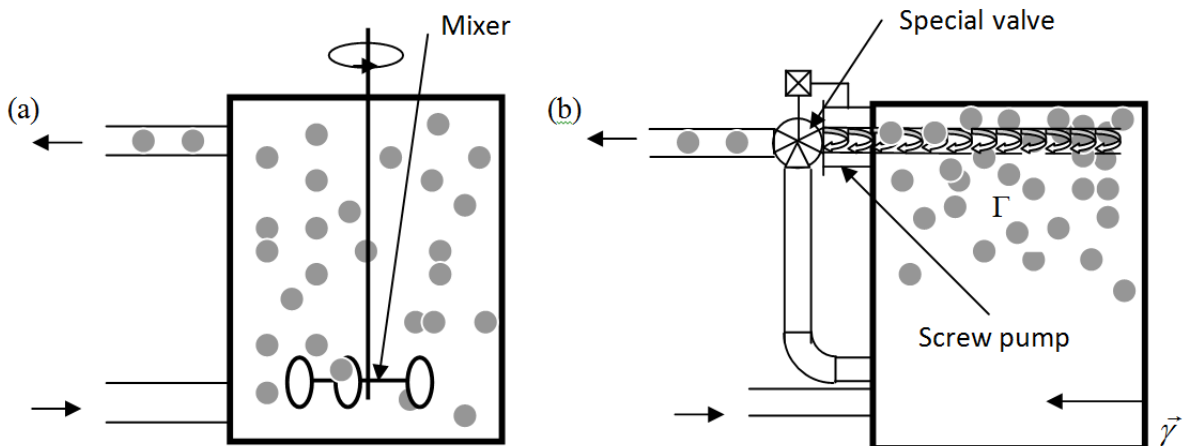
Figure 2.6:Schematic drawing of (a) usual method of storage with mixing and (b) a proposal for an alternative system without a mixer in the tank (Egolf et al., 2008)

2.2 Latent cold storage materials

Latent cold storage materials, which are mainly PCMs, can be produced in various chemical formulations, and they usually can be designed to melt and freeze at a suitable phase change temperature range for air conditioning systems. With the superiority of high latent heat, they have shown a promising ability to reduce the size of storage systems. PCMs have been used for various heat storage applications since the 1800s, but they have been used as a kind of cold storage media or a secondary loop fluid only recently.

In this section, materials with solid-to-liquid phase change with minor volume changes are the primary topic of discussion for practical applications. Early in 1983, Abhat (1983) suggested a useful classification of the substances used for thermal energy storage, as shown in Figure 2.7: Classification of PCMs (Abhat, 1983). The melting temperature and fusion heat of existing PCMs are shown in Figure 2.8 (Dieckmann, 2006). Obviously, the promising PCMs for air conditioning application are salt hydrates, eutectics, paraffin waxes, fatty acids, and refrigerant hydrates. Figure 2.9 shows thermal properties of the PCMs studied in this section. In addition to PCM materials, PCM slurries as secondary loop fluids including clathrate slurries, microencapsulated phase change slurries, phase change emulsions are also discussed and summarized.
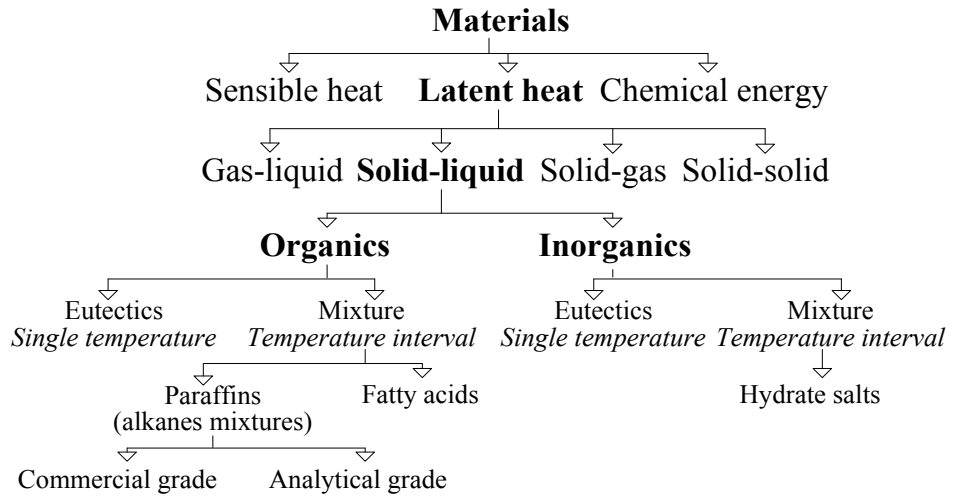
Figure 2.7: Classification of PCMs (Abhat, 1983)
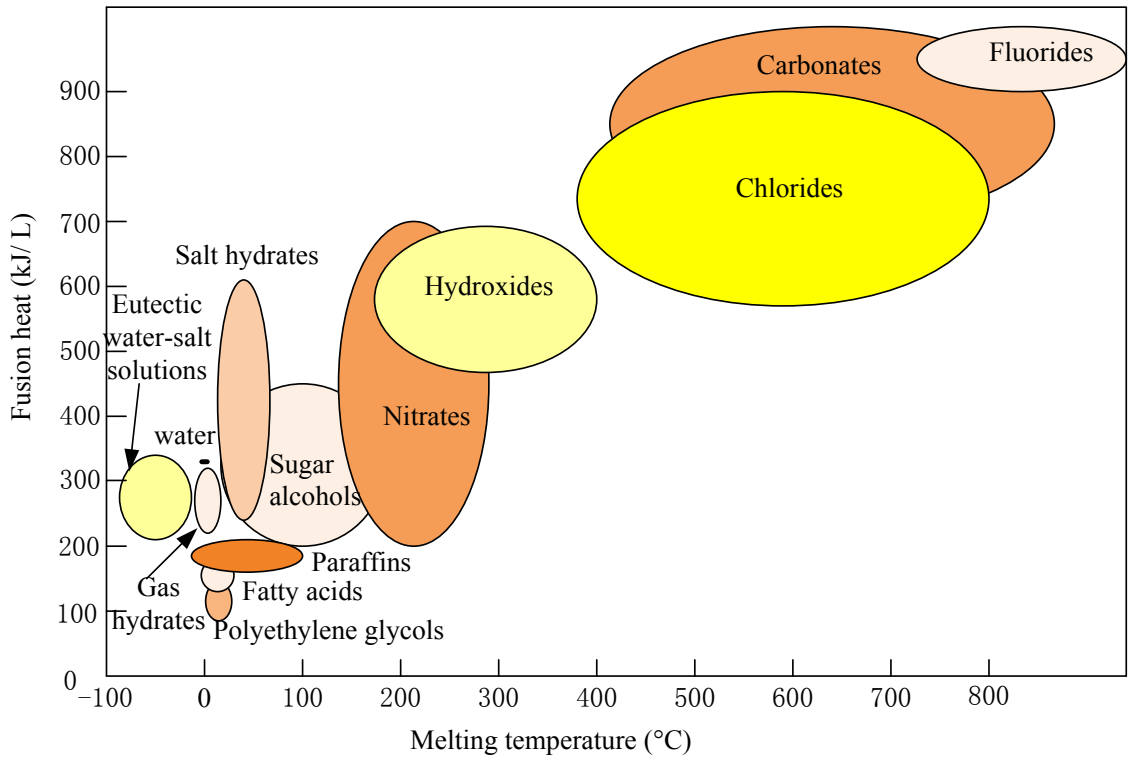
Figure 2.8: Melting temperature and fusion heat of existing PCMs (Dieckmann, 2006)

(a) Fusion heat by mass

(b) Fusion heat by volume
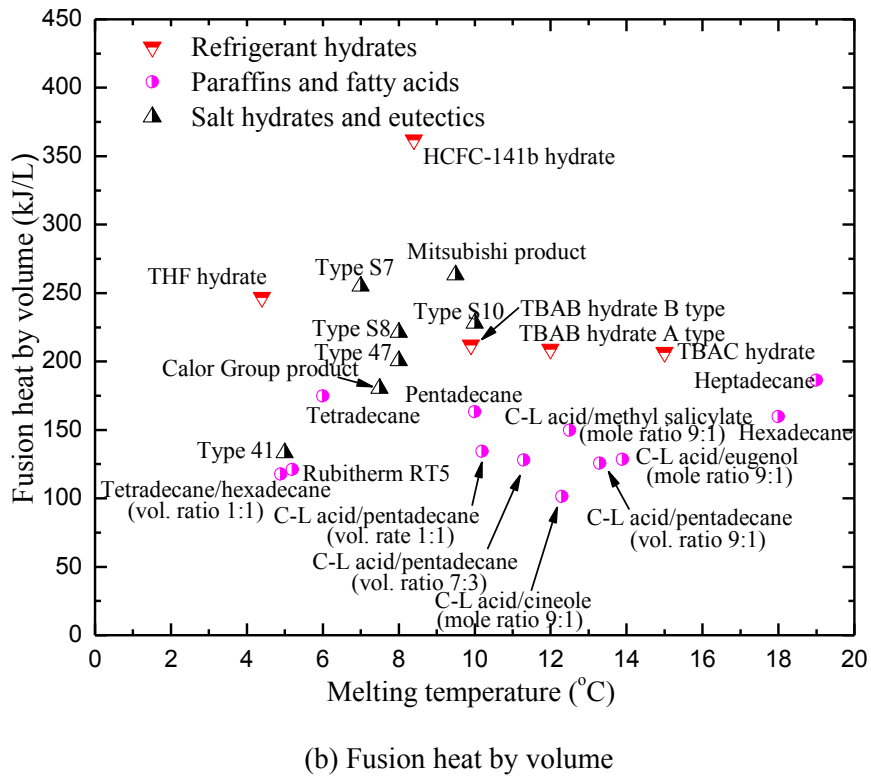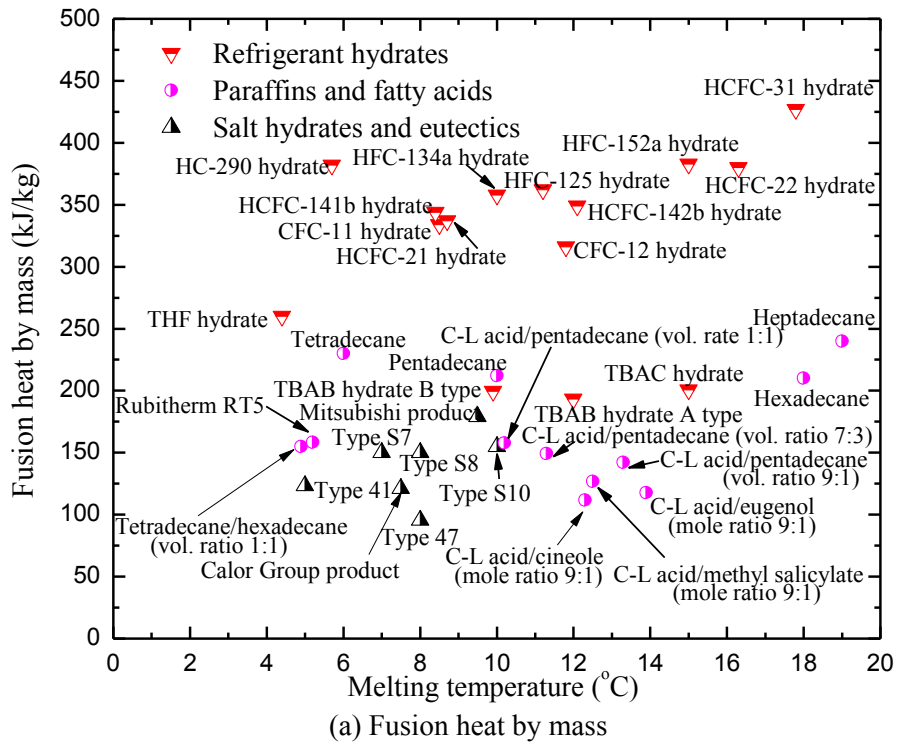
Figure 2.9: Thermal properties of PCMs for air conditioning application

2.2.1 Selection criteria for PCMs or PCM slurries

Requirements for common solid-liquid PCMs or PCM slurries for cold storage in air conditioning applications are summarized as follows:

- Proper phase change temperature range (5~12°C) and pressure (usually near atmospheric pressure), which involves the use of conventional air conditioning equipment and a storage tank for the chiller operation in buildings;

- Large fusion heat, which helps to achieve high cold storage density compared to sensible heat storage and allows for a more compact storage tank;

- Reproducible phase change, also called cycling stability, which can use the materials many times for storage and release of thermal energy with consistent performance. Usually the phase separation, which separates phases with different composition from each other macroscopically, is an important issue for cold storage. If phase has a composition different from the initial design composition optimized for cold storage, it will show a significantly reduced energy storage capacity;

- Good thermal conductivity to speed up phase change progress, and low supercooling;

- Stable chemical properties, low corrosivity, and low environmental impact factors, such as zero Ozone Depletion Potential (ODP) effect and low Global Warming Potential (GWP) effect;

- Low viscosity, good flow and heat transfer characteristics for PCM slurries;

- Easy manufacturing and low price.

Usually it is hard for a material to satisfy the entire requirements listed above so that here the primary four requirements are discussed here. A brief comparison of the thermal properties of the different types of PCMs is shown in Figure 2.10.

(a) Salt hydrates and eutectics   (b) Paraffin waxes

(c) Fatty acids   (d) Refrigerant hydrates
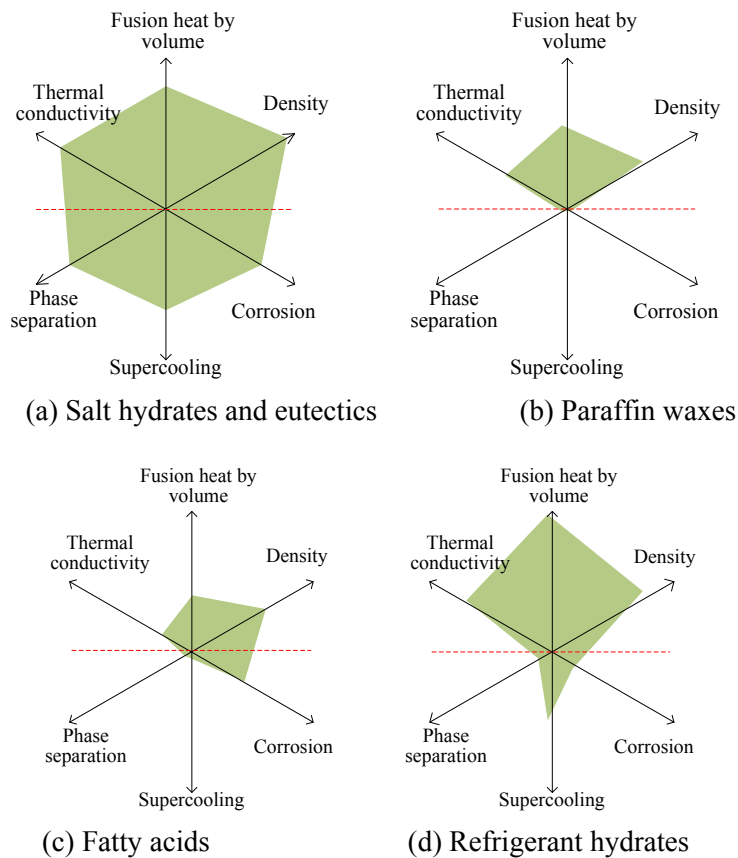
Figure 2.10: Comparison of thermal properties of different PCMs
Note: The farther the colored shape extends along a given axis, the better the performance along that dimension. It can be applied in other similar figures in this study.

2.2.2 Salt hydrates and eutectics

Much of the research on PCMs is focused on salt hydrates and eutectics due to their high fusion heat and suitable phase change temperature range. To provide a general

understanding for different storage systems, Hasnain (1998) discussed the primary features of chilled water, ice, and eutectic salt cold storage systems, as shown in Table 2.1. In the following section, material selection is first introduced. Generally, salt hydrates have a higher fusion heat. However, their major issues of phase separation, supercooling and corrosion, which are directly related to the cycle stability, are introduced later.

Table 2.1: Comparison of various thermal storage systems (Hasnain, 1998)

Primary features	Chilled water storage	Ice storage	Eutectic salt storage
Specific heat (kJ/kg K)	4.19	2.04	-
Latent heat of fusion (kJ/kg)	-	333	80~250
Maintenance	High	Medium	Medium
Warranty availability	Low	High	Medium
Tank interface	Open tank	Closed system	Closed tank
Discharge fluid	Water	Secondary coolant	Water
Charging temperature (°C)	4 to 6	-6 to -3	-20 to 4
Chiller	Standard water	Low temp. secondary coolant	Standard water
Packaged system	Medium	High	High
Heating capability	Low	High	Medium
Chiller charging efficiency	5.0~5.9 COP	2.9~4.1 COP	5.0~5.9 COP
Storage installed cost ($/kW˙h)	8.5~28	14~20	28~43
Discharge temperature (°C)	Above 1~4	1~3	9~10

2.2.2.1   Material selection

Hydrated salts consist of a salt and water in a discrete mixing ratio. The word eutectic is derived from Greek and means "easy melting". It refers to a mixture of two or more components having the lowest melting point of any composition and combination of the same components. At this eutectic point, all of the components will crystallize simultaneously, like a pure substance. In this study for air conditioning application, the eutectics are mostly inorganic salts.

The most commonly used eutectic salt is Glauber salt ($Na_2SO_4·10H_2O$), which contains

44 wt.% Na_2SO_4 and 56 wt.% H_2O (Telkes, 1952). With a melting temperature of about

32.4°C and a high latent heat of 254 kJ/kg (377 MJ/m^3), it is one of the least expensive

materials that can be used for thermal energy storage. To make the phase change

temperature range appropriate for air conditioning applications, more proper

$Na_2SO_4·10H_2O$-related PCMs were developed, as summarized by Liu (2005), and shown

in Table 2.2. The thermal properties of several commercial salt hydrates and eutectics,

which could be used for air conditioning applications, are listed in Table 2.3 (Liu, 2005;

PCM Products, 2011).

Table 2.2: Components of eutectics salt with phase change temperature of 12.8°C (Liu, 2005)

Component	wt.% (salt)	Function	Component	wt.% (salt)	Function
Na_2SO_4	32.5	PCM	$Na_2B_4O_7·10H_2O$	2.6	Nucleating agent
H_2O	41.4	PCM	H_3BO_3	1.73	Equilibrium pH agent
NaCl	6.66	Temp. adjustment agent	Na_5P_3O10	0.25	Dispersing agent
NH_4Cl	6.16	Temp. adjustment agent	MinUGel200	8.7	Thickening agent

Table 2.3: Thermal properties of eutectics slat and salt hydrates (Liu, 2005; PCM Products Ltd., 2011)

PCM component/ PCM type	Phase change temperature (°C)	Fusion heat (kJ/kg)	Thermal conductivity (W/m·K)	Density (kg/m^3)	Specific heat capacity (kJ/kg K)	Company
Na_2SO_4, H_2O, NaCl, NH_4Cl	7.5	121	0.55 (liquid), 0.70 (solid)	1,490	-	Calor Group
$Na_2SO_4·10H_2O$, NaCl, NH_4Cl, $Na_2B_4O_7·10H_2O$, NH_4Br	9.5~10 (melting point) 8.0 (freezing point)	179, 122 (after 100 recycles)	0.75 (liquid), 0.93 (solid)	1,470	-	Kyushu Electric Power, Mitsubishi
Type 41	5.0~5.5	123.3	-	-	-	Transphase
Type 47	8~9	95.4	-	-	-	Transphase
S7	7	150	0.40	1,700	1.85	PCM Products
S8	8	150	0.44	1,475	1.90	PCM Products
S10	10	155	0.43	1,470	1.90	PCM Products

2.2.2.2   Phase separation minimization

As reported by Cantor (1978), phase separation, or incongruent melting, can cause a loss
in enthalpy of solidification. Since phase separation can severely reduce the storage
density, necessary solutions should be offered. Changing the properties of the salt hydrate
with the addition of another material such as water with a gelling or thickening agent can
hinder the separation and sinking of heavier phases. A gelling agent is a cross-linked
material (e.g. polymer) that is added to the salt in order to create a three-dimensional
network that holds the salt hydrate together. A thickening agent is a material added to the
salt hydrate to increase the viscosity and holds the salt hydrate together.

In considering appropriate cross-linked materials for gelling, Ryu et al. (1992) studied the
effects of two different polymeric hydrogels: a super absorbent polymer (SAP) made
from acrylic acid copolymer and carboxymethyl cellulose (CMC). Thixotropic
(attapulgite clay) and alginate have also been tested (Telkes, 1976). Thickening agents
can be starch and various types of cellulose derivatives, such as silica gel (Ryu et al.,
1992; Telkcs, 1974).   Sodium acetate trihydrate ($NaCH_3COO \cdot 3H_2O$), used as a PCM,
was studied by thickening it with each of four different thickening materials: starch,
methyl cellulose, hydroxyethyl methyl cellulose, and bentonite (Cabeza et al., 2003). In
addition, Biswas (1997) investigate the extra water to prevent the formation of heavy
anhydrous salt. A comparison by Biswas (1997) using pure Glauber salt and a mixture of
68.2 wt.% $Na_2SO_4 \cdot 10H_2O$ and 31.8 wt.% H_2O showed that the nucleation of the
decahydrate occurred readily and even without the addition of borax. It should be noted

22

that although the method of adding extra water makes the system stable with cycling, it may lead to a reduction of the storage density and the system should be operated with a large temperature swing. In addition, encapsulating the PCM, mechanical stirring, can also be good solutions to deal with the issue of phase separation. For all solutions, the issue of phase separation invites the meaningful perspectives for further study of salt hydrates and eutectics in air-conditioning application.

2.2.2.3 Supercooling minimization

Supercooling is another serious issue. The use of nucleating agents, cold finger, and porous heat exchange surfaces has been utilized effectively to deal with this issue (Abhat, 1983). Many factors, such as crystal structure, solubility, and hydrate stability, were studied to determine whether a particular additive could promote nucleation. Good nucleating agents can be carbon nanofibers, copper, titanium oxide, potassium sulfate, and borax (Ryu, 1992; Elgafy and Lafdi, 2005). Studies show that 0.95 wt.% to 1.9 wt.% of pulverized borax in Glauber's salt was found to be the most effective in supercooling minimization (Lane, 1992; Onwubiko and Russell, 1984). Other promising nucleating agents to limit the degree of supercooling from 20°C to 2°C could be $Na_2P_2O_7 \cdot 10H_2O$, $BaCO_3$, $BaCl_2$, BaI_2, $Ba(OH)_2$, CaC_2O4, K_2SO_4, $MgSO_4$, $SrCl_2$, $SrCO_3$, $SrSO_4$, $Sr(OH)_2$, and TiO_2.

2.2.2.4 Corrosion suppression

Corrosion is another significant issue. It is also an important engineering design criterion for the material, which is subject to open to the atmosphere for a longer period of time. For salt hydrates and eutectics, the primary limiting factor to widespread use of these latent heat storage materials is the life of PCM container systems associated with the corrosion between the PCM and container. In an effort to address this issue, Kimura and Kai (1984) used NaCl to improve the stability of salt hydrates and eutectics.

Porisini (1988) studied the corrosion rates on stainless steel, carbon steel, aluminum alloys and copper. Following thermal cycling tests, he concluded that stainless steel was the most corrosion resistant among these metals for use with salt hydrates, though copper had a corrosion zone that did not increase even after long periods of time. Farid et al. (2004) summarized the stability of thermal properties under extended cycling. In addition, the corrosion rates of aluminum alloys and copper used in heat exchangers in the air conditioning industry was studied along with metallographic examinations after corrosion tests by Farrell et al. (2006), and ways of preventing corrosion of copper and aluminum by these PCM materials were discussed.

Salt hydrates and eutectics have a high latent heat per unit volume, high thermal conductivity, and are non-flammable and low in cost. However, they have not only phase separation and supercooling issues, but also corrosion issue to most metals. This leads to poor cyclic stability. Therefore, it is necessary to address such issues.

2.2.3 Paraffin waxes and fatty acids

Typical paraffin waxes are saturated hydrocarbon mixtures, and normally consist of a mixture of mostly straight chain n-alkanes such as $CH_3–(CH_2)_n–CH_3$. The crystallization of the $(CH_2)_n$ chain can release a large amount of latent heat. A fatty acid is characterized by the formula $CH_3(CH_2)_{2n}COOH$. Paraffin waxes and fatty acids are both organic and different from inorganic PCMs so that they are mostly chemically inert, stable and recyclable, exhibit little or no supercooling (i.e. they can be self-nucleating), and show no phase separation and a non-corrosive behavior (with the exception of fatty acids for the natural characters of acids). However, they have the disadvantages of low thermal conductivity and volumetric storage (less than 10^3 kg/m^3), and flammability that are opposite from those of inorganic PCMs.

2.2.3.1 Material selection

The various paraffin waxes, which are mainly products of petroleum refining process, are available with a range of melting points. This characteristic can lead to a good match between the melting temperature range and the air conditioning system operating temperature range.

Table 2.4: Thermal properties of paraffin waxes and fatty acids (Mehling and Cabeza, 2008; He and Setteerwall, 2002; Dimaano and Escoto, 1998; Dimaano and Watanabe, 2002a, 2002b)

	PCM	Melting temperature (°C)	Fusion heat (kJ/kg)	Density (kg/m^3)	Thermal conductivity (W/m·K)	Specific heat (kJ/kg·K)
Single paraffin wax	$C_{14}H_{30}$ (n-Tetradecane)	6	230	760 (liq.)	0.21 (sol.)	-
	$C_{15}H_{32}$ (n-Pentadecane)	10	212	770 (liq.)	-	-
	$C_{16}H_{34}$ (n-Hexadecane)	18	210, 238	760 (liq.)	0.21 (sol.)	-
	$C_{17}H_{36}$ (n-Heptadecane)	19	240	776 (liq.)	-	-
Paraffin wax mixture[*]	50:50Tetradecane: Hexadecane (vol.%)	Sensor: 4~6 DSC: 4.9	154.84	-	-	-
	Rubitherm RT5	Sensor: 4~6 DSC: 5.2	158.33	-	-	-
Fatty acid[**] with pentadecane or additives	90:10 C-L Acid:P (vol.%)	13.3	142.2	883.2 (liq.) 891.3 (sol.)	-	2.42 (liq.) 2.08 (sol.)
	70:30 C-L Acid:P (vol.%)	11.3	149.2	858.0 (liq.) 872.7 (sol.)	-	2.57 (liq.) 2.27 (sol.)
	50:50 C-L Acid:P (vol.%)	10.2	157.8	827.8 (liq.) 850.4 (sol.)	-	2.89 (liq.) 2.44 (sol.)
	90:10 C-L Acid: Methyl Salicylate(mol. %)	12.5	126.7	1,182.0 (liq.) 1,272.9 (sol.)	-	2.41 (liq.) 1.92 (sol.)
	90:10 C-L Acid: Cineole(mol. %)	12.3	111.6	927.0 (liq.)	-	2.37 (liq.) 1.71 (sol.)
	90:10 C-L Acid: Eugenol(mol. %)	13.9	117.8	1,091.0 (liq.)	-	2.63 (liq.) 2.01 (sol.)

[*]Carbon distribution of Rubitherm RT5 is 33.4wt.% C14 (No. of carbon atoms), 47.3 wt.% C15, 16.3 wt.% C16, 2.6 wt.% C17 and 0.4wt.% C18. Freezing temperature for paraffin wax mixture by test is 7.0 °C.
[**]C-L Acid is composed with 65 mol % capric acid and 35 mol % lauric acid.

Examples of some single paraffin waxes that have been investigated as PCMs, are shown in Table 2.4 (Mehling and Cabeza, 2008). From the table, it can be easily determined that tetradecane and pentadecane have a great potential as a PCM in conventional cold storage systems for air conditioning application. Also, binary mixtures of tetradecane and hexadecane have also been tested well, and are excellent candidates (He et al., 1999).

A binary mixture of laboratory-grade tetradecane and hexadecane, and the technical grade paraffin wax-Rubitherm RT5, were studied using differential scanning calorimetry

(DSC) (He and Setteerwall, 2002). Dimaano and Escoto (1998) and Dimaano and Watanabe (2002a, 2002b) systemically studied the capric-lauric (C-L) acid mixtures for PCM energy storage, from an initial assessment of thermal properties and investigation for lowest eutectic point with a suitable component compositions, to analysis for mixtures with pentadecane or proper additives in order to make the melting points in the range for cold storage, as shown in Table 2.4. With theoretical calculation and the experimental study of the liquid-solid equilibrium phase diagram on several kinds of fatty acid mixtures, the caprylic-lauric acid mixture (in the mass composition ratio of 80 and 20) was also suggested as good cold storage material with a freezing point of 4.6°C and a fusion heat of 152 kJ/kg (Cen et al., 1997). For other research related to fatty acids for air conditioning application, one may refer to the literature by Li et al. (1996).

2.2.3.2   Thermal conductivity improvement

For paraffin waxes and fatty acids, one of their serious issues is their low thermal conductivities. One possible solution is to add materials having a larger thermal conductivity. Mettawee and Assassa (2007) investigated a method of enhancing the thermal conductivity of paraffin wax by embedding aluminum powder in paraffin wax in a water base collector for solar energy storage unitization. It was found that the useful heat gain was increased by adding aluminum powder in the wax as compared to the case of pure paraffin wax.

Another solution is embedding graphite matrix in PCMs to increase the thermal conductivity. Thermal conductivity of paraffin wax can be increased by two orders of

magnitude through impregnating porous graphite matrices with the paraffin (RT-42, Rubitherm, Germany) (Mills et al., 2006). Also, a technical grade paraffin (melting point 48~50°C) embedded with expanded graphite was studied and showed a good thermal conductivity (Zhang and Fang, 2006). For the two above solutions, they provide insight for thermal conductivity improvement for air conditioning application although the examples listed are for utilization other than the air conditioning application.

Last, the use of finned tubes can also improve heat transfer performance for cold storage. All the previous studies for thermal conductivity improvement listed above can be used as guideline for enhancing PCM cold storage performance for air conditioning application. It should be noted that in order to prevent the liquid leakage during the solid–liquid phase change of the paraffin, a general solution is to encase the paraffin in spherical capsules or microcapsules.

2.2.3.3 Flame retardant improvement

For paraffin waxes and fatty acids, another serious issue is their high flammability. Usually the shape-stabilized PCM composites consist of the paraffin wax, which acts as a dispersed phase change material, and a polymer material (such as high density polyethylene (HDPE)), which acts as a supporting material. As long as the operating temperature is below the melting point of the supporting material, the shape-stabilized PCM can keep its shape even when the paraffin changes from solid to liquid. However, the high flammability property of paraffin waxes has severely restricted their wide

applications. Usually improving flame retardant of polymer materials (with the addition of some flame retardant to polymer materials) can relieve this issue.

There has been much concern worldwide over developing halogen free flame retardant (HFFR) polymeric materials. Intumescent flame retardant (IFR) material is used as an environmental, halogen-free additive (Cai et al., 2006). In order to improve the effective capacity to retard flames, synergistic agents have been used in IFR systems, such as some nanocomposites (Xia et al., 2007; Zhou et al., 2008). The influences of metal (iron, magnesium, aluminum, and zinc) on flame retardancy for paraffin/IFR as a phase change material were studied by Zhang et al. (2010a). Microscale combustion calorimetry (MCC) and cone calorimetry (CONE) were used to characterize the sample. The results revealed that the flame retardant efficiency of IFR in paraffin could be improved by adding metal. Also, the flame retardant mechanism for paraffin/IFR with metal was proposed.

In another study (Song et al., 2010), PCMs based on ethylene-propylene-diene terpolymer (EPDM) (supported material), paraffin (dispersed phase change material), nano-structured magnesium hydroxide (nano-MH) and red phosphorus (RP) with various compositions were prepared. The thermogravimetric analysis (TGA) analysis also indicates that the introduction of nano-MH into the form-stable PCMs (i.e. EPDM/paraffin blends) has significantly increased the fire resistance due to the formation of MgO during the combustion of nano-MH. MgO builds up char layers on the surface and insulates the underlying material and slows the escape of the volatile products generated during decomposition, and therefore improving fire resisting performance. In

29

addition, expanded graphite can also be a good material to improve flame retardant of polymer materials. All these studies can be used as guideline for enhancing PCM cold storage performance for air conditioning application.

2.2.4 Refrigerant hydrates

Gas hydrates, or clathrate hydrates, are ice-like crystals that are composed of host lattices (cavities) formed by water molecules linking with each other through hydrogen bonding, and other guest molecules. The guest molecules are firmly enclosed inside the host cavities under the weak van de Waals force. Usually there are three types (S-I, S-II and S-H) as shown in Figure 2.11 (Khokhar et al., 1998). Different types of hydrates can be formed under different conditions. For this study, refrigerant hydrates, which are mainly the type S-II gas hydrates (i.e., M·nH$_2$O, where M is a molecule of guest material and n is hydrate number) are discussed.
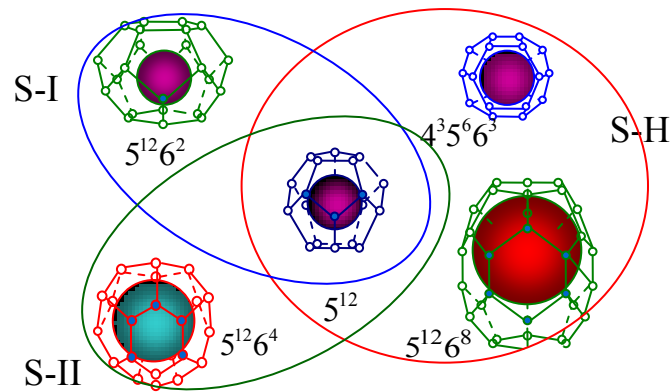
Figure 2.11: Types of hydrate structures and their cage arrangements
(Khokhar et al., 1998)

In addition, CO_2 hydrate (type S-I gas hydrate) and TBAB hydrate and TBAC hydrate (semi-clathrate hydrates) are also discussed in this section. Most refrigerant hydrates can be formed under low pressure (below 1 MPa) with suitable phase change temperature for air-conditioning and large fusion heat (270~430 kJ/kg). Unlike some liquid-solid PCMs discussed above, some refrigerants discussed here are in the gaseous state under atmospheric pressure, so pressure is noted for hydrate formation. Obviously, refrigerant hydrates have a larger fusion heat than eutectic salts, paraffin waxes and fatty acids. A hydrate storage system with the hydrate fusion heat near to that of ice shows the advantage of allowing use of chilled water as circulation medium rather than antifreeze coolant or brine, which are used in ice storage systems.

Many research efforts have been conducted since this type of novel cold storage medium was first proposed by Tomlinson (1982). A series of outstanding achievements were made in the research of hydrate cold storage technology (Ternes, 1983; Akiya et al., 1997; Mori and Mori, 1989; Fournaison et al., 2004; Guo et al., 1998).

2.2.4.1   Material selection

(1) HFC hydrate

In the 1990s, researchers first studied cold storage characteristics of chlorofluorocarbons (CFCs) and hydrochlorofluorocarbons (HCFCs) hydrates, such as CFC-11, CFC-12, HCFC-21, HCFC-22 and HCFC-141b gas hydrates. With the phase out of CFCs and HCFCs for environmental protection, more attention should be paid for alternative substitutes for guest materials of refrigerant hydrates like hydrofluorocarbon (HFC)

hydrate. Oowa et al. (1990) studied the phase equilibrium of HFC-134a hydrate. HFC-32 and HFC-125 hydrates were researched by Akiya et al. (1997). HFC-134a and HFC-152a hydrates were researched as cold storage media, and the energy charge and discharge processes were studied in a transparent apparatus (Guo, 1996). Thermal properties of some new HFC gas hydrates are presented in Table 2.5. It can be seen that the melting temperature of some refrigerant hydrates is a little higher. Through the addition of NaCl, $CaCl_2$, and ethylene glycol (Tanii et al., 1997), the melting temperature can be reduced to make hydrates more suitable for air conditioning applications. HFC-245fa, HFC-236ea, and HFC-365mfc are considered to be the primary alternative fluids for HCFC-141b, and they possibly form gas hydrates for air conditioning application.

Table 2.5: Thermal properties of guest materials for refrigerant hydrate and hydrate

Guest materials of refrigerant hydrate	Hydrate melting point		Hydrate fusion heat (kJ/kg)
	Temperature (°C)	Pressure (atm)	
HC-290	5.7	5.45	382
CFC-11	8.5	0.54	334
CFC-12	11.8	4.39	316
HCFC-22	16.3	8.15	380
HCFC-21	8.7	1.00	337
HCFC-31	17.8	2.82	427
HCFC-141b	8.4	0.42	344
HCFC-142b	12.1	2.25	349
HFC-152a	15.0	4.34	383
HFC-134a	10.0	4.10	358
HFC-125	11.2	9.44	362

(2) CO_2 hydrate slurry

CO_2 hydrate slurries, which are mixtures of solid CO_2 hydrate crystal and liquid aqueous solution, can also be used as secondary working fluids (Marinhas et al., 2006). They have the advantage of being produced by a non-mechanical generation process based on a simple CO_2 injection in a pre-cooled aqueous solution. Moreover, the heat of fusion of

32

solid CO_2 hydrate crystal (500 kJ/kg) is higher than that of ice (334 kJ/kg). As a recently developed secondary refrigerant, CO_2 hydrate slurry should contain sufficient solid crystals in order to release plentiful latent heat in delayed time as a cold source. In addition, the solid hydrate crystal should not affect the flowing conditions of hydrate slurry. The melting point of CO_2 hydrate slurry is adjustable according to the production conditions and can be applied to positive temperature range (+5°C or +7°C or even higher) for air conditioning application.

(3) TBAB hydrate slurry, TBAC hydrate slurry, THF hydrate slurry

Since most refrigerants (HFCs, CO_2, etc) are not very immiscible with water, it is necessary to search for water-soluble materials for rapid hydrate formation such as tetra-*n*-butyl ammonium bromide (TBAB), tetra-*n*-butyl ammonium chloride (TBAC), tetrahydrofuran (THF) and acetone. In addition, unlike other clathrate hydrates, which are usually produced under high pressure and low temperature conditions, the materials listed here can form hydrate under one atmosphere pressure and room temperature. It should be noted that the structures of TBAB hydrate and TBAC hydrate crystals are different from common type S-II hydrates, and they can form semi-clathrate hydrates, in which TBAB or TBAC molecules are both the host and guest in the structure. Also two types of hydrate crystals can be formed for TBAB hydrate and TBAC hydrate with different hydration numbers. Schematic structure of one type for TBAB hydrate crystal (type A with hydration number: 26) is shown in Figure 2.12 (Shimada et al., 2003). It is a semi-clathrate hydrate. Tetra-*n*-butyl ammonium located at the center of three

33

tetrakaidecahedrons and one pentakaidecahedron. Broken bonds are shown by dotted lines. The dotted lines represent bonds which have disappeared from the classical hydrate structure. The dodecahedral cages are empty as shown by the hatched areas.
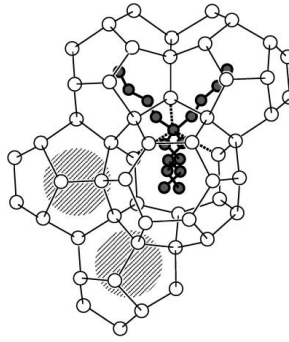
Figure 2.12: Schematic structure of type A TBAB hydrate crystal (Shimada et al., 2003)

Table 2.6: Thermal properties of TBAB/TBAC/THF hydrate crystals

Hydrate guest material	Hydration number	Melting temperature (°C)	Latent heat (kJ/kg)	Density (kg/m³)	Specific heat (kJ/kg·K)	Thermal conductivity (W/m·K)	Literature
TBAB	26/38	12.0/9.9	193.2/199.6		[a]1.86~2.61/ 2.0~2.54		Oyama et al. (2005)
	26/36	12.3/9.6		1,082/1,067			Darbouret et al.(2005)
	26/36	11.8/–	193/205	1,082/1,030	2.22/–	0.42/–	Hayashi et al. (2000) Ogoshi and Takao (2004)
TBAC	30	15.0	200.7				Nakayama (1987)
	29.7/32.1	15.0/14.7		1,034/1,029			Dyadin and Udachin (1984) Leaist et al., (1982)
THF	17	4.4	~260	~950	[b]1.930~2.020	[b]0.489~0.496	Waite et al. (2005)

[a]Between 20 and 0.2°C, [b]Between -25 and -7.5°C. Hydration number for type A TBAB hydrate crystal is 26, while for type B TBAB hydrate crystal it is 36 or 38.

Thermal properties of three hydrate crystals are listed in Table 2.6. Zhang et al. (2010b) gave a detailed introduction to determine thermal properties of clathrate hydrate slurries.

Also hydrate mixtures, such as TBAB/THF mixtures, have been also studied for air conditioning application by Li et al. (2010). Since published literature on environment friendly clathrate hydrate mixture is limited, it is not discussed here in detail.

2.2.4.2   Hydrate formation improvement and storage apparatus designation

Most refrigerants are insoluble in the water, leading to slow hydrate formation (also called crystallization) with a supercooling effect and a slightly longer induction time. To deal with these shortcomings, enhancement methods are very necessary, and are summarized as follows:

(1) One solution is to stir the reaction materials. A mechanical agitator inside the tank can stir the reaction materials directly, or the guest materials and the water can be mixed by continuously being pumping out separately from the tank (Shu et al., 1999), or mixed with the help of an injector (Tong et al., 2000).

(2) Another solution is the inclusion of additives to reduce induction time, the supercooling degree, or to change melting temperature more suitable in air conditioning application. Useful additives are sodium dodecyl sulfate (SDS) (Zhang et al., 2002), ethylene glycol, *n*-butyl alcohol (Zhang et al., 1999), metals or metaloxide compound powders such as copper, zinc, and iron (Isobe and Mori, 1992), inorganic salts, and organic fungi.

(3) The third solution is applying the outfields. A special magnetic field has remarkable influence on the refrigerant gas hydrate formation process, by reducing induction time

and increasing the amount of formed hydrate (Liu et al., 2003a). Ultrasonic waves were also studied for hydrate formation (Liu et al., 2003b). The induction time was longer under the function of a staircase-like supersonic probe than with that of the index–cone-like probe. The range of the ultrasonic wave power that has a good effect on hydrate formation was 58 ~1,000 W.

(a) Direct contact charge and direct contact discharge system

(b) Direct contact charge and indirect contact discharge system

(c) Indirect contact charge and direct contact system

(d) Indirect contact charge and indirect discharge contact discharge system
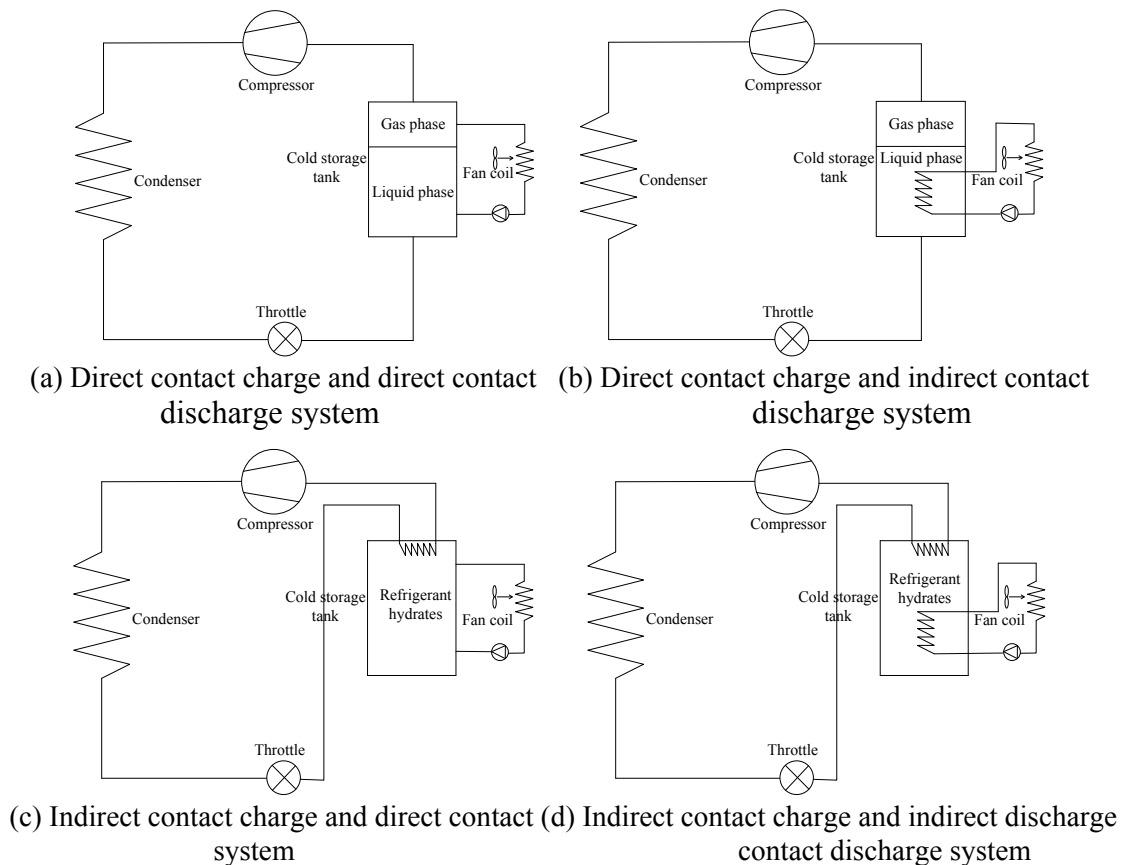
Figure 2.13: Different types of hydrate charge and discharge system (Xie et al., 2004)

For a clear understanding of the heat transfer modes between the cold storage media and the refrigerant or the coolant, it is necessary to study the hydrate storage apparatus design. Xie et al. (2004) summarized this by studying both the direct contact heat transfer mode

and the indirect contact heat transfer mode. In the indirect contact heat transfer mode, the cold storage medium and the refrigerant (or the coolant) exchange heat through the heat exchanger. In the direct contact heat transfer mode, the cold storage medium and the refrigerant (or the coolant) exchange heat through direct contact. The hydrate storage apparatus types can be classified based on direct or indirect-contact charging and direct or indirect-contact discharging system, as shown in Figure 2.13.

Several researchers (Mori and Mori, 1989; Carbajo, 1985; Najafi and Schaetzle, 1991) conducted detailed research on type (a) direct contact charge and direct contact discharge system. Researchers (McCormack, 1990; Dini and Saniei, 1992; Zhang et al., 1999) conducted detailed research on type (d) indirect contact charge and indirect contact discharge system. A comparison between direct-contact and indirect-contact systems is shown in Table 2.7.

Table 2.7: Comparison of direct-contact and indirect-contact systems

System type	Advantage	Disadvantage
Charge process Direct contact	Evaporator heat exchanger not needed; high heat transfer performance; high temperature of refrigerants returning to compressor; defrosting equipment not needed; low energy consumption	Oil-free compressor and water separator needed; high investment
Charge process Indirect contact	Regular compressor used; regular refrigeration cycle; low investment	Evaporator heat exchanger needed; relatively poor heat transfer performance; low temperature in the evaporator and reduced compressor performance; defrosting equipment needed when ice exists; high energy consumption
Discharge process Direct contact	Heat exchanger not needed; low temperature difference between cold storage medium and coolant; low energy consumption	Sophisticated pump needed to make liquid refrigerant to be pumped without cavitations' problem or leaks at the seals
Discharge process Indirect contact	Regular pump	Heat exchanger needed; high temperature difference between cold storage medium and coolant; high energy consumption

From a more practical viewpoint, the hydrate storage apparatus is usually an indirect-contact system. Shu et al. (1999) developed a new hydrate cold storage system for this type of system, which had an internal heat exchanger and a small, external rotating crystallizer, which was the pump. This system could achieve a high-efficiency and high-density cold storage performance. Tong et al. (2000) proposed one type of cold storage system using an injector to spray the refrigerant liquid into the cavity where the liquid could be vaporized and completely mixed with the water to enhance heat mass transfer during hydrate formation.

2.2.4.3 Thermal and hydraulic characteristics of hydrate slurry

In the following introduction, TBAB slurry is mainly discussed as an example since it has been the topic of most intensive studies. Clathrate hydrate slurry is usually considered as non-Newtonian fluid for its solid-liquid two-phase mixture feature. Only when the solid fraction is very small it can be possibly be treated as Newtonian fluid. Darbouret et al. (2005) indicated that there was a critical volume fraction for TBAB hydrate slurry at which its flow behavior changed from Newtonian fluid flow to Bingham fluid flow. Hydrate slurry in higher volume fraction has higher yield stress and apparent viscosity. It was also found that the viscosity of type B TBAB hydrate slurry was a little larger than that of type A due to the different shapes of two types of hydrate crystals.

When compared to the chilled water, clathrate hydrate slurry exhibited a higher overall heat transfer coefficient due to the associated phase change. Results in literature (Ogoshi and Takao, 2004) show the cooling capacity of TBAB clathrate hydrate slurry is about

2.5~3.5 times larger than that of the chilled water at the flow rate of 1~5 kg/min. Xiao et al. (2007) conducted experimental study on the heat transfer characteristics of TBAB slurry in a horizontal copper tube with 8 mm inner diameter.

Results indicated that the influence of the volume fraction of solid phase on Nusselt number was small even with the change of Reynolds numbers. Ma et al. (2010) studied forced convective heat transfer characteristics of TBAB clathrate hydrate slurry with the volume fraction 0~20.0%. Heat transfer correlations of TBAB hydrate slurry flowing through straight circular tubes under constant heat flux were developed for the laminar, transition, and turbulent flow regimes. It was found that the volume fraction was the major factor which influenced the heat transfer in the laminar region while the flow velocity was more important in the transition and turbulent flow regions. In another study, Xiao et al. (2006) tested the flow characteristics of TBAB slurry in a PVC pipe with 21 mm inner diameter. Power law fluid equation was applied, which showed that the apparent viscosity of 0~16 vol.% TBAB slurry was 3~8 times higher than that of water. Therefore, it is necessary to make reasonable considerations for hydrate application in air conditioning systems. In fact, thermal and hydraulic characteristics of clathrate hydrate slurry are usually be affected by many factors, such as volume fraction of hydrate crystal particles, the pipe shape and size, which make the flow characteristics very complicated and need further investigations.

2.2.5 Microencapsulated PCMs or PCM slurries and phase change emulsions

2.2.5.1 Microencapsulated PCMs or PCM slurries

Microencapsulated PCM (MPCM) is the encapsulation of PCM particles (the core) with a continuous film of polymeric material (the shell). The PCM core particles vary in size, ranging from 1 μm to 1000 μm in diameter. There are two processes used in microencapsulation: physical and chemical. The physical processes are spray drying, centrifugal and fluidized bed processes, or coating processes involving rolling cylinders. The chemical processes are in-situ encapsulations like complex coacervation with gelatin, interfacial polycondensation resulting in a polyamide or polyurethane shell, and precipitation due to polycondensation of amino resins. The in-situ processes have the ability to yield microcapsules with the best quality in terms of diffusion-tightness of the wall. The surface morphology of microcapsules, as observed using a scanning electron microscope (SEM), is shown in Figure 2.14 (Hawlader et al., 2003).
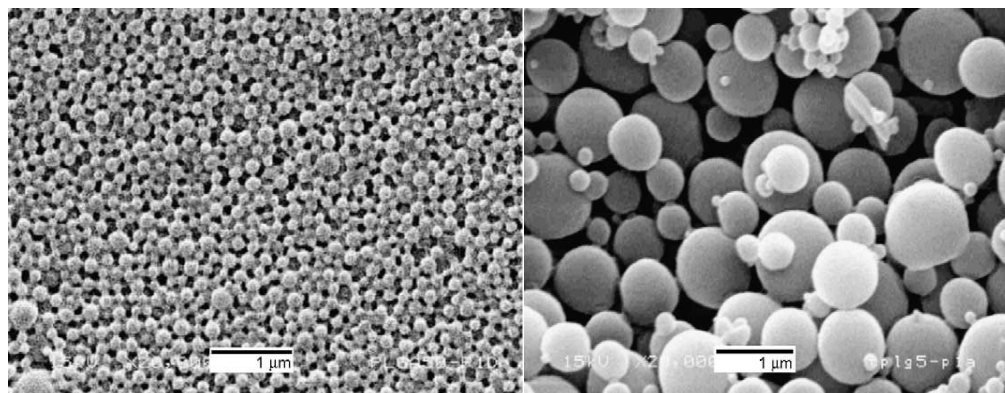
(a) Spray-dried microparticles   (b) Coacervated microparticles

Figure 2.14: Surface morphology of microcapsules studied by a scanning electron microscope (SEM) (Hawlader et al., 2003)

40

The advantages of MPCMs are: (1) reduction of the reactivity of the PCMs with the outside environment, (2) improvement of heat transfer to the surroundings due to the large surface to volume ratio of the capsules, (3) improvement in cycling stability since phase separation is restricted to microscopic distances, and (4) no leakage during its liquid phase for some PCMs. Thermal properties of two MPCM products are listed in Table 2.8 (Microtek Laboratories Inc., 2011). The appearance of the two products is white to slightly off-white color with good thermal cycling. The form of MPCM 6 is a wet cake (70% solids, 30% water), and MPCM 6D is a dry powder.

Table 2.8: Thermal properties of microencapsulated phase change materials (slurries) (Microtek Laboratories Inc., 2011; Diaconu et al., 2010)

MPCM type	Phase change temperature(°C)	Latent heat (kJ/kg)	Comments
MPCM 6	6 (melting)	157~167 (melting)	Specific gravity: 0.9 Core material: Tetradecane Mean particle size: 17~20 micron
MPCM 6D	6 (melting)	157~167 (melting)	Capsule composition: 85~90 wt.% PCM 10~15 wt.% polymer shell
Microencapsulated RT6 slurry	4.1~7.5 (melting) 2.2~5.8 (freezing)	53 (melting) 56 (crystallization)	DSC scanning rate: 0.1°C/min
Microencapsulated RT6 slurry	4.0~6.8 (melting) 3.6~6.0 (freezing)	55 (melting) 49.4 (crystallization)	DSC scanning rate: 0.01°C/min

When the MPCM is dispersed into the carrier fluid, e.g. water, a suspension of MPCM slurry is formed. In the fabrication process, the proper amount of surfactants is used for helping MPCM fully disperse into the carrier fluid, thus increasing the lifetime of the MPCM slurry. Because the phase change with latent heat is involved, the effective specific heat of the fluid is remarkably increased with results in the heat transfer enhancement. Obviously, MPCM slurries can be used as both thermal energy storage and

heat transfer fluid. The thermal properties of MPCM slurries, like effective thermal conductivity, viscosity and effective specific heat, are different from those of the bulk PCM so that the influence of carrier fluids should be considered. The effective thermal conductivity with flowing condition is generally higher than that predicted by Maxwell's equation due to the interaction between the particle and fluid. A detailed introduction has been developed by Zhang et al. (2010b).
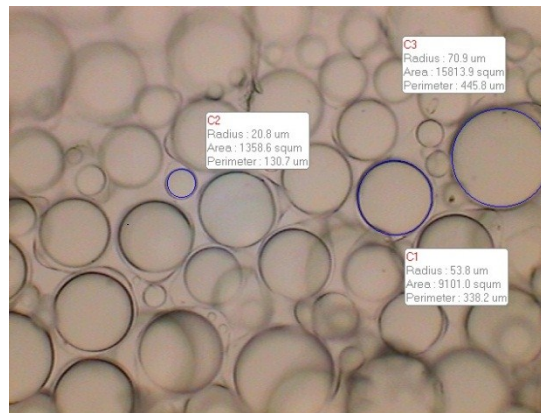
Figure 2.15: Micrograph of one kind of MPCM (*n*-Tetradecane with gelatin)
(Alvarado et al., 2004)

In one study (Alvarado et al., 2004), MPCM particles were made by microencapsulating 99% pure tetradecane with gelatin through the process of complex coacervation. The average microcapsules diameter is 145 μm. On average, the particles contained 2% by weight of an effective nucleating agent. Based on microscopic observations and DSC analysis, each capsule is made of about 88% PCM and 12% shell material. A characteristic micrograph of MPCM can be seen in Figure 2.15. Thermal properties of an MPCM slurry with a different MPCM mass fraction is shown in Figure 2.16, which

shows that this kind of MPCM slurry has the potential to become a successful heat transfer fluid for cold storage for air conditioning application.
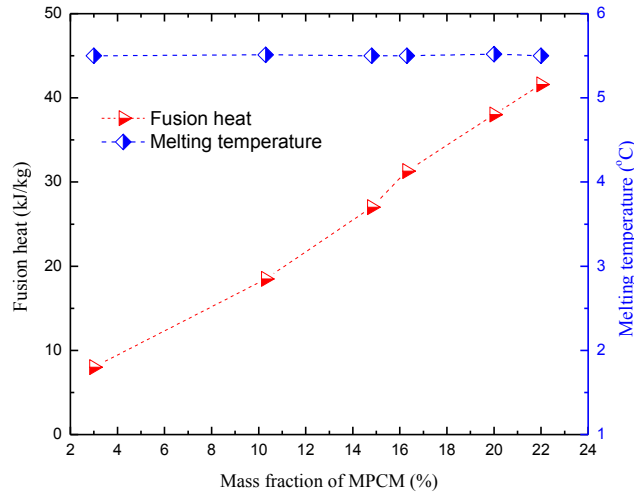
Figure 2.16: Thermal properties of one kind of MPCM slurry (Alvarado et al., 2004)

Diaconu et al. (2010) also studied a kind of MPCM slurry for air conditioning applications. It consisted of an aqueous dispersion of PCM (Rubitherm RT6) encapsulated in a polycyclic cell, resulting in microcapsules with a volume mean diameter of 2.24 μm. RT6 is a commercial PCM, and the PCM mass fraction of the slurry was 45%. Thermal properties of the MPCM slurry by DSC study are shown in Table 2.8. From this table, one can conclude that the narrower phase change temperature range is suitable for air conditioning application.

2.2.5.2   Phase change emulsions

Phase change emulsion, similar to the MPCM slurry, is a novel two-phase fluid composed of PCM particles as a dispersed phase and water as a continuous phase. Due to

the large surface to volume ratio of the dispersed phase, it also has greater apparent specific heats and higher heat transfer abilities in the phase change temperature range than the conventional single-phase heat transfer fluids such as water. Also, phase change emulsion systems store energy not only by using the sensible heat capacity of the carrier fluid, but also by using the latent heat capacity of the media. Thus they are advantageous in the field of the convective heat transfer enhancement and energy transport for both a dynamic type cold storage system and a secondary loop. In addition, a nucleating agent is often used to prevent the effect of supercooling of the emulsion. Illustration of a phase change emulsion is shown in Figure 2.17.
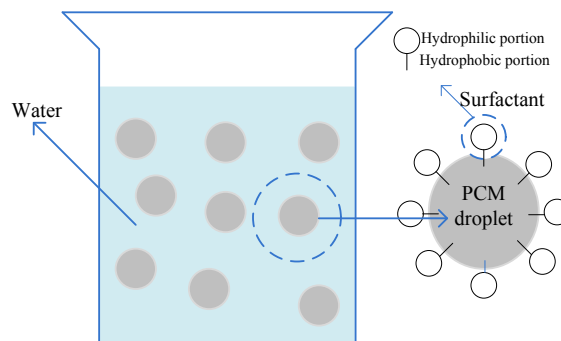
Figure 2.17: Illustration of a phase change emulsion
Note: PCM-in-water emulsions, where fine PCM droplets are directly distributed in water and maintained in dispersion by a surfactant

Rubitherm RT10 (Huang et al., 2009), which is paraffin mixture of tetradecane, pentadecane, and hexadecane, is presented as a PCM, as shown in Figure 2.18. The total heat capacity of the paraffin/water emulsions and the ratio of heat capacity of the emulsions to that of water versus RT10-concentration in the temperature range of 5~11°C are shown in Figure 2.19. Obviously, the paraffin/water emulsion is an attractive candidate for air conditioning application.
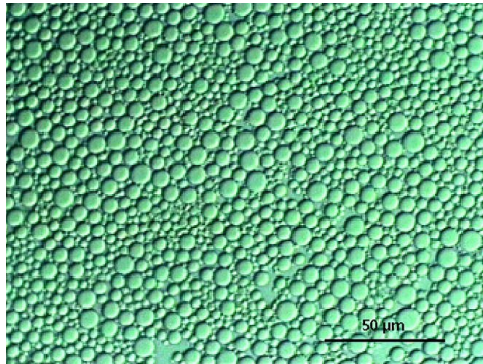
Figure 2.18:Micrograph of the emulsion containing 30 wt.% RT10 at 20°C
(Huang et al., 2009)
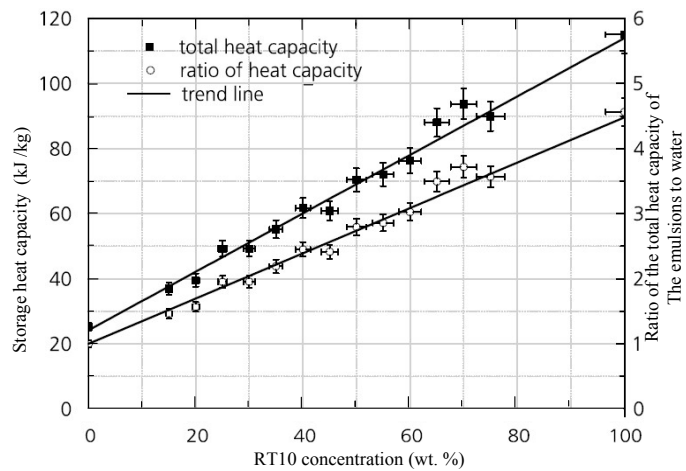
Figure 2.19: Total heat capacity of the phase change emulsions and ratio of heat capacity
of the emulsions to that of water (Huang et al., 2009)

The thermal properties of tetradecane-based phase change emulsions have been studied

by many researchers (Inaba, 1996; Zhao et al., 2001; Zhao et al., 2002.), and are

considered attractive candidates for air-conditioning applications. The melting point of

tetradecane is 5.8ºC and the fusion heat is 229 kJ/kg. A study of tetradecane-based phase

change emulsions is shown in Table 2.9 (Xu et al., 2005a).

Table 2.9: Thermal properties of tetradecane-based phase change emulsions (Xu et al., 2005a)

Phase change emulsion (tetradecane/water)	Melting point (°C)	Fusion heat (kJ/kg)	Average specific heat in the phase change region (kJ/kg·K)	Average specific heat in non-phase change region (kJ/kg·K)
10:90 tetradecane: water (wt.%)	4.36	18.69	5.7	3.9
20:80 tetradecane: water (wt.%)	4.57	31.56	6.6	3.7
30:70 tetradecane: water (wt.%)	4.51	73.47	10.1	3.6

2.2.5.3   Supercooling minimization

Though the core materials (PCMs) for microencapsulated PCM slurries and phase change emulsion are usually paraffin waxes, which are insoluble with water, supercooling is an important issue to deal with. Nucleation agents can be used to relieve this issue. In one study by Huang et al. (2009), a nucleation agent was added to the paraffin to prevent supercooling before the emulsifying process for the paraffin emulsion in cooling applications. The necessary surface can be offered by the agent to start nucleation in the interior of the paraffin droplets, therefore the agent works as the nucleation catalyzer. The supercooling was reduced to 0.1°C with the nucleation agent, while it was 7°C without that. In another study by Alvarado et al. (2006), a concentration of 2% tetradecanol resulted to be sufficient to suppress supercooling both in tetradecane and microencapsulated tetradecane, and the heterogeneous nucleation was more favorable in the presence of tetradecanol. Also additional consideration should be given that the amount of nucleation agent for suppressing supercooling effect should be the smallest possible because adding excessive amount of nucleation agent will lead to a reduction of the latent heat of the PCM. Yamagishi et al. (1996) added l-tetradecanol as nucleation

agent with good results for two *n*-tetradecane and *n*-dodecane microencapsulated slurries. In addition, cold finger and porous heat exchange surfaces has been utilized effectively to deal with this issue.

2.2.5.4 Thermal and hydraulic characteristics

Since the working fluids studied in this section are mainly used for the secondary loop systems in air conditioning application, it is necessary to study the thermal and hydraulic characteristics. Note that MPCM should be durable during its long term operation, because it might be broken by the circulating pump. The MPCM slurry is generally considered as the Newtonian fluid when the volume fraction of MPCM is less than 25%. The viscosity of the working fluid is a critical factor for cold energy transportation. Based on literature (Wang et al., 2008; Yamagishi et al., 1999), results indicated that the working fluid showed the Newtonian fluid behavior and the apparent viscosity was about 1.5~10 times of the water as the mass fraction of MPCM increased from about 5 to 30%. The MPCM slurry can be treated as the homogeneous fluid at low volume fraction.

Inaba et al. (2004) investigated the mixing effect of the large size PCM (*n*-docosane) particles under the condition without a phase change and the small size PCM (*n*-tetradecane) slurry with a phase change. Results showed that the flow drag reduction could be achieved in the turbulent flow regime, while the pressure drop was increased in the laminar flow regime in the case of higher mass fraction of large size particles. The ratio between the heat transported by MPCM slurry (including both latent heat and sensible heat) and the pumping power of the circulating pump was larger than that for

47

water in the turbulent flow regime. In the laminar flow regime, the ratio decreased from larger than that for water to less than that for water as increasing the fraction of the larger MPCM particles. Therefore, reasonable consideration for both the energy transportation and pumping power should be paid in practical application.

In another study by Alvarado et al. (2007), MPCM (*n*-tetradecane as the core material) with the diameter of smaller than 10 mm was proven to be durable and impact-resistant in the durability test with a cavity pump. MPCM slurry with low mass fraction had much smaller pressure drop than that of water. Moreover, the difference was reduced with an increased mass fraction of MPCM. The drag reduction effect of slurry would be the possible reason. Around melting temperature of *n*-tetradecane, the heat transfer coefficient of slutty reached its peak.

Study by Diaconu (2009) revealed that the convective heat transfer coefficient between the MPCM particles and the carrier fluid (water) played a very critical role during charging/discharging processes. In addition, MPCM mass fraction and particle diameter were studied for optimizing the thermal storage system. Study by Yamagishi et al. (1996) also investigated MPCM (core material: *n*-tetradecane and *n*-dodecane) slurries. From this study the tolerance against the shear force induced by pumping is quite essential in practical application. Large apparent viscosity can be achieved with high volume fraction, and this can increase the pressure drop and pumping power. Pressure drop can be effectively reduced by using the drag reduction additives in the case of high volume fraction of MPCM. Based on the discussion above, viscosity, pressure drop, pumping

power, convective heat transfer coefficient, laminar/tubular flow regime, are all important factors when investigating thermal and hydraulic characteristics, which still need further study.

2.3   Sorption cold storage

For sensible and latent cold storage in air conditioning application, the temperature of the cold storage tank is lower than the ambient temperature. Accordingly, the cold energy loss from the storage tank must be considered in such a system during the storage period. This may be disadvantageous for the system, especially when it is used for a long term storage period. In the following, the sorption cold storage is introduced as a solution for a long term storage period, especially for adsorption storage. Sorption cold storage uses sorption working pairs (sorbents/refrigerants) in air conditioning applications. The sorbents, which can induce physical or chemical attraction with an active refrigerant gas for a refrigeration effect, can either be in liquid phase (absorption technology) or in solid form (adsorption technology). The cooling capacity can be preserved for a long term with no pollution and no cooling energy losses.

Also it can be readily discharged when needed only by connecting the generator (for absorption storage) or adsorbent bed (for adsorption storage) to the evaporator. This kind of cold storage system, which can be driven by electricity, industry waste heat, or solar energy, contributes significantly to the concept of sustainable system development. In addition, especially for an adsorption cold storage system, after energy charging, can be moved to another place that cannot provide energy by itself to produce refrigeration

power for short term air conditioning. Usually a sorption system uses alternative clean refrigerants, with no pollution other than the CFC or HCFC refrigerants in a conventional vapor compression system. Also, it can be operated without few moving parts, other than some magnetic valves, is mechanically simple, and has high reliability, low vibration and a long lifetime. A general comparison of absorption and adsorption storage technologies is shown in Fig. 2.20.

(a) Absorption (b) Adsorption (c) Ideal sorption
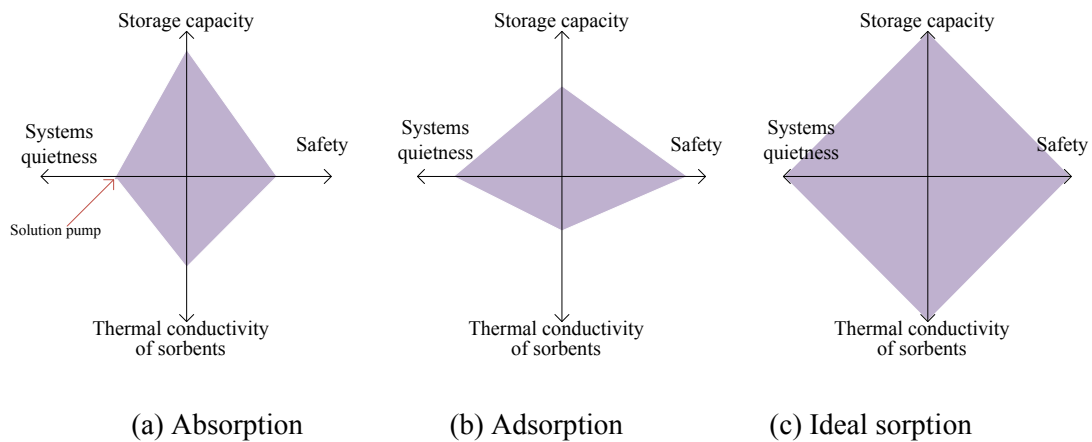
Figure 2.20: Comparison of absorption and adsorption storage technologies

2.3.1 Basic storage principle

2.3.1.1 Absorption cold storage

A schematic drawing of the basic principle for absorption storage is shown in Figure 2.21(a). Using the working pair LiBr/H_2O as an example, with the shut-off valve after the poor solution opened, the poor solution (low concentration of absorbent) is pumped towards the high-pressure zone, and then the mixture is heated in the generator during the charging process. The contribution of heat (driving heat) allows the separation of the refrigerant (H_2O) from the absorbent (LiBr solution). The refrigerant vapor is sent to the

50

condenser, where it is condensed to liquid by a cooling fluid. The liquid refrigerant is stored in a container for cold storage, while the rich solution from the generator is also stored in a container. The liquid refrigerant in the container as the cold storage can be used to produce the cooling effect for air conditioning application. During the discharging process, the shut-off valve after the poor solution is closed, the liquid refrigerant is expanded with the shut-off valve on the liquid refrigerant side opened and sent to the evaporator, and rich solution flows to the absorber with the shut-off valve on the rich solution side opened. Thus, the water vapor in the evaporator is absorbed by the rich solution and the cooling effect is produced in the evaporator at low pressures. And the rich solution absorbs the water vapor and releases absorption heat, which can be used for heating purposes. Gradually, the poor solution from the absorber is stored in a container. Because the absorption refrigeration system has been well developed for the market, only a brief introduction is given in this chapter.

(a) Absorption storage   (b) Adsorption storage
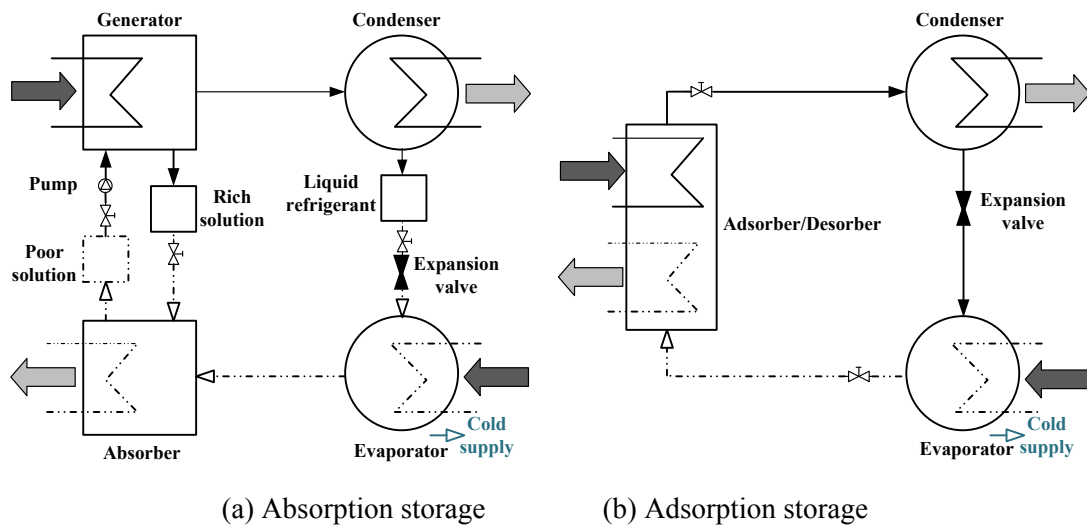
Figure 2.21: Schedule drawing of basic principle for sorption storage

2.3.1.2 Adsorption cold storage

A schematic drawing of the basic principle for adsorption storage is shown in Figure 2.21(b). Adsorption is the general phenomenon resulting from the interaction between a solid (adsorbent) and a gas (refrigerant), based on a reversible physical or chemical reaction process. During the charging process, a desorber (can also be an adsorber during the discharging process) connected to a condenser is heated by a heat-driving source with the shut-off valve after the desorber opened. Next, the refrigerant vapor flows from the desorber to the condenser and is cooled to a liquid state. It then passes through the expansion valve and is stored in an evaporator under low-pressure condition for cold storage. During the discharging process, the shut-off valve after the adsorber is closed. The adsorber is cooled by a heat transfer fluid and its pressure drops. When the pressure drops below that of the evaporator, the shut-off valve after the evaporator is opened and the refrigerant is evaporated and moves to the adsorber because of the pressure difference. Cold temperatures are then produced in the evaporator for air conditioning application.

2.3.2 Working pair selection

During charge or discharge processes, important heat and mass flows are produced with frequent use of sorption working pairs. The thermal properties of these working pairs play a very important role for storage used in air conditioning applications. Here, the thermal property mainly refers to the storage capacity or the ratio of the amount of cold storage by evaporation of refrigerant to the mass or volume of the sorbent. It is one of the basic criteria required for designing an efficient storage process.

To provide a general understanding on thermal properties of different working pairs, Mugnier and Goetz (2001) summarized and compared their storage capacities. Based on the data, and with a rigorous calculation protocol obtained from the literature (Mugnier and Goetz, 2001), thermal properties of working pairs for air conditioning applications were extracted and summarized as shown in Figure 2.22. The summary examines them under the same conditions of an ambient temperature of 35°C and evaporation temperature of 5°C. Storage capacity and minimum heating temperature of different sorption working pairs under same conditions is shown in Figure 2.23. From the figures above, the most suitable and efficient working pair for the sorption storage system is water and solid/gas reaction used as the refrigerant and sorbent, respectively.

For the requirements of a working pair, the refrigerant should have environment safety, large latent heat per volume, no toxicity, no flammability, no corruption, good thermal stability, low material cost, and better volatility of the solution in the absorption system. For the sorbent, especially for the adsorbent, it should have the large adsorption capacity, large change of adsorption capacity with temperature variation, a more flat desorption isotherm, and good compatibility with refrigerant. Generally speaking, there are no perfect working pairs meeting all of these requirements.
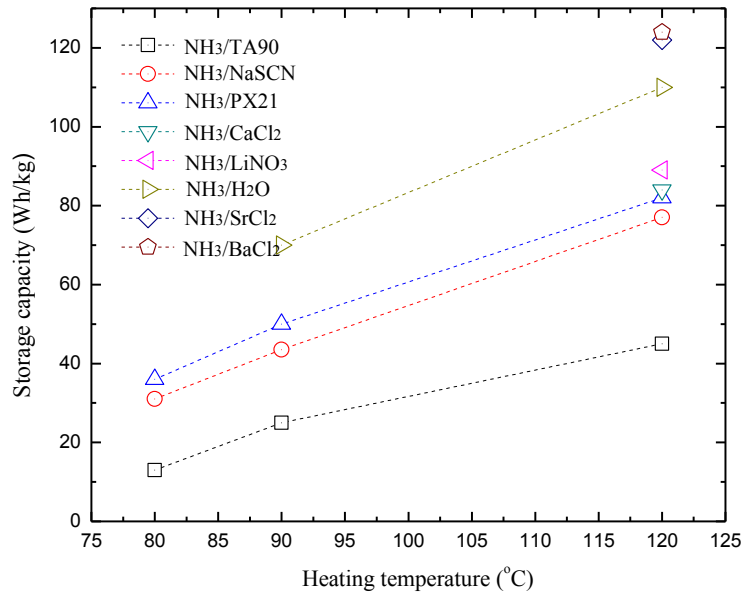
(a) NH₃ as refrigerant

(b) H₂O as refrigerant
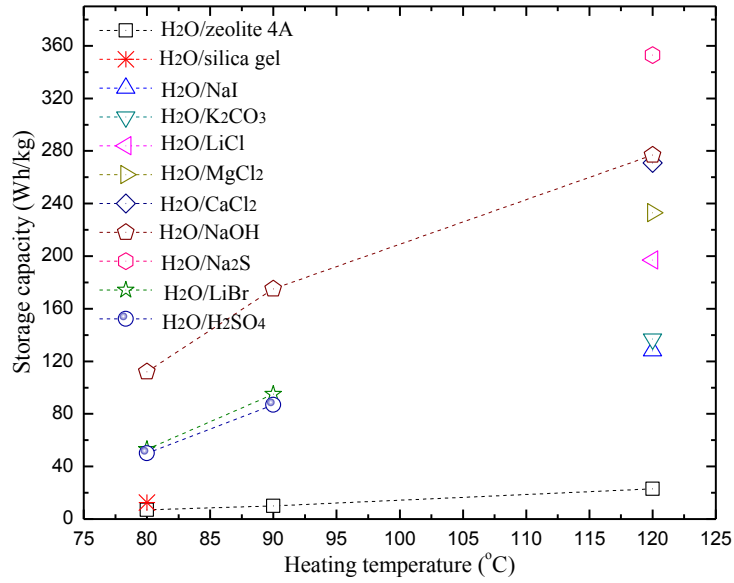
(c) Other materials as refrigerant
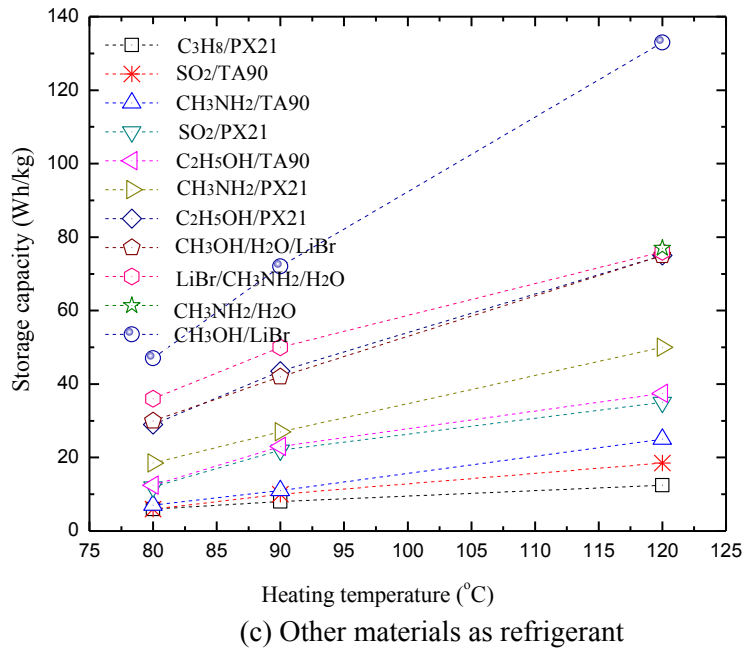
Figure 2.22: Storage capacity of different sorption working pairs with ambient temperature of 35°C and evaporation temperature of 5°C (Mugnier and Goetz, 2001)
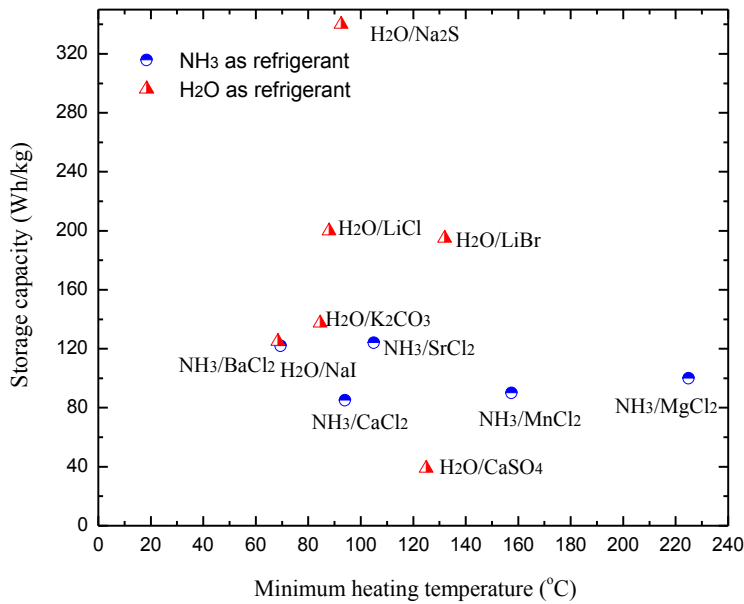
Figure 2.23: Storage capacity and minimum heating temperature of different sorption working pairs with ambient temperature of 35°C and evaporation temperature of 5°C (Mugnier and Goetz, 2001)

55

2.3.2.1 Absorption working pairs

Among the absorption absorbent/refrigerant pairs, $H_2O/LiBr$ and NH_3/H_2O are the most common ones. The former is usually used for air conditioning application and the latter can be used for subzero applications, such as ice making. In addition, NH_3/H_2O has several disadvantages: (1) higher generator inlet temperature (about 90~180°C, while it is about 70~90°C for $H_2O/LiBr$), (2) higher pressures and hence higher pumping power needed, (3) a more complex system needed due to a rectifier to separate ammonia and water vapor at the generator outlet, and (4) hazards by the use of ammonia. Therefore, $H_2O/LiBr$ is more suitable for air conditioning application. In addition, the comparison of working pairs, $H_2O/LiBr$, $H_2O/NaOH$, $H_2O/LiCl$, and $H_2O/CaCl_2$, has also been studied. As shown in Table 2.10, different working pairs were compared under the same conditions of a temperature of absorption of 25°C, a temperature of evaporation of 10°C and a temperature of condensation of 30°C (Liu et al., 2009). From this table, and based on the analysis from literature (Liu et al., 2009), the $H_2O/NaOH$ and $H_2O/LiCl$ pairs have excellent performance on storage capacity. The NaOH has the advantage of a low price, but has the disadvantage of a temperature requirement for solar energy utilization (84~135°C). The $CaCl_2$ is the least expensive material, but its storage capacity is low so that the volume of storage tanks would be bigger than for the other pairs. The $H_2O/NaOH$ could be the most economic material because of its low price and high storage capacity. However, due to its high temperature requirement for solar energy utilization, the system's solar collector would be operated at low efficiency. This solution is also highly corrosive.

Table 2.10: Evaluation points of different absorption working pairs (Liu et al., 2009)

Working pairs	Absorbent price (Euro/ton)	Without crystallization			With crystallization		
		Concentration Maximum (%) (kg absorbent/kg solution)	Capacity (kJ/kg)	Temperature requirement for heat driving (°C)	Concentration Maximum(%) (kg absorbent /kg solution)	Capacity (kJ/kg)	Temperature requirement for heat driving (°C)
H_2O/LiBr	6,000	60	1,535	74	69	2,068	93
H_2O/LiCl	3,400	46	2,922	68	70	5,271	78
H_2O/NaOH	300	53	3,442	84	69	5,225	135
H_2O/CaCl$_2$	140	45	628	50	51	1,103	56

2.3.2.2   Adsorption working pairs

The commonly used working pairs of H_2O/silica gel and H_2O/zeolite, which closely meet these requirements, are introduced here.

(1) H_2O/silica gel

Based on Faninger (2004), the storage density of silica gel is up to four times that of water. From the literature by Yang (1991), the adsorption heat of H_2O/silica gel is about 2,500 kJ/kg and the desorption temperature can be very low, but above 50°C. Normally the desorption temperature should not be higher than 120°C, and it is usually below 90°C. Approximately 4~6wt.% water is connected with a single hydroxyl group on the surface of a silica atom to maintain the adsorption capacity. If the desorption temperature is too high (above 120°C), adsorption performance will drop significantly, even to the point of losing its adsorption capacity. In addition, the adsorption quantity of this pair is low, about 0.2 kg/kg (Wang et al., 2009).

(2) H$_2$O/zeolite

Zeolites are alumina silicates with high microporosity (Nielsen, 2003), and are considered to be reliable even in the harshest environmental conditions (Zeolith-Technologie GmbH, 2008). Since synthetic zeolites are expensive, Han et al. (1994) conducted a contrast study of natural zeolites to the synthetic zeolite 13X. They reported that natural zeolites could be used as a storage material instead of the 13X synthetic zeolite when the heating temperature is below 100°C. For the H$_2$O/zeolite pair, the adsorption heat is about 3,300~4,200 kJ/kg, higher than that of H$_2$O/silica gel pair (Wang et al., 2009). Additionally, with desorption temperature high than 200°C, the H$_2$O/zeolite can be still stable. The zeolites are usually employed for air conditioning application with a heat source between 200 and 300°C. Several kinds of crystal cell units of zeolite are shown in Figure 2.24 (Yang, 1991). The volume of pores for type X and Y zeolites, whose void ratio can be as high as 50% when there is no water adsorbed, is larger than that of other types of pores. One crystal unit can have 235 molecules of water after adsorption, and most of the molecules would accumulate in the center pore.
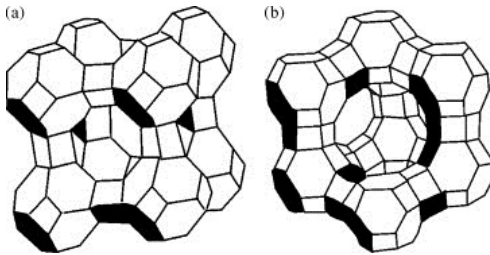
(a) Crystal cell unit of type A zeolite   (b) Crystal cell unit of type X, Y zeolite or faujasite

Figure 2.24: Crystal cell unit of zeolite (Yang, 1991)

The adsorption process of the working pairs discussed above is physical adsorption, which is caused by the van de Walls force between the molecules (Ponec et al., 1974) of the adsorbent containing mesopores or micropores, and the refrigerant. For details about chemical adsorption, please refer to literature (Wang et al., 2009).

2.3.3   Heat transfer and system performance enhancement

The sorption cold storage is closely related to the sorption cooling technologies. The absorption storage was initially studied in conjunction with solar energy, and the system design was gradually improved based on the technologies of absorption refrigeration system. Components of absorption systems were studied for improving heat transfer. An example of such a study involves the optimization of liquid refrigerant tank with reasonable volume to make the system operate in an improved state for better storage capacity (Sheridan and Kaushik, 1981).   Additionally, various recycle system configurations have been used to improve system performance (Li and Sumathy, 2000; Yang et al., 2011). Based on the literature review (Wan et al., 2006; Qiu et al., 2009; Xu et al., 2008; Rizza, 2003; Xu et al., 2005b), Yang et al. (2011) summarized related absorption cold storage technologies. The research works were extracted for air conditioning application with most commonly used working pair, $H_2O/LiBr$, is shown in Table 2.11.

Table 2.11: Review of absorption cold TES storage technologies (Yang et al., 2011)

Absorption pair	Driving source	Thermal storage density (kWh/m^3)	Standard for thermal storage volume
H$_2$O/LiBr	Compressor cycle	111.7 (full storage type) 109.4 (part storage type)	Mixed storage volume and water volume
H$_2$O/LiBr	Solar energy, single effect	58.2	Dilute solution volume, concentrated solution and water volume
H$_2$O/LiBr	Solar energy	116.7	Mixed storage volume and water volume
H$_2$O/LiBr	Heat pump	90	Optimized dilute solution volume, concentrated solution
H$_2$O/LiBr	Compressor cycle	32.78	Mixed storage volume and water volume

For the adsorption storage, the adsorption cold storage system with H$_2$O/zeolite working pair was studied by Lu et al. (2003). Results showed that the adsorption cold storage system could be successful used for the locomotive air conditioning system. This system is simple and can be handled easily compared with other multi-bed adsorption systems. Also, the operating process of the system is in conformity with the running time of the locomotive. An average refrigeration power of about 4.1 kW was obtained, which was enough to make the driver's cabin fairly comfortable. However, this study also mentioned that the heat and mass transfer of the adsorber needs to be improved to get better performance. Here the main issue of the poor heat and mass transfer of adsorbent beds, especially the low thermal conductivities and poor porosity characteristics of adsorbents, are discussed.

Li and Wang (2002) reached the conclusion that adding packing density to an adsorbent, adopting double glass covers, using selective coating material, and using heat transfer fins or plate heat exchangers could enhance the heat transfer and thermal conductivity of the adsorbent beds. Additionally, composite adsorbents, which are normally a combination of physical sorbents (silica gel or zeolite) and chemical sorbents (metal

chlorides) can experience increases physical adsorption capacity through the addition of extra chemicals. For improving system performance of adsorption storage, there are two main parameters to with which to evaluate the performance for adsorption refrigeration: COP, which is the ratio of cold production from the evaporator to the heat supplied by driving energy, and SCP, which is the ratio of cooling power for the semi-cycle to the adsorbent mass in one adsorbent bed. To improve the COP, in addition to adapting advanced heat exchanger, adsorption storage with different advanced cycles has been studied extensively (Sumathy et al., 2003). To improve the SCP, more technologies are needed to improve heat and mass transfer of adsorbent beds, which are discussed above to some extent. Wang et al. (2009) summarized the performance of the COP and SCP with a fair comparison of different working pairs from the literature (Lai, 2000; Eun et al., 2000; Wang et al., 2005a; Wang et al., 2005b). The water-based working pairs for air conditioning applications are compared as shown in Table 2.12.

Table 2.12: Performance comparison of different adsorption working pairs (Wang et al., 2009)

Adsorption working pair	Evaporating temp. (°C)	COP	SCP (W/kg)	Characteristics
Water/graphite/silica gel	3		70	Composite adsorbent to intensify the heat transfer
Water/silica gel	10	0.4	85	Split heat pipe type evaporator
Water/zeolite	5	0.9	250	Intermittent convective thermal wave cycle

For the adsorption storage technologies, the main factors impeding the commercialization of this storage technology for air conditioning application are high equipment and maintenance cost, big size, and the need for an auxiliary energy system. There is still

much more work to do for optimizing and reducing the cost of these systems with more advanced technologies.

2.4   Challenges and technology perspective

Different kinds of available cold storage materials that can be used for air conditioning applications are introduced in this section. Technology perspectives, with regard to water storage, ice storage, PCM storage and sorption storage are summarized as follows:

(1) Water storage and static ice storage, which are already well-established technologies, have little need for further study. The important issue concerning the dynamic ice slurry application is its generation method, relating to the efficiency and reliability of a water or aqueous solution converting to ice crystals or ice slurry, which needs to be investigated further.

(2) Salt hydrates and eutectics, and refrigerant hydrates are material candidates for cold storage, and demonstrate high latent heat of fusion, high thermal conductivity, and low flammability. However, salt hydrates have more serious issues of phase separation, supercooling, and corrosion. Paraffin waxes and fatty acids are mostly chemically inert, stable and recyclable, exhibit little or no supercooling. They show no phase separation or non-corrosive behavior (with the exception of fatty acids for the natural characters of acids). However, they have the shortcomings of low thermal conductivity and high flammability. Some works have been done for such issues by past researchers, which were introduced and summarized in this paper.

(3) Thermal and hydraulic characteristics of phase change slurries (mainly about clathrate slurries, microencapsulated phase change slurries, and phase change emulsions) are discussed and summarized. Viscosity, pressure drop, pumping power, convective heat transfer coefficient, and laminar/tubular flow regime, are all important factors for thermal and hydraulic characteristics and reasonable consideration should be made for practical application.

(4) The suitable and efficient working pair that can be used for the sorption storage system is water and solid/gas reaction used as the refrigerant and sorbent, respectively. One of main issues is the poor heat and mass transfer of adsorbent beds, especially for the low thermal conductivities and poor porosity characteristics of adsorbents. Additionally, the main factors impeding the commercialization of this storage technology are high equipment and maintenance cost, large size, and the need of an auxiliary energy system. Therefore, there is still much further work to do with regards to optimizing and reducing the costs of these systems with more advanced technologies.

3 Critical Literature Review of Cold TES Technologies for Subzero Application

Based on the literature published, still less information is available or introduced systematically for review of cold storage for subzero applications. Therefore, I tried to provide extensive reviews on the cold storage for subzero applications. In this chapter, different kinds of subzero applications are classified as shown in Figure 3.1. The phase change materials (PCMs), and sorption working pairs, are mainly introduced.
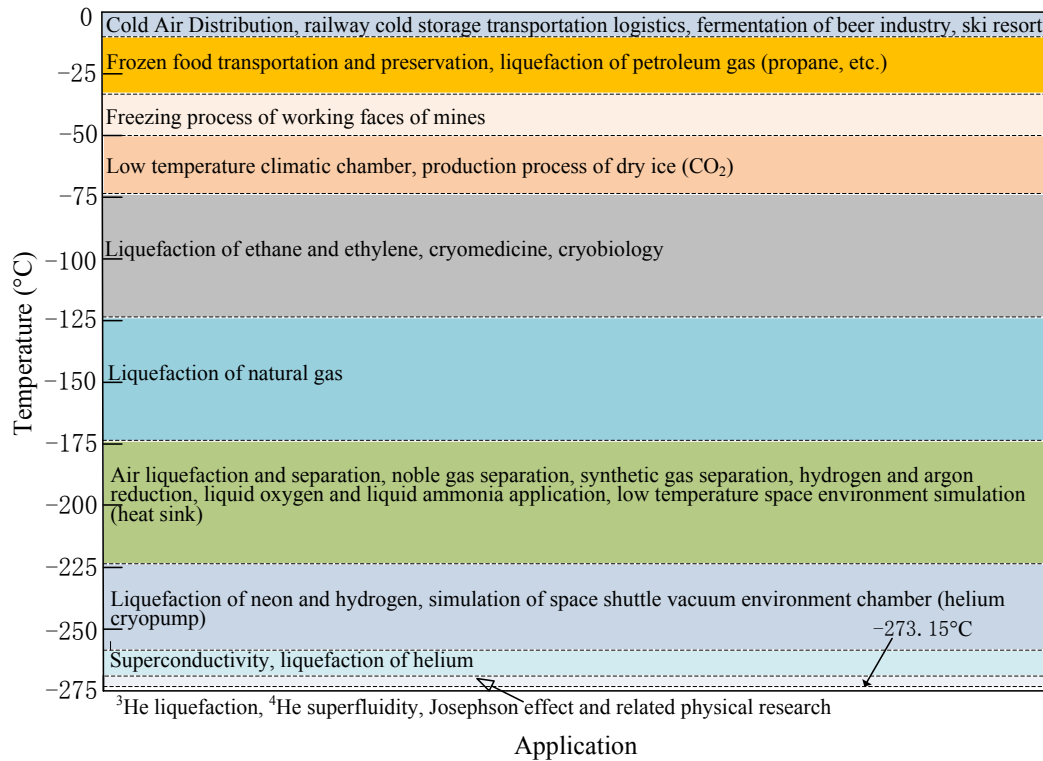
Figure 3.1: Classification of different kinds of subzero cold storage application

3.1 Latent cold storage materials

Early in 1983, Abhat (1983) gave a useful classification of the substances used for thermal energy storage, as shown in Figure 2.7 in Chapter 2. From Figure 2.7, PCMs with

solid-liquid changes for all applications are divided into two main families: inorganic and organic. The melting temperature and phase change enthalpy (fusion heat) of existing PCMs are shown in

Figure 2.8 (Dieckmann, 2006). Based on the review of recent development of PCM storage research for subzero applications, the commonly used PCMs can be eutectic water-salt solutions (non-eutectic water-salt solutions like paraffins also included with a very small part). Here the thermal storage technologies for subzero applications will be discussed and summarized according to this PCM classification. Figure 3.2 shows thermal properties of PCMs studied in this section.
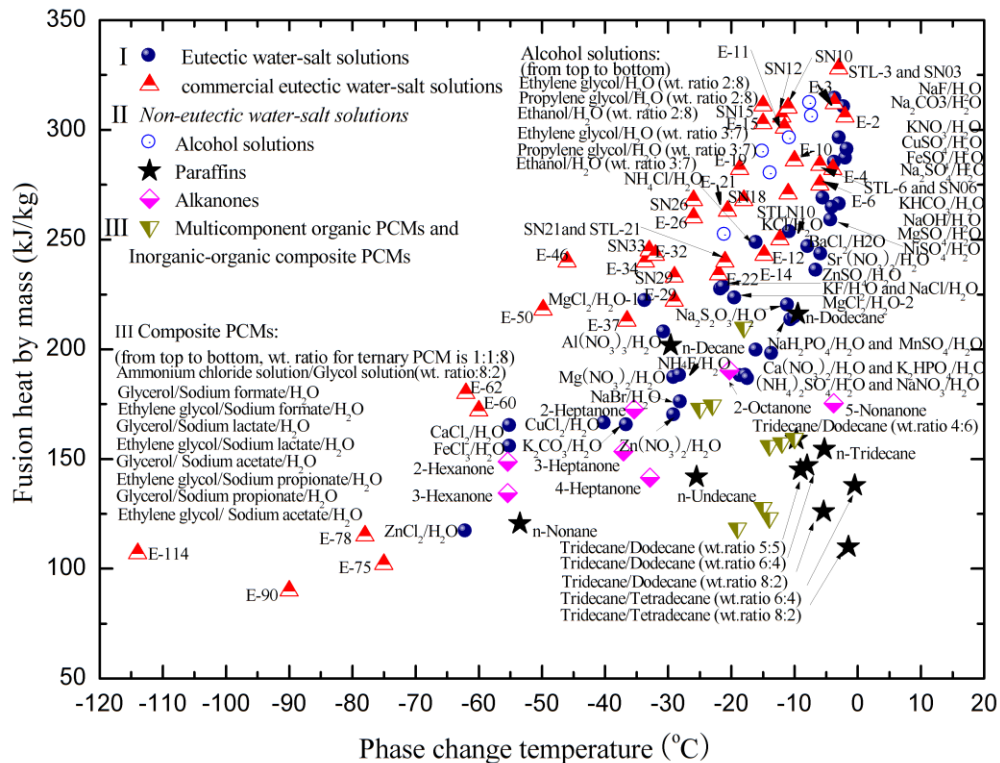
Figure 3.2: Thermal properties of PCMs for subzero application

3.1.1 Selection criteria for common PCMs

For solid-liquid PCMs for cold storage in subzero applications, a suitable phase change temperature and a larger fusion heat are two most obvious and important requirements. It has similar requirements to that for air conditioning application (more details please refer to Chapter 2.2.1), except for the phase change temperature for subzero application.
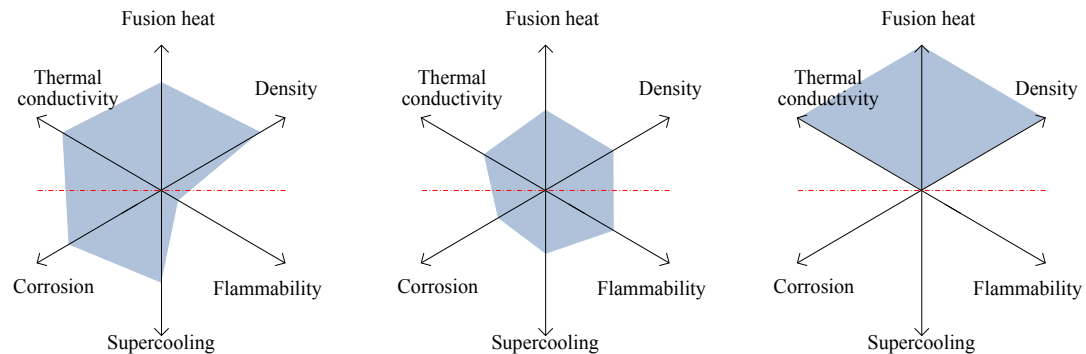
(1) Eutectic water-salt solutions (2) Non-eutectic water-salt PCMs (3) Ideal common PCMs
Note: This is a general comparison. Among non-eutectic water-salt PCMs, it should be noted that alcohol solutions have relatively higher fusion heat and density, and paraffins exhibit little or no supercooling, and show non-corrosive behavior

Figure 3.3: Thermal property comparison of common PCMs

In fact, there are no ideal common PCMs for subzero applications. However, a comparison of thermal properties of common PCMs is shown in Figure 3.3. Good thermal properties of thermal conductivity, fusion heat, and density are above the red dot line, and issues of corrosion, supercooling, and flammability, are listed below the dot line. The farther the colored shape extends along a given arrow, the better the performance along that dimension. From the comparison it can be found that usually eutectic water-

salt solutions have good advantages of better thermal conductivity, larger fusion heat and density, and low flammability, but they have serious issues of corrosion and supercooling.

While usually non-eutectic water-salt PCMs do not have these advantages of eutectic water-salt solutions, while they do have those serious issues. Among non-eutectic water-salt PCMs, it should be noted that alcohol solutions have relatively higher fusion heat and density, and paraffins exhibit little or no supercooling, and show non-corrosive behavior. Different kinds of materials will be discussed in detail in later introduction.

3.1.2   Eutectic water-salt solutions

A majority of the research on PCMs is focused on eutectic water-salt solutions for their high fusion heat and suitable phase change temperature range. Generally speaking, the freezing point of water will be depressed when salts are added to water, and this can be used to explain why gritting or salting roads and pathways melts snow on them. With more salt added, the freezing point will be depressed further, but the water solutions may not freeze from a pure liquid state to a solid state. To make clear about this, the phase diagram for eutectic water-salt solutions is shown in Figure 3.4. Starting from the left of the curve, the composition is 100% water with freezing point of 0°C. With more salt added the freezing point of the salt/water mixture decreases. Under this situation, only pure water freezes out of the solution and the salt remains in solution. With more salt added the freezing point depresses further until the eutectic point (point P) is reached at the lowest freezing point on the curve. At this point both the salt and the water freeze out of the solution, and the composition of the frozen material is exactly the same as that of

the solution. With more salt added the mixture freezing temperature starts to increase and anhydrous salt precipitates out on freezing. Under a particular salt concentration (point P), the solution freezes and melts completely from liquid/solid to solid/liquid at a constant temperature (point P), releases and stores large amounts of energy. This kind of PCM is called a eutectic water-salt solution.
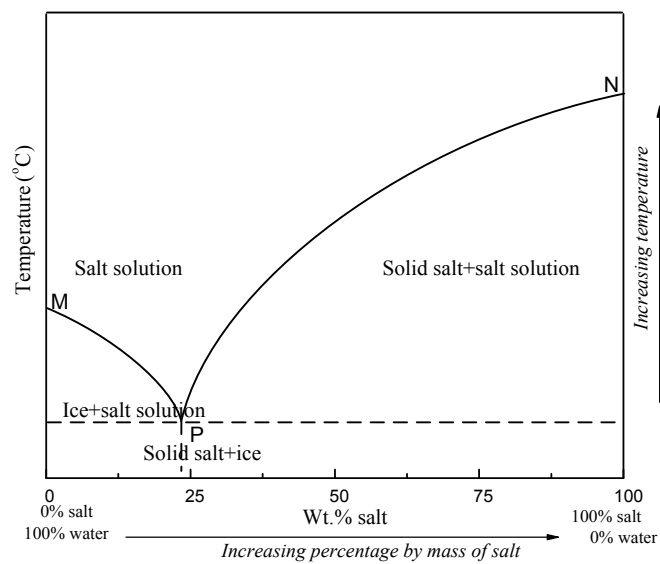
Figure 3.4: Phase diagram of eutectic water-salt solutions

3.1.2.1   Material selection

Zheng and Wu (2002) gave the thermal properties of eutectic water-salt solutions at different temperature level from −62°C to −1.6°C, as shown in Table 3.1. Commercial eutectic water-salt solutions are shown in Table 3.2 (Sub-zero eutectic PCM solutions, 2012; Zalba et al.,2003) and Table 3.3 (PLUSS, 2011). These PCMs have the advantages of higher fusion heat and density. But they also have issues of phase separation and

supercooling. Commercial solutions have relatively less issues as these, as efficient improvements have been made by manufacturers.

Table 3.1: Thermal properties of eutectic water-salt solutions (Zheng and Wu,2002)

PCM	wt.% of salt	Phase change temperature (°C)	Fusion heat (kJ/kg)
$ZnCl_2/H_2O$	0.51	−62	116.84
$FeCl_3/H_2O$	0.331	−55	155.52
$CaCl_2/H_2O$	0.298	−55	164.93
$CuCl_2/H_2O$	0.36	−40	166.17
K_2CO_3/H_2O	0.396	−36.5	165.36
$MgCl_2/H_2O$-1	0.171	−33.6	221.88
$Al(NO_3)_3/H_2O$	0.305	−30.6	207.63
$Mg(NO_3)_2//H_2O$	0.346	−29	186.93
$Zn(NO_3)_2/H_2O$	0.394	−29	169.88
NH_4F/H_2O	0.323	−28.1	187.83
$NaBr/H_2O$	0.403	−28	175.69
KF/H_2O	0.215	−21.6	227.13
$NaCl/H_2O$	0.224	−21.2	228.14
$MgCl_2/H_2O$-2	0.25	−19.4	223.10
$(NH_4)_2SO_4/H_2O$	0.397	−18.5	187.75
$NaNO_3/H_2O$	0.369	−17.7	187.79
NH_4NO_3/H_2O	0.412	−17.35	186.29
$Ca(NO_3)_2/H_2O$	0.35	−16	199.35
NH_4Cl/H_2O	0.195	−16	248.44
K_2HPO_4/H_2O	0.368	−13.5	197.79
$Na_2S_2O_3/H_2O$	0.3	−11	219.86
KCl/H_2O	0.195	−10.7	253.18
$MnSO_4/H_2O$	0.322	−10.5	213.07
NaH_2PO_4/H_2O	0.324	−9.9	214.25
$BaCl_2/H_2O$	0.225	−7.8	246.44
$ZnSO_4/H_2O$	0.272	−6.5	235.75
$Sr (NO_3)_2/H_2O$	0.245	−5.75	243.15
$KHCO_3/H_2O$	0.1695	−5.4	268.54
$NiSO_4/H_2O$	0.206	−4.15	258.61
Na_2SO_4/H_2O	0.127	−3.55	284.95
NaF/H_2O	0.039	−3.5	314.09
$NaOH/H_2O$	0.19	−2.8	265.98
$MgSO_4/H_2O$	0.19	−3.9	264.42
KNO_3/H_2O	0.097	−2.8	296.02
Na_2CO_3/H_2O	0.059	−2.1	310.23
$FeSO_4/H_2O$	0.1304	−1.8	286.81
$CuSO_4/H_2O$	0.119	−1.6	290.91

Table 3.2: Thermal properties of commercial eutectic water-salt solutions (Sub-zero eutectic PCM solutions, 2012; Zalba et al.,2003)

PCM type	Phase change temperature (°C)	Fusion heat (kJ/kg)	Specific heat (kJ/kg·K)	Density (kg/m^3)	Thermal conductivity (W/m·K)
E-114	−114.0	107	2.39	782	0.170
E-90	−90.0	90	2.56	786	0.140
E-78	−78.0	115	1.96	880	0.140
E-75	−75.0	102	2.43	902	0.170
E-62	−62.0	180	4.01	1300	0.580
E-60	−60.0	172	2.90	1280	0.440
E-50	−49.8	218	3.28	1325	0.560
E-46	−46.0	240	3.05	1205	0.540
E-37	−36.5	213	3.15	1500	0.540
E-34	−33.6	240	3.05	1205	0.540
SN33	−33	245	–	1240	–
E-32	−32.0	243	2.95	1290	0.560
E-29	−29.0	222	3.69	1420	0.640
SN29	−29	233	–	1150	–
E-26	−26.0	260	3.67	1250	0.580
SN26	−26	268	–	1210	–
E-22	−22.0	234	3.34	1180	0.570
SN21	−21	240	–	1120	–
STL-21	−21	240	–	1120	–
E- 21	−20.6	263	3.13	1240	0.510
E-19	−18.7	282	3.29	1125	0.580
SN18	−18	268	–	1210	–
E-15	−15.0	303	3.87	1060	0.530
SN15	−15	311	–	1020	–
E-14	−14.8	243	3.51	1220	0.530
E-12	−12.3	250	3.47	1110	0.560
SN12	−12	306	–	1060	–
E-11	−11.6	301	3.55	1090	0.570
STLN10	−11	271	–	1050	–
SN10	−11	310	–	1110	–
E-10	−10.0	286	3.33	1140	0.560
E-6	−6.0	275	3.83	1110	0.560
STL-6	−6	284	–	1070	–
SN06	−6	284	–	1070	–
E-4	−3.9	282	3.78	1060	0.580
E-3	−3.7	312	3.84	1060	0.600
STL-3	−3	328	–	1010	–
SN03	−3	328	–	1010	–
E-2	−2.0	306	3.80	1070	0.580

Table 3.3: Thermal properties of commercial eutectic water-salt solutions (PLUSS, 2011)

PCM type	Contents	Phase change temperature (°C)	Latent heat (kJ/kg)	Liq. density (kg/m^3)	Appearance
HS 37N	Inorganic salts	−37 to −39	60(minimum)	–	Light white/grey/blue
HS 26N	Inorganic salts	−25 to −26	205	1200	Light blue to dark
HS 23N	Inorganic salts	−22 to −24	200	1180	Light white/grey
HS 7N	Inorganic salts	−7 to −5	230	1120	Light white/grey

3.1.2.2   Phase separation and supercooling minimization

Phase separation, or incongruent melting, can cause a loss in enthalpy of solidification as reported by Cantor (1978), which can lead to poor storage density. This issue can be addressed by adding water, with gelling or thickening. Gelling, means adding a cross linked material (e.g. polymer) to the salt in order to create a three dimensional network that holds the salt solution together. Thickening means that by adding a material to the salt solution the viscosity can be increased and therefore the salt solution can be hold together. For cross-linked materials for gelling, as discussed in Chapter 2, effect of two different polymeric hydrogels, such as a super absorbent polymer (SAP) made from acrylic acid copolymer and carboxymethyl cellulose (CMC), were studied by Ryu et al. (1992). Thixotropic (attapulgite clay) and alginate have been tested as well (Telkes, 1976). For thickening agents, they can be starch and various types of cellulose derivatives (Ryu et al., 1992; Telkcs, 1974). These solutions listed above for the issue of phase separation invites the meaningful perspectives for further study of eutectic water-salt solutions for subzero application.

In order to introduce another issue of supercooling, the cooling process of eutectic water-salt solution is shown in Figure 3.5. The process can be divided into four stages. $A{\rightarrow}B$ is the sensible thermal storage process. Though temperature of the solution decreased below eutectic point (Point C), it still remains in the state of liquid. $B{\rightarrow}C$ is the nucleation process. B is the point for occurrence of nucleation. Temperature difference between point B and C is regarded as supercooling degree (temperature), which should be reduced

71

to improve storage efficiency. Then crystal nucleus diffuses to the surroundings, and at *C* initial solid layer is formed. *C*→*D* is the latent thermal storage process, where solid layer grows fast. *D*→*E* is the sensible thermal storage process, where solution remains solid.
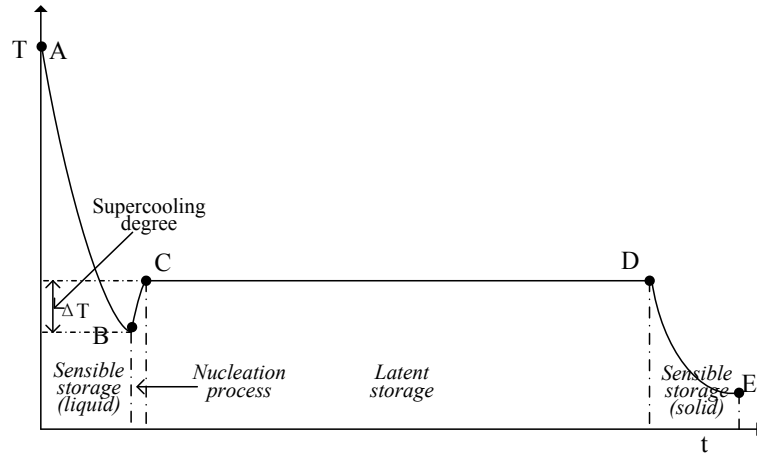
Figure 3.5: Cooling process of a eutectic water-salt solution

Similar to the solutions in Chapter 2, the use of adding nucleating agents, cold fingering method and exerting physical fields (ultrasonic field, electromagnetic field and magnetic field) can been utilized effectively to deal with the issue of supercooling. Many factors were studied to determine whether a particular additive will promote nucleation or not, such as crystal structure, solubility and hydrate stability. Good nucleating agents can be carbon nanofibers, copper, titanium oxide as well as potassium sulfate and borax. Vonnegut (1947) suggested silver iodide serves as a very effective nucleus for the formation of ice crystals because it very closely resembles ice in crystal structure. Other promising nucleating agents to limit supercooling could be $Na_2P_2O_7 \cdot 10H_2O$, $BaCO_3$, $BaCl_2$, BaI_2, $Ba(OH)_2$, CaC_2O_4, K_2SO_4, $MgSO_4$, $SrCl_2$, $SrCO_3$, $SrSO_4$, $Sr(OH)_2$ and TiO_2. Surface roughness is another important factor. With larger surface roughness, it is better

for heterogeneous nucleation. In addition, Fang (2011) studied the effect of magnetic field on water and inorganic salt solutions (5% NaCl solution, 7% KCl solution and 5% NH_4Cl solution). Results showed that it could reduce the supercooling degree and shorten supercooling time of inorganic salt solutions. And the effect is more evident with higher magnetic field intensity. For the crystallization process, it can advance crystal growth and increase crystal amount and diameter of crystal particles. While only for water in the crystallization process, the magnetic field increases the diameter of crystal particles, making the ice crystal softer and easier to melt.

3.1.2.3   Cyclic stability

Cyclic stability is another important issue. The main reason for poor cyclic stability is the poor stability of the materials properties and/or corrosion between the PCM and the container. PCMs only show great potential for wide application when they have repetitive cycles of heating and cooling process. It should be noted that with more cycles of use, its performance will be reduced. This is because during melting process, some kinds of salt hydrates can be formed, this would lead to the irreversible process. To address this issue, some studies try to apply the PCM-water solution in a direct contact system. They can exchange heat with another fluid which is not indissoluble with water solution to prevent phase seperation. In addition, for the issue of corrosion between PCMs and the container, Porisini (1988) studied the corrosion characteristics of salt hydrates on stainless steel, carbon steel, aluminum alloys and copper. Following thermal cycling tests, Porisini concluded that stainless steel was the most corrosion resistant among these metals for use

with salt hydrates, though copper had a corrosion zone that did not increase even after long periods of time. This study can also be used as a guideline for eutectic water-salt solutions for subzero applications.

3.1.2.4 Performance improvement and energy saving potential

Since the majority of cold storage materials for subzero applications is eutectic water-salt solutions, therefore it is necessary to provide reasonable analysis and summary for their performance improvement and energy integration potential, especially for application of frozen food storage.

Temperature fluctuations during the storage in freezers could cause dramatic effect on the quality of the frozen food. Phimolsiripol et al. (2008) studied the effects of freezing and temperature fluctuations during frozen storage on frozen dough and bread quality. The rates of quality and weight loss increased significantly with larger temperature fluctuations and/or higher storage temperatures. In addition, high fluctuations due to door opening, defrost system and electrical power failure can also lead to the poor quality of frozen food for the temperatures inside the freezer change significantly. In another study by Gormley et al. (2002), some quality parameters of selected food products with the effect of fluctuating (fluctuations cycles of −30ºC to −10ºC to −30ºC) versus constant frozen storage temperatures regimes (−60ºC and −30ºC) were studied. Temperature fluctuations cycles could cause stress damage and other deleterious effects such as fat oxidation and changes in color and texture.

Regarding these issues, Onyejekwe (1989) incorporated a PCM into a domestic freezer. The study showed the optimal performance of the container inside the freezer, and made the possibility of using an easily available and very cheap PCM (NaCl + H_2O) for cold storage. Azzouz et al. (2008) used a dynamic model and applied a PCM (a eutectic water-salt solution with phase change temperature chosen in the range from −9°C to 0°C) on the back side of a refrigerator evaporator to achieve in a higher evaporating temperature, and claimed 5%~15% increase in the coefficient of performance (COP) and a significant decrease in the number of starts and stops of the compressor with smaller air temperature fluctuations in the freezer. Later, Azzouz et al. (2009) conducted an experimental investigation and claimed that the addition of the PCM (a eutectic water-salt solution with a phase change temperature of −3°C) on the back evaporator in a household refrigerator (as shown in Figure 3.6) improved its performance in comparison with conventional system and allowed several hours of refrigeration without electrical power supply.
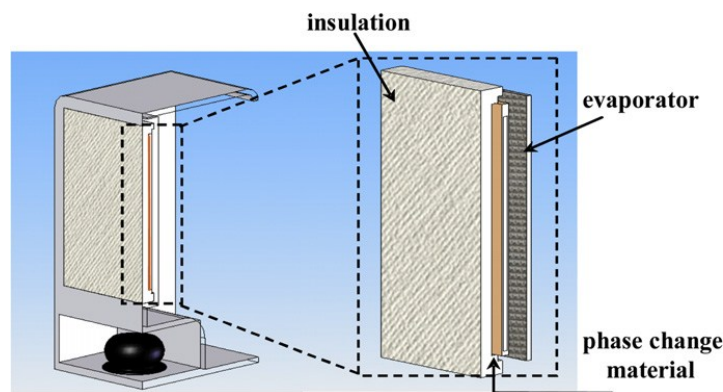
Figure 3.6: Schematic diagram of the refrigerator with PCM (Azzouz et al. (2009)

One study by Gin et al. (2010) investigated the incorporation of PCM (a eutectic water-salt solution: mixture of water and 19.5wt.% NH_4Cl salt with a melting and freezing point of $-15.4°C$) panels placed against the internal walls of a domestic freezer to maintain stable temperature in the presence of heat loads. Energy consumption tests showed that heat loads resulting from door openings and defrost cycles had increased the energy consumption of the freezer by 11~17% and 15~21%, respectively. The inclusion of the PCM into the freezer had decreased the energy consumption during a defrost cycle by 8%, and by 7% during door openings in this system. Further study by Gin and Farid (2010) showed that the introduction of the PCM improved the quality of the frozen foods during the storage. Drip loss in meat was found to be lower and ice crystal sizes in the ice cream were found to be smaller in the freezer with PCM compared to without PCM. PCM panels were placed against the walls of the freezer as shown in Figure 3.7.
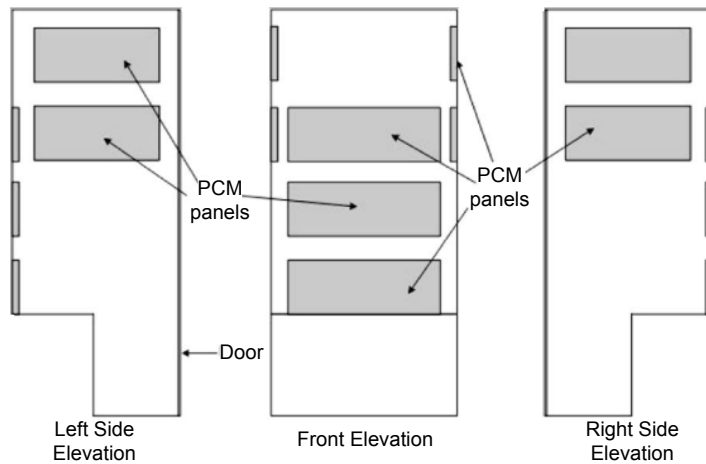
Figure 3.7: Schematic of the internal airspace of the freezer showing the placement of the PCM panels against their inner walls (Gin and Farid, 2010)

Oró et al. (2012) studied the thermal performance of commercial freezers using PCMs under door openings and electrical power failure. A commercial PCM of Climsel-18 was

selected (Sodium nitrate dissolved in water with some additives, with melting temperature of −18°C). The PCM is contained in 10 mm thick stainless steel panels placed at different locations in the freezer. During 3 hours of electrical power failure, it showed that the use of PCM maintained the freezer temperature 4~6°C lower and that of the frozen products could remain at acceptable levels for a longer time. For the condition of frequent door openings, the PCM could benefit the thermal performance especially when the temperature of the cabinet is near the melting temperature of the PCM.

A novel dual evaporator based on a domestic refrigerator with PCM was designed by Subramaniam et al. (2010) to provided thermal storage in order to improve food quality and prolong compressor off time. New PCM based refrigeration cycle is shown in Figure 3.8. It has two benefits: a) fresh food cooling by using high temperature refrigeration cycle during on time, and an off time period extension prolonging by using PCM; b) storing excess energy at high refrigeration temperature to be used subsequently as sub-cold energy for the relatively less efficient low temperature refrigeration cycle. The theoretical estimation of the energy saving and COP improvement with the existing and new cycle is shown in Figure 3.9. The existing cycle COP of 1.5624 changes to 2.007 and 1.808 for charging and discharging processes with the new PCM based system. This study showed that there could be potential of 8% savings in energy as compared to the existing refrigerator model.
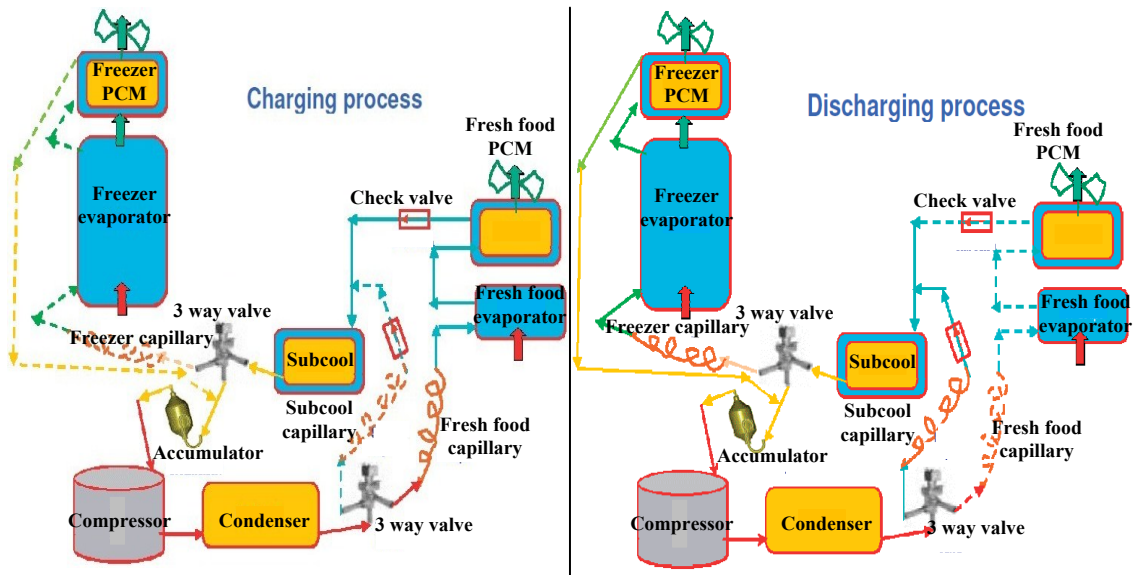
Figure 3.8: Schematic of new PCM based refrigeration cycle (Subramaniam, et al., 2010)
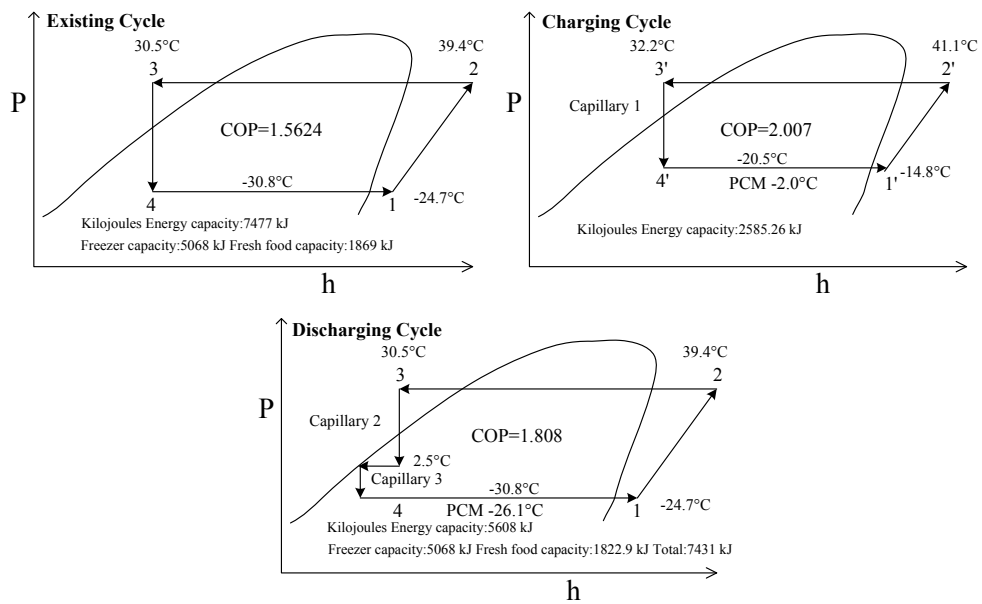
Figure 3.9: Energy saving & COP improvement of new PCM based refrigeration cycle (Subramaniam, et al., 2010)

3.1.3　Non eutectic water-salt solution PCMs

3.1.3.1　Material selection

(1) Alcohol solutions

Alcohol is a class of organic compounds. The main functional group of alcohols (alkanols) is the hydroxyl or -OH group. Alcohols differ in the number of carbon atoms in the molecules and with the placement of the -OH group in the molecule. The most common alcohol is ethanol which is commonly produced by fermentation. The structural formula of ethanol is shown in Figure 3.10(a).
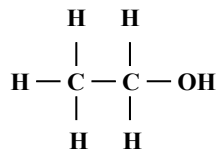
(a). Ethanol
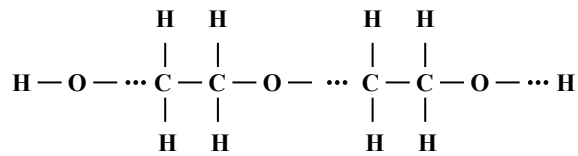
(b). Polyethylene glycols.
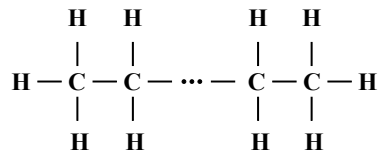
(c). Linear paraffins.
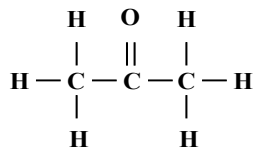
(d). Alkanone containing three carbon atoms.

Figure 3.10: Chemical structure of different materials

For cold storage in subzero applications, the alcohol solutions, which is mainly the mixture of alcohols and water, serve as heat transfer fluid (ice slurries) for supermarkets and industry refrigeration. Usually alcohol solutions have larger fusion heat and density, high heat transport abilities, as well as low pressure drop to facilitate small pumping power. Hägg (2005) studied the relationship between the freezing point and the concentration of different freezing point depressants (alcohols), as shown in Figure 3.11. Based on different cold storage requirements, different freezing points are needed. In addition, this can be achieved by choosing different concentration of depressants in Figure 3.11. Figure 3.12 shows the relationship between freezing point curve and the latent heat of different alcohol solutions (Kumano et al., 2007). Latent heat decreases in combination with a lowered freezing point, and ethylene glycol solution has a larger latent heat than other solutions with same freezing point.
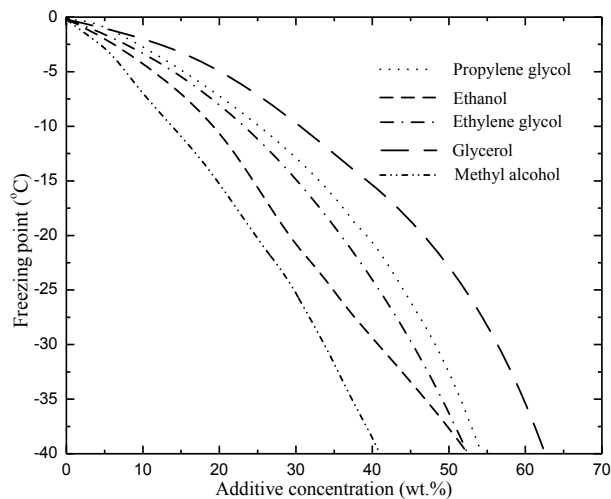
Figure 3.11: Freezing point curves of common freezing depressants (Hägg, 2005)
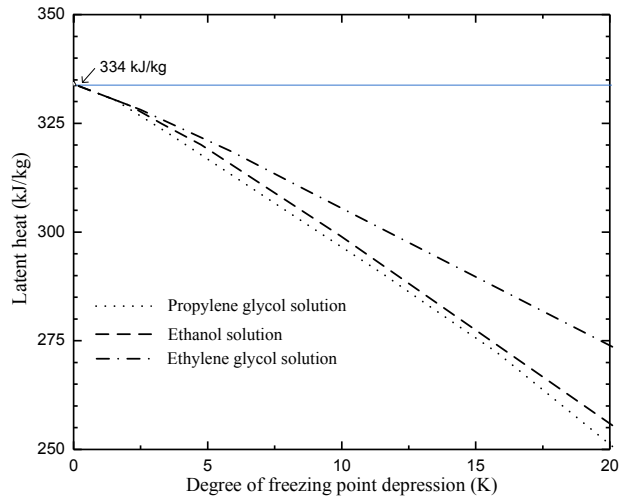
Figure 3.12: Latent heat of ice fusion in different alcohol solutions (Hägg, 2005)

In addition to the introduction of alcohol solutions, there are other close materials. One is polyethylen glycol (Mehling and Cabeza, 2008), or short peg, which is a polymer with the general formula $C_{2n}H_{4n+2}O_{n+1}$. It is produced from ethylenglycol. The base units of a linear PEG chain are monomers of $-CH_2-CH_2-O-$, as shown in Figure 3.10(b). The monomers have a molecular weight of 44 g/mole. Polyethylene glycols are available in a molecular weight range from about 200 to 35,000; this corresponds to 5 monomers to about 800 monomers.

For practical application, apart from the mentioned factors of alcohol solutions, it is also necessary to pay attention for environmental pollution and toxicity, flammability, material compatibility, corrosion and handling security. Usually alcohols have the issue of flammability and toxicity. When choosing a fluid, it is important to find out which

parameter is crucial for the particular application and which one is the best fluid for the current case.

(2) Paraffins

Typical paraffins, which are usually saturated hydrocarbon mixtures, normally consist of a mixture of mostly straight chain n-alkanes, CH_3–$(CH_2)_n$–CH_3. A large amount of latent heat can be released because of the crystallization of the $(CH_2)_n$ chain. Various types can be acquired from petroleum refining. The most commonly used organic PCM are made of paraffins. Paraffin is a technical name for an alcane, but often it is specifically used for linear alkanes with the general formula C_nH_{2n+2}, as shown in Figure 3.10(c).

Examples of some single paraffin waxes that have been investigated as PCMs, are shown in Table 3.4 (Domalski and Hearing, 2011). In addition, Rubitherm product RT-4 has a melting temperature of –4°C and a fusion heat of 179 kJ/kg (RUBITHERM, 2011). In comparison with inorganic PCMs, usually paraffin waxes are advantageous for they are mostly chemically inert, stable and recyclable, they exhibit little or no supercooling (i.e. they can be self-nucleating), and they show no phase separation and non-corrosive behavior. In comparison with inorganic PCMs, paraffin waxes are superior in general as they are chemically inert, stable and recyclable. They exhibit little or no supercooling (i.e. they can be self-nucleating), and they show no phase separation and non-corrosive behavior. However, they have relatively low thermal conductivity and volumetric storage (less than 10^3 kg/m^3), and they are flammable, which are opposite for organic PCMs.

Table 3.4: Thermal properties of paraffins (Domalski and Hearing, 2011)

PCM	Formula	Melting temperature (°C)	Enthalpy of fusion (kJ/kg)	Liquid density (kg./m^3)
n-Nonane	C_9H_{20}	−53.5	120.6	720
n-Decane	$C_{10}H_{22}$	−29.6	201.8	730
n-Undecane	$C_{11}H_{24}$	−25.5	141.9	740
n-Dodecane	$C_{12}H_{26}$	−9.5	216.2	748
n-Tridecane	$C_{13}H_{28}$	−5.3	154.5	756

Yilmaz et al. (2009) developed new binary mixtures of paraffins to be used as phase change materials (PCMs) for thermal energy storage in cooling applications. Experimental results are shown in Table 3.5. This melting/freezing range can be suitable for a variety of subzero applications. Further experimental study also showed that none of the mixtures as expected from organics showed any supercooling.

Table 3.5: Thermal properties of paraffin mixture (Yilmaz et al., 2009)

PCM	On-set temperature for freezing by DSC (°C)	Heat of fusion (kJ/kg)
40:60 Tridecane:Dodecane (wt.%)	−9.7	159
50:50 Tridecane:Dodecane (wt.%)	−9.1	145
60:40 Tridecane:Dodecane (wt.%)	−8.0	147
80:20 Tridecane:Dodecane (wt.%)	−5.4	126
80:20 Tridecane:Tetradecane (wt.%)	−1.5	110
60:40 Tridecane:Tetradecane (wt.%)	−0.5	138

(3) Alkanones

Alkanones can be produced by the oxidation of a secondary alkanol. Alkanones are usually similar in structure to alkanes. However, on one of the carbons, two of the hydrogens have been replaced by an oxygen. For example, the alkanone containing three carbon atoms is shown in Figure 3.10 (d). Here thermal properties of alkanones containing carbon atoms from 6 to 10 is shown in Table 3.6 (Chickos et al., 2011). Usually this kind of

materials has the issues of flammability and toxicity, and these issues have impeded their cold storage applications.

Table 3.6: Thermal properties of alkanones (Chickos et al., 2011)

PCM	Formula	Melting temperature(°C)	Enthalpy of fusion (kJ/kg)	Liquid density (kg/m^3)
2-Hexanone	$C_6H_{12}O$	−55.4	148.7	812
3-Hexanone	$C_6H_{12}O$	−55.4	134.5	815
3-Heptanone	$C_7H_{14}O$	−37.1	153.5	818
2-Heptanone	$C_7H_{14}O$	−35.4	172.6	820
4-Heptanone	$C_7H_{14}O$	−32.9	141.5	820
2-Octanone	$C_8H_{16}O$	−20.3	190.4	819
5-Nonanone	$C_9H_{18}O$	−3.8	175.3	826

3.1.3.2   Thermal property improvement

Among non-eutectic water-salt solution PCMs for subzero applications, alcohol solutions have the advantages of high fusion heat, no phase separation and relatively low cost, but they have issues of supercooling and corrosion. To deal with such issues, solutions should be adapted similar to eutectic water-salt solutions. Also enough attention should be paid to flammability of alcohol solutions. At present little information about alkanones is available for subzero thermal storage applications. Usually this kind of materials has the limits of flammability and toxicity.

For paraffins, they are mostly chemically inert, stable and recyclable, exhibit little or no supercooling (i.e. they can be self-nucleating), and show no phase separation and non-corrosive behavior. However, they have the issue of low thermal conductivity, which may lead poor heat transfer characteristics for subzero applications. Here several solutions are listed as follows. One possible solution is to add materials with larger

thermal conductivity. Mixture of water and a paraffin as PCM by adding aluminum foams of different porosity was studied by Hackeschmidt et al. (2007).

Results showed that with a relative density of 6%, which means with 94% porosity, a thermal conductivity of about 6 W/m·K can be achieved. Other solutions can be to embed the PCM in the metal matrix structure or the graphite matrix (Mills et al., 2006; Mehling et al., 1999; Fukai et al., 2000; Py et al., 2001). In addition, heat transfer for thermal storage can also be improved by the use of finned tubes (Padmanabhan and Murthy, 1986; Morcos, 1990; Sadasuke and Naokatsu, 1991; Costa et al., 1998). All the previous studies or resolutions regarding thermal conductivity improvement and heat transfer enhancement show perspective of applying PCM technologies to subzero cold storage application.

For paraffins, another serious issue is their high flammability. Usually the shape-stabilized PCM composites consist of the paraffins, which act as a dispersed phase change material, and a polymer material (such as high density polyethylene (HDPE)), which acts as a supporting material. As long as the operating temperature is below the melting point of the supporting material, the shape-stabilized PCM can keep its shape even when the paraffin changes from solid to liquid. Usually improving flame retardant of polymer materials (with the addition of some flame retardant to polymer materials) can relieve this issue. A short summary for flame retardant improvement was done Chapter 2, and possible ways can be done by adding metal, nano structured magnesium hydroxide or

expanded graphite. These studies can be used as guideline for paraffins for subzero application.

3.1.4   Multi-component organic PCMs and inorganic-organic composite PCMs

(1) Multicomponent organic PCMs

Guo (2008) also studies several multi-component organic PCMs from ethylene glycol, sodium formate, sodium formate, sodium acetate, sodium lactate, ethacetic acid, glycerol, sodium propionate, ethylene glycol and H_2O. Results are shown in Table 3.7. Renewable Alternatives products (Thermester–(14)B and Thermester–(12)M) (Renewable alternatives products, 2011.) are also listed in Table 3.7. These PCMs are made from a "green" technology, in that underutilized bio-based products-namely beef tallow, palm oil, coconut oil and soybean oil - are converted into PCMs. They are non-toxic and they are capable of thousands of melting and freezing cycles without performance degradation. There is no concern for oxidation or concern that these fat and oil products will become rancid because they are fully hydrogenated. Fully hydrogenated fats can be stable for decades because they do not have chemical sites for oxidation to occur.

Chlorobenzene and bromobenzene (Michaud et al., 1996), which are liquid substances at room temperature, crystallize with very similar structures, without any known polymorphism at ordinary pressures. They are isomorphous, showing complete solid state solubility, with little deviation from ideality. The mixture could be regarded as suitable as

86

phase change materials for cold storage application if one needs precise temperature control at a temperature between −31°C and −45°C.

Table 3.7: Thermal properties of multi-component organic PCMs

PCM	Component ratio by mass	Phase change temperature (°C)	Fusion heat (kJ/kg)
Sodium lactate/H_2O	85.15:14.85	−49	28.3
Sodium acetate/H_2O	23.96:76.04	−43	29.7
Sodium formate/H_2O	1:4	−18	250.2
Ethylene glycol/Sodium formate/H_2O	1:1:8	−25	173.1
Glycerol/Sodium formate/H_2O	1:1:8	−23	174.5
Ethylene glycol/ Sodium acetate/H_2O	1:1:8	−19	118.5
Ethylene glycol/Sodium propionate/H_2O	1:1:8	−15	127.8
Glycerol/ Sodium acetate/H_2O	1:1:8	−14	156.0
Glycerol/Sodium propionate/H_2O	1:1:8	−14	123.2
ethylene glycol/Sodium lactate/H_2O	1:1:8	−12	157.4
Glycerol/Sodium lactate	1:1:8	−10	159.3
Thermester-(14)B	Organic mixture	−14	150
Thermester-(12)M	Organic mixture	−12	170

 (2) Inorganic-organic composite PCMs

Usually inorganic PCMs (such as inorganic salt solutions) have high fusion heat, but they have the serious issues of corrosion and phase separation. Adding organic PCMs (such as alcohol solutions) can alleviate those issues. Shen (2008) studied a kind of hybrid solution of ammonium chloride solution (25 wt.%~30 wt.% NH_4Cl) and glycol solution (25 wt.% glycol) with their certain solution mass ratio of 3:2 ammonium chloride solution and glycol solution). The hybrid solution has the phase-change temperature from −16°C to −21°C and latent heat from 207 kJ/kg to 212 kJ/kg, which can be regarded as a good candidate of PCMs for cold storage in freezers.

3.1.5   Microencapsulated PCMs and PCMs with nanoparticle additives

In this section, microencapsulated PCMs, which have larger surface area to volume, and PCMs with nanoparticle additives, which have higher thermal conductivities, will be discussed in this section.

3.1.5.1   Microencapsulated phase change materials (MPCMs) and MPCM slurries

Microencapsulation is the encapsulation of PCM particles (the core) of 1 μm to 1000 μm diameter with a continuous film of polymeric material (the shell). Generally speaking, two processes are sued in microencapsulation: physical process, which can be spray drying, centrifugal and fluidized bed processes, or coating processes (e.g. in rolling cylinders), and chemical process, which are in-situ encapsulations like complex coacervation with gelatine, interfacial polycondensation to get a polyamide or polyurethane shell, precipitation due to polycondensation of amino resins, and others. The in-situ processes have the ability to yield microcapsules with the best quality in terms of diffusion-tightness of the wall. MPCMs have several benefits, such as reduction of the reactivity of the PCMs with the outside environment, improvement of heat transfer to the surrounding because of the large surface to volume ratio of the capsules, improvement in cycling stability since phase separation is restricted to microscopic distances, and no leakage during its liquid phase for some PCMs.

Several MPCM products from a company named Microtek are listed as follows in Table 3.8 (Standard microPCM products, 2011). The mean particle size is 17~20 microns. The

appearance of two products is white to slightly off-white color with good thermal cycling. The form for MPCM (10) is wet cake (70% Solids, 30% Water), and for MPCM (-10)D it is dry powder.

Table 3.8: Thermal properties of microencapsulated phase change materials (MPCMs) (Standard microPCM products, 2011)

Product Number	Core material	Melting temp. (°C)	Fusion heat (kJ/kg)	Specific gravity	Capsule composition	Final form
MPCM (-30)	*n*-Decane	−30	140~150	0.9	85~90% wt.% PCM 10~15 wt.% polymer shell	Wet filter cake
MPCM (-30)D	*n*-Decane	−30	140~150	0.9	85~90% wt.% PCM 10~15 wt.% polymer shell	Dry powder
MPCM (-10)	*n*-Dodecane	−9.5	150~160	0.9	85~90% wt.% PCM 10~15 wt.% polymer shell	Wet filter cake
MPCM (-10)D	*n*-Dodecane	−9.5	150~160	0.9	85~90% wt.% PCM 10~15 wt.% polymer shell	Dry powder

When the MPCM is dispersed into the carrier fluid, e.g. water, a suspension of MPCM slurry is formed. In the fabrication process, the proper amount of surfactants is used for helping MPCM fully disperse into the carrier fluid, thus increasing the lifetime of the MPCM slurry. Because the phase change with latent heat is involved, the effective specific heat of the fluid is remarkably increased with results in the heat transfer enhancement. Obviously, MPCM slurries can be used as both thermal energy storage and heat transfer fluid.

Regarding the MPCMs/MPCM slurries, some additional attention should be paid to the supercooling for it may drastically deteriorate the system performance as cold storage materials. Chapter 2 provided a summary for supercooling minimization for air conditioning application, such as adding nucleation agents for suppressing supercooling

effect, and this can also be a good reference for subzero application. In addition, enough attention should be paid to the cycle stability for a MPCM slurry may be limited by its performance attenuation after long-term running. Based on the literature review, still limited study exists for thermal performance of MPCMs for subzero application.

3.1.5.2   PCMs with nanoparticle additives

PCMs with nanoparticle additives can exhibit properties, such as thermal conductivity enhancement for the thermal transport and storage. It has been recognized that significant enhancement in thermal conductivity can be shown with suspensions of nanoparticles in fluids. Therefore, PCMs with nanoparticle additives can exhibit thermal conductivity enhancement. The enhanced thermal conductivity contributes to improve the efficiency of heat transfer fluids. This can also enable a possible reduction in the sizes of heat exchangers and pumps in industrial thermal storage application.

New nanofluid systems by utilizing semiconductor nanorods, hybrid nanoparticles, phase-change liquid nanodroplets and phase-change metallic nanoparticles as the dispersed phases were developed systematically by Han (2008). A nanoemulsification technique had been developed and used to synthesize nanofluids. Results showed that thermal conductivity was increased greatly in these nanofluid systems, e.g., 52% enhancement in thermal conductivity was found in water-in-FC72 nanofluids. Though this work is studied for nanofluids, it can provide good information for subzero application for PCMs. He (2005) studied the relationship between thermal conductivity and volume fraction of nanoTiO$_2$ particles in nanofluid PCMs (nanoTiO$_2$ particles with

20nm in BaCl$_2$/H$_2$O solution), as shown in Figure 3.13. Obviously, thermal conductivity increased with increasing nanoTiO$_2$ particles.
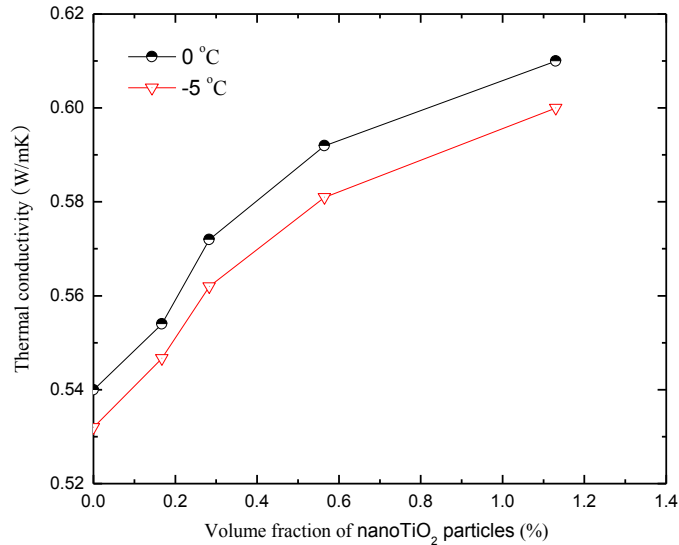
Figure 3.13: Relationship between thermal conductivity and volume fraction of nanoTiO$_2$ particles in nanofluid PCMs (He, 2005)

He (2005) also studied the kinetic characteristics and thermal properties of nanofluid PCMs, as shown in Table 3.9. It can be found that nanofluids could reduce supercooling degree with increased addition of volume fraction of nanoTiO$_2$ particles. Thermal properties tested by differential scanning calorimetry (DSC) showed that the changes of melting temperature were small, while it should be noted that the latent was reduced with increased addition of volume fraction of nanoTiO$_2$ particles. Therefore, the fraction of nano particles for PCMs should not be excessive. In addition, during the fifty cold charge/discharge experiments, its latent heat and phase change temperature remained constant, which shows that the material's stability is good. Experimental study showed

that the time for freezing of nanofluids is much less than eutectic salt solutions, the charge/discharge capacity, charge/discharge rate and heat transfer coefficient of nanofluids are higher than eutectic salt solution.

Table 3.9: Kinetic characteristics and thermal properties of nanofluid PCMs (He, 2005)

PCM	Experimental kinetic characteristics		Thermal properties by DSC	
	Phase change temperature (^{o}C)	Supercooling degree (^{o}C)	Melting temp. (^{o}C)	Latent heat (kJ/kg)
$BaCl_2/H_2O$ ($BaCl_2$ 22.5wt%)	−8.16	3.78	-8.4	281.1
$TiO_2/BaCl_2/H_2O$ (TiO_2 0.167vol.%)	−8.61	2.93	-8.5	279.5
$TiO_2/BaCl_2/H_2O$ (TiO_2 0.283vol.%)	−8.61	2.51	-8.6	258.3
$TiO_2/BaCl_2/H_2O$ (TiO_2 0.565vol.%)	−8.61	1.88	-8.2	257.4
$TiO_2/BaCl_2/H_2O$ (TiO_2 1.13vol.%)	−8.72	0.57	-8.5	254.2

3.2   Sorption cold storage

Different from PCM solid-liquid thermal storage, sorption storage uses the sorption working pairs (sorbents/refrigerants) for cold storage in subzero application. The sorbents can make physical or chemical attraction with an active refrigerant gas for refrigeration effect. Usually there are two common sorption storages: absorption technology (sorbents in liquid phase) and adsorption technology (sorbents in solid phase). The cooling capacity can be kept for a long term with no pollution and no cooling energy losses. Also it can be discharged for immediate use with connecting the generator (for absorption storage) or adsorbent bed (for adsorption storage) to the evaporator. This kind of cold storage system contributes significantly to the concept of sustainable system development with driving source of electricity, industry waste heat, or solar energy. In addition, an adsorption system after energy charging can be moved to another place easily where refrigeration power is not enough for short term subzero application. Usually in a sorption system,

alternative clean refrigerants, with no pollution other than the CFC or HCFC refrigerants (in a conventional vapor compression system), are adopted. Also, it can be operated without major moving parts (such as pumps, fan motors, etc.) so that it is mechanically simple, and has high reliability, low vibration and a long lifetime. A general comparison of absorption and adsorption storage technologies is quite similar to Figure 2.20 in Chapter 2. Absorption storage usually has larger storage capacity and larger thermal conductivity of sorbents, while adsorption storage usually proves its features of better reliable operation and quietness.

3.2.1   Basic storage principle

3.2.1.1   Absorption cold storage

For absorption storage, a schematic drawing of the basic principle is shown in Figure 2.21 (a) in Chapter 2. When the shut-off valve after the poor solution is opened, the poor solution (low concentration of absorbent) is pumped towards the high-pressure zone, and then the mixture is heated in the generator during the charging process. The driving heat makes the separation of the refrigerant (take NH_3 for example) from the absorbent (NH_3 solution). The refrigerant vapor is sent to the condenser, where it is condensed to liquid by a cooling fluid. The liquid refrigerant is stored in a container and can be used to produce the cooling effect for subzero application (ice making). The rich solution from the generator is also stored in a container. During the discharging process, with the shut-off valve after the poor solution closed, the liquid refrigerant is expanded with the shut-off valve on the liquid refrigerant side opened and sent to the evaporator, and rich

93

solution flows to the absorber with the shut-off valve on the rich solution side opened. Thus, water vapor from the evaporator is absorbed by the rich solution, and the cooling effect is produced in the evaporator at low pressures. Meanwhile, the rich solution absorbs the water vapor and absorption heat can be released, which can be used for heating purposes. Gradually, the poor solution from the absorber is stored in a container. The principle of absorption storage is very similar to that of the intermittent absorption refrigerator, in which working pairs can be heated or cooled by turns. Here only a brief introduction of absorption storage is made as it has been commercially well developed.

3.2.1.2 Adsorption cold storage

For adsorption storage, a schematic diagram of its basic principle is shown in Figure 2.21 (b). The phenomenon of adsorption is resulting from the interaction between a solid (adsorbent) and a gas (refrigerant), which can be a reversible physical or chemical reaction process. During the charging process, with the shut-off valve after the desorber (can also be an adsorber during the discharging process) opened, the desorber connected to a condenser is heated by a heat-driving source. Next, the refrigerant vapor flows from the desorber to the condenser and is cooled to a liquid state. It then passes through the expansion valve and is stored in an evaporator under low-pressure condition for cold storage. During the discharging process, with the shut-off valve after the adsorber closed, the adsorber is cooled by a heat transfer fluid and its pressure drops. When the pressure drops below that of the evaporator, the shut-off valve after the evaporator is opened and

the pressure difference makes the refrigerant be evaporated and move to the adsorber. Then the cooling can be produced in the evaporator for subzero application.

3.2.2 Working pair selection

For sorption storage, thermal property of working pairs is very important for storage efficiency because heat and mass flows are produced with working pairs during charge or discharge process. In this section, high storage capacity, which is the ratio of amount of storage by evaporation of refrigerant to the mass or volume of the sorbent, is one of the basic criteria required for designing an efficient storage process. To have a better understanding for properties of different working pairs, Mugnier and Goetz (2001) summarized and compared their storage capacity. Here based on the data with a rigorous calculation protocol from literature (Mugnier and Goetz, 2001), thermal properties of working pairs for subzero application (such as ice making) were extracted and summarized in Figure 3.14 under the same conditions that ambient temperature is 35°C and evaporation temperature is −20°C. Storage capacity and minimum heating temperature of different sorption working pairs under same conditions is shown in Figure 3.15.
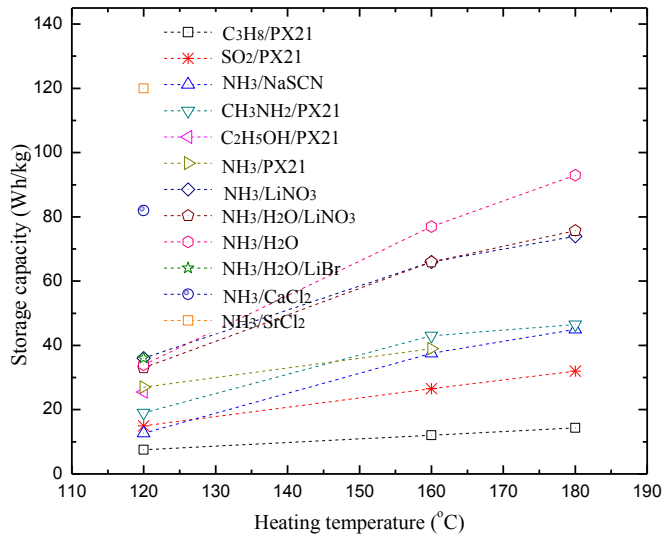
Figure 3.14: Storage capacity of different sorption working pairs with ambient
temperature of 35°C and evaporation temperature of –20°C (Mugnier and Goetz, 2001)
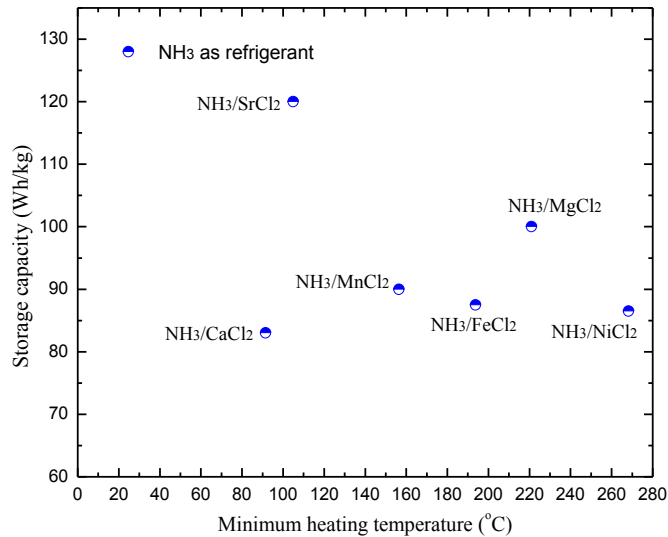
Figure 3.15: Storage capacity and minimum heating temperature of different sorption
working pairs with ambient temperature of 35°C and evaporation temperature of –20°C
(Mugnier and Goetz, 2001)

From the figures above, the suitable and efficient working pairs for sorption storage system is NH_3 used as the refrigerant and solid/gas reaction as the sorbent. The main sorption types, absorption storage, which has been commercially well developed, and adsorption storage, which is still under the development stage, is introduced later.

3.2.2.1   Absorption working pairs

Working pairs was a key role for storage process. Usually it needs better volatility of the solution. For working pairs it has other requirements, such as environment safety, non-toxicity, low GWP and ODP and low material cost. For working pairs in subzero application, the selection of absorbent/refrigerant pair is mainly NH_3/H_2O for refrigerant NH_3 can evaporate at lower temperatures (i.e. from −10°C to 0°C). Several working pairs for subzero application are summarized as follows.

(1) NH_3/H_2O

NH_3/H_2O pair is commonly used for subzero application such as ice making. Related research were conducted both theoretically (Sun, 1996) and experimentally (Bogart, 1981). Although it is commonly used, it has the disadvantages that ammonia is toxic and the system needs high operating pressure conditions and needs a column of rectifier because NH_3 and H_2O can both exist in vapor state.

(2) Other working pairs

Generally speaking, NH_3/H_2O systems exhibit a relatively low COP, therefore it is necessary to search for better working fluid pairs to improve system performance. Infante (1984) studied thermal properties of the lithium ammonia/nitrate ($NH_3/LiNO_3$) and ammonia/sodium thiocyanate ($NH_3/NaSCN$) solutions. Sun (1998) and Abdulateef et al. (2007) made detailed comparisons between NH_3/H_2O, $NH_3/LiNO_3$ and $NH_3/NaSCN$ absorption systems. Results showed that the $NH_3/LiNO_3$ and $NH_3/NaSCN$ cycles give better performance than the NH_3/H_2O cycle. The $NH_3/NaSCN$ cycle cannot operate at evaporator temperatures below −10°C for the possibility of crystallization. With a theoretical analysis of the absorption refrigeration cycle by Zhu and Gu (2009), it was found that the $NH_3/NaSCN$ solution is advantageous for lower generator temperatures in comparison with NH_3/H_2O solution. This is because COP is about 10% higher than that for NH_3/H_2O system at the same working conditions.

For other working pairs, Fan et al. (2007) gave a state-of-the-art review on the solar sorption research refrigeration technologies. A unit of 1.5 kWh/day using NH_3 as refrigerant and IMPEX material (80% $SrCl_2$ and 20% Graphite) as absorbent was reported by Bansal et al. (1997). Theoretical maximum overall COP of the unit is 0.143, and it is closely related to the climatic conditions. Potential of using organic fluid mixtures trifluoroethanol (TFE)/tetraethylenglycol dimethylether (TEGDME or E181) and methanol/TEGDME, as working pairs in series flow and the vapour exchange double-lift absorption cycles was discussed by Medrano et al. (2001). The simulation results showed that the COP of the vapor exchange cycle working with TFE/TEGDME is 15% higher than that NH_3/H_2O.

3.2.2.2   Adsorption working pairs

To make adsorption storage more efficient, there are several requirements for working pairs. As for the adsorbent, large adsorption capacity, large change of adsorption capacity with temperature variation, more flat desorption isotherm and good compatibility with refrigerant are the main requirements. As for the refrigerant, it should have large latent heat per volume, no toxicity, non-flammable, no corruption and good thermal stability. In fact, no perfect working pairs meeting all requirements above exist. In the following, common working pairs of methanol/carbon and ammonia/carbon are mainly introduced as an example of physical adsorption, and ammonia/Calcium chloride is introduced as an example of chemical adsorption.

(1) Methanol/carbon

Methanol/carbon working pair system is most commonly used for low desorption temperature, low adsorption heat, high latent heat of evaporation of methanol and good supply with low price. Methanol/carbon and methanol/activated carbon fiber are two kinds of working pairs. Carbon fibre has better mass transfer performance than granular activated carbon for the specific surface area of former is larger than that of latter, and the pores of activated carbon fiber are more uniform. When compared with activated carbon-methanol, the carbon fiber has an increased COP by 10~20% and an increased cyclic adsorption capacity by 2~3 times (Wang, 1997). In addition, it should be noted that the former has the issues of the anisotropic thermal conductivity and higher contact thermal resistance between the fiber and the adsorber wall. As to methanol/carbon working pair

system, it has the disadvantage of operating under sub-atmospheric pressure (i.e. high vacuum condition) and limited desorption temperature range (no higher than 120°C) to ensure better system performance. Other attentions should be paid to its high toxicity of methanol and relatively low thermal conductivity of carbon-based materials.

(2) Ammonia/carbon

The adsorption heat of this working pair is similar to that of methanol/carbon. However, it has higher working pressure (1.6 MPa under condensation temperature of 40°C), which can lead to better mass transfer performance and shorter adsorption time. This may also make the system to be ponderous. Another difference is that it can use heat source higher than 200°C. However, it also has disadvantages, such as toxicity and corrosion of ammonia to cuprum material.

(3) Ammonia/calcium chloride

Ammonia/calcium chloride, which has large adsorption quantity (as high as more than 1 kg/kg for most chlorides, is commonly used in chemical adsorption storage systems. Related reaction between calcium chloride and ammonia is shown as follows:

$$CaCl_2 \cdot n_1 NH_3 + n_2 \Delta Hr \leftrightarrow CaCl_2 \cdot (n_1 - n_2)NH_3 + n_2 NH_3 \qquad \text{Equation 3.1}$$
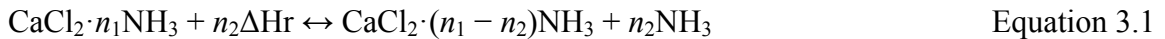
where ΔH_r is the reaction enthalpy (J/mol), the numbers of n_1 and n_2 could be 2, 4 and 8.It should be noted in the calcium chloride/ammonia adsorption systems, issues of expansion, deterioration and corrosion should be solved out for its commercialization.

(4) Working pairs with consolidated/composite adsorbents

In addition to the single working pairs listed above, there are more efficient working pairs with consolidated/composite adsorbents. Consolidated adsorbent, which has high thermal conductivity, can be considered as the most promising alternative to enhance the heat transfer within the adsorber. Wang et al. (2004) studied adsorption performances with the additive of activated carbon in solidified compound adsorbent (mixture of $CaCl_2$ and activated carbon) for ice making. Results showed that solidified compound adsorbent (sample No.6 in his study) made the adsorption quantity to be improved about 0.15 kg/kg in comparison with simple $CaCl_2$ adsorbent (sample No.4 in his study) at the evaporating temperature of −15°C. This is because the mass transfer performance is improved by the additive of activated carbon. Also the volume cooling density of solidified compound adsorbent is about 35% improved at least in comparison with that of $CaCl_2$ at same evaporating temperature. In recent work, composite adsorbents ($CaCl_2$ and expanded graphite) have better adsorption performances and thermal conductivity for the additive of expanded graphite in $CaCl_2$ powder has restrained the agglomeration phenomenon in adsorption process and improved the adsorption performance of $CaCl_2$ (Wang et al., 2006). They are suitable to be used as adsorbent for ice making on fishing boats because they have higher thermal conductivity, larger volumetric cooling capacity, higher SCP values and better anti-sway performance than simple composite adsorbents.

3.2.3 Heat transfer and system performance improvement

Absorption technologies have been well developed as compared with adsorption technologies. Components of absorption system were improved for better heat transfer and system performance. In a study by Rivera and Rivera (2003), a compound parabolic concentrator (CPC) with a glass cover, operates as the generator-absorber of the cooling system. Since lithium nitrate does not evaporate during the generation, it is not necessary to use a rectifier. The theoretical efficiencies of the CPC varied from 0.33 to 0.78 depending on the time of the day and the season. In a typical Mexico weather, it was possible to produce up to 11.8 kg of ice and the thermal COPs were between 0.15 and 0.4 depending on the generation and condensing temperatures. In addition, various recycle forms such as double-effect convertible system, dual-cycle system, and multistage system has been used to improve system performance (Li and Sumathy, 2000; Yang et al., 2011). Yang et al. (2011) summarized related absorption thermal storage technologies. Here the works using working pair NH_3/H_2O were summarized as shown in Table 3.10.

Table 3.10: Review of absorption cold TES technologies for subzero application (Yang et al., 2011)

Absorption pair	Driving source	Cold storage density with theoretical analysis (kW h/m^3)	Standard for thermal storage volume
NH_3/H_2O	Compressor cycle	182.7	Concentrated solution volume (Xu and Zhang, 2007)
NH_3/H_2O	Heat pump	33 (evap. temp. –27 °C)	Optimized dilute solution volume and concentrated solution volume (Rizza, 1998)

One of main issues of the adsorption storage is the poor heat and mass transfer of adsorbent beds, particularly for the low thermal conductivities and poor porosity

characteristics of adsorbents. To evaluate the performance for adsorption refrigeration, there are two main parameters: COP, which is the ratio of cold production from evaporator to heat supplied by driving energy, and SCP, which is the ratio of cooling power for semi-cycle to the adsorbent mass in one adsorbent bed. Adding the materials with higher thermal conductivity into the adsorbent and developing consolidated and composite adsorbents (as discussed in section 3.2.2) are good ways to improve heat performance of adsorbents. A good example is the thermal conductivity of activated carbon with added cuprum powder can be improved by 2~25% (Eltom and Sayigh, 1994). Obviously, such solutions are beneficial for SCP improvements. However, it should be noted that the heat transfer enhancement here usually reduces the mass transfer performance of the adsorbent. Therefore, it is more convenient for the solutions here to be used in the occasions where heat transfer rather than mass transfer is the dominating factor for system performance. A reasonable analysis for both heat and mass transfer is necessary during sorption storage process.

Furthermore, extended surfaces, such as finned tubes and plate-in heat exchangers, can also help improve heat transfer. The adsorbent bed with an expanded graphite plate can be also a good way for heat transfer enhancements. It should be noted for such solutions an efficient heat management solution is needed to achieve a reasonable COP. In addition, heat pipes used in adsorption refrigeration systems can improve the system performance. Moreover, adsorption storage with different advanced cycles has been studied extensively for system performance improvements (Sumathy et al., 2003; Wang et al., 2010). The typical adsorption refrigeration cycles are: basic cycle, continuous heat recovery cycle,

mass recovery cycle, thermal wave cycle and convective thermal wave cycle. Some work about the optimization for system design (adsorber and the cycle mode) should be done for system performance. Wang and Oliveira (2006) summarized performance of COP and SCP with a fair comparison for different working pairs, and the working pairs for subzero application (ice making) are extracted based on literature (Pons and Guilleminot, 1986; Tamainot-Telto and Critoph, 1997; Li et al., 2002; Li et al., 2004; Khattab, 2004; Wang and Wang, 2005; Lu et al., 2006), as shown in Table 3.11.

Table 3.11: Performance of adsorption systems for subzero application (Wang and Oliveira, 2006)

Application	Heat source temperature or insolation	Working pair	COP	SCP or ice production	Reference
Ice making	20 MJ/m^2 day	AC-Methanol	0.12	6 kg/m^{2}day	(Pons and Guilleminot, 1986)
Ice making	105°C	AC-NH$_3$	0.10	35 W/kg	(Tamainot-Telto and Critoph, 1997)
Ice making	18.1~19.2 MJ/m^2 day	AC-Methanol	0.12~0.14	5.0~6.0 kg/m^{2}day	(Li et al., 2002)
Ice making	17~20 MJ/m^2 day	AC-Methanol	0.13~0.15	6.0~7.0 kg/m^{2}day	(Li et al., 2004)
Ice making	20 MJ/m^2 day	AC+blackened steel-Methanol	0.16	[a]9.4 kg/m^{2}day	(Khattab, 2004)
Ice making	< 120°C	AC-Methanol	0.18	27 W/kg	(Wang and Wang, 2005)
Ice making	115°C	AC+CaCl$_2$/NH$_3$	0.39	[b]770 W/kg	(Lu et al., 2006)

[a]Based on the area of the adsorber, which was different from the area of the reflector panels.
[b]The SCP is based on the mass of CaCl$_2$ inside one adsorbent bed and only in the duration of the adsorption phase

In addition, the ISAAC solar icemaker, which is an intermittent solar ammonia-water absorption cycle, as shown in Figure 3.16, was developed by Energy Concepts Company (The ISAAC solar icemaker, 2012). The ISAAC uses a parabolic trough solar collector and a compact and efficient design to produce ice with no fuel or electric input, and with no moving parts. During the day, solar energy is used to generate liquid ammonia

refrigerant. During the night, the generator is cooled by a thermosyphon and ice is formed in the evaporator compartment as ammonia is reabsorbed to the generator. The daily ice production of the ISAAC is about five kilograms per square meter of collector, per sunny day. The construction of the ISAAC solar icemaker involves only welding, piping and sheet metal work, and there are no expensive materials. And the quantity of ice is sufficient to support small scale business while maintaining sustainability in harsh environments, or provide low cost household refrigeration. It is a good example of sorption storage for subzero application.
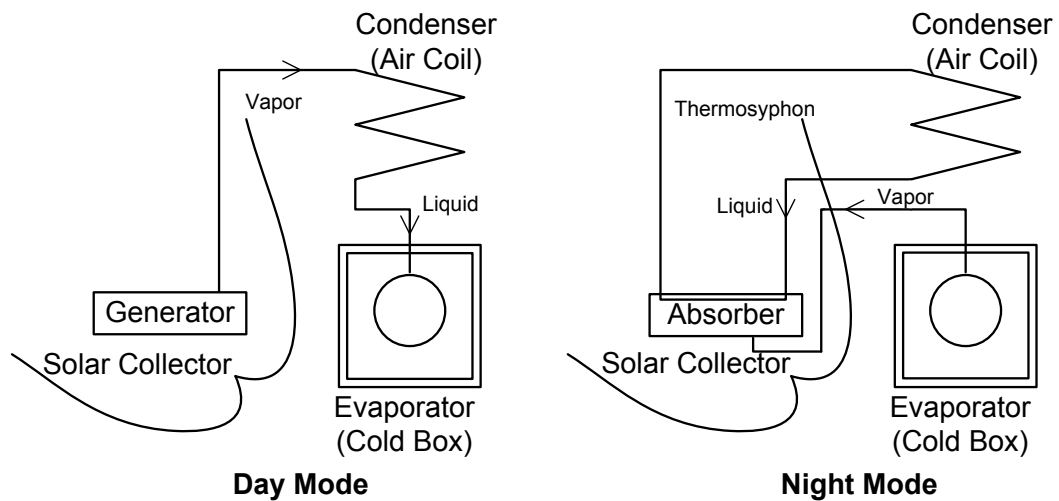
Figure 3.16: Design of ISAAC solar icemaker (The ISAAC solar icemaker, 2012)

Based on the adsorption storage technologies discussed above, it can be found that it has a great potential in subzero application, while the main factors impeding the commercialization of this storage technology may include poor heat and mass transfers of adsorbent beds, high equipment and maintain cost and large size. Further work is still

needed to improve heat and mass transfer characteristics during adsorption storage process and reduce the system cost.

3.3 Challenges and technology perspective

Different kinds of available cold storage materials for subzero application are introduced in this paper. Technology perspectives with regard to PCM storage and sorption storage are mainly summarized as follows:

(1) For PCMs, eutectic water-salt solutions have the benefits of higher fusion heat than other PCMs, but have the issues of phase separation and supercooling effect. Among non-eutectic water-salt solution PCMs, most used alcohol solutions have relatively higher fusion heat and no phase separation, but usually have issues of supercooling, corrosion, etc. Also, paraffins have the advantages of that they are mostly chemically inert, stable and recyclable, exhibiting little or no supercooling (i.e. they can be self-nucleating), no phase separation, and non-corrosive behavior. However, they have relatively low thermal conductivity and density. Usually non-eutectic water-salt solution PCMs are flammable. Issues of each kind of PCMs are discussed in this chapter. Multicomponent PCMs are also discussed.

(2) In addition, two other kinds of materials, microencapsulated PCMs, which have better heat transfer with larger surface area to their volume, and PCMs with nanoparticle additives, which have higher thermal conductivities, are mainly introduced here. Further research on the inherent mechanism of heat transfer and transport characteristics

including convective heat transfer characteristics, viscosity and stability, would be good to do.

(3) Working pair selection, heat transfer enhancement and system performance improvement are made for sorption storage for subzero applications, absorption storage (which has been developed well), and adsorption storage (which has made a great progress for further marketing). Related issues include poor heat and mass transfer of adsorbent beds, especially for the low thermal conductivities and poor porosity characteristics of adsorbents. The sorption system is usually more complicated for subzero applications than for air conditioning application. For example, NH_3/H_2O system is commonly used for subzero applications such as ice making. However, the system needs high operating pressure conditions and needs a column of rectifier because NH_3 and H_2O can both exist in vapor state during the storage process, and because ammonia is toxic. Further research also includes optimizing and reducing the cost of these systems with more advanced technologies for sorption storage.

4 Critical Review of Heat TES Technologies for Residential Application

In addition to air conditioning and subzero application, TES has another important aspect for residential application, such as space heating, domestic hot water production, heat supply for cloth dryers, etc. In this section, the heat storage technologies for residential application are mainly discussed. As shown in Figure 2.8 discussed early in Chapter 2, the main introduced materials here have the phase transition at around 30~100°C. In this section, the sensible, latent and sorption heat storage are introduced.

4.1 Sensible heat storage materials

Sensible heat storage means energy can be stored by changing the temperature of the storage materials. The amount of stored heat is proportional to the density, specific heat, volume, and temperature variation of the storage materials. Basically, specific heat, density and thermal conductivity are the main thermal properties of sensible heat storage materials. Figure 4.1 shows the main thermal properties of sensible heat materials.
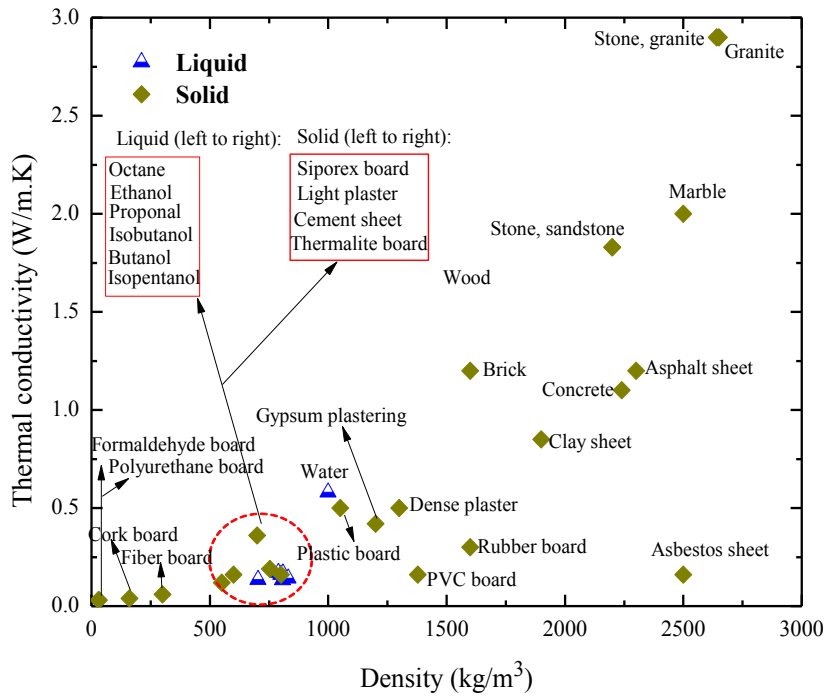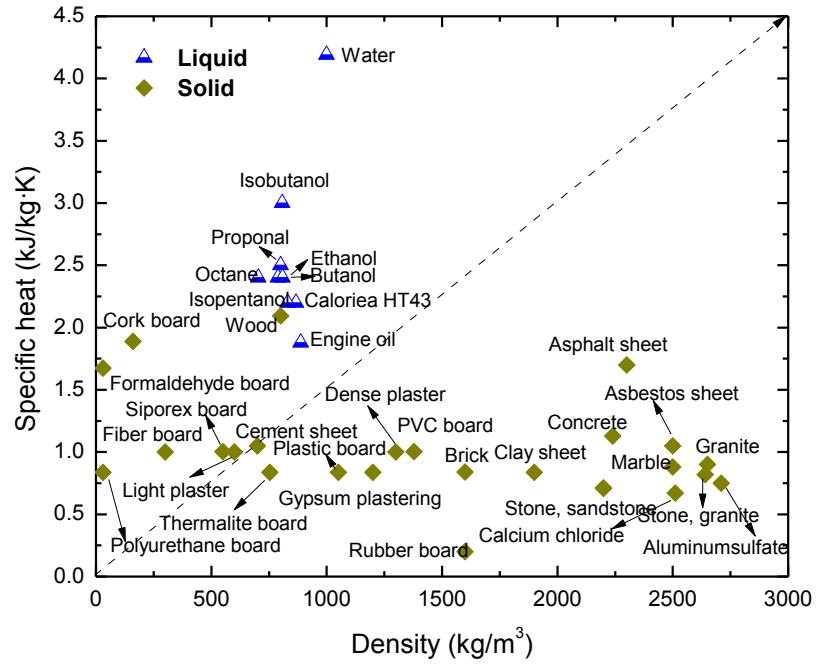
Figure 4.1: Thermal properties of sensible heat materials

4.1.1 Selection criteria for sensible heat materials

Requirements for common sensible heat storage materials in residential application are summarized as follows:

- Minimum service temperature of 30ºC;

- High energy density (high density and specific heat);

- Good thermal conductivity (higher than 0.3 W/m·K);

- Good thermal diffusivity

- Easy manufacturing and low price

- Stable chemical properties, low corrosivity, and low environmental impact factors, such as zero ODP effect and low GWP effect

Sensible heat storage is a relatively mature technology that has been implemented and evaluated among many large-scale residential applications. Water and rock bed are commonly used as storage materials and a brief comparison of their thermal properties is shown in Figure 4.2.

(a) Water and aquifer　　　　　(b) Rock bed
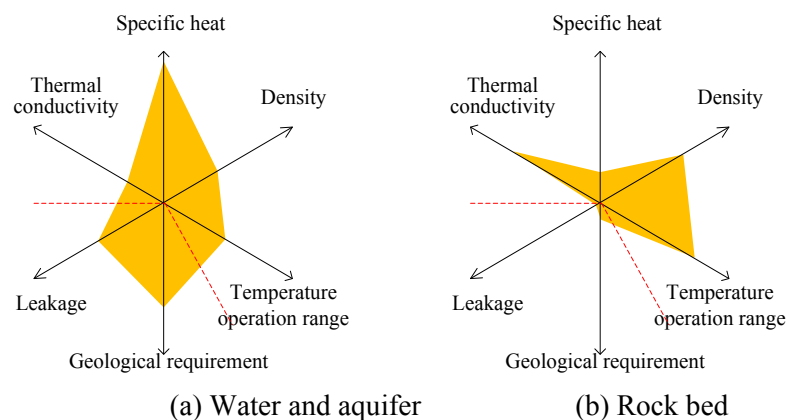
Figure 4.2: Comparison of sensible heat materials' thermal properties

4.1.2 Water and aquifer

Water is a favorable material for heat storage in residential application due to its high specific heat as compared with other sensible heat storage media. Water tank and aquifer storage system are two common water-based storage systems.
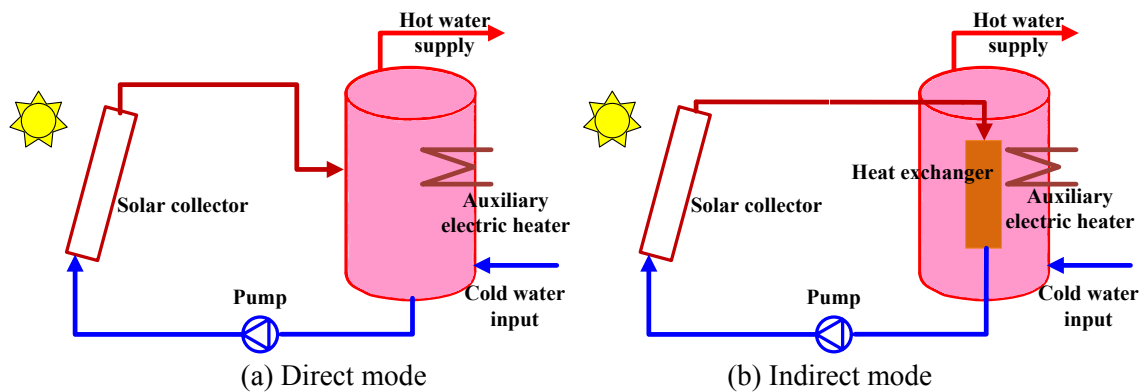
Figure 4.3: Schematic of domestic hot water system with electrical heater

Regarding water tank, water stratifies naturally because of increasing density at lower temperature: the hot water flows to the top, the cold water remains at the bottom, and the intermediate region is the thermocline. For sensible heat storage, typical temperature difference is usually in the range of 5~10°C. Temperature scale for space heating and domestic hot water production is usually at the operating range of 25~80°C. One of the common applications is the solar hot water tank, as shown in Figure 4.3. For the direct (open loop) configuration, the collector directly transfers the heat to water tank without any intermediate heat exchanger and the heat transfer fluid is water. Cold Water enters at the bottom of the hot water tank and in turn passes through the solar collector, gets heated and delivers heat at the top portion of hot water tank. For the indirect (closed loop)

configuration, the heat transfer fluid does not mix with water in the tank. Usually the hot water requirement is typically at constant temperature and solar radiation varies during the day. Therefore, auxiliary heater, attached to the tank, is used to compliment the demand at constant temperature.

Usually the thermal stratification in the water storage tank is affected by several factors, such as tank size and shape, location and geometry of inlets and outlets, temperature and flow rates during charging and discharging. In addition, necessary strategies should be investigated to improve stratification. Water storage tank should be operated in a stratified manner with water at the top if the tank being hotter than that in the bottom due to thermal buoyancy. It should be noted that mixing effect caused by the temperature difference could degrade the heat source level and negative effect on the system storage efficiency. The horizontally partitioned water tank was proved to achieve good thermal stratification performance and was efficient for heat storage application. Another important point for water tank is the heat losses during storage tank. Effects on water tank design and selection of insulation materials (glass wool and polyurethane) have been made recent years for reduction of heat losses.

Aquifers are geological formations containing ground water, and water in aquifers is sometimes mixed with gravel or sand. Aquifers have the advantages of storing heat/cold for long periods, especially when large storage volumes are available. Heat storage in aquifers consists in extracting ground water from a well, heating this water with an available heat source, and then re-injecting it back into the aquifer in the other well, as

illustrated in Figure 4.4. Aquifer heat storage systems have lower investment and operating cost than classical water storage tanks. However, the allowable temperature change, the natural ground flow and potential environmental consequences should be considered for design and operation. Usually the hydro-geological conditions make the aquifer storage system quite complex and conditional.
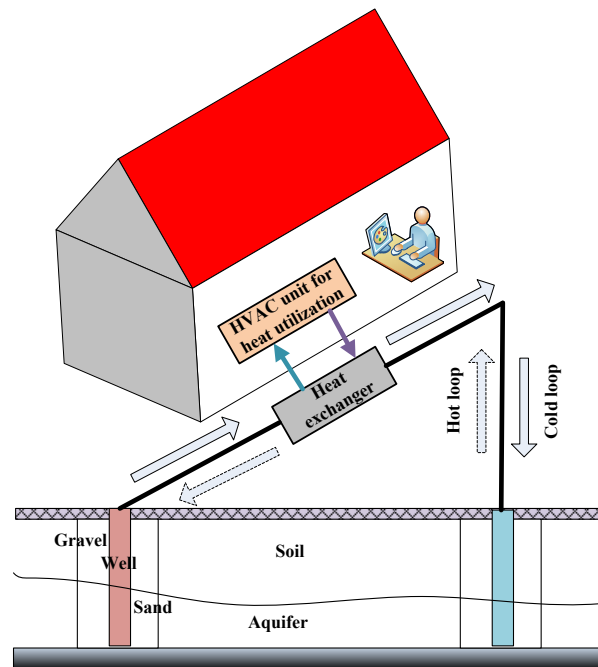
Figure 4.4: Schematic of aquifers

4.1.3   Rock and bricks

In addition to the water, other commonly used materials can be solid materials, such as rock, metal, concrete, sand, brick, etc. The operating temperature range can be over 100°C. As compared with water storage, solid storage has several inherent advantages: it can endure much higher temperatures; it has no leakage problem with their containment;

sold heat storage material has good conductivity. Rock is the commonly used heat storage material. Even though it has a lower volumetric thermal capacity, it can work at temperatures higher than 100°C. One example is Harry Thomason's technique using both water and stone as storage media, as shown in Figure 4.5. The collected heat can be stored both in the stone and water tank. The stored energy could warm the cool air.
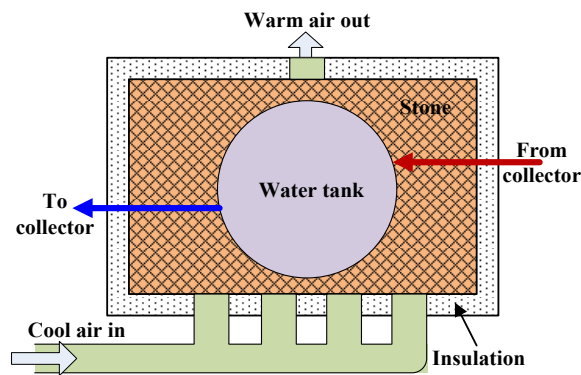
Figure 4.5: Harry Thomason's technique using both water and stone as storage media
(Dincer and Rosen, 2011)

Another example is shown in Figure 4.6. During off-peak periods (i.e. charging process) electric energy is converted to heat which is stored in high mass units, or bricks, made of dense ceramic material. During the peak hours (i.e. discharging process), the power is shut off and an electric fan begins to transfer the heat from the brick to the house. The temperature is controlled by outside sensors. The sensors can adjust the amount of power intake to keep the room at the required comfort temperature. In addition, sensible heat storage can use large amount of water, such as underground reservoirs or solar ponds.
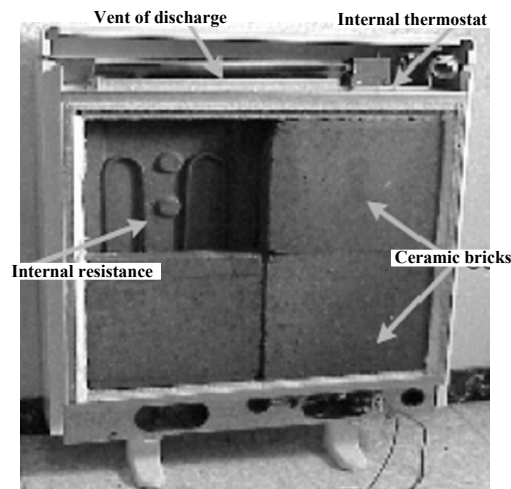
Figure 4.6: Sensible heat storage (Molina et al., 2003)

Regarding solid storage materials, the compatibility of the material with heat transfer fluid used is very important. The storage performance is strongly dependent on the solid material's size, shape, the packing density, the type of heat transfer fluid, etc. While, the main drawback for solid storage materials is their low specific heat capacity (~1200 $kJ/m^3 \cdot K$, where water is ~4200 $kJ/m^3 \cdot K$), which makes a relatively lower storage density by volume. To achieve the same amount of heat storage, solid storage usually needs three times more space than water-based storage system.

In addition, there are other kinds of storage systems, such as ground and soil storage. Since sensible heat storage technologies have already developed well and there are already many large-scale practical applications, it will not be discussed in detail here.

4.2 Latent heat storage

4.2.1 Selection criteria for latent storage materials

For latent heat storage materials, inorganic materials (salt hydrates and metals), and organic materials (paraffins and no parafins) are mainly introduced here, as shown in Figure 4.7. Table 4.1 and Table 4.2 provide for a review of their thermal properties.

- Phase change service temperature of 30~100 ºC;

- Large fusion heat and good cycling stability;

- Good thermal conductivity to speed up phase change progress, and low supercooling;

- Stable chemical properties, low corrosivity, and low environmental impact factors;

- Easy manufacturing and low price.

Usually it is hard for a material to satisfy the entire requirements listed above so that here the primary four requirements are discussed here. A brief relative comparison of the thermal properties of the different types of PCMs is shown in Figure 4.8.

Figure 4.7: Thermal properties of heat storage materials for residential application

Table 4.1: Inorganic phase change materials (Sharma et al., 2009; Naumann and Emons, 1989; Belton and Ajami, 1973; Lindner, 1996; Wikipedia, 2013)

PCM	Phase change temp. (°C)	Fusion heat (kJ/kg)	PCM	Phase change temp. (°C)	Fusion heat (kJ/kg)
Salt hydrates			**Salt hydrates**		
$LiNO_3 \cdot 2H_2O$	30.0	296	$Na_2S_2O_3 \cdot 5H_2O$	48.5	210
$LiNO_3 \cdot 3H_2O$	30	189	$MgSO_4 \cdot 7H_2O$	48.5	202
$Na_2CO_3 \cdot 10H_2O$	32.	267	$Ca(NO_3)_2 \cdot 3H_2O$	51	104
$Na_2SO_4 \cdot 10H_2O$	32.4	241	$Zn(NO_3)_2 \cdot 2H_2O$	55	68
$KFe(SO_4)_2 \cdot 12H_2O$	33	173	$FeCl_3 \cdot 2H_2O$	56	90
$CaBr_2 \cdot 6H_2O$	34	138	$Ni(NO_3)_2 \cdot 6H_2O$	57	169
$LiBr_2 \cdot 2H_2O$	34	124	$MnCl_2 \cdot 4H_2O$	58	151
$Zn(NO_3)_2 \cdot 6H_2O$	36.1	134	$MgCl_2 \cdot 4H_2O$	58	178
$FeCl_3 \cdot 6H_2O$	37.	223	$CH_3COONa \cdot 3H_2O$	58	265
$Mn(NO_3)_2 \cdot 4H_2O$	37.1	115	$Na(CH_3COO) \cdot 3H_2O$	58	226
$Na_2HPO_4 \cdot 12H_2O$	40	279	$Fe(NO_3)_2 \cdot 6H_2O$	60.5	126
$CoSO_4 \cdot 7H_2O$	40.7	170	$NaAl(SO_4)_2 \cdot 10H_2O$	61	181
$KF \cdot 2H_2O$	42	162	$NaOH \cdot H_2O$	64.3	273
$MgI_2 \cdot 8H_2O$	42	133	$Na_3PO_4 \cdot 12H_2O$	65	190
$CaI_2 \cdot 6H_2O$	42	162	$Na_2B_4O_7 \cdot 10H_2O$	68.1	-
$K(CH_3COO) \cdot 3/2H_2O$	42	-	$LiCH_3COO \cdot 2H_2O$	70	150
$K_2HPO_4 \cdot 7H_2O$	45	145	$Al(NO_3)_2 \cdot 9H_2O$	72	155
$Zn(NO_3)_2 \cdot 4H_2O$	45	110	$Ba(OH)_2 \cdot 8H_2O$	78	265
$Mg(NO_3) \cdot 4H_2O$	47	142	$Al_2(SO_4)3 \cdot 18H_2O$	85.8	-
$Ca(NO_3) \cdot 4H_2O$	47	153	$Al(NO_3)_3 \cdot 8H_2O$	88	-
$Fe(NO_3)_3 \cdot 9H_2O$	47	155	$Mg(NO_3)_2 \cdot 6H_2O$	89.9	167
$Na_2SiO_3 \cdot 4H_2O$	48	168	$KAl(SO_4)_2 \cdot 12H_2O$	91	184
$K_2HPO_4 \cdot 3H_2O$	48	99	$MgCl_2 \cdot 6H_2O$	117	167
Metals			**Metals**		
Gallium	30.0	80.3	Cerrolow 203	70	159
Cerrolow 136	47.2	68.2	Cerrolow 117	95	-
Cerrolow 158	58	90.9			

Table 4.2: Organic PCMs for heat storage residential application (Sharma, et al., 2009; Lane, 1980; Hawes et al., 1993)

PCM	Phase change temp.(°C)	Fusion heat kJ/kg)	PCM	Phase change temp. (°C)	Fusion heat (kJ/kg)
Paraffins			**Paraffins**		
C19	32.0	222	C29	63.4	240
C20	36.7	246	Paraffin wax	64	173.6
1-Tetradecanol	38	205	C30	65.4	251
C21	40.2	200	Polyglycol E6000	66	190
C22	44.0	249	C31	68	242
C23	47.5	232	C32	69.5	170
C24	50.6	255	Biphenyl	71	119.2
C25	49.4	238	C33	73.9	268
C26	56.3	256	C34	75.9	269
C27	58.8	236	Propionamide	79	168.2
C28	61.6	253	Naphthalene	80	147.7
No paraffins			**No paraffins**		
Camphenilone	39	205	Lauric acid	49	178
Docasyl bromide	40	201	9-Heptadecanone	51	213
Caprylone	40	259	Methyl behenate	52	234
Heptadecanone	41	201	Hypophosphoric acid	55	213
1-Cyclohexylooctadecane	41	218	Palmatic acid	55	163
4-Heptadacanone	41	197	Trimyristin	33~57	201~213
Cyanamide	44	209	Heptaudecanoic acid	60.6	189
Methyl eicosanate	45	230	Bee wax	61.8	177
Eladic acid	47	218	Bees wax	61.8	177
3-Heptadecanone	48	218	Stearic acid	69.4	199
2-Heptadecanone	48	218	Acetamide	81	241

C19 means the no. of carbon atoms for paraffins is 19.

(a) Salt hydrates   (b) Metals

(c) Paraffins   (d) Fatty acids
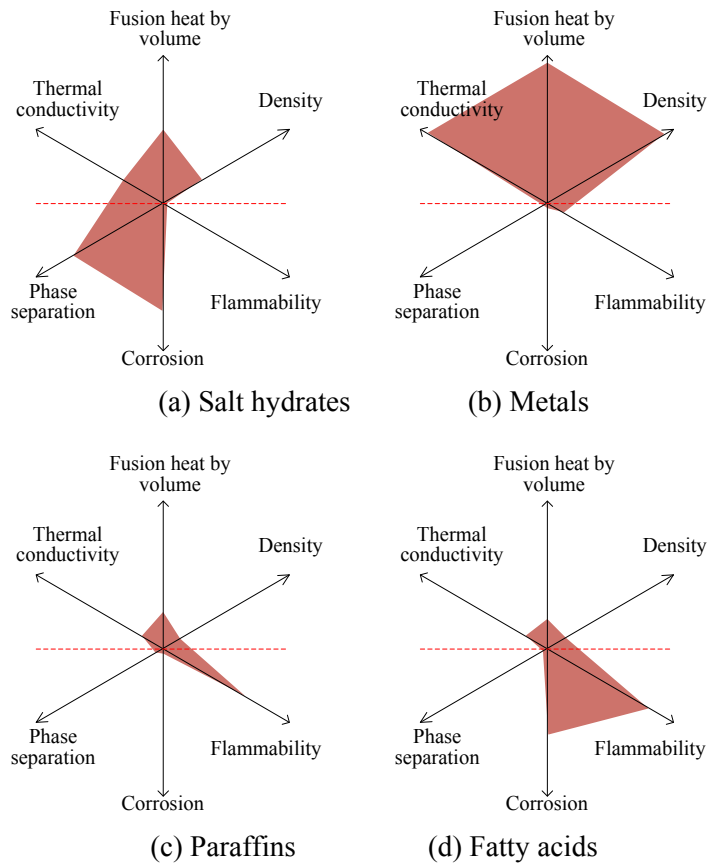
Figure 4.8: Comparison of latent heat materials' thermal properties

4.2.2 Salt hydrates and metals

The inorganic heat storage materials are mainly salt hydrates and metals for residential application. As discussed in the Chapter 2 and Chapter 3, salt hydrates have the advantages that they have relatively high volumetric storage density and high thermal conductivity, and they are cheaper as compared with organic materials. However, they have the issues of poor cycle stability, corrosion and supercooling. Regarding these issues, the resolutions are quite similar to Chapter 2 and 3, and it will not be discussed in detail here. The metals can be excellent heat storage candidates because of their high

volumetric fusion heat. The main drawbacks for use of metals are their scare availability and high cost.

4.2.3 Paraffins and no paraffins

The organic heat storage materials are mainly paraffins and no paraffins (mainly fatty acids). As discussed in Chapter 2 and 3, usually organic materials have negligible supercooling, non-corrosiveness, chemical stability, self-nucleation, no phase segregation, and low cost operation. However, they have the issues of low thermal conductivity ($\sim$0.2W/m·K), significant volume change and flammability. Pure paraffins are very expensive and therefore only technical grade paraffins (mixture of pure substances) are used for latent heat storage applications. Non-paraffin organic PCMs (fatty acids) also have corrosion issues. Regarding these issues, the resolutions are quite similar to Chapter 2 and 3, and it will not be discussed in detail here. The organic heat storage materials should not be exposed to intense temperature, flames.

4.2.4 Heat transfer enhancement and system application examples

The materials listed in Table 4.1 and Table 4.2 still have issues, such as phase separation, supercooling, corrosion for inorganic PCMs, or low thermal conductivity and flammability for organic PCMs. Related solutions regarding these issues are similar to that for air conditioning application. Repeated introduction for each issue is not listed here. More details are referred to Chapter 2. Figure 4.9 summarized the possible techniques (Agyenim et al., 2010). The performance of micro-encapsulated PCMs is

expected to exceed conventional PCMs since small PCM particles provide larger heat transfer area per unit volume and can provide a higher heat transfer rate. PCMs in metal structures have also be prove to be a good way for thermal conductivity enhancement. In addition, PCMs with high conductivity porous materials and nanoparticles, can still constitute a promising alternative for improving the heat transfer processes in PCMs.
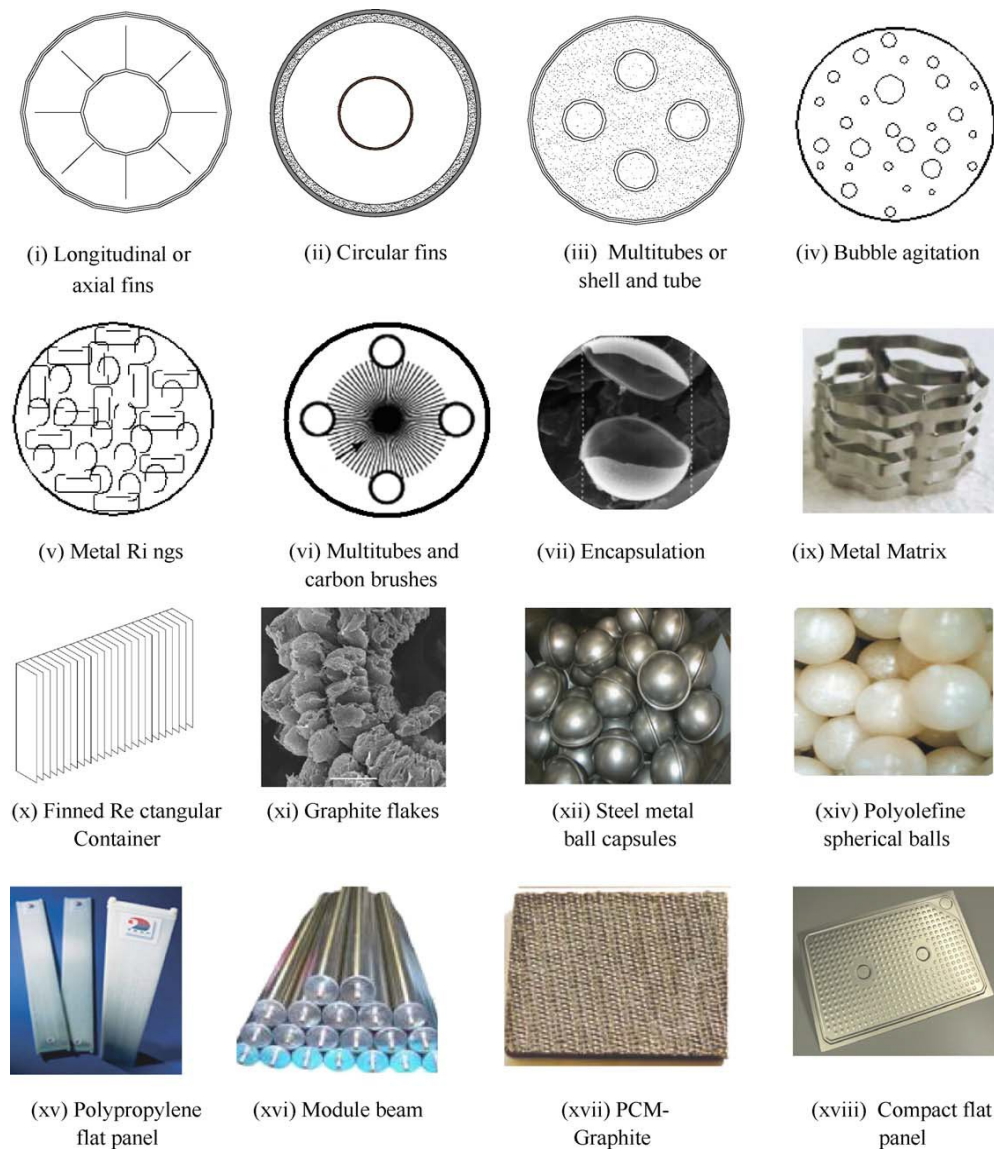
Figure 4.9: Heat transfer enhancement methods employed in latent heat material research (Agyenim et al., 2010)

For latent heat storage, the system is composed of a heat storage medium that undergoes the phase change, a container for the storage medium and a heat exchanger surface for transfer heat to and from the storage medium. There are three heat transfer type of heat storage system: heat transfer at the outside surface of storage system (usually employed in space temperature control application), heat transfer at the inside surface within the storage system and heat transfer with exchanging the storage medium, as shown in Figure 4.10.

(a)　　　　　　　　　　　　　　　(b)　　　　　　　　　　　　　　　(c)

(a) Heat transfer at the outside surface of storage system
(b) Heat transfer at the inside surface within the storage system
(c) Heat transfer with exchanging the storage medium
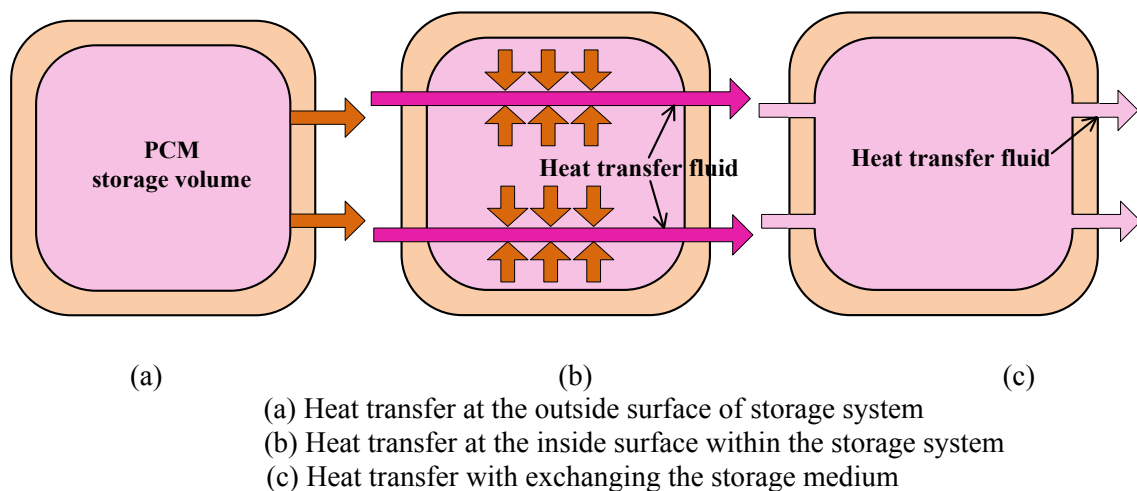
Figure 4.10: Heat transfer type of heat storage system

An under-floor electric heating system with the shape-stabilized PCM plates is shown in Figure 4.11 (Lin et al., 2005). The under-floor heating system included polystyrene insulation, electric heaters, PCM, some wooden supporters, air layer and wood floor. Different from conventional PCM, shape-stabilized PCM can keep the shape unchanged during phase change process. Therefore, the PCM leakage danger can be avoided. This system can charge heat by using cheap night time electricity and discharge the heat stored at day time.
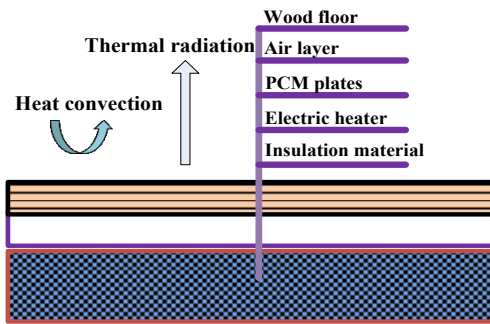
Figure 4.11: PCM assisted under-floor electric heating system (Lin et al., 2005)

Canbazoglu et al. (2005) compared PCM-charged solar water heater (SWH) systems with that of the conventional SWH systems without PCM. PCM-filled polyethylyne bottles were set in their storage system in three rows. The cross-sectional view of the system is shown in Figure 4.12. Without drawing-off the hot water during night, the system could attain about 46°C. The storage time of hot water, the produced hot water mass, and total heat accumulated in the solar water-heating system having the heat storage tank combined with PCM were approximately 2.59~3.45 times of that in the conventional solar water-heating system. In addition, there are other application, such as PCM filled glass windows, PCM integrated roof, PCM assisted ceiling, which are not discussed here.
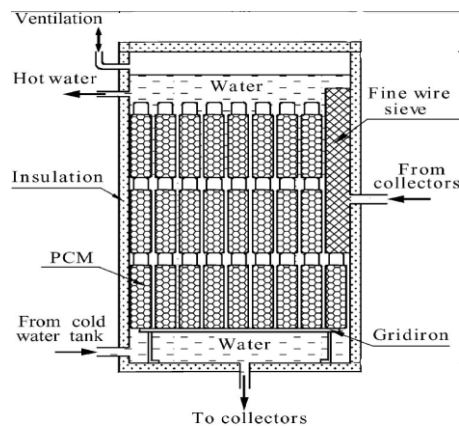
Figure 4.12: Cross-sectional view of heat storage tank combined with PCM
(Canbazoglu et al. 2005)

4.3 Sorption heat storage

4.3.1 Operating principle

(a) Absorption storage   (b) Adsorption storage
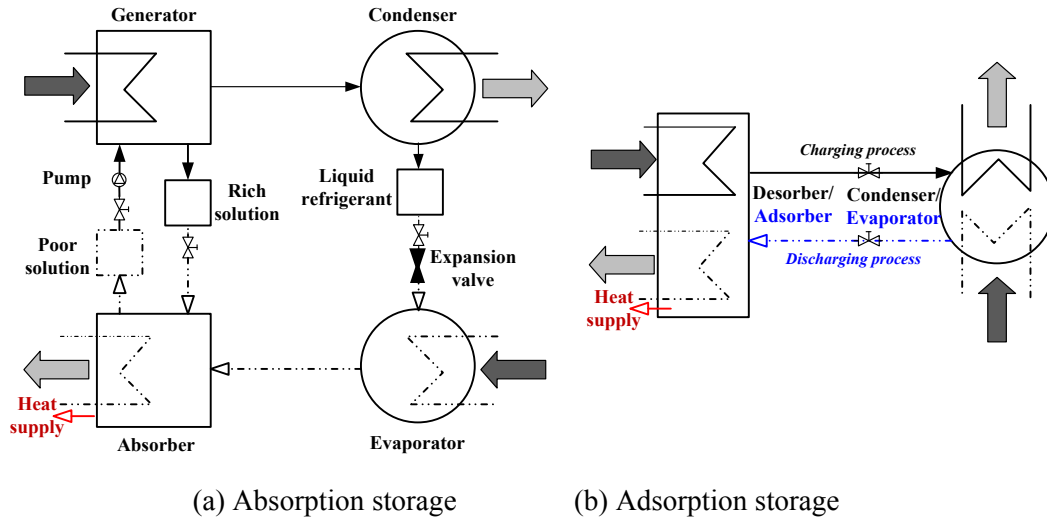
Figure 4.13: Schedule drawing of basic operating principle for sorption storage

A schematic drawing of the basic operation principle for absorption storage is shown in Figure 4.13(a). The operating principle is same as that for absorption air conditioning application. The difference is that for heating purpose, during discharging process, the heat supply from absorber is utilized, while for air conditioning application, the cold supply from evaporator is utilized. The basic operating principle of adsorption storage is shown in Figure 4.13(b). During the charging process, a desorber (can also be an adsorber during the discharging process) heated by a heat source connected to a condenser (can also be an evaporator during the discharging process). After a period of storing process (it can be short-term period or long-term period), discharging process begins. The adsorber is cooled by a heat transfer fluid and its pressure drops. The pressure is lower than that of evaporator, and the refrigerant from evaporator will flow to

the adsorber. The adsorption heat will make the heat transfer fluid temperature in the adsorber increases. Then the fluid with higher temperature flows to buildings for heating.

4.3.2 Working pair selection

Usually the working pairs should have the requirements of high thermal conductivity and high heat transfer with the heat transfer fluid for sorption process. They also have the requirements of environmental safety, non-toxicity, low global warming potential and ozone depletion potential. Several common sorption work pairs for heat storage purpose are listed in Table 4.3. Water /silica gel, water/lithium bromide, and water/lithium chloride appear to be at the most extensively studied. As to other chemical reaction working pairs, please refer to literature (Tatsidjodoung et al. 2013) for details.

Table 4.3: Sorption heat storage performance of different working pairs

	Sorption working pair	Storage density (MJ/m^3)	Performance characterization level	Operation condition	Reference
Absorption heat storage	H_2O/NaOH	900 (single stage reactor)	Reactor scale	Charge: 100~150°C Discharge: 40~65°C	Weber and Dorer, 2008
	H_2O/LiCl	910.8 (with crystallization in the storage tank)	Reactor scale	Charge: 46~87°C Discharge: 30°C	Bales et al., 2008
	H_2O/CaCl$_2$	428 (solution)	Reactor scale	Charge: 70~80°C Discharge: 21°C	Le-Pierrès et al., 2011
	H_2O/LiBr	907.2 (solution)	Reactor scale	Charge: 40~90°C Discharge: 30~33°C	N'Tsoukpoe et al., 2012
Adsorption heat storage	H_2O/zeolite 13X+MgSO$_4$	597.6	Material scale	Charge: 150°C Discharge: 30~50°C	Hongois et al., 2011
	H_2O/expanded natural graphite +SrBr$_2$	216	Reactor scale	Charge: 70~80°C Discharge: 35°C	Mauran et al., 2008
	H_2O/expanded vermiculite+LiNO$_3$	450	Reactor scale	Charge: 62~65°C Discharge: 33~36°C	Sapienza et al., 2012

4.3.3 Thermal property and system performance improvement

Despite high theoretical storage potential exists, sorption heat storage systems generally have very low performance when experimented, especially for adsorption heat storage in reactor-scale or system-scale. The main reasons are the poor heat and mass transfers involved and the thermodynamic cycle of the processes and it is necessary to improve thermal conductivity of the reactant sorbents. In addition, swelling and agglomeration phenomena often occur during the sorption process with water. Regarding these issues, several solutions are offered, which are quite same to that for air conditioning application (not introduced in detail here), such as adding an additive with the sorbent in absorption, using porous elaborated materials, or natural expanded graphite for sorption heat storage.

Regarding the adsorption heat storage for residential application, based on the literature review, this aspect is still marginal compared to sensible and latent heat storage technologies. For further research, developing new high-efficient and environmental-friendly sorption working pairs is one important direction. In addition, the use of carrier materials with a high porous structure with a reactive material dispersed inside to improve the heat and mass transfers is another important direction. Other future work still needs to focus on the integration of sorption storage into residential systems.

4.4 Challenges and technology perspective

(1) For sensible heat storage, the use of water, rock and ground has been investigated deeply and has proven to be feasible for large-scale district heating.

(2) Latent heat storage has a higher energy density than sensible heat storage. Current the issues of corrosion, flammability and compatibility with building materials, should be taken into account in details. Search for novel PCMs and gaining better understandings of their physicochemical mechanisms are quite necessary for further technical developments.

(3) Sorption heat storage currently remains in the laboratory study stages. Current studies are mainly on the selection and modification of working pairs in accordance with the thermodynamic requirements and operation conditions. Finding the proper sorbent materials and optimizing the reaction bed structure for both better heat/mass transfer and more compact system are critical steps.

5 Critical Literature Review of Energy and Exergy Analysis on TES System Performance Evaluation

Facing the issue of the gap between the availability and the demand in traditional energy sources, the performance assessment of TES units requires a sound and comprehensive knowledge on their thermal behavior. The energy efficiency of a TES system, the ratio of the energy recovered from storage to that originally provided, can be conventionally used to measure TES performance. With energy analysis, lots of work had been done both numerically and experimentally for configurations, various geometries, operating and design parameters of TES units for various applications. However, they are not sufficient because they did not take into account all the considerations necessary in TES evaluation. It does not evaluate how nearly the performance of the system approaches the ideal storage performance. The thermodynamic losses which occur within a system are often not accurately identified and assessed with energy analysis.

Here it is important to mention the popular quote by Bejan (1978), which is,

"*the primary purpose of a thermal energy storage system is not, as the name implies, to store the energy, rather, to store useful work*".

Exergy analysis allows to overcome many shortcomings of energy analysis. Based on the second law of thermodynamics, exergy analysis is very useful in identifying the causes, locations, and magnitudes of process inefficiencies. It can be predicted that in the near future, exergy analysis would be the major part for TES performance assessment.

Reasonable energy and exergy analysis for storage system performance evaluation can achieve an optimized system for the application of interest. As discussed in the section of Chapter 1, storage system performance evaluation can be investigated through two approaches, which are introduced in detail later. They are:

- Energy conservation principle based on first law of thermodynamics.
- Exergy analysis based on second law of thermodynamics.

5.1   Energy analysis

Usually for thermal storage systems, performance can be evaluated by efficiency or effectiveness. The efficiency is usually nothing but a way to measure how effectively the heat or cold energy is stored or removed. It is related to the storage process, i.e. "charging process", and "discharging process". The term "charging" or "discharging" is related to its actual application. If it is for cooling purpose, "charging" can be a solidifying process for PCM storage. While for heating purposes, it can be a melting process for PCM storage. Similarly, the charging or discharging process has been interpreted in earlier section, and its operation principle will not be explained here. The system performance can be calculated separately for charging and discharging process or done as an overall parameter.

One study by Kaizawa et al. (2008) showed the term of "heat storage ratio" and "heat release ratio" to evaluate the energy storage system performance.

$$Heat\ storage\ ratio = \frac{Total\ energy\ storaed\ in\ the\ unit}{Maximum\ storage\ capacity\ of\ the\ unit} \qquad \text{Equation 5.1}$$

$$Heat\ release\ ratio = \frac{Total\ energy\ released\ by\ the\ unit}{Maximum\ storage\ capacity\ of\ the\ unit}$$ Equation 5.2

Usually the heat stored and released can be calculated from the heat absorbed and released, respectively, by the HTF. The maximum heat storage capacity takes into account the sensible, latent, or sorption heat capacity of the unit. It can be easily predicted that both the performance ratios increase with increase of the mass flow rate of HTF at all times. In addition, thermal efficiency (η) is defined for charging process, discharging process and overall process.

$$\eta_{charg} = \frac{Total\ energy\ stored\ in\ the\ unit}{Total\ energy\ delivered\ to\ the\ unit}$$ Equation 5.3

$$\eta_{disch} = \frac{Total\ energy\ recovered\ from\ the\ unit}{Total\ energy\ stored\ in\ the\ unit}$$ Equation 5.4

$$\eta_{overall} = \frac{Total\ energy\ recovered\ from\ the\ unit}{Total\ energy\ delivered\ to\ the\ unit}$$ Equation 5.5

It should be noted that based on the literature review, lots of researchers did not include the work from pump in their system evaluation. One possible reason is that the pump work of HTF is relatively small when compared with the total storage energy. One would expect it to produce the maximum possible efficiency. Different influence factors and operating parameters on the energy efficiency should be investigated extensively. For sensible, latent and sorption TES storage, higher mass flow rates of HTF can result in higher storage efficiency. One study by El Qarnia (2009) calculated the storage efficiency of latent heat storage system used for solar water heater, with the storage efficiency expressed as a ratio between the latent heat stored in the PCM and the total solar radiation.

Results showed that higher HTF mass flow rate and more tubes in the heat exchanger lead to higher storage efficiency. In another study by Kaygusuz (2003), the storage efficiency of latent heat unit of a solar heat pump increased with higher HTF mass flow rate. Similar results were also achieved by Seeniraj et al. (2002). In another experimental study of a compact PCM solar collector by Mettawee and Assassa (2006), it showed that in the charging process, the average heat transfer coefficient increased sharply with increasing the molten salt layer thickness, as the natural convection grew strong. In the discharge process, the useful heat gain was found to increase as the water mass flow rate increases. The research work was conducted less for sorption storage process than that for sensible and latent storage process. However, it can still reveal that a large HTF mass flow rate is beneficial for thermal storage efficiency.

5.2   Exergy analysis

As discussed above, exergy analysis is more important for it can establish a clear understanding of the system storage performance. This section overviews the concepts of exergy, entropy and their influence in the second law of thermodynamics-based analysis.

5.2.1   Basic concepts

5.2.1.1   Exergy and entropy

In the second law of thermodynamics, the quality of energy is gauged from the state of system in relation to the surrounding conditions. This quality or usefulness of energy is termed as "exergy". It has other equivalent terms, like availability, available energy,

essergy, work capability and utilizable energy. Based on the literature review, the term "exergy" is more commonly employed than others. Therefore, in this section the term "exergy" is used. The corresponding analysis is called exergy analysis.

Exergy is defined as maximum quantity of work that can be produced by a system as it comes to equilibrium with surrounding. It is a measure of potential of the system to cause change in case that it is in non-equilibrium condition with surrounding. It should be noted that a system can hold exergy when it is not in equilibrium with surroundings and the exergy can be larger when the system deviates more from surroundings. The exergy is zero when it has achieved the equilibrium state. Exergy cannot be conserved, but can be consumed or destroyed. Therefore, energy is getting degraded automatically.

Regarding the entropy, the exergy content of a system or a matter can be obtained using the thermodynamic relations within it. It is well-known that all real processes are irreversible and hence, any irreversibility is associated with the process can be stated as responsible for the exergy destruction. It is necessary to know that to what extent exergy can be destroyed in order to quantify the true potential of the systems. From this viewpoint, entropy is very useful. It is a measure of irreversibility. In practical application, entropy is always generated and exergy is destroyed. It is easy to find that exergy is proportional to the generated entropy. A simple expression with flow condition for the relationship is expressed as follows:

$$\psi = (h - h_0) - T_0(s - s_0)$$
<div style="text-align:right">Equation 5.6</div>

ψ is the flow (specific) exergy, h is enthalpy, s is entropy, and the subscript zero indicates properties at the dead state of P_0 and T_0.

5.2.1.2 Exergy efficiency

The first law of thermodynamics-based efficiency can be stated as the ratio of energy output and energy input. In practical thermal systems the energy output is less than energy input because of energy loss. The first law of thermodynamics-based efficiency indicates the amount of loss that occurs during the process in the system. Hence, efficiency can be improved only by reducing losses. However, the losses do not reflect the degradation of energy. The second law or exergy efficiency of a thermal system is defined as the ratio of exergy output and exergy input. For a given quantity of exergy, the output exergy is lessened due to exergy destruction. As we know exergy destruction is due to irrerversibilities.

Thus, exergy efficiency (ϵ) is a measure of irrerversibilities and is defined as,

for total charging process,

$$\epsilon_{char} = \frac{Total\ exergy\ stored\ in\ the\ unit}{Total\ exergy\ delivered\ to\ the\ unit} \qquad \text{Equation 5.7}$$

for total discharging process,

$$\epsilon_{disch} = \frac{Total\ exergy\ recovered\ from\ the\ unit}{Total\ exergy\ stored\ in\ the\ unit} \qquad \text{Equation 5.8}$$

for overall process,

$$\epsilon_{overall} = \frac{Total\ exergy\ recovered\ from\ the\ unit}{Total\ exergy\ delivered\ to\ the\ unit} \qquad \text{Equation 5.9}$$

$$\epsilon_{overall} = \epsilon_{char}\epsilon_{disch} \qquad \text{Equation 5.10}$$

Since heat transfer during charging or discharging process is time dependent, it is also very important to investigate the exergy efficiency at different times. Therefore, the exergy efficiency in terms of exergy rate is defined as,

$$\epsilon_{char} = \frac{Rate\ of\ exergy\ storaed\ in\ the\ unit}{Rate\ exergy\ delivered\ to\ the\ unit} \qquad \text{Equation 5.11}$$

$$\epsilon_{disch} = \frac{Rate\ of\ exergy\ recovered\ from\ the\ unit}{Rate\ of\ exergy\ stored\ in\ the\ unit} \qquad \text{Equation 5.12}$$

It should be noted that still lots of studies did not include the pump work for exergy efficiency evaluation. Energy usually cannot reflect the destroyed quantity as well as lost quantity. Because of this reason, the exergy efficiency is usually found to be less than energy efficiency. Jegadheeswaran et al. (2010) summarized latent TES comparison for energy and exergy efficiency, which is redrawn in Figure 5.1.
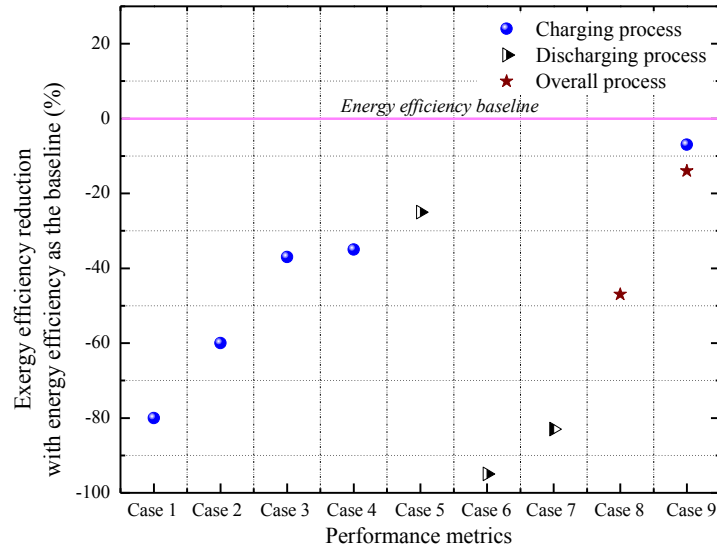
Figure 5.1: Energy and exergy efficiency comparison for latent TES
(Jegadheeswaran et al., 2010)

5.2.2   Exergy based system performance evaluation

As discussed earlier, appropriate values of operating and design parameters can benefit the system storage performance. This section reviews the research work with exergy based system performance evaluation and optimization. Basically, the influencing parameters can be HTF inlet temperature, mass flow rate or velocity and heat exchanger geometry.

For latent TES system, with larger the difference between the inlet HTF temperature and PCM unit temperature, the entropy generation is greater. Entropy generation is directly proportional to finite temperature difference. Therefore, in order to minimize the entropy generation and maximize exergy efficiency, the difference between the inlet HTF temperature and PCM unit temperature should be small. But smaller temperature difference will lead to lower heat transfer rate. There exists a compromise between the heat transfer charging rate and exergy efficiency.

One study by El-Dessouky and Al-Juwayhel (1997) proved that entropy generation number could be reduced by increasing the HTF (air/water) inlet temperature during discharging. Based on the literature review, the mass flow rate of HTF can also influence the exergy efficiency a lot. As for the mass flow rate, the well-known dimensionless number called Reynolds (Re) number is widely used. Higher Re number indicates higher mass flow rate and vice versa. One study by Kousksou et al. (2007) reported that the effect of velocity of HTF on the entropy generation number is almost negligible. This is because in the numerical model, the pressure drop is neglected and the effects of

variation in velocity (responsible for pressure drop) on entropy generation number could not be explored. In theory, with a larger Re number, the pressure drop is higher, and thus, entropy generation is higher. However, the research on latent TES by Kousksou et al. (2008) and Erek and Dincer (2008) did not show the effect. Other researchers argued that the higher value of mass flow rate of HTF does not increase heat transfer rate considerably either charging or discharging process for latent heat storage unit, and the reason was given that HTF side heat transfer coefficient has very small role in determining the phase change rate. Basically the HTF inlet temperature has greater influence than mass flow rate, as shown in Figure 5.2 for latent TES system (Akif Ezan et al., 2010). From the discussion above, it is necessary to mention that the inherent mechanism for effect of mass flow rate on exergy efficiency should be further investigated.
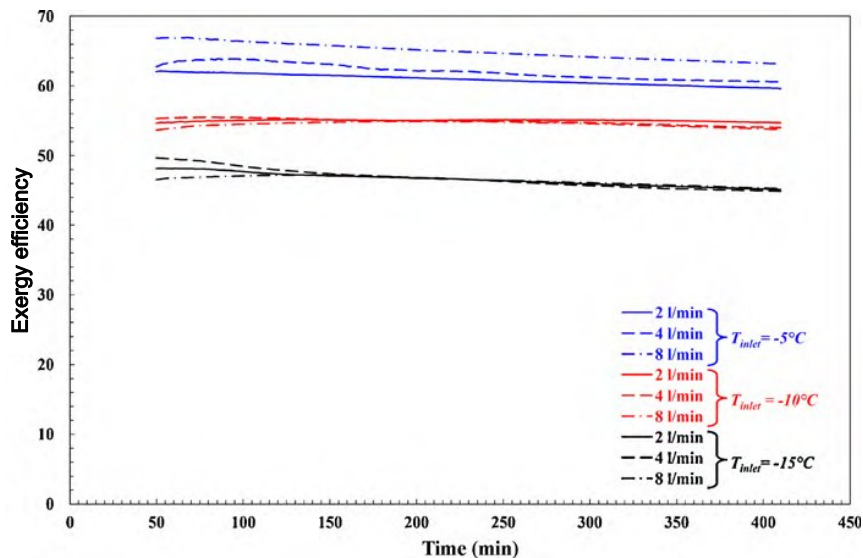
Figure 5.2: Effect of the inlet temperature and flow rate on the exergy efficiency-charging mode (Ezan et al., 2010)

In addition, tube material and length can also influence the exergy. As shown in Figure 5.3 (Ezan et al., 2010), with larger thermal conductivity of tube material, the exergy efficiency is also increased. In another study by Ezan et al. (2011), energy and exergy efficiencies increase with increasing the length of the tube. Besides, with increasing the tube length, effect of the flow rate on exergy efficiency becomes clearer. With increased tube length (as shown in Figure 5.4), even the pressure drop is larger, the thermal efficiency is increased. Further research still need to determine the main contributions for entropy generation, such as pressure drop irreversibility and heat transfer irreversibility.
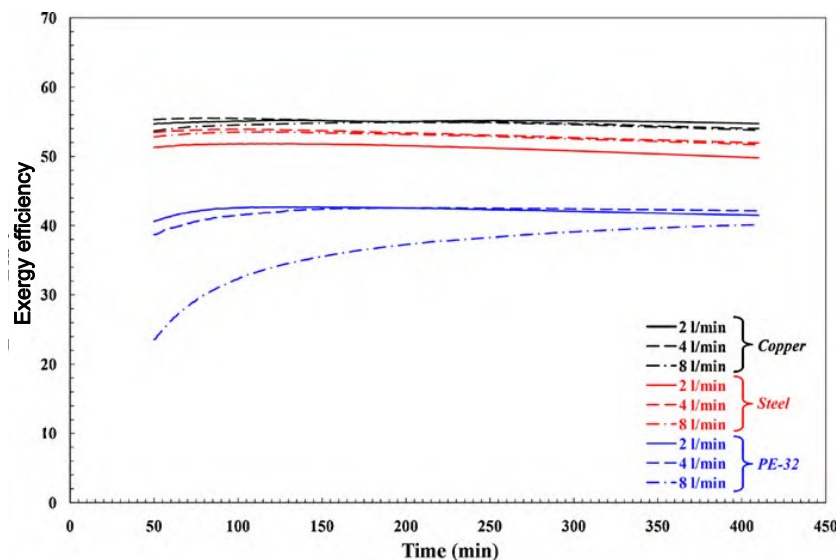
Figure 5.3: Effect of the tube material on the exergy efficiency—charging mode
(Ezan et al., 2010)
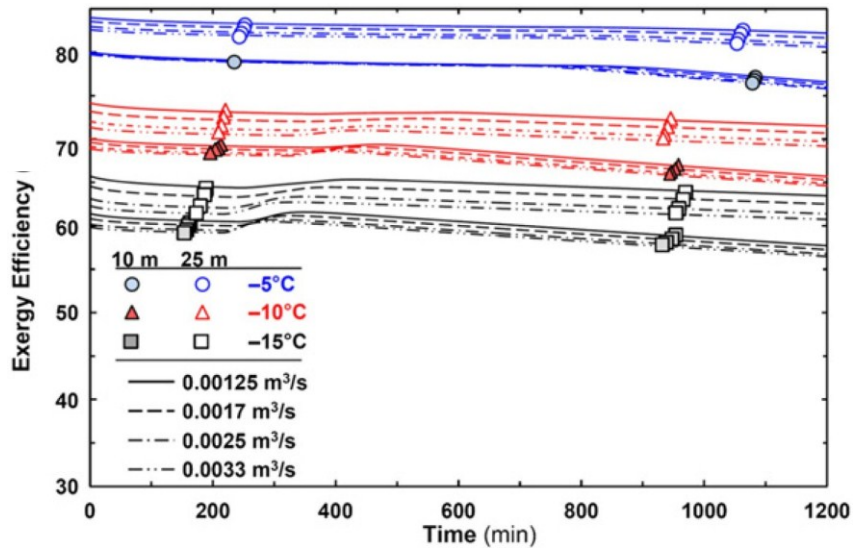
Figure 5.4: Effects of tube length and flow rate of HTF on Exergy efficiency
(Ezan et al. 2011)

Some studies also did some work on the influence of system dimensions, as shown in
Figure 5.5. It is understood that increasing the diameter and decreasing the length of unit
can lead to the pressure drop in the HTF flow. Erek and Dincer (2008, 2009) have
reported for discharging process, that increasing shell radius reduces the entropy
generation number considerably. While with a larger shell radius, the natural convection,
which is dominated in the melting process, will lead to a larger heat transfer rate. It may
also lead to larger irreversibilities because of the faster interface motion and liquid
viscosity. Therefore, more work need to be investigated to reveal the main contribution
for irreversibilities: heat transfer irreversibilities and pressure drop irreversibilities.
Currently there are limited rearch regarding the exergy evaluation with influencing
factors for sorption storage. More future work should be developed for exergy-based
system performance evaluation.
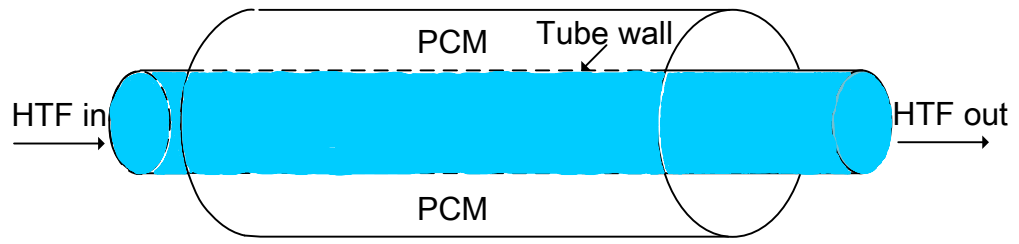
Figure 5.5: Shell and tube heat storage unit

6 Experimental Apparatus and Procedure for Adsorption Storage

This chapter introduces the experimental apparatus and procedure for adsorption heat and cold storage. The operation principle and test facility are introduced first. Then instrumentation and DAQ system, test procedure and data analysis together with test matrix are introduced.

6.1 Test facility

6.1.1 Operation principle

First, the principle of heat storage is introduced as shown in Figure 6.1. During the charging process, thermal energy is used to regenerate the adsorbent in the desorption bed. The adsorbate vapor (i.e. refrigerant) is separated from desorption bed and condensed into liquid phase by ambient cooled coils in the condenser. The liquid refrigerant is stored in the condenser. At the beginning of the charging process, the pressure in the desorption bed and condenser increases greatly. Finally, the pressures of desorption bed, condenser are at the saturation pressure of the ambient temperature. Desorption bed and condenser during charging process become adsorption bed and evaporator during discharging process, respectively. At the beginning of discharging process, lower HTF temperature of adsorption bed makes adsorption chamber pressure lower than saturation pressure of the ambient temperature. With the valve between adsorption bed and evaporator opens, the pressure of the two chambers decreases and the adsorbate (refrigerant) is forced to be in adsorption phase inside adsorbent and the reaction latent heat is released, carried by the

141

heat transfer fluid to meet the loads. During the discharging process, falling film coils is used as evaporator to supply heat for liquid adsorbate evaporation.

Regarding cold storage, during the charging process, thermal energy is used to regenerate the adsorbent in the desorption bed. The adsorbate vapor (i.e. refrigerant) is separated from desorption bed and condensed into liquid phase by ambient cooled coils in the condenser. The liquid refrigerant flows to the evaporator and is stored there. Finally, the pressures of desorption bed, condenser and evaporator are at the saturation pressure of the ambient temperature. Before the discharging process, the adsorption bed is first cooled at the ambient conditions (i.e. pre-discharging process) refrigerant vapor is adsorbed by the adsorbents. Therefore, its pressure decreases greatly and is below the saturation pressure of the ambient temperature. As discharging process begins, the refrigerant is evaporated by absorbing heat from the chilled water coil so that the cooling is produced in the evaporator to meet the loads. The pressure difference between the evaporator and adsorption bed forces refrigerant flows from evaporator to adsorption bed. The irreversibility in this process is the mass transfer driving force, i.e. finite pressure difference and the sequence is a temperature difference between stored thermal energy and released thermal energy.
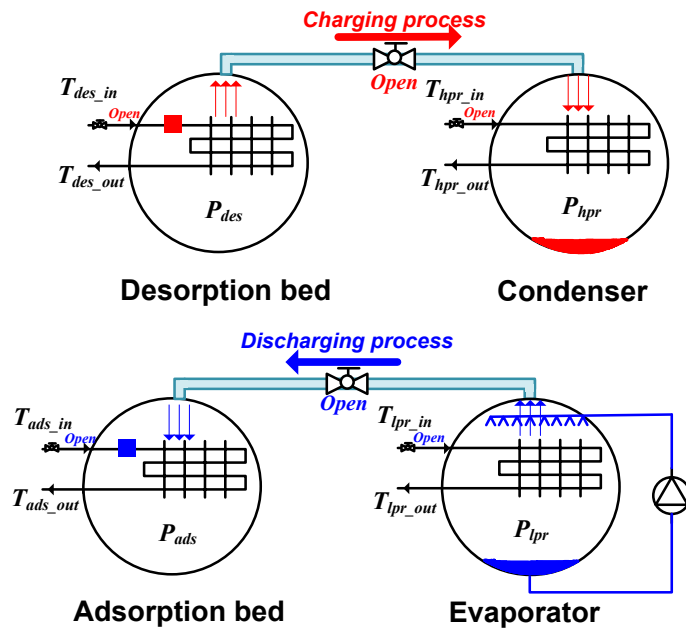
(a) Heat storage
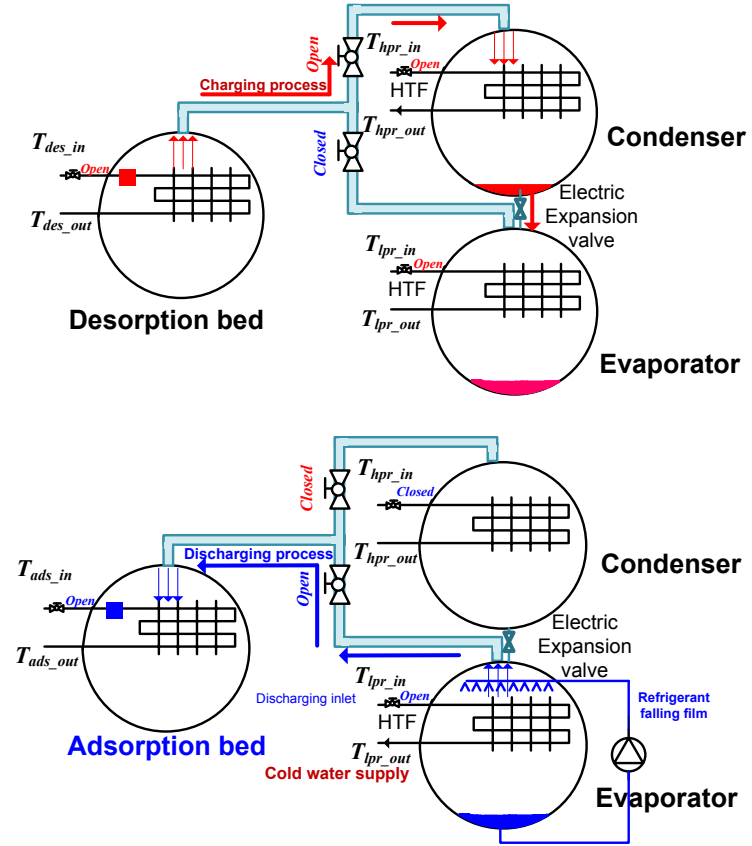
(b) Cold storage

Figure 6.1: Operation principle for adsorption thermal energy storage

In this project, Mitsubishi Plastic (MPI) FAM-Z01 is proposed as the adsorbent bed material and water is the refrigerant. The isotherm curves in Figure 6.2 shows the mass fraction (also loading) of adsorbate in equilibrium state as a function of pressure ratio between adsorbate reservoir and saturation pressure of adsorbent bed. At the end of charging process, the regenerated adsorbent has less adsorbate residual and the mass fraction is low, i.e. blue point. At the end of discharging process, the mass fraction reaches a high value, i.e. red point. The differential loading between two operating points contributes to the thermal energy storage.
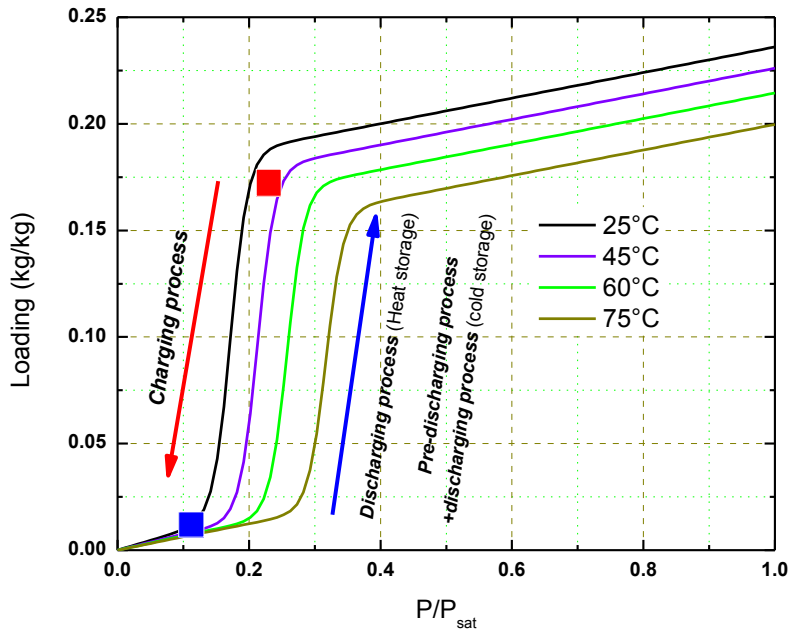
Figure 6.2: Charging/discharging process of adsorption heat storage on Z01 isotherm chart

6.1.2 Experimental apparatus

Different chambers of sorption beds and condenser/evaporator, which were housed in each own cylindrical vacuum chamber, are shown in Figure 6.3. A steel flange on one side of each chamber supported a one inch thick plate of Lexan to enable viewing inside of the heat exchangers during adsorption thermal storage operation. The hot water can be supplied by a 220-gallon water storage thermal buffer tank, which is heated by the prime mover, named "ecopower" (currently a reciprocating internal combustion spark ignition engine). Three constant speed pumps circulate heat transfer fluid (water) for sorption bed, condenser and/or evaporator. The heat flows between components are regulated by electronically actuated mixing/diverting valves that control the amount of water recirculation. Thermocouples and mass flow meters throughout the system are used to test the system storage performance. Specifications are provided in Table 6.1 as follows.

Table 6.1: Specifications of adsorption thermal storage system

Component/operation parameter of adsorption thermal storage system	Specification
Working pair (refrigerant/adsorbent)	water/zeolite
Adsorber HX finned-volume dimensions (excludes headers and u-tubes)	600 x 264 x 102 mm
Calculated adsorbent mass (per HX)	2.80 kg
Adsorbent substrate area (per HX)	16.7 m^2
Charge of HTF (per HX, excl. headers)	2.47 L
Nominal driving temperature	around 70°C
Heat transfer fluid (HTF) type	water
Refrigerant falling film flow rate	40~70 g/s
CHW flow rate	30~100 g/s
HTF flow rate – condenser	40~60 g/s
HTF flow rate – adsorber	10~80 g/s
HTF flow channels and feedthroughs	20.0 mm ID steel/copper/PEX
HTF ball valves	19.1 mm ID stainless steel
Refrigerant vapor feedthroughs	63.5 mm ID steel
Refrigerant vapor flow channels	50.8 mm ID steel/copper
Refrigerant vapor ball valves	50.8 mm ID brass
Vacuum chamber interior volume (empty)	52~61 L (various lengths)
Condenser/Evaporator tube surface area	0.0023 m^2

(a) Heat storage
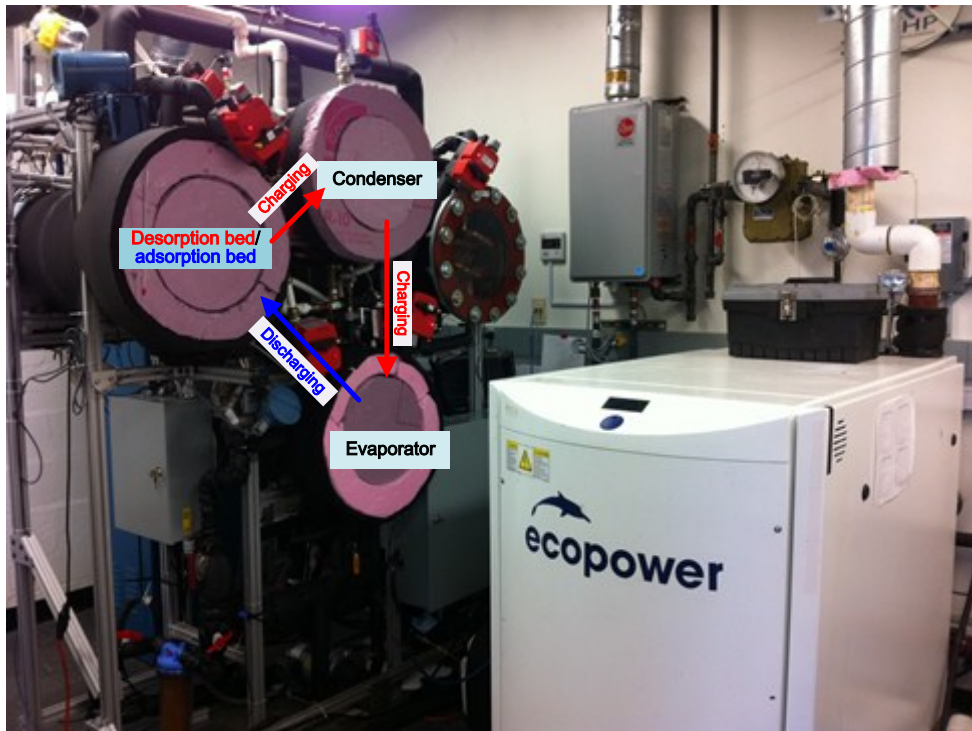
(b) Cold storage

Figure 6.3: Schematic of test facility

The adsorber heat exchanger (Figure 6.4), which was inside of the sorption bed were obtained through a donation from Mitsubishi Plastic. They are copper tube and aluminum plain fin type with 12 parallel four-pass circuits and a 0.25 mm thickness coating of Z01 zeolite on all fin and tube surfaces. Headers are 25.4 mm in outer diameter.
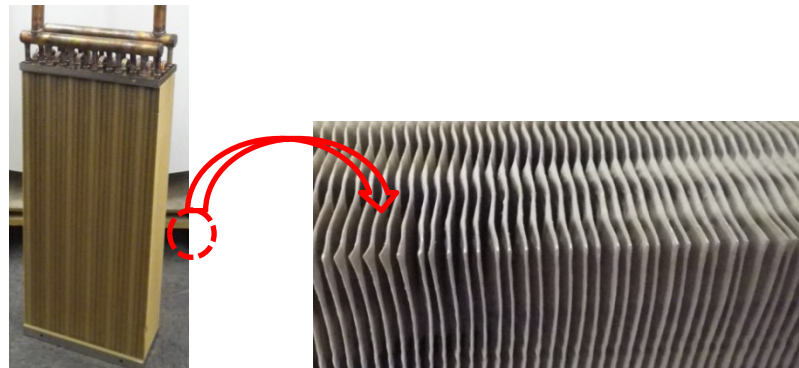
(a) Prototype of adsorber heat exchanger (b) Close-up of adsorber heat exchanger coated fins
(1.8 mm fin spacing, 0.115 mm fin thickness, 0.25 mm zeolite coating thickness)

Figure 6.4: Adsorber heat exchanger used in sorption bed

The condenser/evaporator, shown in Figure 6.5, was also soldered together with 22.23 mm OD copper pipe and fittings. The horizontal tubes were stacked vertically in two columns so that refrigerant dripping off would fall directly to the chamber bottom. It will be evaporator chamber during discharging process, and the tubes were carefully leveled so that the refrigerant would fall in film form from one tube onto the next. Distribution of the falling film was implemented with a combination of an orifice tube (the copper tube with many small orifices shown in the top of Figure 6.5(b)) to ensure even longitudinal distribution, and V-shaped aluminum distributor trays that made sure the orifice jets landed on the middle of the first tube in the evaporator. The HTF flowed on the inside and refrigerant flowed around the outside.

147
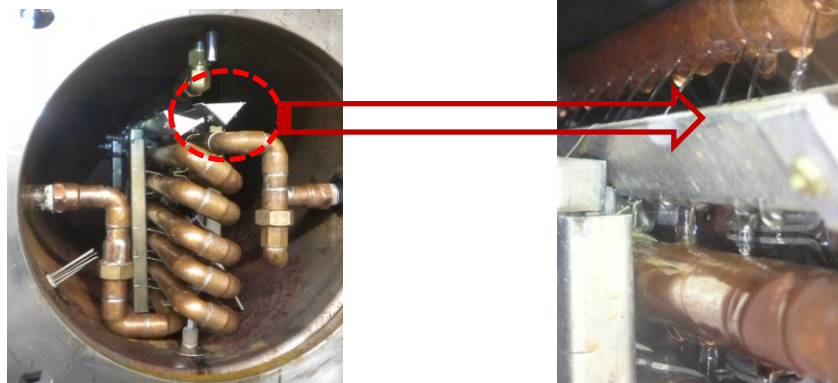
(a) Condenser/evaporator plumbed to chamber feed-through (b) Close up of falling film distributor

Figure 6.5: Condenser/evaporator chamber

6.2 Instrumentation and Data Acquisition (DAQ) system

The structure of the data acquisition process (DAQ) is shown in Figure 6.6. The measuring instruments (thermocouple, pressure transducer, mass flow rate meter) sends output signals (4~20 mA or 0~5 VDC) to National Instrument Field Point modules. Then the signals are received by the modules and transferred to a data acquisition personal computer. The LabVIEW main DAQ in the computer reads the signal and further processes them. The DAQ can convert signals to the unit of measure, such as temperature, pressure and mass flow rate for further data reduction techniques. Part of the processed data from DAQ can be used to control the mass flow rate, inlet temperature of the HTF for different chambers. The control was based on proportional- integral-derivative (PID) algorithm. In addition, the DAQ can also benefit of visualizing processes real time on the personal computer monitor. An array of all collected and processed data can be written to a Microsoft Excel spreadsheet, which can be used for further data analysis and visual formatting. The heat transfer fluid property database is also written in the DAQ software.

148
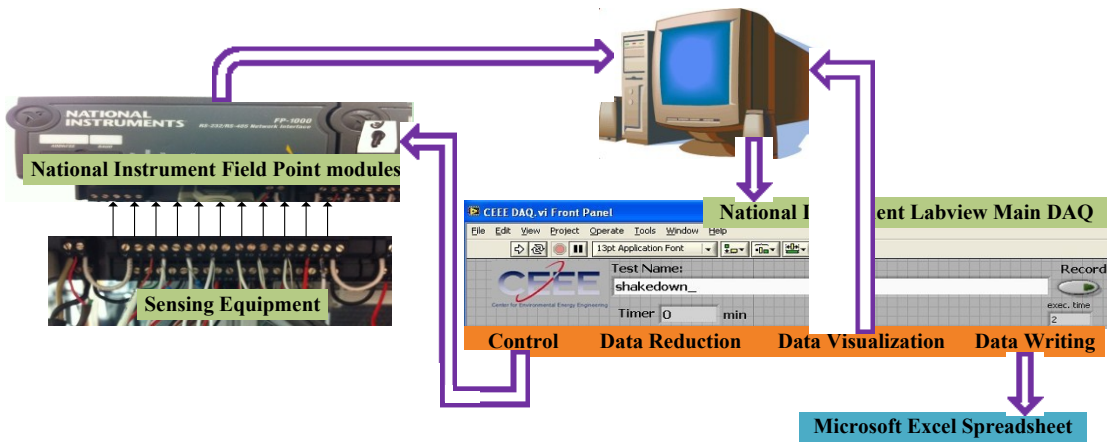
Figure 6.6: Data acquisition process structure

6.3 Data reduction process

Data reduction was performed within the LabVIEW data acquisition program. Property subroutines of HTF are an essential part of converting measurable data, such as temperature and pressure, into calculated parameters, such as specific heat capacity, and enthalpy. The HTF properties are used in LabVIEW to calculate fluid exchanger heat directly. Thermal energy storage performance is calculated as follows:

For charging process, the instant capacity for desorption bed is calculated as,

$$\dot{Q}_{des} = \dot{m}_{w,des} C_{p,w}(T_{des,in,w} - T_{des,out,w}) \hspace{3cm} \text{Equation 6.1}$$

$\dot{m}_{w,des}$ is HTF mass flow rate of the desorption bed, $T_{des,in,w}$ and $T_{des,out,w}$ are inlet and outlet HTF temperature.

Similarly, the instant capacity around condenser side is calculated as,

149

$$\dot{Q}_{cond} = \dot{m}_{w,cond} C_{p,w} (T_{cond,out,w} - T_{cond,in,w})$$

Equation 6.2

The total delivered energy into desorption bed during charging process is,

$$Q_{delivered} = Q_{des} = \int_{0}^{t_{charg}} \dot{Q}_{des} \, dt$$

Equation 6.3

The instant exergy flow and total exergy delivered into the desorption bed are,

$$\dot{Ex}_{delivered} = \dot{m}_{w,des} (\psi_{des,in,w} - \psi_{des,out.w})$$

Equation 6.4

$$Ex_{delivered} = Ex_{des} = \int_{0}^{t_{charg}} \dot{Ex}_{des} \, dt$$

Equation 6.5

For discharging process, the instant capacity for adsorption bed is calculated as,

$$\dot{Q}_{ads} = \dot{m}_{w,ads} C_{p,w} (T_{ads,in,w} - T_{ads,out,w})$$

Equation 6.6

Similarly, the instant capacity around evaporator side is calculated as,

$$\dot{Q}_{evap} = \dot{Q}_{evap,HTF} + \dot{Q}_{evap,falling\ film}$$
$$= \dot{m}_{w,evap} C_{p,w} (T_{evap,in,w} - T_{evap,out,w}) +$$
$$\dot{m}_{w,falling\ film} C_{p,w} (T_{falling\ film,in,w} - T_{falling\ film,out,w})$$

Equation 6.7

The total recovered energy during discharging process is,

$$Q_{recovered} = abs(Q_{ads}) = abs(\int_{0}^{t_{disch}} \dot{Q}_{ads} \, dt)$$ (Heat storage) Equation 6.8

$$Q_{recovered} = abs(Q_{evap}) = abs(\int_{0}^{t_{disch}} \dot{Q}_{evap} \, dt)$$ (Cold storage) Equation 6.9

The energy storage density (ESD) can be calculated as,

$$ESD = \frac{Q_{recovered}}{m_{adsorbent}}$$
Equation 6.10

The instant exergy flow, total exergy recovered and total exergy loss or destroyed from

the total process are,

$$\dot{Ex}_{ads} = \dot{m}_{w,ads}(\psi_{ads,in,w} - \psi_{ads,out,w})$$ (Heat storage)   Equation 6.11

$$Ex_{recovered} = abs(Ex_{ads}) = abs(\int_0^{t_{disch}} \dot{Ex}_{ads}\, dt)$$ (Heat storage)   Equation 6.12

$$\dot{Ex}_{evap} = \dot{m}_{w,evap}(\psi_{evap,out,w} - \psi_{evap,in,w}) +$$ (Cold storage)
$$\dot{m}_{w,falling\, film}(\psi_{falling\, film,out,w} - \psi_{falling\, film,in,w})$$
Equation 6.13

$$Ex_{recovered} = abs\,(Ex_{evap}) = abs(\int_0^{t_{disch}} \dot{Ex}_{evap}\, dt)$$ (Cold storage)   Equation 6.14

$$Ex_{destruction\, and\, loss} = Ex_{delivered} - Ex_{recovered}$$
Equation 6.15

The total energy efficiency and exergy efficiency are,
$$\eta = \frac{Q_{recovered}}{Q_{delivered}}$$
Equation 6.16

$$\epsilon = \frac{Ex_{recovered}}{Ex_{delivered}}$$
Equation 6.17

In addition, for discharging process for heat storage purpose, the HTF from the

adsorption bed is utilized to meet the load. The outlet HTF temperature from the

adsorption bed changes from high (such as 70°C) to low (such as 30°C) with time. In the

case that it is needed to determine the average outlet HTF temperature for adsorption bed,

the term target-based hot water temperature T_{target}, for example, 45°C, which can be the

bath water temperature for one kind of residential application, is used. If the outlet HTF

whole-discharging-mass-based average temperature can be regarded as the target

temperature during the discharging process at time t_{target}, it will be convenient to use the outlet HTF from adsorption bed to evaluate system performance.

$$\int_0^{t_{target}} \dot{m}_{ads} T(t)_{ads\_out} \, dt = T_{target} \int_0^{t_{target}} \dot{m}_{ads} \, dt \quad \text{(Heat storage)} \qquad \text{Equation 6.18}$$

The target based energy recovered, exergy recovered from adsorption bed, ESD and whole exergy lost are,

$$Q_{target\ recovered} = abs(\int_0^{t_{target}} \dot{Q}_{ads} \, dt) \qquad \text{(Heat storage)} \qquad \text{Equation 6.19}$$

$$Ex_{target\ recovered} = abs(\int_0^{t_{target}} \dot{Ex}_{ads} \, dt) \qquad \text{(Heat storage)} \qquad \text{Equation 6.20}$$

$$ESD_{target} = \frac{abs(\int_0^{t_{target}} \dot{Q}_{ads} dt)}{m_{adsorbent}} \qquad \text{(Heat storage)} \qquad \text{Equation 6.21}$$

$$Ex_{target\ lost} = Ex_{delivered} - abs(\int_0^{t_{target}} \dot{Ex}_{ads} \, dt) \qquad \text{(Heat storage)} \qquad \text{Equation 6.22}$$

The target based energy efficiency, exergy efficiency and total volume of hot water supply are calculated as,

$$\eta_{target} = \frac{Q_{target\ recovered}}{Q_{delivered}} \qquad \text{(Heat storage)} \qquad \text{Equation 6.23}$$

$$\epsilon_{target} = \frac{Ex_{target\ recovered}}{Ex_{delivered}} \qquad \text{(Heat storage)} \qquad \text{Equation 6.24}$$

$$V_{target\ recovered} = \frac{abs(\int_0^{t_{target}} \dot{m}_{ads} dt)}{\rho_{ads}} \qquad \text{(Heat storage)} \qquad \text{Equation 6.25}$$

After all these calculations, it will be convenient to compare system performance under different operation conditions. The loading difference is the difference of loading at the end of charging process and the loading at the end of discharging process, which can be obtained from the isotherm chart.

152

6.4   Uncertainty analysis

Uncertainty in an experimental testing has two components, namely systematic uncertainty and random uncertainty. The former comes from measurement device itself. On the other hand, the latter is due to the fluctuation in every data measured. Typically, the standard deviation is used for the random uncertainty. Then total uncertainty is the sum of systematic and random uncertainties. The temperature, pressure, and mass flow rate are measured directly. While during the data reduction process, non-measurable fluid properties, such as state enthalpy, state exergy, were calculated based on measured physical properties. These non-measurables were further used to determine system performance metrics, such as total energy delivered and recovered energy and exergy efficiency. Random uncertainty of non-measurables and performance metrics can be computed as their respective standard deviation, using following equation.

$$STD_{x_1,x_2,...,x_n} = (\frac{1}{n}((x_1 - \overline{x})^2 + (x_2 - \overline{x})^2 + \cdots + (x_n - \overline{x})^2))^{1/2} \qquad \text{Equation 6.26}$$

For any calculated parameter, the systematic uncertainty needs to be propagated by means of Pythagorean addition, shown for a function f and coefficients x_i from x_1 through x_n as follows:

$$\omega_{f(x_1,x_2,...,x_n)} = \left(\left(\frac{\partial f}{\partial x_1}\omega_{x_1}\right)^2 + \left(\frac{\partial f}{\partial x_2}\omega_{x_2}\right)^2 + \cdots + \left(\frac{\partial f}{\partial x_n}\omega_{x_n}\right)^2\right)^{1/2} \qquad \text{Equation 6.27}$$

The above equation implies that the relationship of any calculated parameter, i.e. enthalpy, to its measurable components, i.e. temperature and pressure, be evaluated.

Since all the tests conducted in this study are in transient process, transient uncertainty analysis should be performed using the uncertainty propagation table option in the Engineering Equation Solver software (EES). The absolute magnitude of a measured data can change significantly during the course of a test. Systematic uncertainty needs to be evaluated in every time step during the test and be integrated over the time of the experiment to determine the total uncertainty of accumulated performance parameters, such as total stored energy and recovered exergy, etc.

$$\omega_{accumulated} = \int_0^t \omega_{instant} dt \hspace{3cm} \text{Equation 6.28}$$

There were several types of measurements acquired during testing, such as mass flow rate, temperature, pressure, power, etc., as shown in Table 6.2. Accumulated uncertainty of transient results is provided by means of error bars in figures shown in Chapter 7.

Table 6.2: Systematic uncertainties of instrumentation and performance parameters

Instrument	Range	Absolute error	Relative error	Units
Ohio Semitronics Watt Transducers	0~1	-	0.01	kW
RTD Sensors	0~90	0.2	-	°C
Coriolis Micro Motion mass Flow Meters	0~0.10	-	0.005	kg/s
Sponsler Turbine Flow Meters	0~0.10	-	0.01	kg/s
T-Type Thermocouples	-200~350	0.5	-	°C
Main performance parameter				
$\dot{Q}_{des}, \dot{Q}_{ads}$			0.014	kW
$\dot{Q}_{cond}, \dot{Q}_{evap}$			0.019	kW
$\dot{Ex}_{des}, \dot{Ex}_{ads}$			0.026	kW
$\dot{Ex}_{cond}, \dot{Ex}_{evap}$			0.030	kW
Q_{des}, Q_{ads}			0.023	kJ
Q_{cond}, Q_{evap}			0.027	kJ
Ex_{des}, Ex_{ads}			0.030	kJ
Ex_{cond}, Ex_{evap}			0.035	kJ
η			0.037[†]/0.043[‡]	-
ϵ			0.047[†]/0.050[‡]	-

The values in this table for performance parameters are average uncertainty. [†]: heat storage. [‡]: cold storage

6.5   Test procedure and test matrix

As mentioned previously, the goal of this study is to investigate the effects of adsorption storage, such as HTF mass flow rate, HTF temperature for different chambers. First, the test procedure is listed as follows:

(1). Before a test, check chamber pressure and temperature, and use vacuum pump to vacuum each chamber to ensure there is no leakage and make each chamber at the initial pre-set condition. Push the green button for Ecopower on the back side, and start the "ecoServ" button in the personal computer to set the tank temperature (i.e. regeneration temperature). Start outdoor chiller and cooling water pump manually.

(2). To begin a test, choose "Adsorption TES" button from LabVIEW profile and wait until tank temperature approaches the pre-set regeneration temperature. Then set each parameter (such as HTF mass flow rate, HTF inlet temperature for charging and discharging process for different chambers) on the LabVIEW profile. After regeneration temperature has been achieved, for heat storage process, press "heat storage charging process" button, or for cold storage process, press "cold storage charging process" button, and start recording data in CEEE DAQ.vi. The charging process then begins. Wait until the inlet and outlet HTF temperature of desorption bed is very close and the difference for inlet and outlet HTF temperature of condenser is also quite small. Then the charging process has been finished and all valves between different chambers are closed at this moment. Then for heat storage process test, press "heat storage discharging process" button to begin discharging process. For cold storage process test, press "cold storage

pre-discharging process" button first to ensure the adsorption bed is cooled at the pre-set ambient conditions for a period of time. Then press "cold storage discharging process" button and discharging process begins. Similarly, the discharging process will be finished when the inlet and outlet HTF temperature of adsorption bed is very close and the difference for inlet and outlet HTF temperature of evaporator is also quite small.

(3). After a test, press "shutdown" button and stop recording data. Stop Ecopower by press "CHP off" button from the "ecoServ" profile. Stop the outdoor chiller and cooling water pump manually.

Usually it takes around one or two hours to ensure normal system operation for each test. If the initial temperature of hot water tank is low (perhaps it is the ambient temperature), it takes a longer time (around three hours) for the water tank to achieve the regeneration pre-set temperature. During the period of shakedown test, it took more than one month to adjust the PID control parameters or change LabVIEW control strategies to minimize the HTF temperature fluctuation during the test. The issue of HTF temperature fluctuation could not be neglected at the early stage of this project, because the water loop from outside chiller to the chamber was long and the response time was so slow, and there are many valves in different HTF loop. Luckily, this issue was eased later with better LabVIEW control strategies, so storage performance could be accessed and analyzed.

The HTF inlet temperature of condenser was pre-set as the ambient temperature. The heat storage test is "short-term" (it can be used in several days), and it assumes that the sorption chamber is in good insulation. The test matrix is shown in Table 6.3.

Table 6.3: Test matrix

(a) Heat storage mode

Effect factor		Charging process			Discharging process			Performance
		T_{des}(℃)	T_{cond}(℃)	$\dot{m}_{des}$(kg/s)	T_{ads}(℃)	T_{evap}(℃)	$\dot{m}_{ads}$(kg/s)	
$\dot{m}_{ads}$		70	30	0.080	30	30	0.050	Energy storage density,
		70	30	0.080	30	30	0.040	
		70	30	0.080	30	30	0.030	
		70	30	0.080	30	30	0.020	
		70	30	0.080	30	30	0.010	Energy efficiency;
$\dot{m}_{des}$		70	30	0.080	30	30	0.028	
		70	30	0.070	30	30	0.028	
		70	30	0.060	30	30	0.028	Exergy efficiency;
		70	30	0.050	30	30	0.028	
		70	30	0.040	30	30	0.028	
T_{ads}		70	30	0.080	45	30	0.028	Exergy destruction.
		70	30	0.080	40	30	0.028	
		70	30	0.080	35	30	0.028	$T_{initial.disch}$ is the initial temperature
		70	30	0.080	30	30	0.028	
T_{des}		76	30	0.080	30	30	0.028	of adsorption bed for discharging process
		73	30	0.080	30	30	0.028	
		70	30	0.080	30	30	0.028	
		67	30	0.080	30	30	0.028	
		64	30	0.080	30	30	0.028	
		61	30	0.080	30	30	0.028	
$T_{cond}=T_{evap}$		70	25	0.080	30	25	0.028	
		70	30	0.080	30	30	0.028	
		70	35	0.080	30	35	0.028	
T_{evap}		70	30	0.080	30	30	0.028	
		70	30	0.080	30	33	0.028	
		70	30	0.080	30	36	0.028	
$T_{sorp.bed\_disch}$	70	70	30	0.080	30	30	0.028	
	60	70	30	0.080	30	30	0.028	
	50	70	30	0.080	30	30	0.028	

(a) Cold storage mode

Effect factor	Charging process			Discharging process			Performance
	T_{des}(°C)	T_{cond}(°C)	$\dot{m}_{des}$(kg/s)	T_{ads}(°C)	T_{evap}(°C)	$\dot{m}_{evap}$(kg/s)	
$\dot{m}_{evap}$	70	30	0.060	30	30	0.040	Energy storage density,
	70	30	0.060	30	30	0.030	
	70	30	0.060	30	30	0.020	
	70	30	0.060	30	30	0.014	
T_{evap}	70	30	0.060	30	15	0.028	Energy efficiency;
	70	30	0.060	30	20	0.028	
	70	30	0.060	30	25	0.028	
	70	30	0.060	30	30	0.028	Exergy efficiency;
T_{ads}	70	30	0.060	20	30	0.028	
	70	30	0.060	25	30	0.028	
	70	30	0.060	30	30	0.028	Exergy destruction.
T_{des}	73	30	0.060	30	30	0.028	
	70	30	0.060	30	30	0.028	
	67	30	0.060	30	30	0.028	

157

7 Energy and Exergy Performance of Adsorption TES

This chapter mainly discusses energy and exergy adsorption TES performance with different influencing factors. At first, a complete charging and discharging process are introduced and then more details are analyzed regarding HTF flow rate and temperatures for different chambers.

7.1 Charging and discharging process performance of adsorption heat storage

The operating conditions for one overall charging and discharging heat storage process are listed as follows: T_{des}=70°C, T_{cond}=T_{evap}=T_{amb}=30°C, T_{ads}=30°C, $\dot{m}_{des,HTF}$=0.080 kg/s, $\dot{m}_{ads,HTF}$ =0.028 kg/s, $\dot{m}_{cond,HTF}$ = $\dot{m}_{evap,HTF}$ =0.050 kg/s. Different process performance is shown with experimental test data as follows.

Temperature profile of HTF during charging and discharging process with experimental investigation is shown in Figure 7.1. During charging process, the heat source temperature at $T_{des,in}$ (70°C) regenerated the desorption chamber, and drove the refrigerate water vapor to the condenser chamber and condensed there. The condense heat made the $T_{cond,out}$ increase about 5°C. After about 18 minutes, the charging process finished. During the discharging process, more refrigerant vapor would flow into the adsorption chamber. And this lead to a lower $T_{evap,out}$ than $T_{evap,in}$. The adsorption heat together with the sensible heat of adsorption chamber made a higher $T_{ads,out}$ (>30°C) for the heat loading purpose for building application. When the inlet and outlet of HTF

158
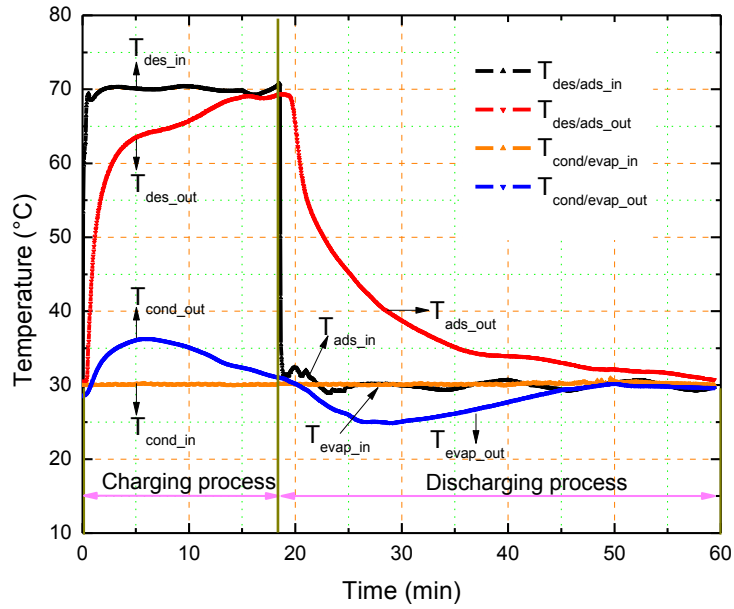
Figure 7.1: Temperature profile of HTF during charging and discharging process
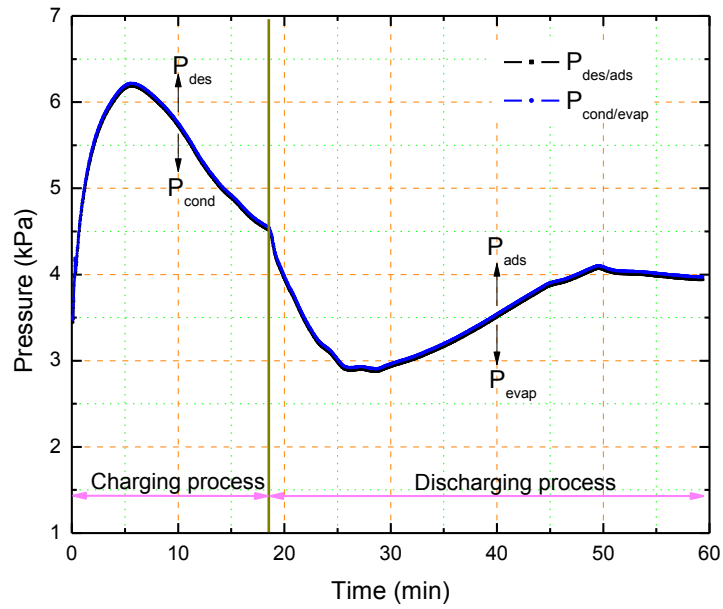
Figure 7.2: Pressure profile of chambers during charging and discharging process

temperature difference is small for adsorption chamber and evaporator chamber, the discharging process is finished. It took 42 minutes for the discharging process. Pressure profile of chambers during charging and discharging process with experimental investigation is shown in Figure 7.2. The high regeneration temperature made the pressure of desorption chamber and condenser chamber high while the low adsorption temperature made the pressure of adsorption chamber and evaporator chamber low.

HTF mass flow rate profile during charging and discharging process with experimental investigation is shown in Figure 7.3. During charging and discharging process, the HTF mass flow rates of condenser and evaporator remained constant while HTF mass flow rate of sorption chamber changed. This is because it is expected to have a quick charging process (larger $\dot{m}_{des,HTF}$) and a reasonable longer discharging process (usually smaller $\dot{m}_{ads,HTF}$).

Instant capacity of sorption bed during charging and discharging process with experimental investigation is shown in Figure 7.4. At the beginning of charging process, larger temperature gradient between inlet HTF and desorption bed together with larger HTF mass flow rate made a larger instant capacity for the desorption bed. Charging process ended when instant capacity was very small. Similarly, instant capacity was larger of the beginning for discharging process.
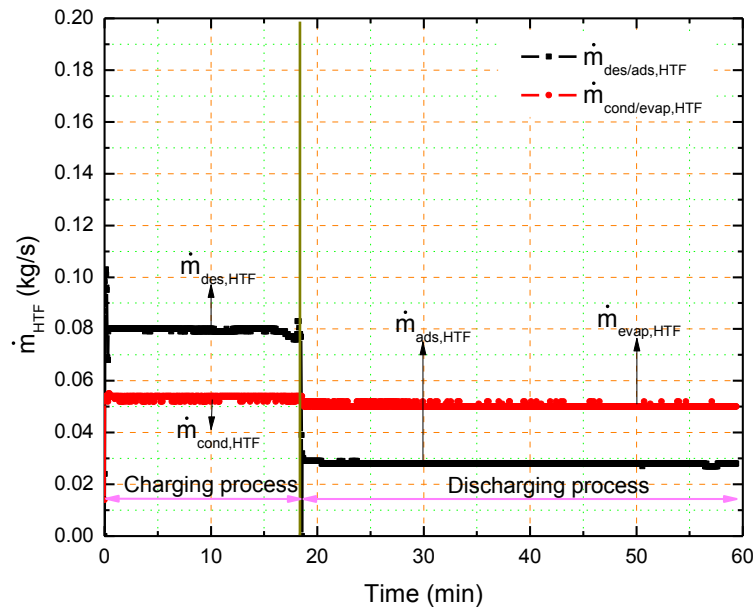
Figure 7.3: HTF mass flow rate profile during charging and discharging process
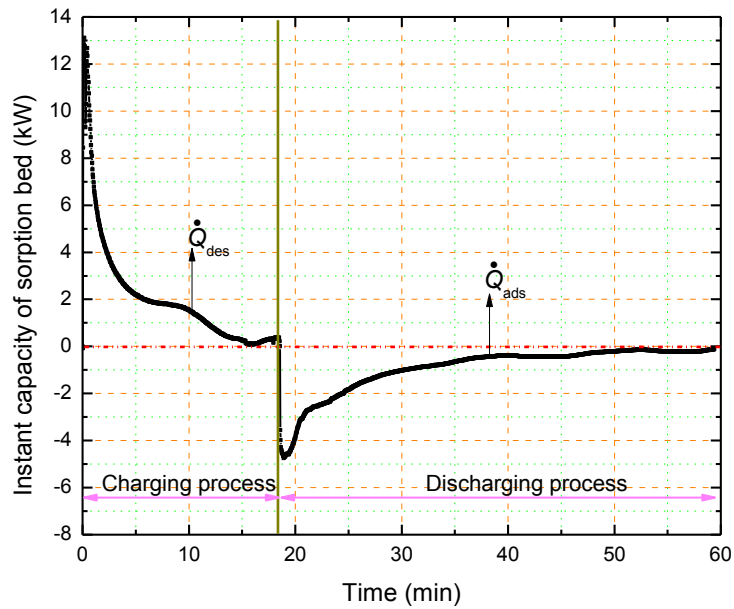
Figure 7.4: Instant capacity of sorption bed during charging and discharging process

161

Accumulated energy by HTF for sorption bed during charging and discharging process is shown in Figure 7.5. With the charging time or discharging time increased, the total energy delivered or energy recovered increased. The calculation showed that the energy efficiency is 95.9%. The loading difference is around 0.164 kg adsorbate/kg adsorbent. The analysis from adsorption bed showed that for the total recovered energy during discharging process, adsorption heat contributes 60.27% while the adsorption bed (including HTF, tubes, fins and adsorbents) sensible heat contributes 39.73%. The distribution for mass and thermal mass inside the adsorption bed is also shown in Figure 7.5. Among the thermal mass, the HTF is around 40% and the adsorbent is 27%.
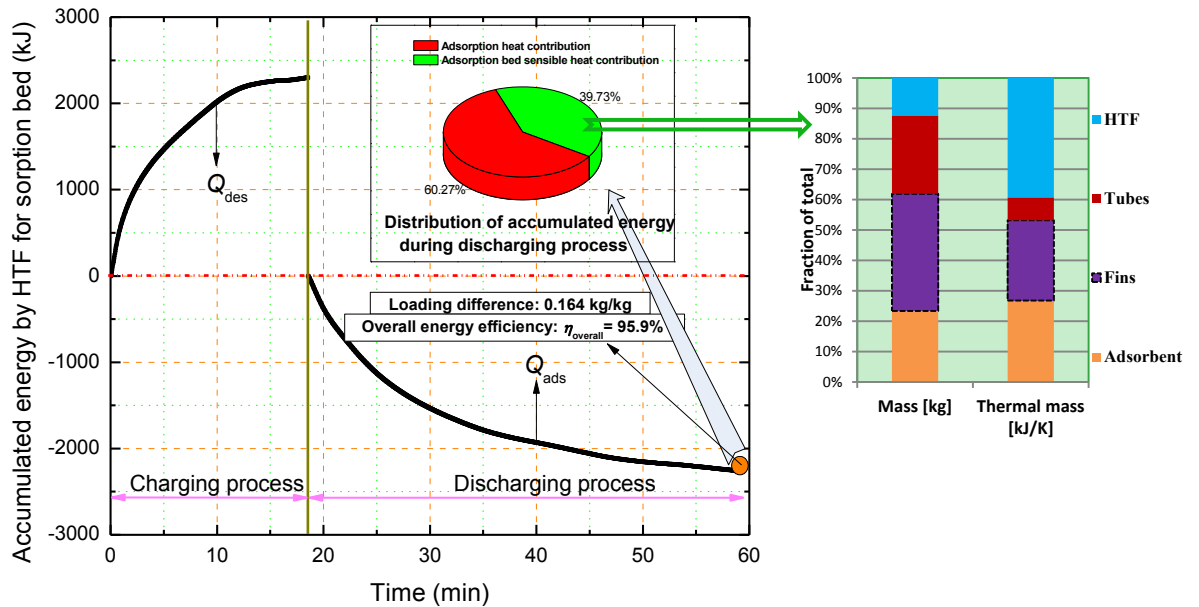
Figure 7.5: Accumulated energy by HTF for sorption bed during charging and discharging process

Instant exergy flow by HTF for sorption bed during charging and discharging process is shown in Figure 7.6. The instant exergy flow is larger at the beginning for the charging and discharging process. Accumulated exergy by HTF for sorption bed during charging and discharging process is shown in Figure 7.7. It showed that after 12 minutes for discharging process, the accumulated exergy did not change much, and the total exergy recovered was small in comparison with exergy delivered. The overall exergy efficiency was 26.7%.
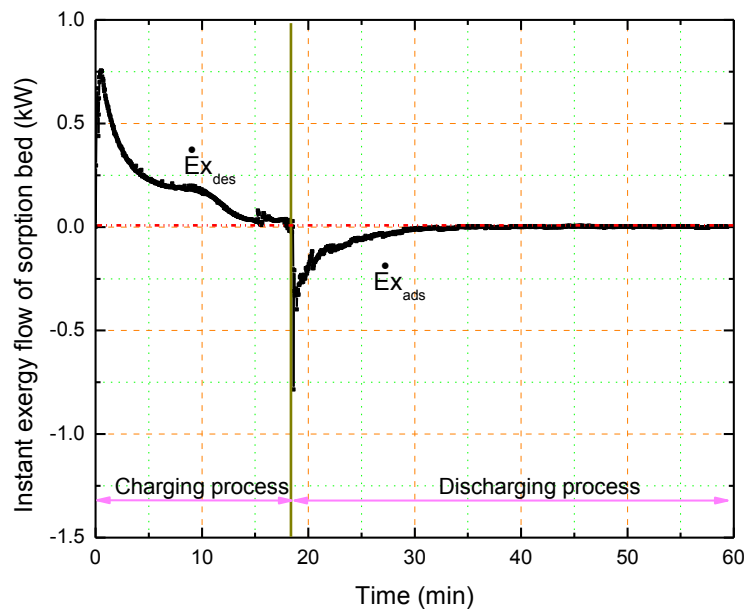
Figure 7.6: Instant exergy flow by HTF for sorption bed during charging and discharging process
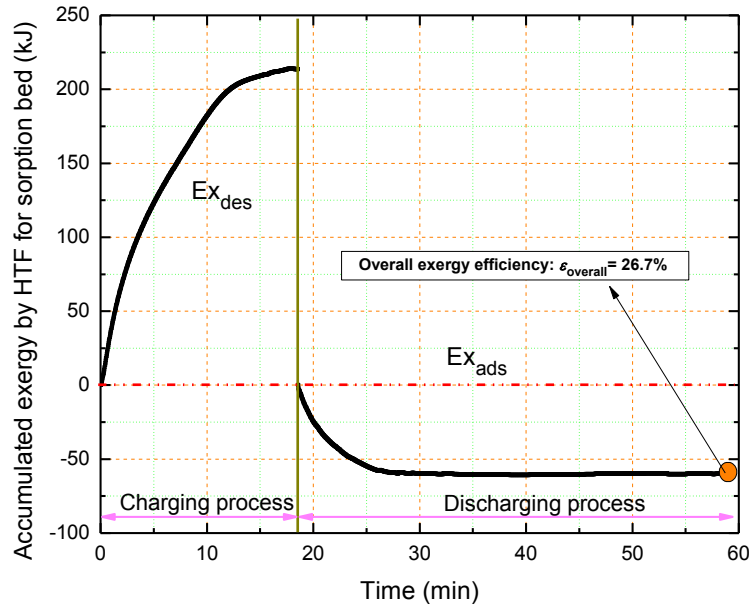
Figure 7.7: Accumulated exergy by HTF for sorption bed during charging and discharging process

Energy storage density and energy efficiency for different target-based hot water supply average temperatures is shown in Figure 7.8. With higher target-based hot water supply temperature, the energy storage density and energy efficiency reduced. The changes in exergy recovered, exergy efficiency and hot water supply volume are shown in Figure 7.9 and Figure 7.10. Similarly, the exergy recovered, exergy efficiency and hot water supply volume reduced with increasing hot water temperature.
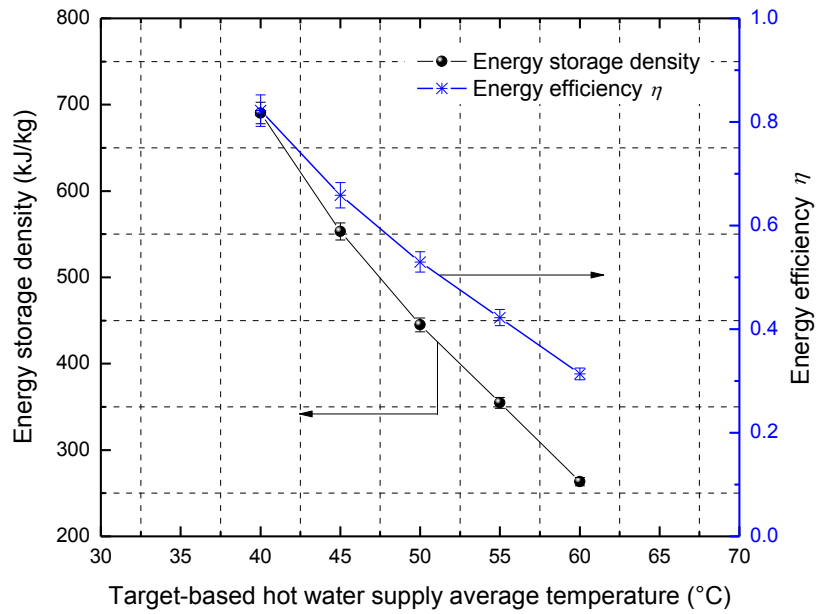
Figure 7.8: Energy storage density and energy efficiency for different target-based hot water supply average temperatures
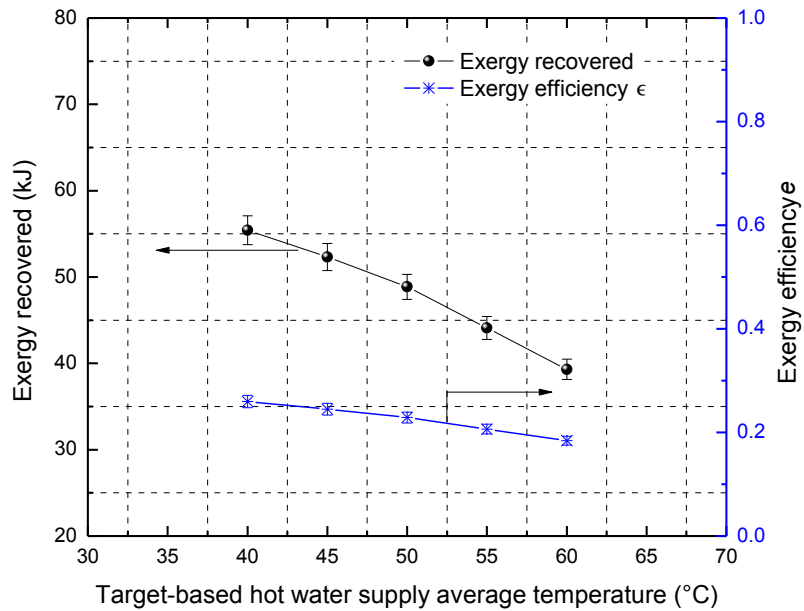
Figure 7.9: Exergy recovered and exergy efficiency for different target-based hot water supply average temperatures
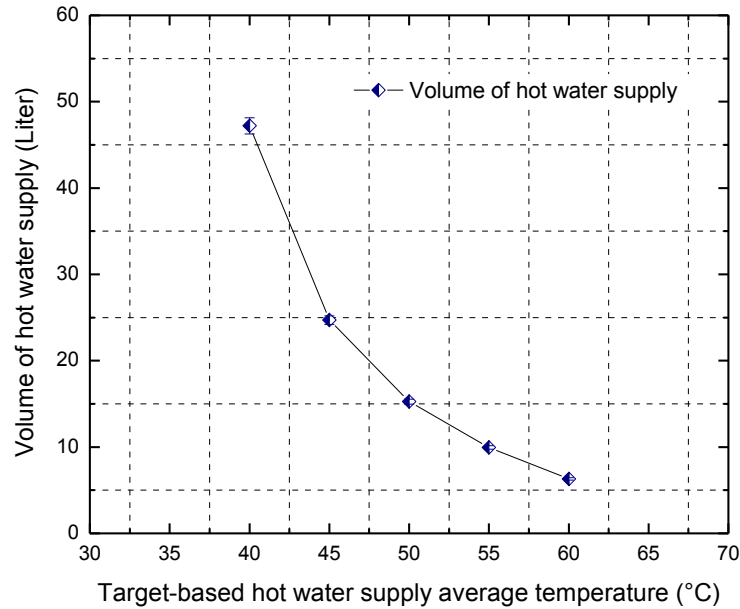
Figure 7.10: Hot water volume for different target-based hot water supply average temperatures

7.2   Effect factors on adsorption heat storage performance

7.2.1   Effect of HTF mass flow rate of adsorption bed on heat storage performance

Effect of HTF mass flow rate of adsorption bed for different target-based hot water supply average temperatures is shown in Figure 7.11 through Figure 7.13. For a single mass flow rate, energy and exergy-related performance including hot water supply volume is same to what discussed in Chapter 7.1. From Figure 7.11, it can be found that with smaller $\dot{m}_{ads,HTF}$, the storage density was higher. For the case of $\dot{m}_{ads,HTF}$=0.010 kg/s, it did not show any data on target-based hot water temperature of 40°C and 35°C, this is because the average hot water supply temperature throughout the discharging process was higher than 40°C. Similarly, there is no data on target-based hot water

temperature of 35°C for case $\dot{m}_{ads,HTF}$=0.020 kg/s and 0.030 kg/s. From Figure 7.12 and

Figure 7.13, it can be found that with smaller $\dot{m}_{ads,HTF}$, the exergy recovered and hot

water supply volume were larger. Possible explanation is that with smaller $\dot{m}_{ads,HTF}$, the

irreversibilities due to pressure drop are smaller. Therefore, more high-quality energy (i.e.

exergy) is recovered. For the experimental test for this project, sometimes the $\dot{m}_{des,HTF}$

was reduced manually at one point during the discharging process, and it could be

noticed that the $T_{ads,out}$ increased immediately. This suggests that if more hot water

(with higher temperature) is required, it would be better to reduce the $\dot{m}_{ads,HTF}$ in order

to fully use of the potential heat especially from adsorption heat.
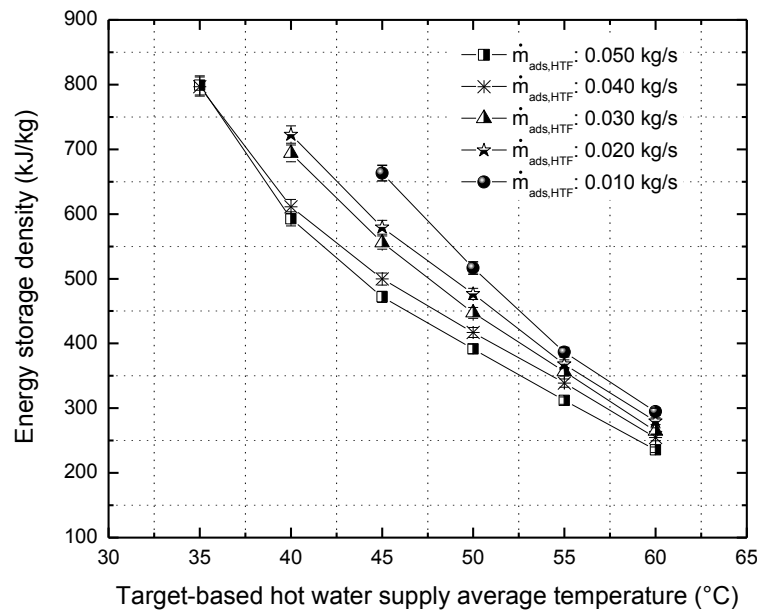
Figure 7.11: Effect of HTF mass flow rate of adsorption bed on energy storage density
for different target-based hot water supply average temperatures
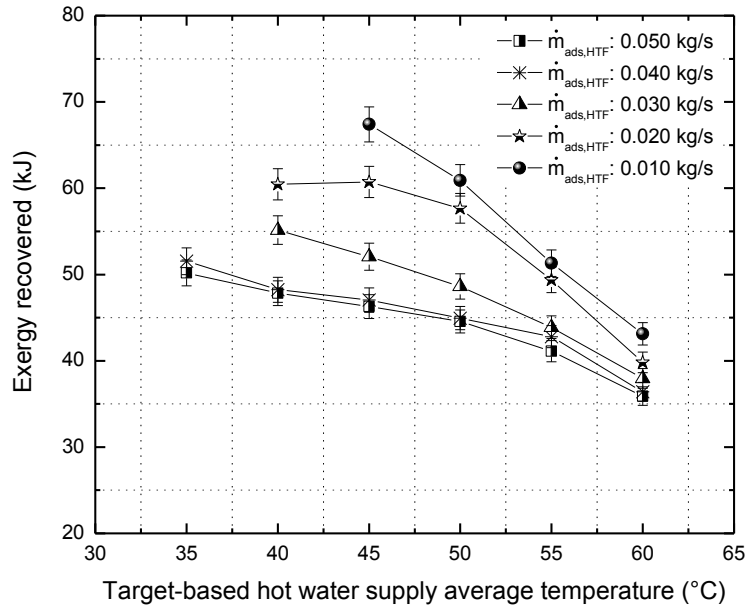
Figure 7.12: Effect of HTF mass flow rate of adsorption bed on exergy recovered for different target-based hot water supply average temperatures
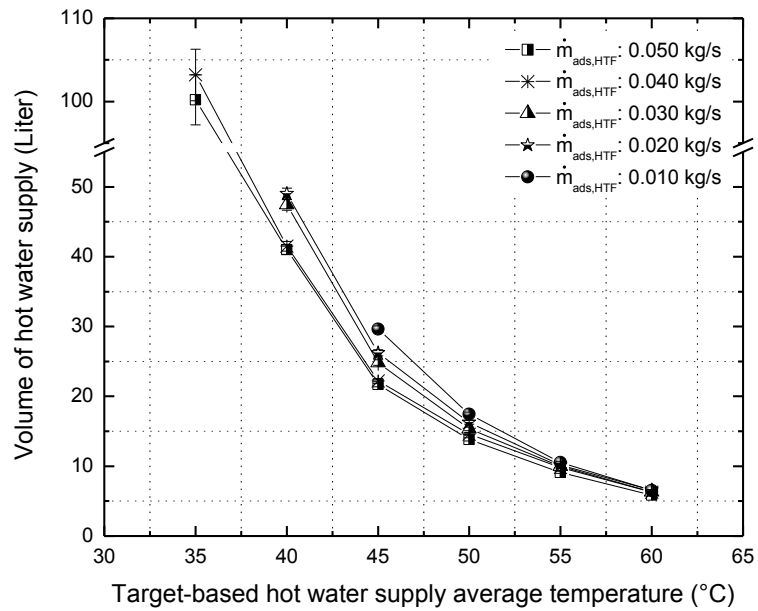
Figure 7.13: Effect of HTF mass flow rate of adsorption bed on hot water supply volume for different target-based water average temperatures

Effect of HTF mass flow rate of adsorption bed on overall storage performance metrics is shown in Figure 7.14. It can be found that total energy storage density, energy efficiency and loading difference increased with larger mass flow rate. While the exergy efficiency reduced. With larger mass flow rate, the total exergy destruction and loss increased, as shown in Figure 7.14, which means larger irreversibilities due to pressure drop are produced. Therefore, the exergy efficiency is reduced. Figure 7.15 through Figure 7.17 show the change of mass flow rate on instant capacity, specific exergy flow and chamber pressure in detail. With mass flow rate decreased in the discharging process, it is easy to get the conclusion that the instant capacity decreased, but the HTF outlet temperature of adsorption bed increased, which made the specific exergy flow (absolute value) and chamber pressure increased.
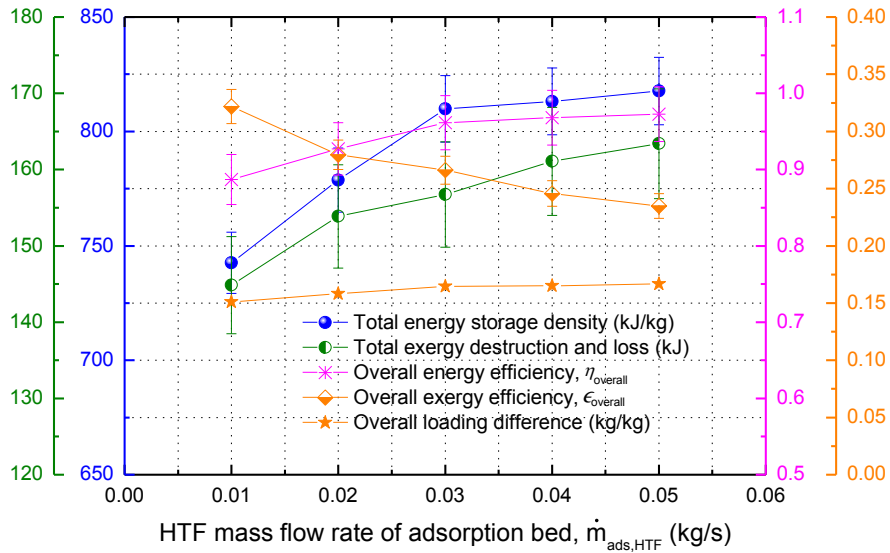
Figure 7.14: Effect of HTF mass flow rate of adsorption bed on storage performance metrics
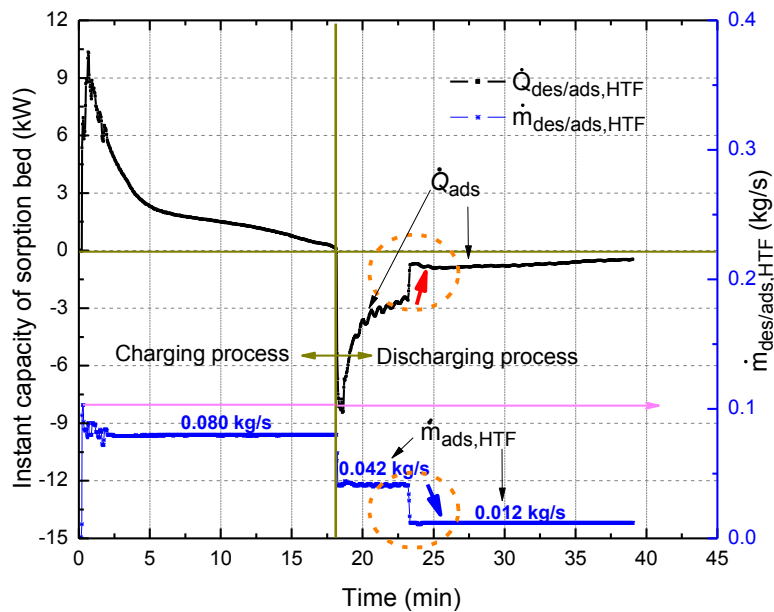
Figure 7.15: Effect of HTF mass flow rate change of adsorption bed on instant capacity
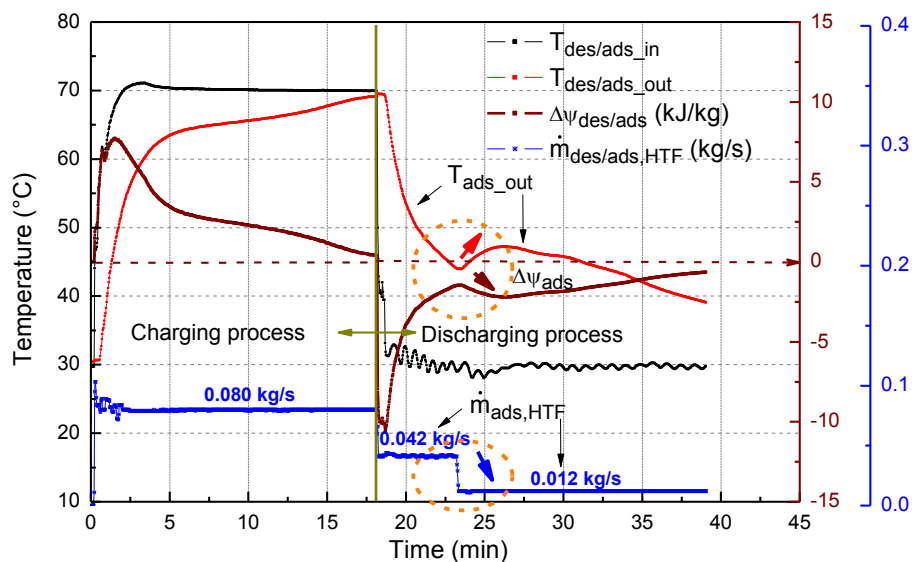
Figure 7.16: Effect of HTF mass flow rate change of adsorption bed on specific exergy flow

170
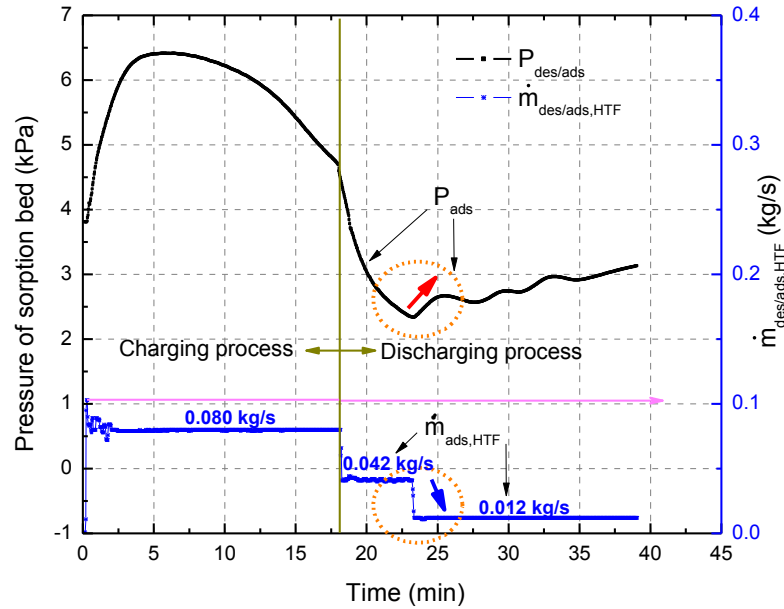
Figure 7.17: Effect of HTF mass flow rate change of adsorption bed on specific exergy flow

7.2.2 Effect of HTF mass flow rate of desorption bed on heat storage performance

Effect of HTF mass flow rate of desorption bed for different target-based hot water supply average temperatures is shown in Figure 7.18 through Figure 7.20. It can be found that even though different values of $\dot{m}_{des,HTF}$ used, the energy and exergy-related performance, and hot water supply volume did not change much. $\dot{m}_{des,HTF}$ is less sensitive than $\dot{m}_{ads,HTF}$ for target-based system performance. Further analysis for $\dot{m}_{des,HTF}$ showed that with larger $\dot{m}_{des,HTF}$, the energy storage density, exergy recovered and hot water supply volume were larger. Possible explanation is that with larger $\dot{m}_{des,HTF}$, the heat transfer rate is also larger, and the more energy and exergy are stored.

171
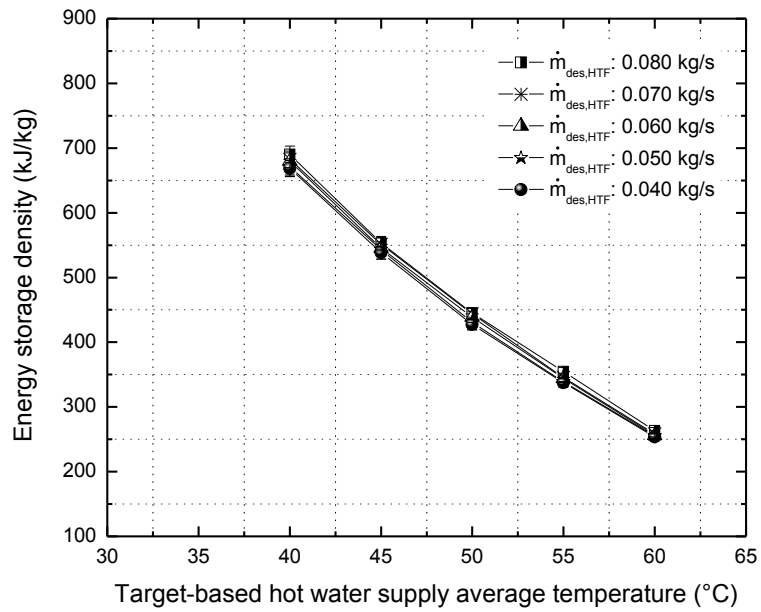
Figure 7.18: Effect of HTF mass flow rate of desorption bed on energy storage density
for different target-based hot water supply average temperatures
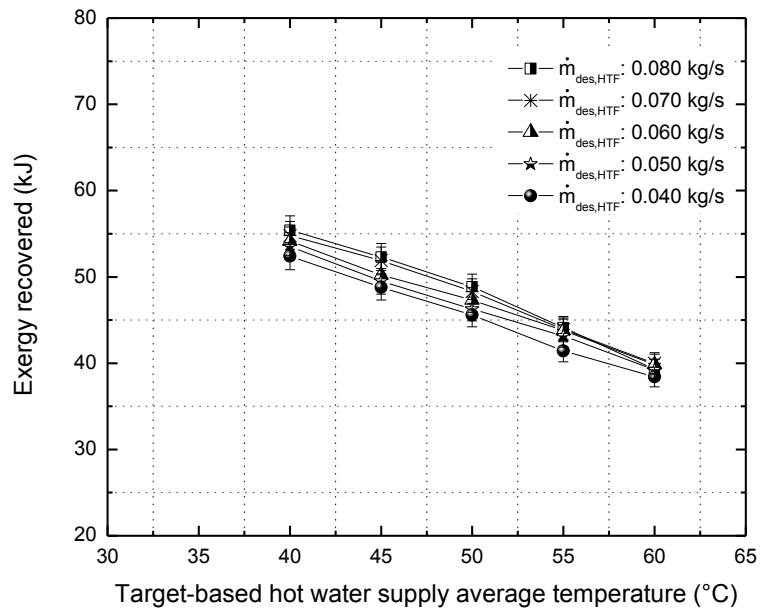
Figure 7.19: Effect of HTF mass flow rate of desorption bed on exergy recovered for
different target-based hot water supply average temperatures

172
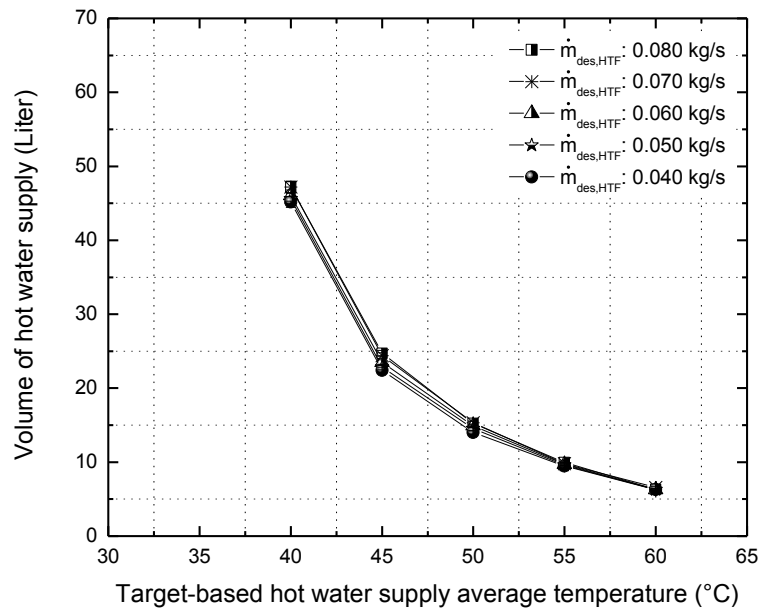
Figure 7.20: Effect of HTF mass flow rate of desorption bed on hot water supply volume for different target-based water average temperatures

Effect of HTF mass flow rate of desorption bed on overall storage performance metrics is shown in Figure 7.21. It can be found that total energy storage density, energy efficiency and loading difference increased a little with larger mass flow rate. While the exergy efficiency reduced. With larger mass flow rate, the total exergy destruction and loss increased, as shown in Figure 7.21, which also means larger irreversibilities due to pressure drop are produced. Therefore, the exergy efficiency is reduced. It should be noted that the exergy efficiency did not change much as compared with effect of $\dot{m}_{ads,HTF}$.
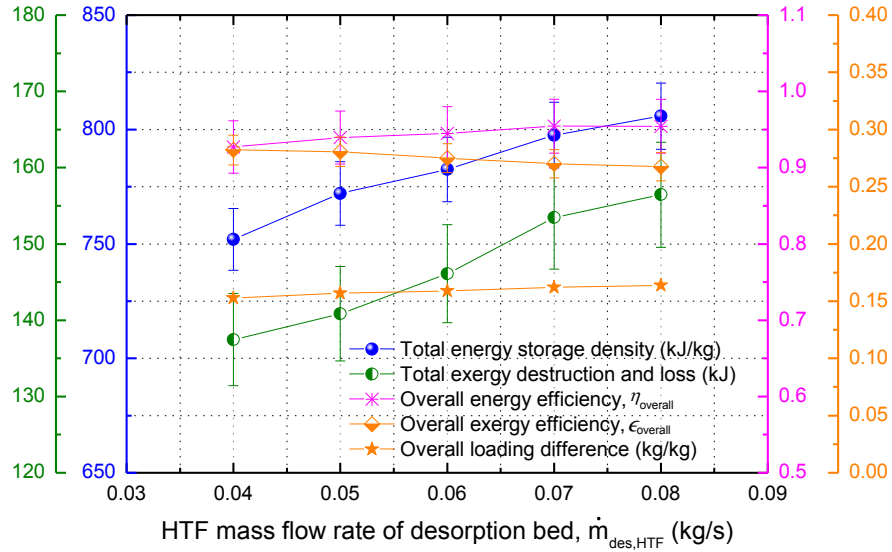
Figure 7.21: Effect of HTF mass flow rate of desorption bed on storage performance metrics

7.2.3   Effect of inlet HTF temperature for adsorption bed on heat storage performance

Effect of inlet HTF temperature for adsorption bed (adsorption temperature) for different target-based hot water supply average temperatures is shown in Figure 7.22 through Figure 7.24. It can be found that for with hot water supply temperature reduced, energy storage density increased greater for higher T_{ads} than that for lower T_{ads}. Similarly, the curve slope for higher T_{ads} is larger than that for lower T_{ads} for the performance of exergy recovered, and hot water supply volume.
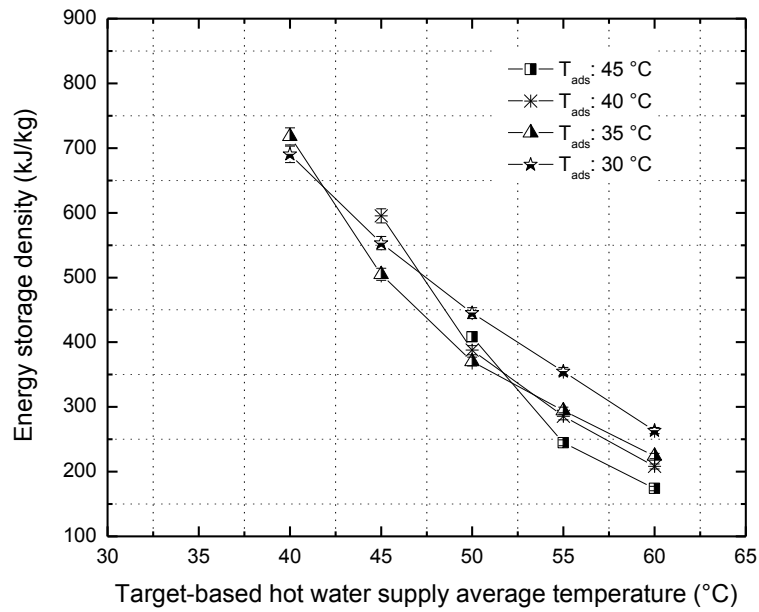
Figure 7.22: Effect of inlet HTF temperature for adsorption bed on energy storage density for different target-based water average temperatures
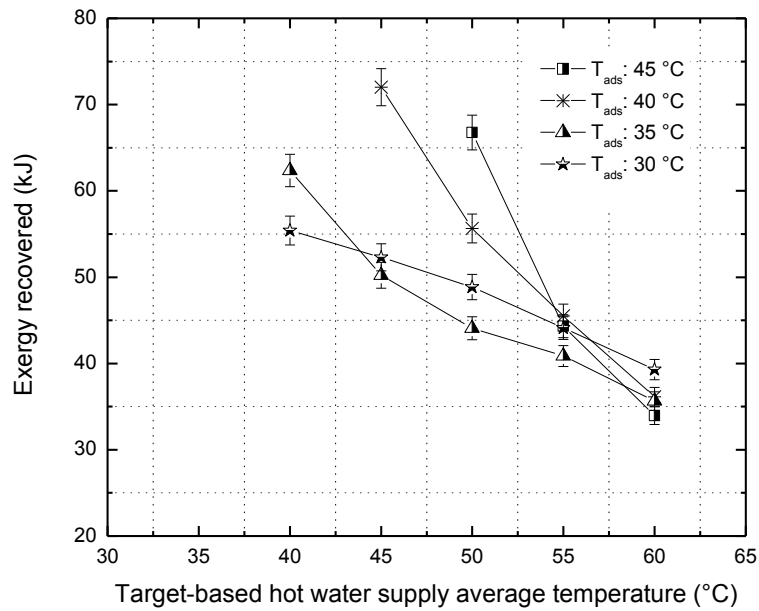
Figure 7.23: Effect of inlet HTF temperature for adsorption bed on exergy recovered for different target-based water average temperatures
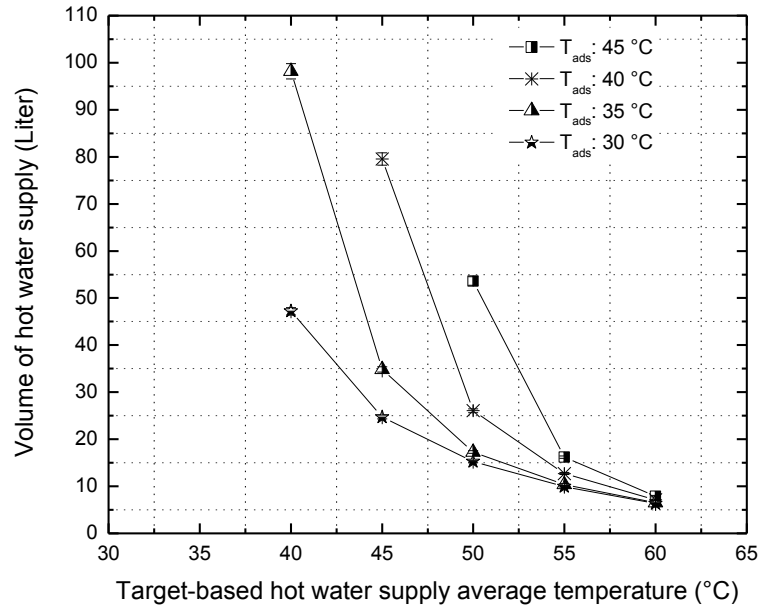
Figure 7.24: Effect of inlet HTF temperature for adsorption bed on hot water supply volume for different target-based water average temperatures

Effect of inlet HTF temperature for desorption bed on overall storage performance metrics is shown in Figure 7.25. It can be found that total energy storage density, energy efficiency and loading difference reduced with increasing adsorption temperature, while the exergy efficiency increased. Possible explanation is that the entropy generation is directly proportional to the finite temperature difference between adsorption temperature and HTF temperature. With higher adsorption temperature, the temperature difference was small, and the total exergy destruction and loss decreased, as shown in Figure 7.25, which also means less irreversibilities due to temperature difference are produced.
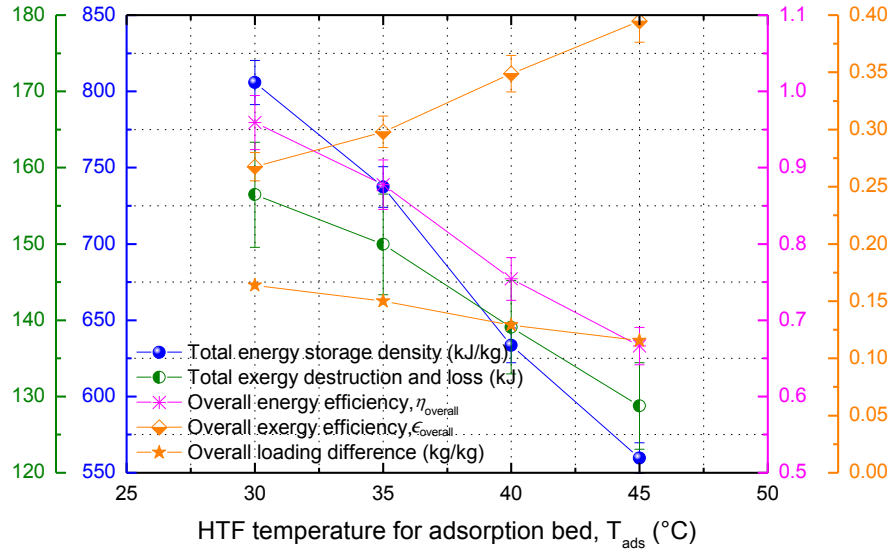
Figure 7.25: Effect of inlet HTF temperature for adsorption bed on storage performance metrics

7.2.4   Effect of inlet HTF temperature for desorption bed on heat storage performance

Effect of inlet HTF temperature for desorption bed (regeneration temperature) for different target-based hot water supply average temperatures is shown in Figure 7.26 through Figure 7.28. It can be found the higher T_{des} lead to a larger value for the energy storage density, exergy recovered, and hot water supply volume. Higher T_{des} leads to a larger heat transfer rate between desorption bed and HTF.
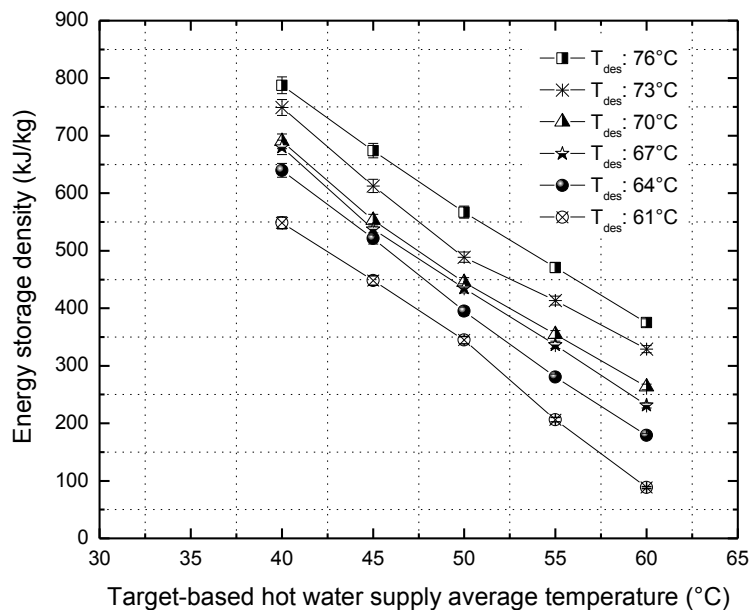
Figure 7.26: Effect of inlet HTF temperature for desorption bed on energy storage density for different target-based water average temperatures
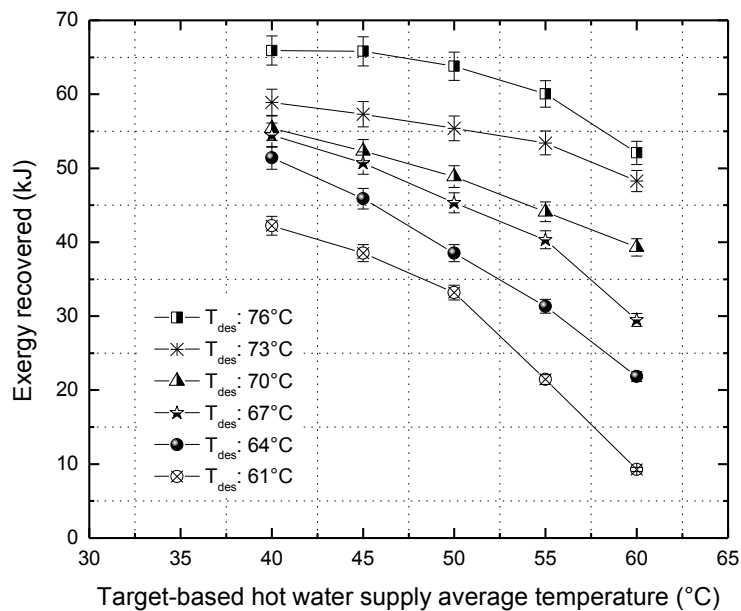
Figure 7.27: Effect of inlet HTF temperature for desorption bed on exergy recovered for different target-based water average temperatures

178
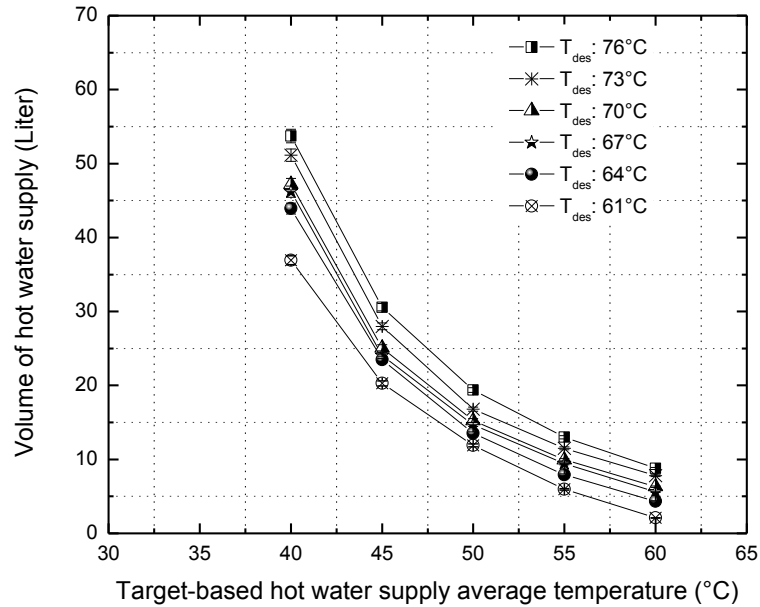
Figure 7.28: Effect of inlet HTF temperature for desorption bed on hot water supply volume for different target-based water average temperatures

Effect of inlet HTF temperature for desorption bed on overall storage performance metrics is shown in Figure 7.29. Similarly, it can be found that total energy storage density, energy efficiency and loading difference increased with desorption temperature. While the exergy efficiency reduced. This is attributed to the fact that the entropy generation is directly proportional to the finite temperature difference between regeneration temperature and HTF temperature. As shown in Figure 7.29, the total exergy destruction and loss increased with higher regeneration temperature, leads larger irreversibilities being produced due to temperature differences.
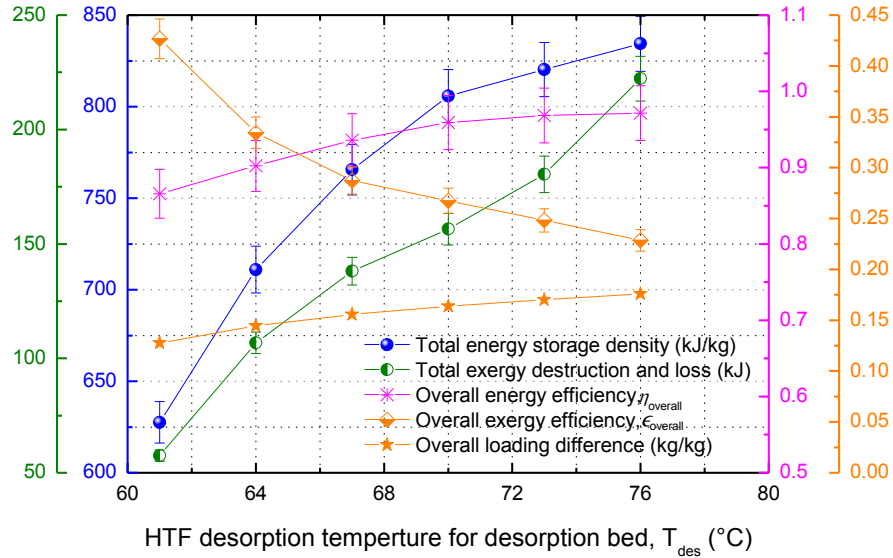
Figure 7.29: Effect of inlet HTF temperature for desorption bed on storage performance metrics

7.2.5 Effect of ambient temperature on heat storage performance

Effect of ambient temperature (condensing temperature and evaporating temperature are same to ambient temperature) for different target-based hot water supply average temperatures is shown in Figure 7.30 through Figure 7.32. It can be found that energy storage density and hot water supply volume were larger for higher ambient temperatureT_{amb}. For the case T_{amb}=25°C (<T_{ads}=30°C), for charging process, it had a higher accumulated energy, which can be calculated as 877 kJ/kg in the charging storage density format. For discharging process, because T_{amb}<T_{ads}, it severed as heat sink and removed a certain amount of energy and the adsorption heat could not be fully utilized. Therefore the storage density during discharging is small. Take target-based hot water

180

temperature 60°C for example, only 250 kJ/kg storage density was achieved. For the case T_{amb}=35°C ($>T_{ads}$=30°C), for charging process, it is easy to understand that it had a lower accumulated energy, which can be calculated as 802 kJ/kg in the charging storage density format. However for the discharging process, for T_{amb}>T_{ads}, it severed as heat source and added a certain amount of energy to supply the hot water. Taking the same supply temperature 60°C for example, around 340 kJ/kg storage density was achieved, which is higher than the case T_{amb}=25°C. Similarly, higher T_{amb} leads to larger hot water volume. As for the exergy recoved, since lower T_{amb} means the reference energy temperature level is low, more exergy would be recovered.
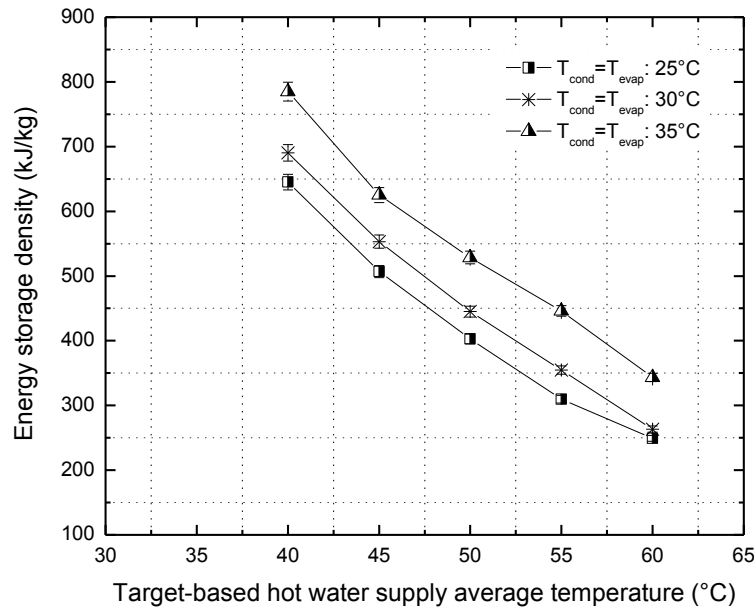
Figure 7.30: Effect of ambient temperature on energy storage density for different target-based water average temperatures
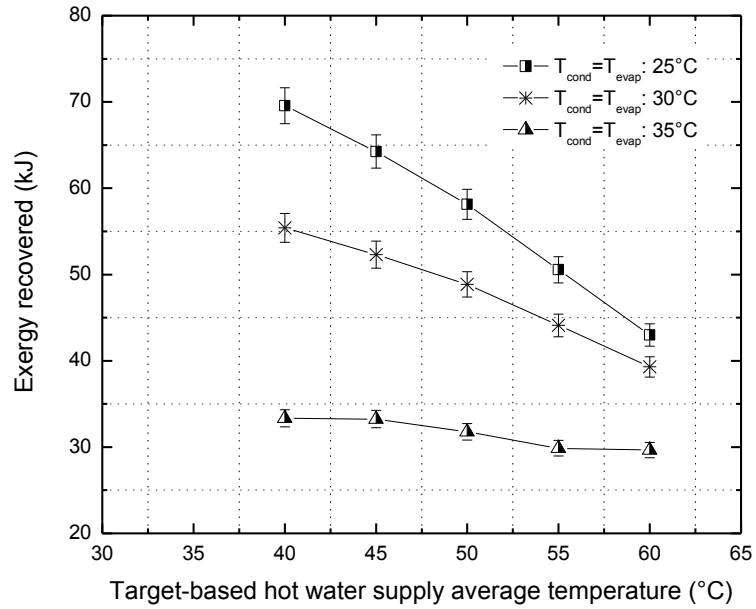
Figure 7.31: Effect of ambient temperature on exergy recovered for different target-based
water average temperatures
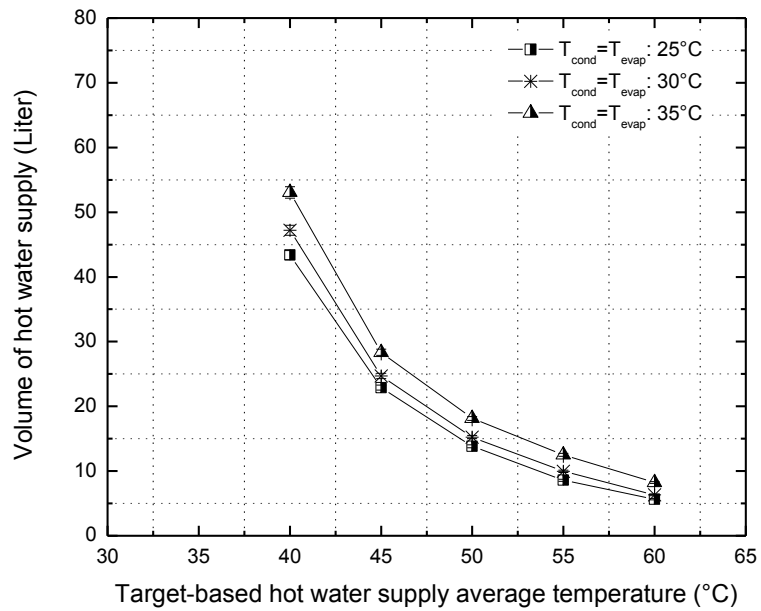
Figure 7.32: Effect of ambient temperature on hot water supply volume for different
target-based water average temperatures

Effect of ambient temperature on overall storage performance metrics is shown in Figure 7.33. It can be found that, with increased T_{amb}, total energy storage density and energy efficiency increased, as is explained earlier. The loading change was not very apparent. It is easy to understand that the exergy lost was lower when the reference temperature (i.e. T_{amb}) is higher. In addition, overall exergy efficiency decreased with increased T_{amb}, due to reference energy temperature level increased.
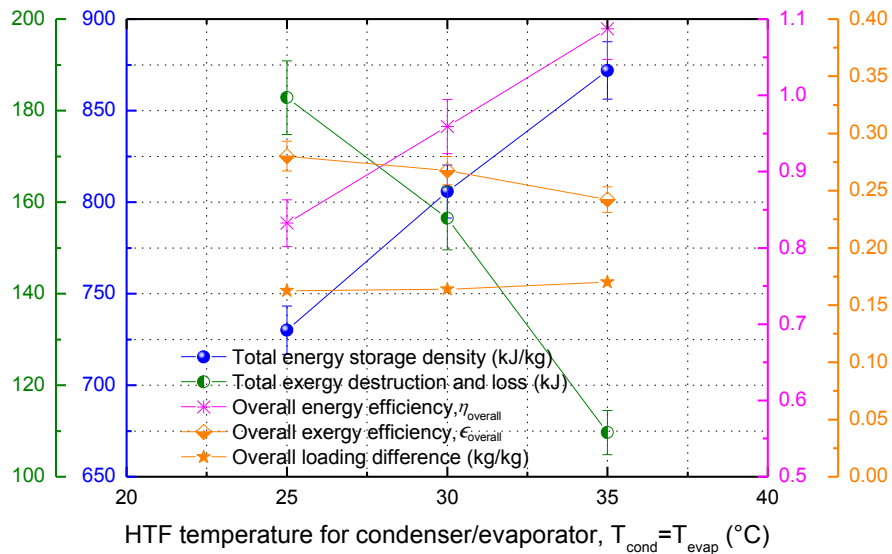
Figure 7.33: Effect of ambient temperature on storage performance metrics

7.2.6   Effect of inlet HTF temperature for evaporator on heat storage performance

Effect of inlet HTF temperature for evaporator different target-based hot water supply average temperatures is shown in Figure 7.34 through Figure 7.36. Here the ambient

temperature T_{amb} for charging process (i.e. T_{cond}) remained constant while T_{amb} for discharging process (i.e. T_{evap}) changed. For this section, since the ambient temperature is different during charging and discharging process, exergy efficiency was not analyzed and exergy recovered was analyzed based on T_{evap} as the reference temperature. It can be found that with higher T_{evap}, the energy storage density and hot water supply volume increased. It is also easy to understand that exergy recovered was smaller when the reference temperature T_{evap} was higher.
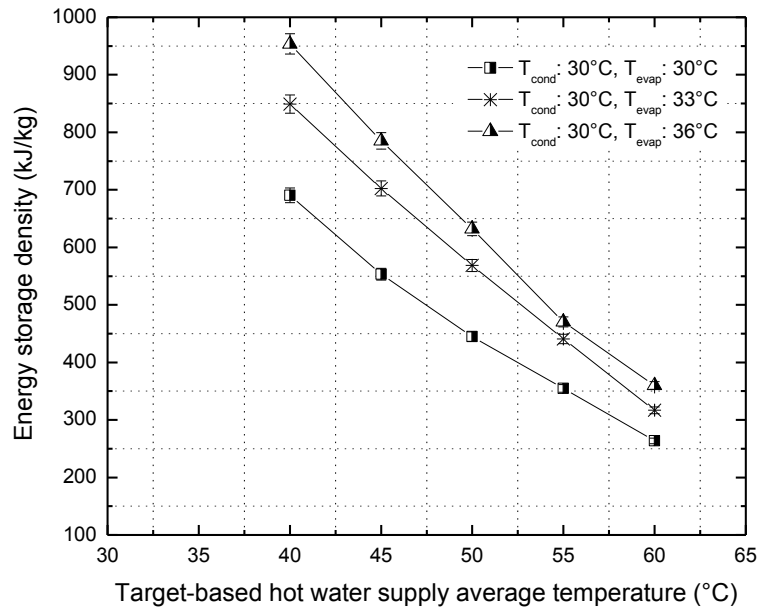
Figure 7.34: Effect of inlet HTF temperature for evaporator on energy storage density for different target-based water average temperatures
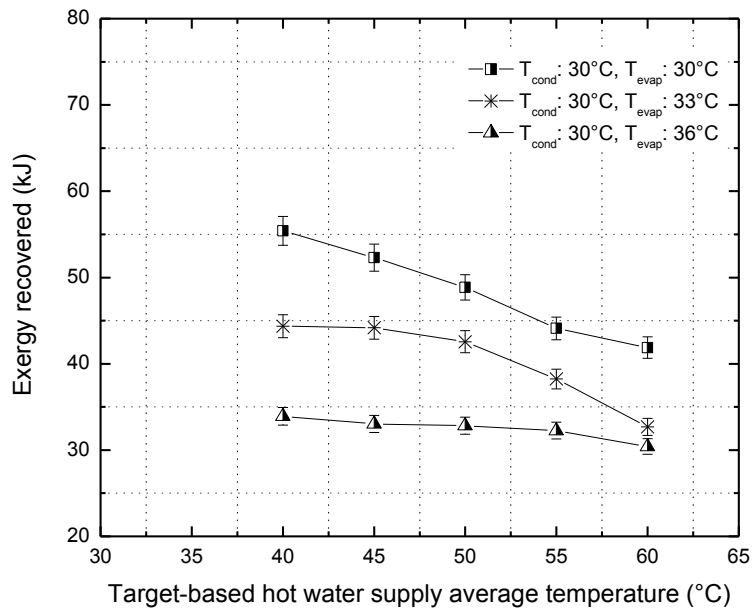
Figure 7.35: Effect of inlet HTF temperature for evaporator on exergy recovered for different target-based water average temperatures
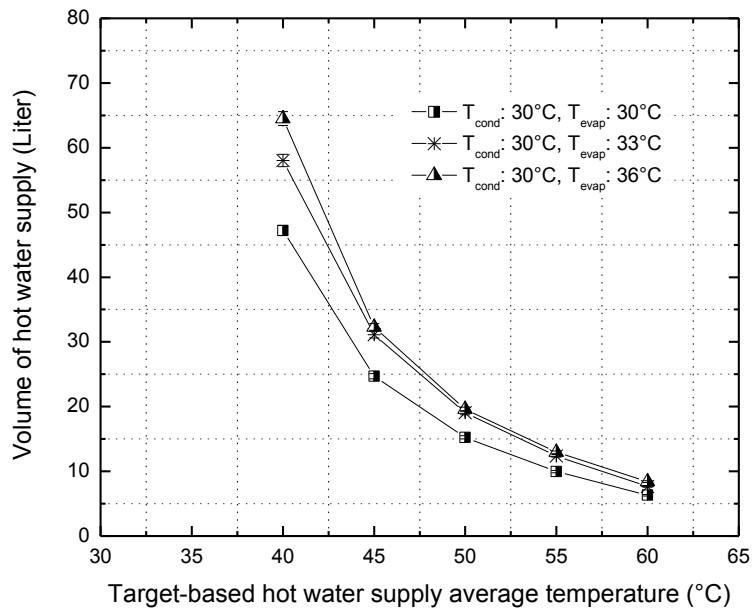
Figure 7.36: Effect of inlet HTF temperature for evaporator on hot water supply volume for different target-based water average temperatures

Effect of T_{evap} on overall storage performance metrics is shown in Figure 7.37. It can be found that, with increased T_{evap}, total energy storage density, energy efficiency and the loading difference increased. A higher T_{evap} means an additional higher temperature heat source to the adsorption process, which can make more contribution for the heat energy recovered.
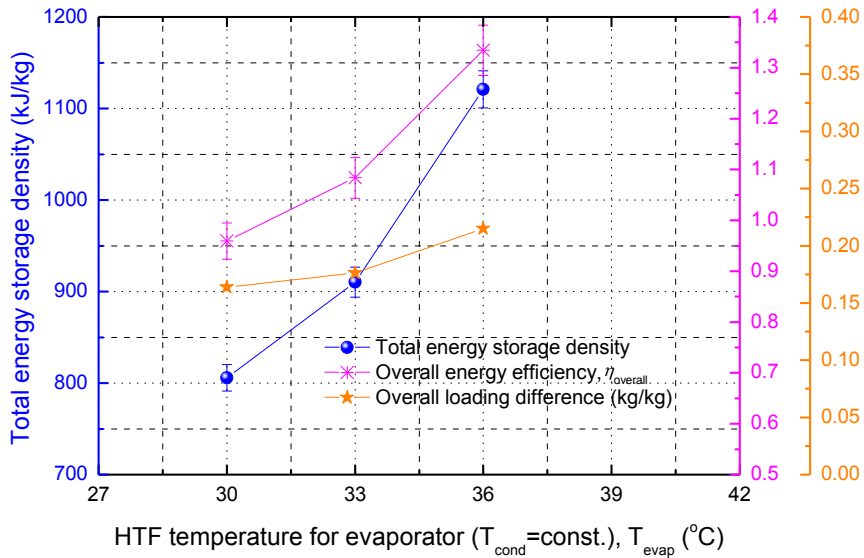
Figure 7.37: Effect of inlet HTF temperature for evaporator on storage performance metrics

7.2.7   Effect of initial state of adsorption bed on heat storage performance

Effect of initial state of adsorption bed ($T_{sorp.bed\_disch}$) for discharging process on storage performance is shown in Figure 7.38 through Figure 7.40. After charging process has been finished, the storing period may influence the storage performance for the initial condition of adsorption bed will be also changed. Therefore in this section, the effect

of $T_{sorp.bed\_disch}$ was investigated. Obviously, higher $T_{sorp.bed\_disch}$ lead to higher energy storage density, exergy delivered and hot water supply volume.
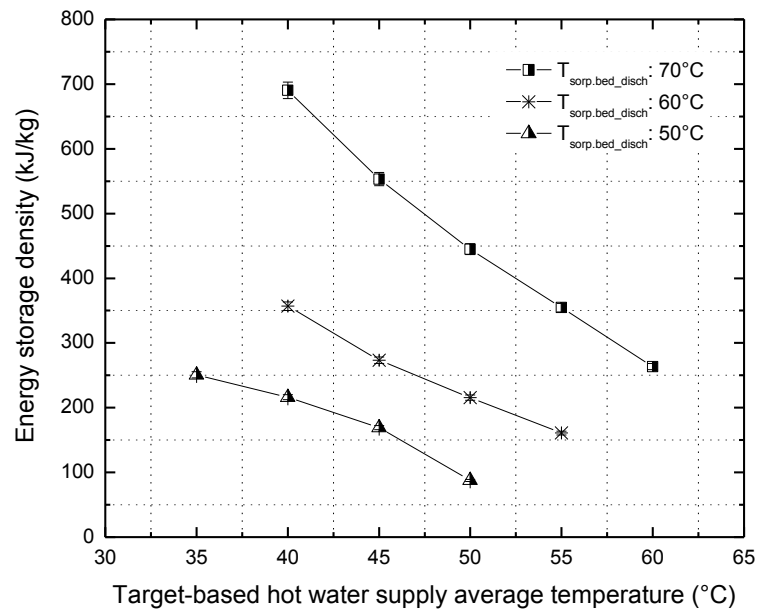
Figure 7.38: Effect of initial state of adsorption bed on energy storage density for different target-based water average temperatures
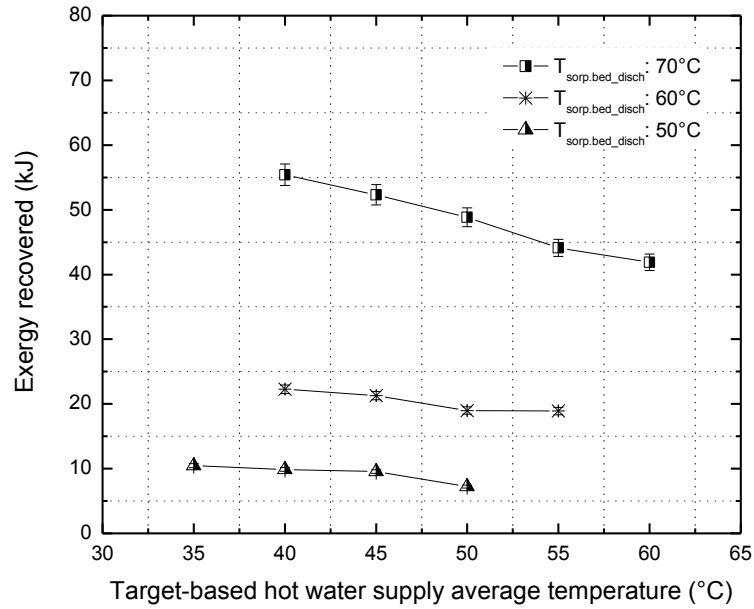
Figure 7.39: Effect of initial state of adsorption bed on exergy recovered for different target-based water average temperatures
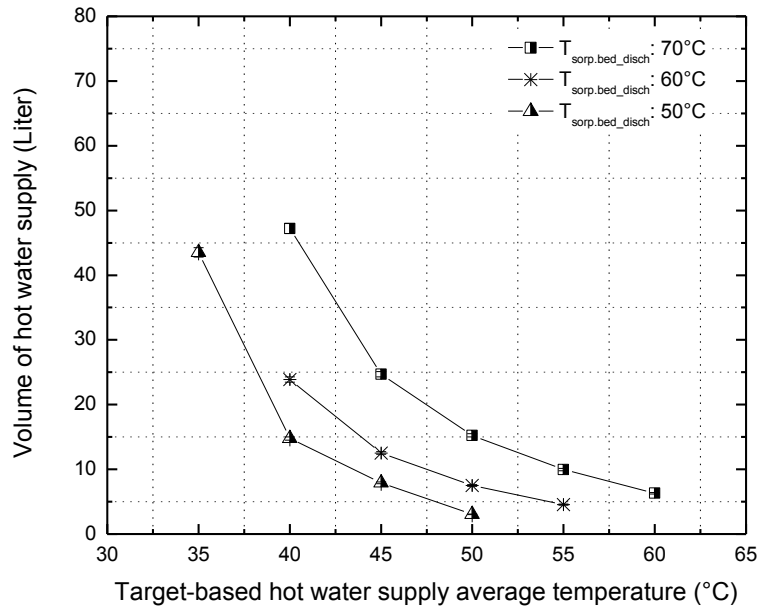
Figure 7.40: Effect of initial state of adsorption bed on hot water supply volume for different target-based water average temperatures

Effect of $T_{sorp.bed\_disch}$ on overall storage performance metrics is shown in Figure 7.41. A higher $T_{sorp.bed\_disch}$ would lead to larger total energy storage density, energy efficiency, and the loading difference. It can also lead to larger exergy recovered and exergy efficiency. It can be noticed that when $T_{sorp.bed\_disch}$ decreased, energy storage density decreased more significantly than other effect factors. One reason is that there was an amount of condensed water at the bottom of adsorption bed during charging process, as shown in Figure 7.42, and the water would be absorbed by the adsorbents during a long storing period and this part of adsorption heat would be wasted before the discharging process. Another reason is that with lower $T_{sorp.bed\_disch}$ during discharging process, part of the adsorption heat would be used to heat the adsorption bed, not to heat the HTF. This can be used to explain that even though there are lots of reports for larger adsorption storage density from material scale (tested by vacuum gravimetric method and thermo-balance) based on the literature review, the storage density was usually lower from the system integration level (with large vacuum chamber and HTF loops).
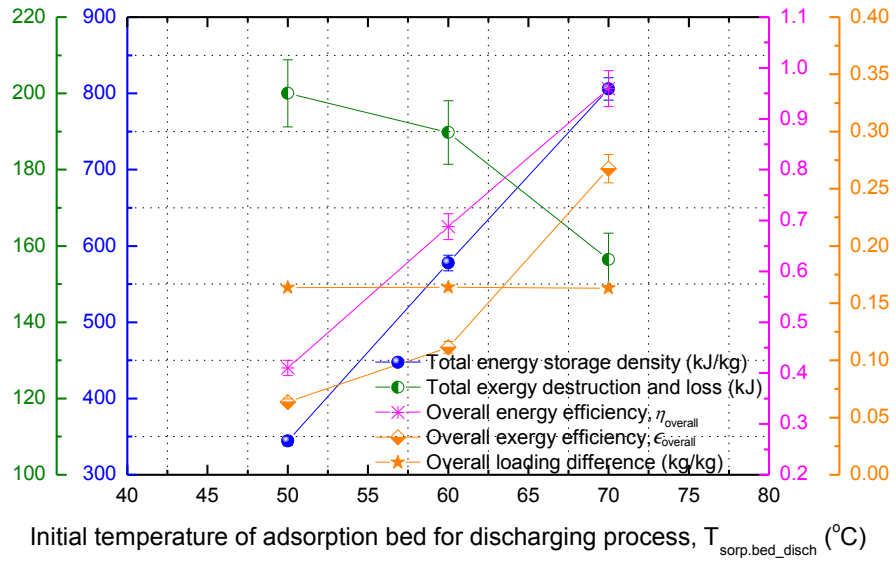
Figure 7.41: Effect of initial state of adsorption bed on storage performance metrics

Figure 7.42: Phenomenon of condensed water at the bottom of adsorption bed during charging process

7.3 Charging and discharging process performance of adsorption cold storage

The operating conditions for one overall charging and discharging cold storage process are listed as follows: T_{des}=70°C, T_{cond}=T_{ads}=T_{amb}=30°C, T_{evap}=30°C, $\dot{m}_{des,HTF}$=0.060 kg/s, $\dot{m}_{evap,HTF}$=0.028 kg/s, $\dot{m}_{cond,HTF}$= 0.050 kg/s, $\dot{m}_{ads,HTF}$= 0.046 kg/s.

Temperature profile of HTF during charging and discharging process with experimental investigation is shown in Figure 7.43. For charging process, the regeneration temperature $T_{des,in}$ (70°C) regenerated the desorption chamber, and drove the refrigerate water vapor to the condenser chamber and condensed there. After about 21 minutes, the charging process finished. Then the pre-discharging process was taken to make the adsorption bed at the ambient condition. For the following discharging process, the lower adsorption chamber temperature (ambient temperature) lead to a lower pressure than that of evaporator chamber and more refrigerant vapor would flow into the adsorption chamber. And this lead to a lower $T_{evap,out}$ than $T_{evap,in}$, and the $T_{evap,out}$ can be used for cold load for residential application. The minimum point for $T_{evap,out}$ was around 20.7°C, which means 9.3°C temperature drop could be produced during the discharging process. When the inlet and outlet of HTF temperature difference was small for adsorption chamber and evaporator chamber or the adsorption process was in a steady state condition, the discharging process would be finished. It took around 51 minutes for discharging process.

191
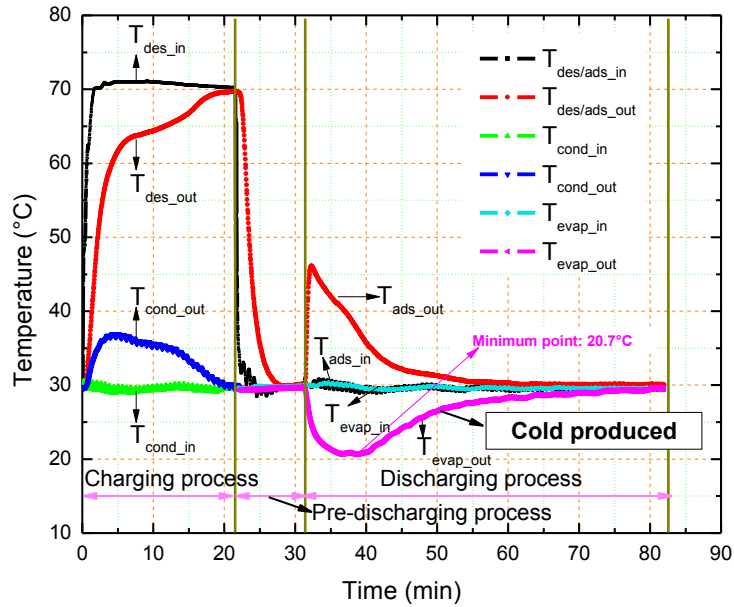
Figure 7.43: Temperature profile of HTF during charging and discharging process

Pressure profile of chambers during the process is shown in Figure 7.44. At the beginning of the charging process, the pressure in the desorption bed and condenser increases greatly. Finally, the pressures of desorption bed, condenser and evaporator are at the saturation pressure of the ambient temperature (4.15 kPa when T_{amb}=30°C as shown in Figure 7.44). During the discharging process, the adsorption bed is first cooled at the ambient conditions (i.e. pre-discharging process) refrigerant vapor is adsorbed by the adsorbents. Therefore, its pressure decreases greatly and is below the saturation pressure of the ambient temperature (the final pressure for pre-discharging process is 0.25 kPa, which is quite lower than saturation pressure 4.15 kPa when T_{amb}=30°C, as shown in Figure 7.44). As discharging process begins, the refrigerant is evaporated by absorbing heat from the chilled water coil so that the cooling is produced in the evaporator to meet

192

the loads. The pressure difference between the evaporator and adsorption bed forces refrigerant flows from evaporator to adsorption bed.
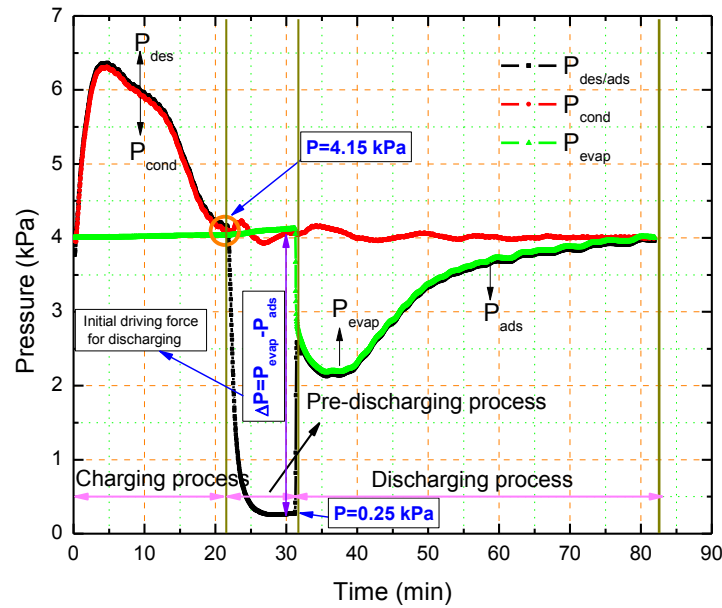
Figure 7.44: Pressure profile of chambers during charging and discharging process

Temperature and pressure change in detail in the evaporator is shown in Figure 7.45. It can be found that when evaporator chamber pressure is above the saturation pressure of falling film water inside the evaporator, both the HTF outlet temperature and falling film water temperature begin to increase.
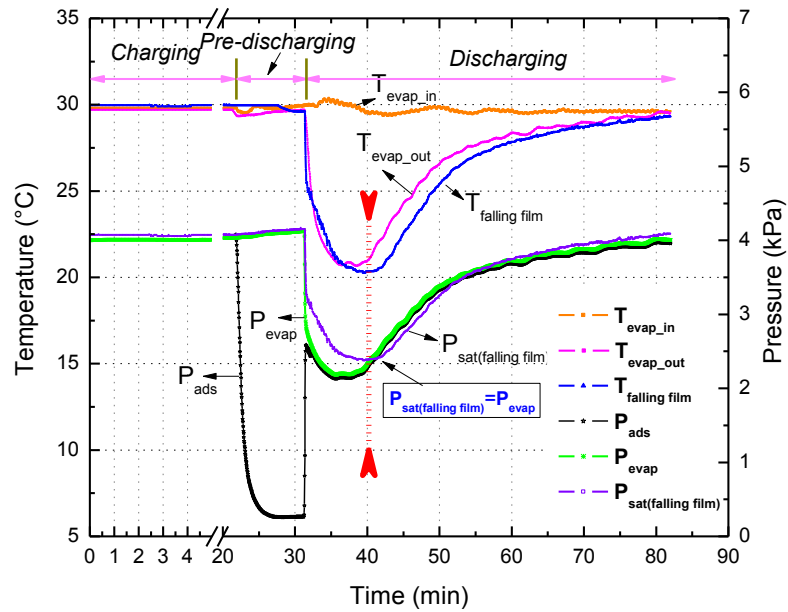
Figure 7.45: Temperature and pressure change in the evaporator

HTF mass flow rate profile during charging and discharging process is shown in Figure 7.46. During charging and discharging process the HTF mass flow rates of condenser and desorption chamber were large while the HTF mass flow rate of evaporator was small. This is because it is expected to have a quick charging process (larger $\dot{m}_{des,HTF}$) and a reasonable longer discharging process (usually smaller $\dot{m}_{evap,HTF}$).
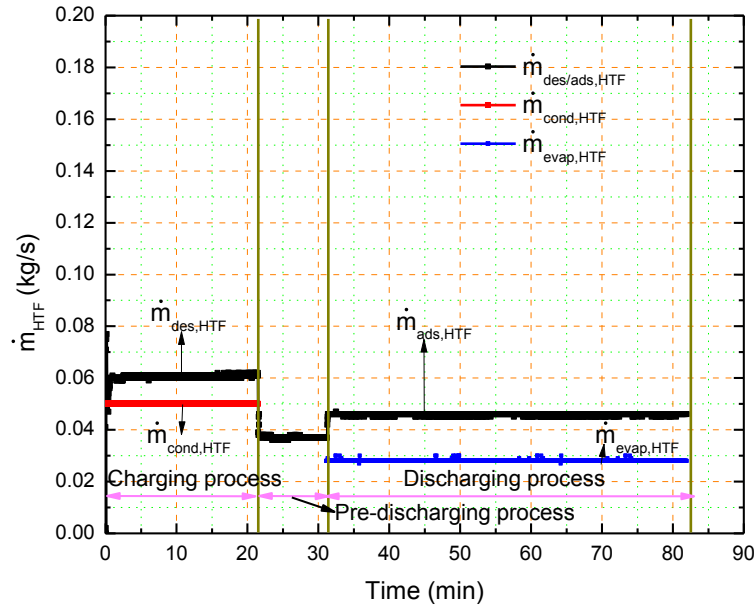
Figure 7.46: HTF mass flow rate profile during charging and discharging process

The instant capacity of sorption bed during charging and the instant capacity of evaporator during discharging process are shown in Figure 7.47. At the beginning of charging process, larger temperature gradient between inlet HTF and desorption bed together with larger HTF mass flow rate made a larger instant capacity for the desorption bed. Charging process ended when instant capacity was very small. Similarly, the instant capacity of evaporator was larger for the beginning of discharging process.

Accumulated energy for sorption bed during charging and for evaporator during discharging process is shown in Figure 7.48. With the charging time or discharging time increased, the total energy delivered or energy recovered increased. The calculation showed that the energy efficiency is around 44.6%. The loading difference is around 0.165 kg adsorbate/kg adsorbent.
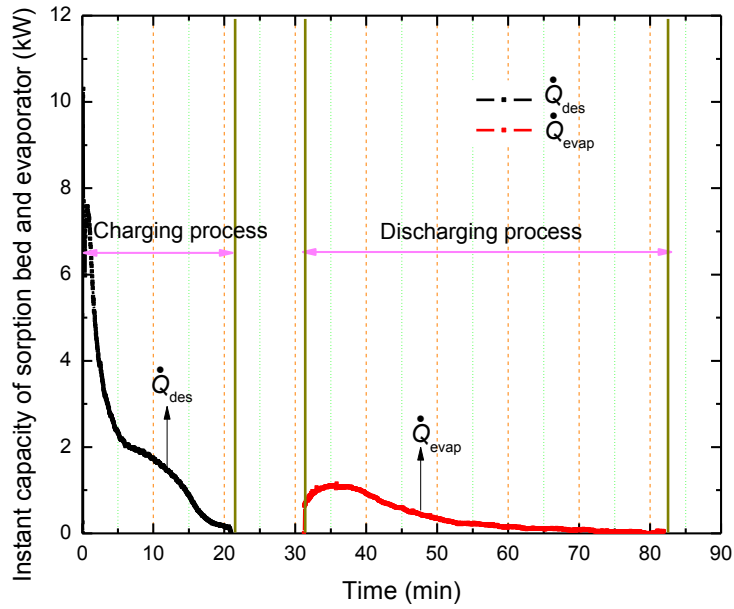
Figure 7.47: Instant capacity during charging and discharging process
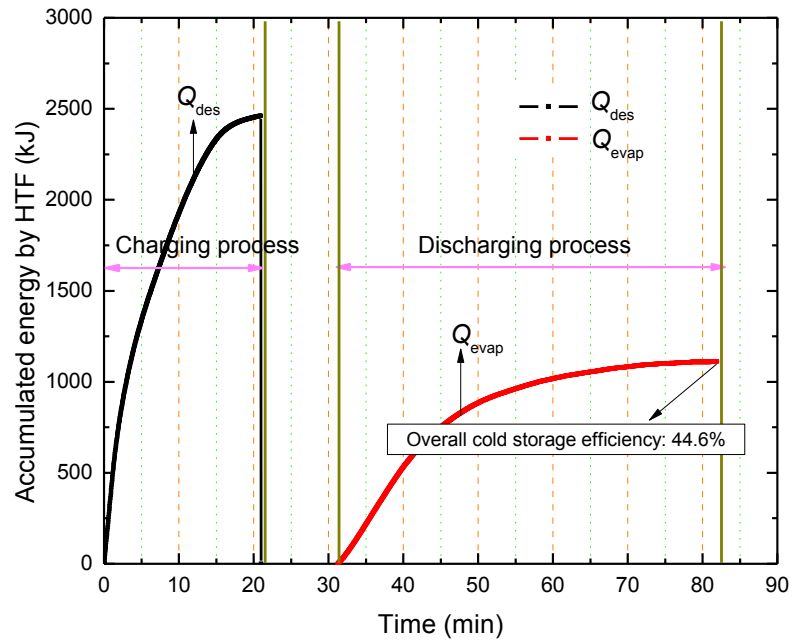
Figure 7.48: Accumulated energy during charging and discharging process

196

Instant exergy flow for sorption bed during charging and for evaporator during discharging process is shown in Figure 7.49. The instant exergy flow (here the absolute value is used for the convenience to explain the discharging process for evaporator) is larger at the beginning for charging and discharging process. But the instant exergy flow for evaporator is quite small in comparison with that for sorption bed. Accumulated exergy (here the absolute value is also used for the convenience to explain the discharging process for evaporator) during charging and discharging process is shown in Figure 7.50. It showed that after 18 minutes for discharging process, the accumulated exergy did not change that much, and the total exergy recovered was quite small as compared with exergy delivered and the overall exergy efficiency was only 4.47%.
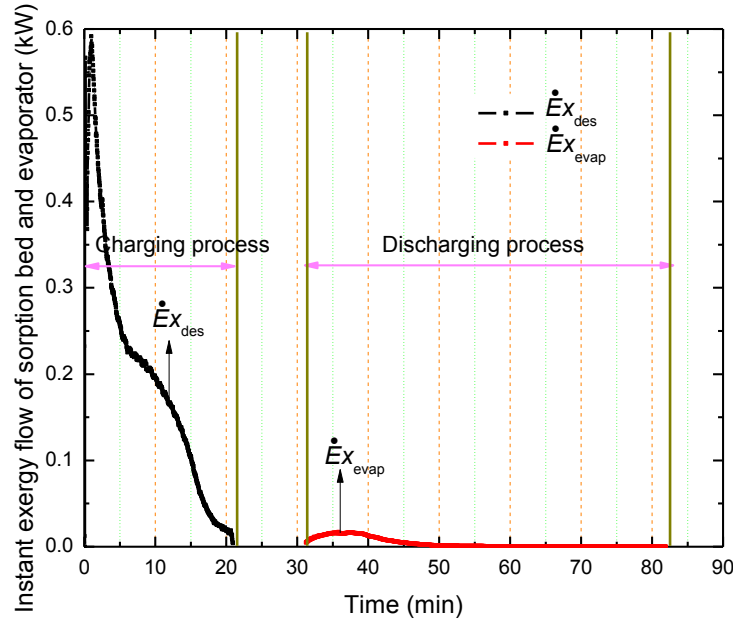
Figure 7.49: Instant exergy flow during charging and discharging process
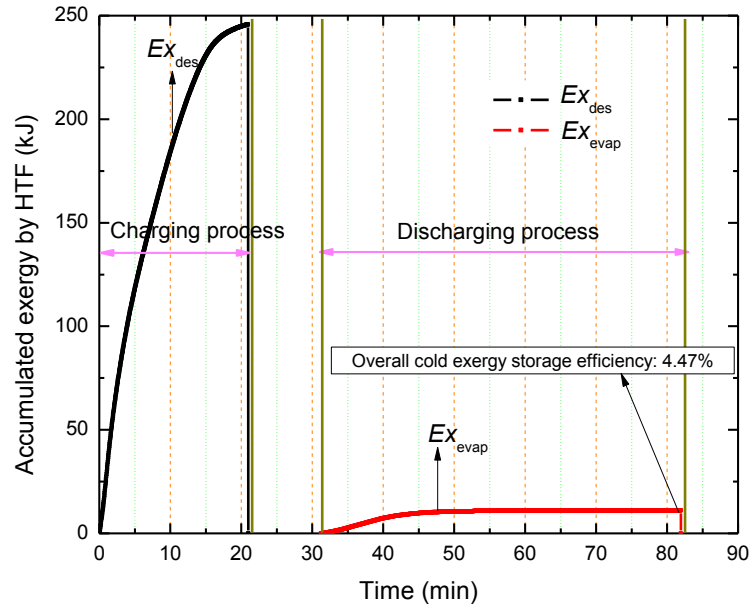
Figure 7.50: Accumulated exergy during charging and discharging process

7.4 Effect factors on adsorption cold storage performance

7.4.1 Effect of HTF mass flow rate of evaporator on cold storage performance

Effect of HTF mass flow rate of evaporator on energy storage density and energy efficiency is shown in Figure 7.51. It can be found that with large mass flow rate, both the energy storage density and cold energy efficiency increased. This is because large mass flow rate can increase the heat transfer rate, and thus can achieve better heat transfer characteristics.
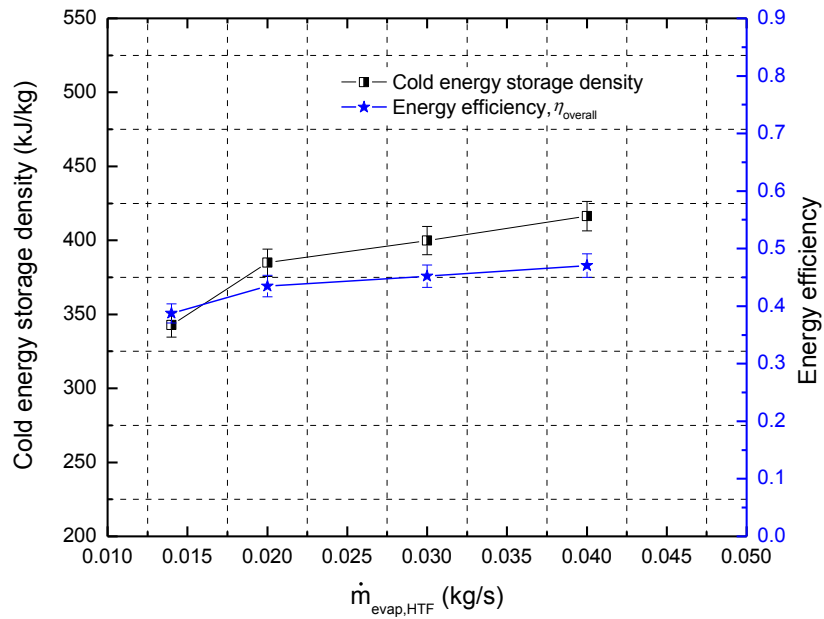
Figure 7.51: Effect of HTF mass flow rate of evaporator on energy storage density and energy efficiency
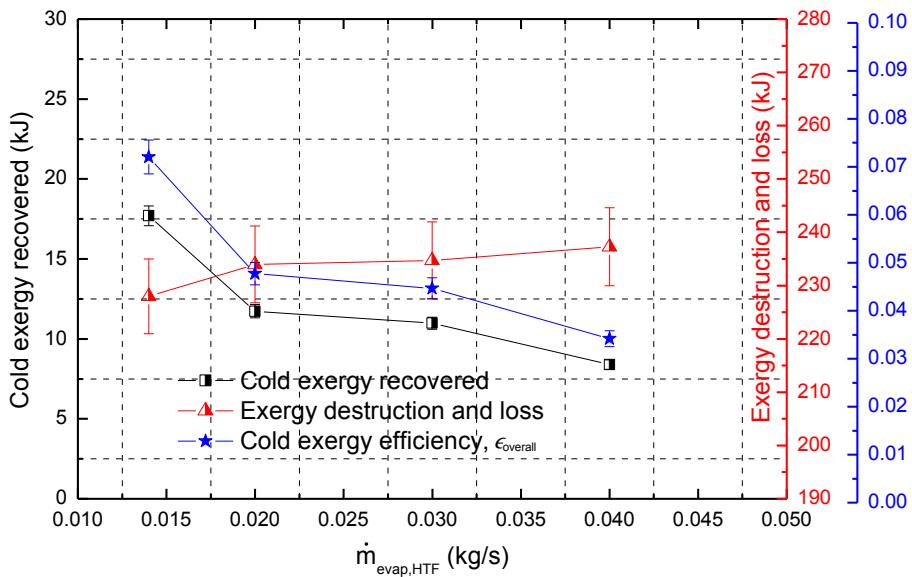
Figure 7.52: Effect of HTF mass flow rate of evaporator on exergy-based performance

Effect of HTF mass flow rate of evaporator on exergy-based performance is shown in Figure 7.52. It can be found that with large mass flow rate, the exergy destruction and loss increased. Possible explanation is that large mass flow rate would lead to large pressure drops, which would produce more irreversibilities. Therefore, with same operation condition for charging process, large exergy destruction and loss would lead to less exergy recovered and cold exergy efficiency would be reduced.

Effect of HTF mass flow rate of evaporator on minimum evaporator outlet HTF temperature and loading difference is shown in Figure 7.53. It can be found that with large mass flow rate, the minimum evaporator outlet HTF temperature increased. Lower minimum evaporator outlet HTF temperature, which can be regarded as the "quality of the cold", could be achieved under small mass flow rate. Small mass flow rate means less irreversibilities, thus high quality of cold can be achieved. It also showed that loading difference increased slightly with increased mass flow rate. This is because large mass flow rate can be beneficial to the heat transfer rate, loading difference increased. From Figure 7.54 through Figure 7.56 it can be found that with a small mass flow rate, the instant evaporator capacity decreased, but the evaporator outlet HTF could achieve a lower temperature, which made the specific exergy flow (here the absolute value is used) increased. In addition, a small mass flow rate can made the evaporator chamber pressure increased slightly.
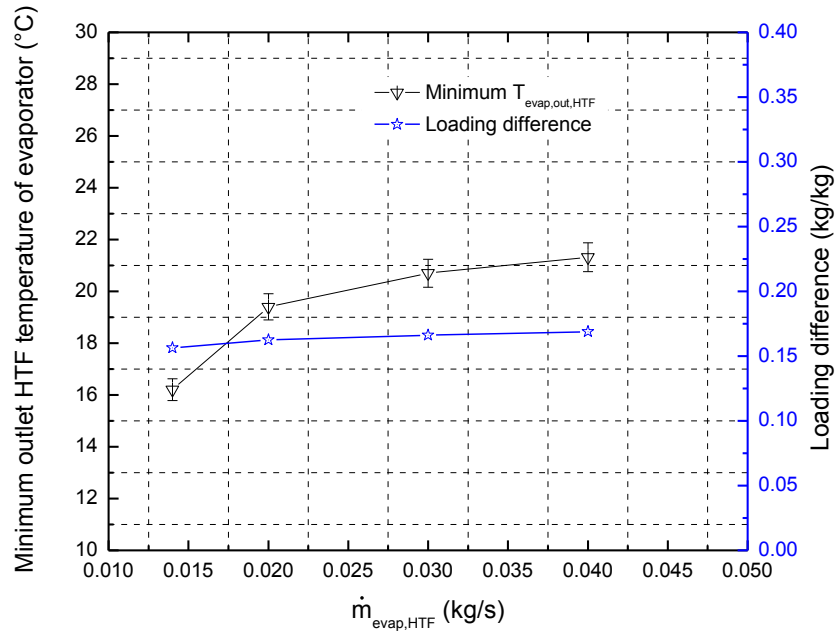
Figure 7.53: Effect of HTF mass flow rate of evaporator on minimum evaporator outlet HTF temperature and loading difference
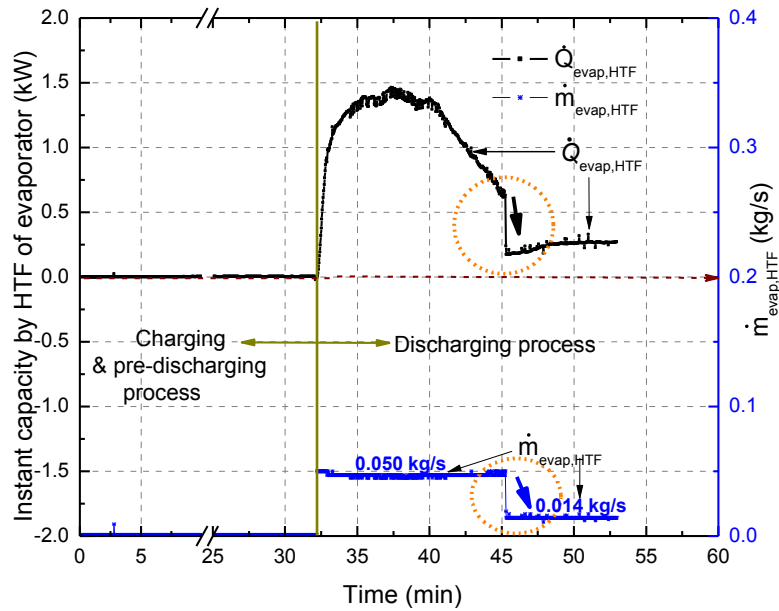
Figure 7.54: Effect of HTF mass flow rate change of evaporator on instant capacity by HTF of evaporator
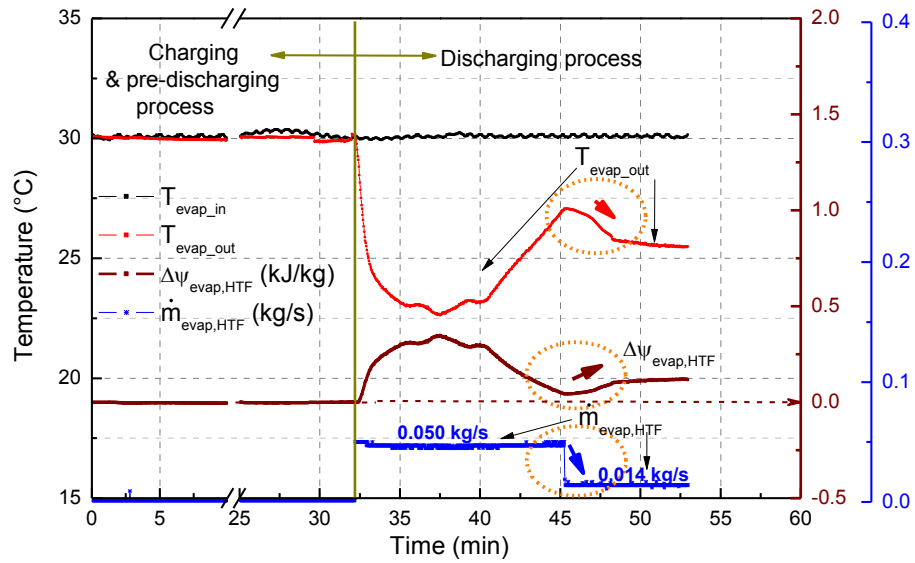
Figure 7.55: Effect of HTF mass flow rate change of evaporator on evaporator outlet HTF temperature and specific exergy flow
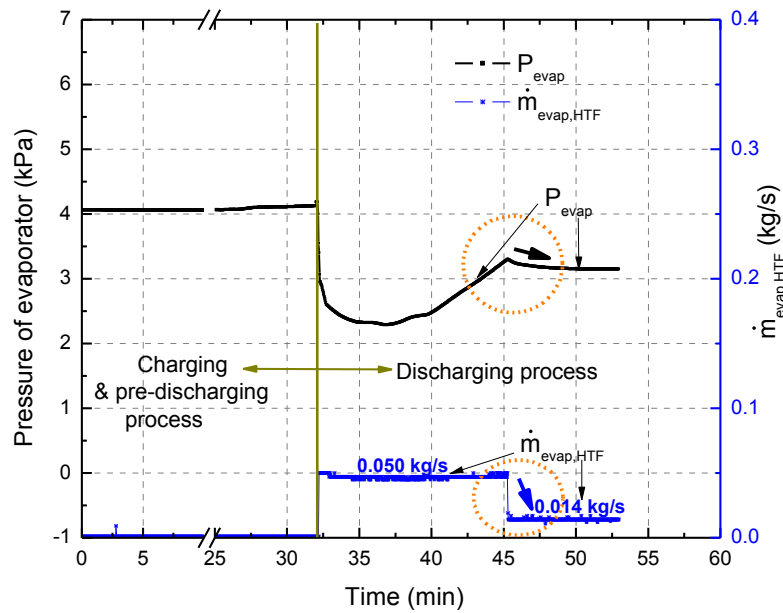
Figure 7.56: Effect of HTF mass flow rate change on evaporator pressure

7.4.2   Effect of inlet HTF temperature for evaporator on cold storage performance

Effect of inlet HTF temperature for evaporator on energy storage density and energy efficiency is shown in Figure 7.57. With higher inlet HTF temperature for evaporator, evaporator pressure would be higher. Thus larger pressure difference between evaporator and adsorption chamber would drive more refrigerant flow from evaporator to adsorption bed. Therefore, with same operation condition for charging process, the energy storage density and energy efficiency increased.
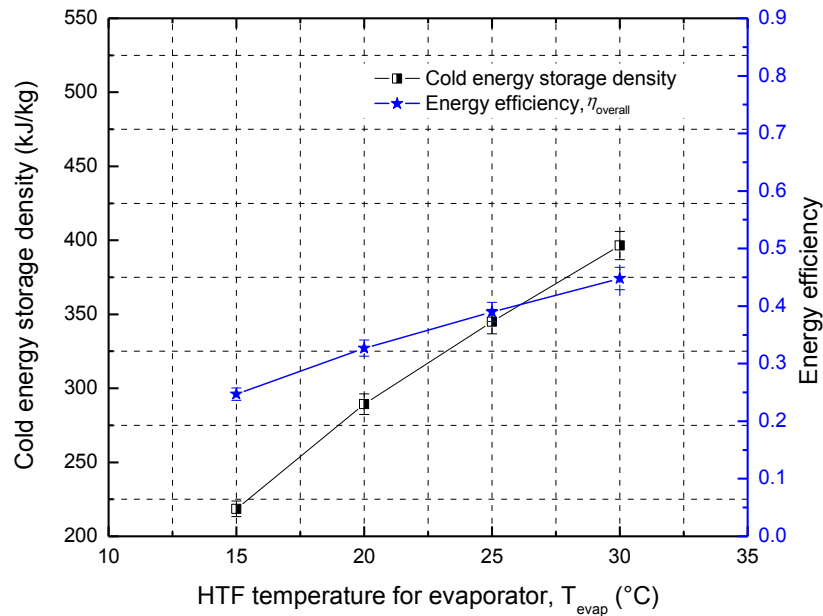
Figure 7.57: Effect of inlet HTF temperature for evaporator on energy storage density and energy efficiency

Effect of inlet HTF temperature for evaporator on exergy-based performance is shown in Figure 7.58. With higher inlet HTF temperature for evaporator, exergy destruction and loss would be larger. This is because the higher pressure difference between evaporator

and adsorption chamber would produce increased irreversibility. With more irreversibilities, the exergy recovered and exergy efficiency decreased, as shown in Figure 7.58.
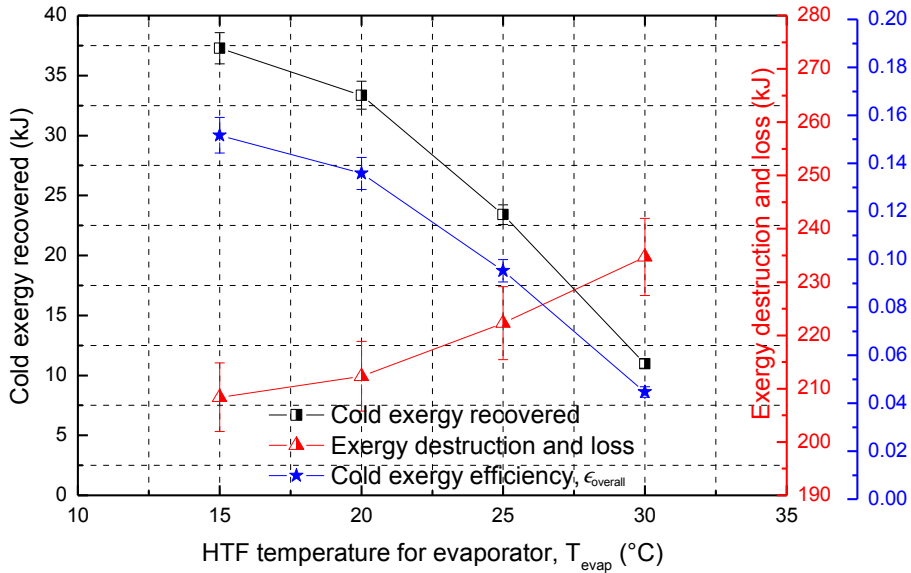
Figure 7.58: Effect of inlet HTF temperature for evaporator on exergy-based performance

Effect of inlet HTF temperature for evaporator on minimum evaporator outlet HTF temperature and loading difference is shown in Figure 7.59. It is easily understood that lower minimum evaporator outlet HTF temperature could be achieved under lower inlet HTF temperature for evaporator. The loading difference increased with higher inlet HTF temperature because higher temperature could lead a larger pressure difference between evaporator and adsorption chamber. It would drive more refrigerant flow from evaporator to adsorption bed. Therefore, with same operation condition for charging process, the loading difference increased.
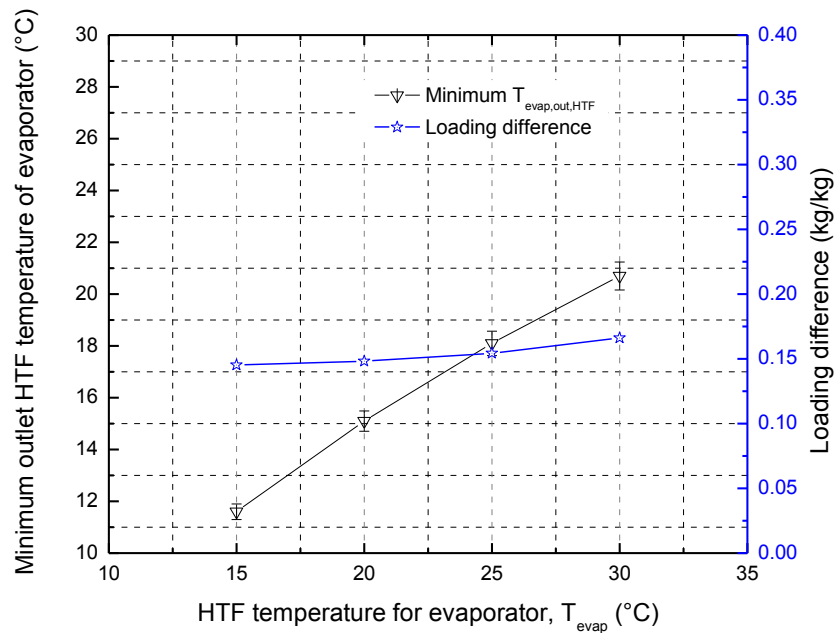
Figure 7.59: Effect of inlet HTF temperature for evaporator on minimum evaporator outlet HTF temperature and loading difference

7.4.3 Effect of inlet HTF temperature for adsorption bed on cold storage performance

Effect of inlet HTF temperature for adsorption bed on energy storage density and energy efficiency is shown in Figure 7.60. Inlet HTF temperature for adsorption bed here can be regarded as the ambient temperature. With higher ambient temperature for adsorption bed, adsorption chamber pressure would be increased while the pressure of evaporator remained constant. Thus pressure difference between evaporator and adsorption chamber would be reduced and less refrigerant flow from evaporator to adsorption bed. Therefore, with same operation condition for charging process, the energy storage density and energy efficiency reduced.
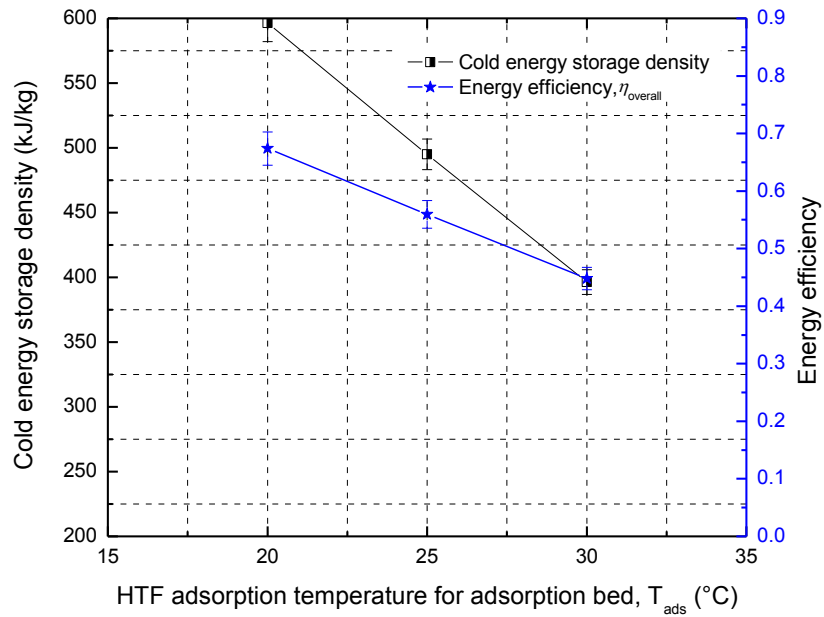
Figure 7.60: Effect of inlet HTF temperature for adsorption bed on energy storage density and energy efficiency

Effect of inlet HTF temperature for adsorption bed on exergy-based performance is shown in Figure 7.61. Exergy-based performance was evaluated based on reference temperature (i.e. ambient temperature). Because the ambient temperature during charging process (i.e. HTF inlet temperature of condenser) may be different from the ambient temperature during discharging process, here the cold exergy efficiency and exergy destruction and loss were not shown. With increased inlet HTF temperature for adsorption bed, the cold exergy recovered decreased due to the increased reference temperature during the discharging process.
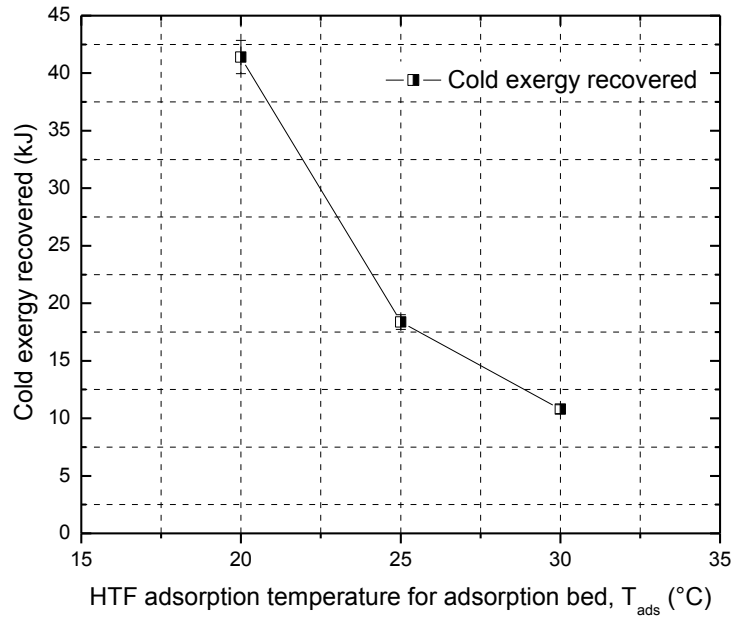
Figure 7.61: Effect of inlet HTF temperature for adsorption bed on exergy-based performance

Effect of inlet HTF temperature for adsorption bed on minimum evaporator outlet HTF temperature and loading difference is shown in Figure 7.62. It is easily understand that lower minimum evaporator outlet HTF temperature could be achieved under lower inlet HTF temperature for adsorption bed. The loading difference decreased with higher inlet HTF temperature because lower pressure difference between evaporator and adsorption chamber would drive less refrigerant flow from evaporator to adsorption bed. Therefore, with same operating condition for charging process, the loading difference decreased.
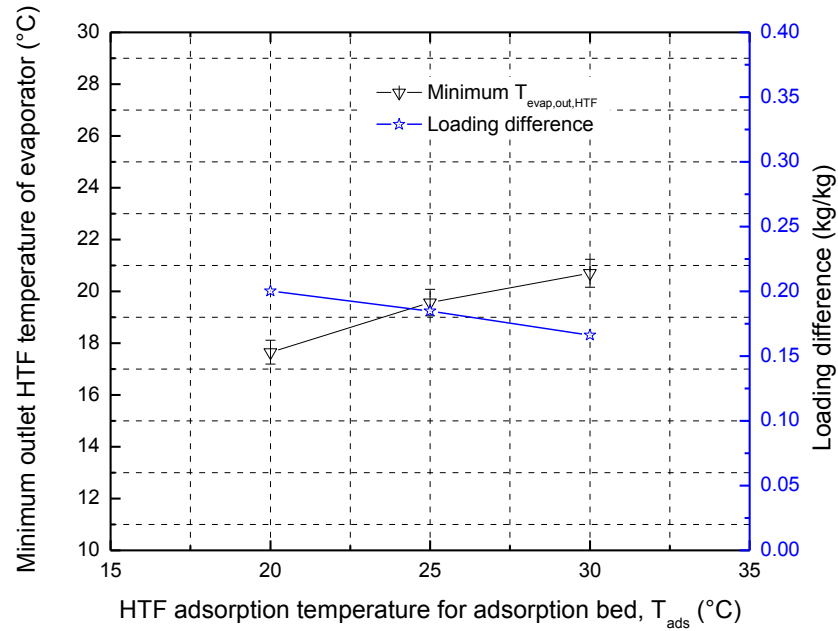
Figure 7.62: Effect of inlet HTF temperature for adsorption bed on minimum evaporator outlet HTF temperature and loading difference

7.4.4   Effect of inlet HTF temperature for desorption bed on cold storage performance

Effect of inlet HTF temperature for desorption bed on energy storage density and energy efficiency is shown in Figure 7.63. With higher regeneration temperature for desorption bed, adsorption chamber pressure at the end of pre-discharging process could reach a lower value while pressure of evaporator remained constant. Thus pressure difference between evaporator and adsorption chamber would be increased and more refrigerant flow from evaporator to adsorption bed. Therefore, the energy storage density and energy efficiency increased. Effect of inlet HTF temperature for desorption bed on exergy-based performance is shown in Figure 7.64. With higher regeneration temperature, exergy recovered increased. But exergy destruction and loss would be larger. With more irreversibilities, the exergy efficiency decreased.
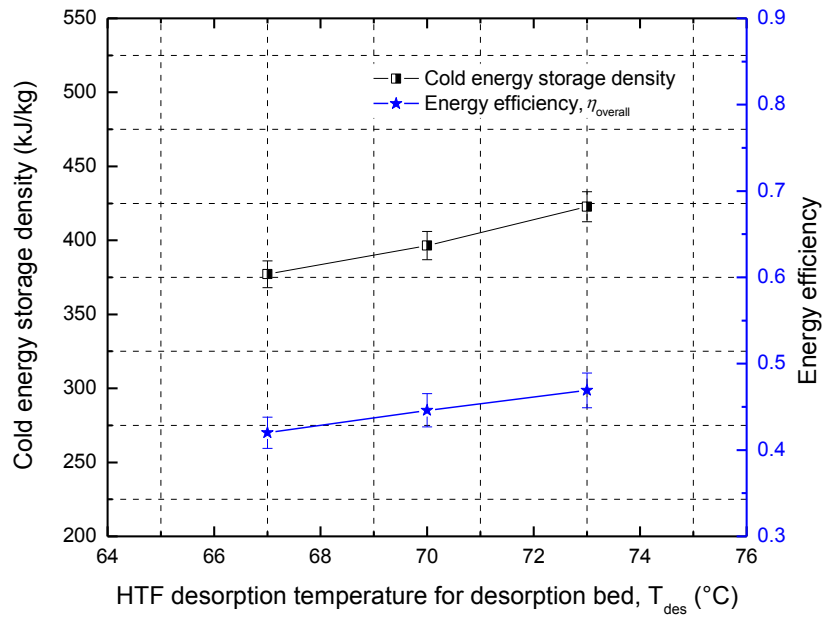
Figure 7.63: Effect of inlet HTF temperature for desorption bed on energy storage density and energy efficiency
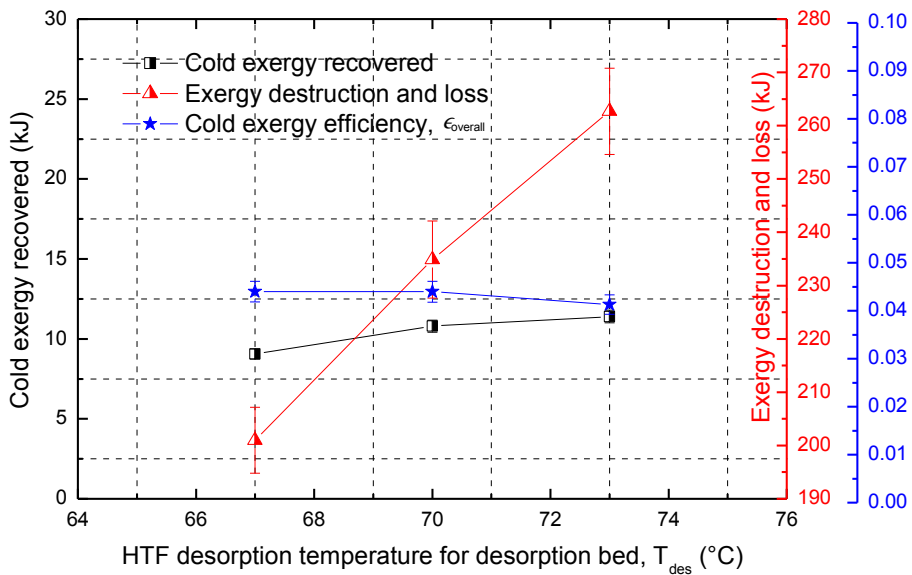
Figure 7.64: Effect of inlet HTF temperature for desorption bed on exergy-based performance

Effect of regeneration temperature on minimum evaporator outlet HTF temperature and loading difference is shown in Figure 7.65. It is easily understand that lower minimum evaporator outlet HTF temperature could be achieved under higher regeneration temperature. The loading difference increased with higher regeneration temperature.
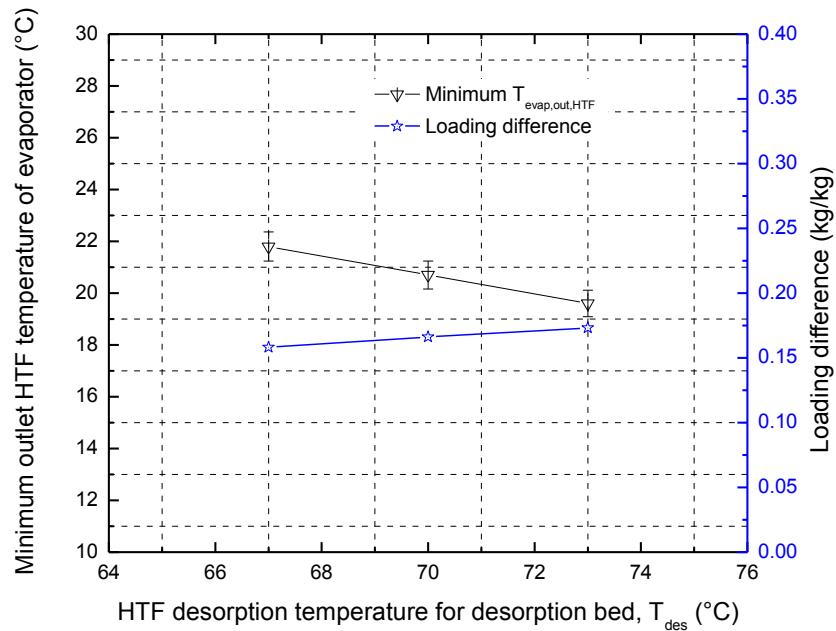
Figure 7.65: Effect of inlet HTF temperature for desorption bed on minimum evaporator outlet HTF temperature and loading difference

7.5   Storage performance improvement potential

This chapter mainly discuss about the storage performance improvement potential. It should be noted that the coated fin thickness is so small that there exists great potential to improve the storage density by volume. Several enhancement methods are listed as follows.

- Add more adsorbents into the fin spacing of adsorbent heat exchanger

As shown in Figure 7.66, it can be easily noticed that the fin spacing is still large and the adsorbent coating thickness is small (fin spacing is ~15 times of fin thickness). The current design has the advantage that the heat transfer between adsorption bed and HTF is very good for the time of charging process (usually around 20 minutes during test). There exists great potential to improve the storage density. Therefore, necessary solutions need to be taken to add more adsorbents into fin spacing. From Figure 7.66 three solutions are shown. Increasing coating thickness will definitely increase energy storage density by volume (usually the volume of adsorbent heat exchanger or reactor chamber may be assumed to be the volume). Also attaching the adsorbent granules into the fin spacing with the aid of resin (such as epoxy resin) without blocking the entrance pores of the granule is another good solution. In addition, a combination of the two solutions above can also be another good way to improve the energy storage density.
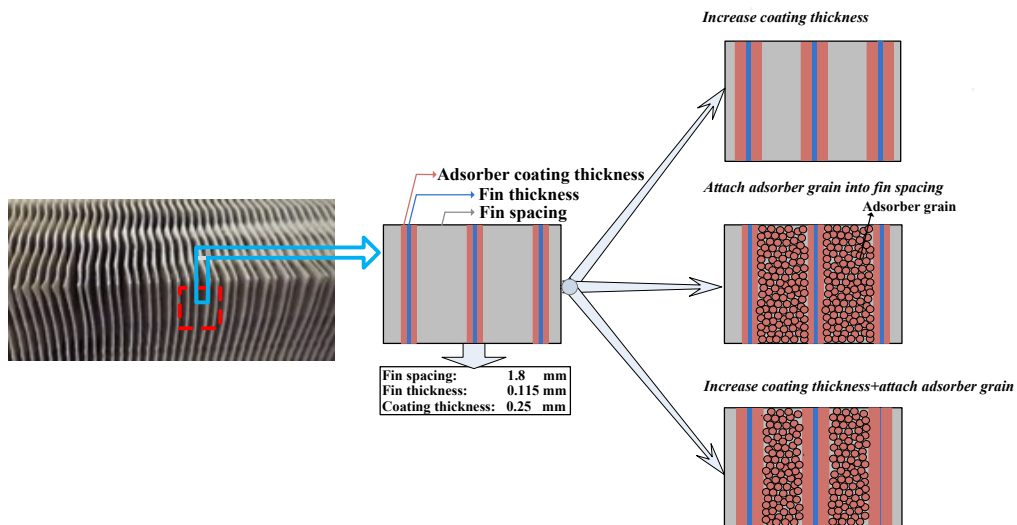
Figure 7.66: Storage performance enhancement by adding more adsorbents into the fin spacing of adsorbent heat exchanger

- Add more adsorbents onto heat transfer tubes to form consolidated adsorbent

As shown in Figure 7.67, more adsorbents can be added onto the bare heat transfer tubes to form consolidated adsorbent. Currently only a small amount of the adsorbents are coated on fins, and there are still lots of bare tubes are inside the sorption bed. Therefore, it is necessary to add adsorbents onto the heat transfer tubes, and the bound structure can also allow an increase in the adsorbent thermal conductivity.
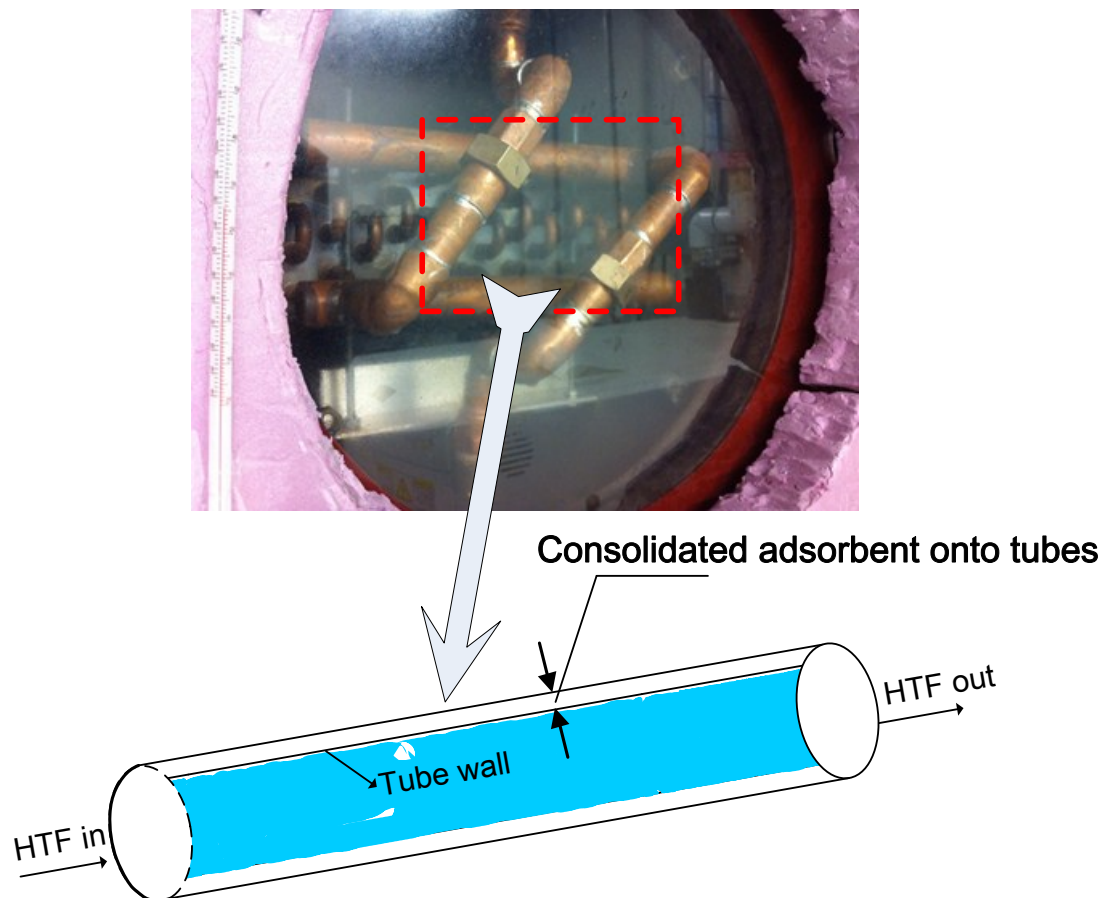
Figure 7.67: Storage performance enhancement by adding more adsorbents onto heat transfer tubes to form consolidated adsorbent

If the adsorbent heat exchanger volume (0.0162 m³) is chosen to calculate the heat storage density, it is about 140 MJ/m³ (T_{des}=70°C, T_{cond}=T_{evap}=T_{amb}=30°C, T_{ads}=30°C, $\dot{m}_{des,HTF}$ =0.080 kg/s, $\dot{m}_{ads,HTF}$ =0.028 kg/s, $\dot{m}_{cond,HTF}$ = $\dot{m}_{evap,HTF}$ =0.050 kg/s). Obviously, there are great potential to increase the storage density by volume.

- Thermal property improvement of adsorbents

As discussed above, if overfull adsorbents are added into the heat exchanger, it is necessary to pay more attention to the poor heat transfer inside the heat exchanger. Adding proper nano-particles into the adsorbents, or composite adsorbents (as discussed in Chapter 2) will improve heat transfer characteristics of sorption bed. Some other new types of adsorbents with special syntheses of novel mesoporous materials, as shown in Figure 7.68 (Vinu et al., 2006), and with metal organic frameworks, as shown in Figure 7.69, had been developed and have promising characteristics for residential application, and are listed because they may show some perspective for improvement of storage performance in this project.
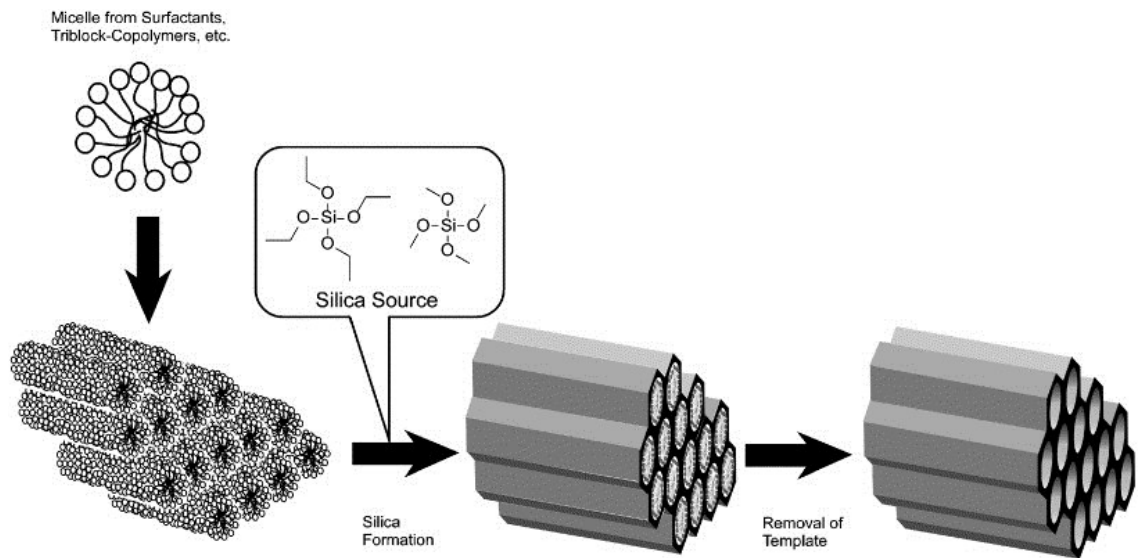
Figure 7.68: General concept for synthesis of mesoporous silica from micelle temple

Figure 7.69: Metal–organic framework adsorbent materials

- Make sorption storage unit more compact and add radiation-shielding materials to reduce heat loss

During the test, the sorption chamber and condenser/evaporator chamber are separate. It is necessary to integrate all the chambers together into a single chamber with HTF loop connected with outside loops. In this way, low weight unit can reduce the heat loss to ambient surroundings and save much space for residential application. In addition,

radiation-shielding materials should also be added onto the surface of chambers to reduce

heat loss.

8 Adsorption Thermal Energy Storage with Vapor Compression Heat Pump Integration

To make full use of low-grade energy source with temperature 25~40°C, a vapor compression heat pump model is integrated in the adsorption thermal energy storage system. In this chapter the vapor compression heat pump performance and adsorption heat storage system performance with heat pump integration are evaluated extensively.

8.1   System description and modeling

There are different integration types between vapor compression heat pump and adsorption thermal storage system, as shown in Figure 8.1. For the type of closed loop, a HTF loop exchange heat from condenser of the vapor compression heat pump to the desorption bed of sorption storage system directly. Open loop involves other equipment like the hot water tank. The condenser heat can be used to regenerate desorption bed and supply the hot water simultaneously. In this chapter, the open loop is considered since the experimental data from Chapter 7 can be used.

(1) Closed loop   (2) Open loop
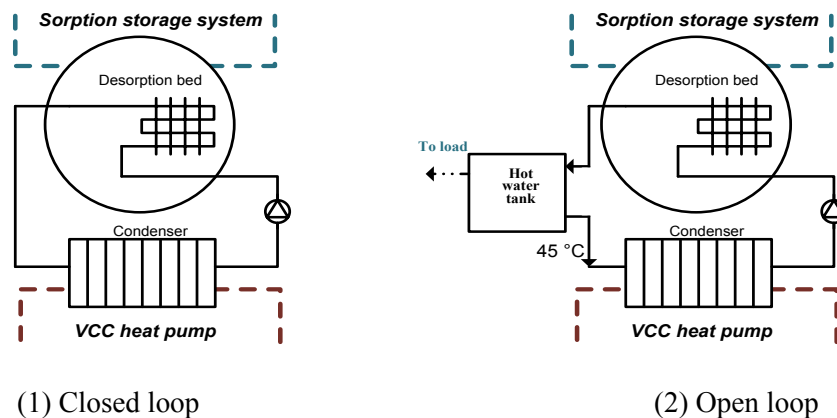
Figure 8.1: Different integration types between vapor compression heat pump and sorption storage system

Schematic of adsorption storage system with heat pump integration with an open loop is shown in Figure 8.2. It can be divided into two parts: vapor compression heat pump system and adsorption heat storage system. Here charging and discharging processes are introduced separately. For charging process, the vapor compression heat pump transfers low grade energy (it can be any waste heat from residential application, around 25~40°C) from evaporator side to high grade energy (around 70°C) at the condenser side. It enables us to utilize and recover the waste heat more efficiently. The condenser heat heats the 45°C water from hot water tank to around 70°C water, which can be used to regenerate the desorption bed. In the meanwhile, the adsorbate vapor (i.e. refrigerant) from desorption bed flows from adsorbent to the condenser chamber forced by the pressure difference and condensing into liquid phase onto ambient cooled coils. The output hot water from desorption bed flows back to the hot water tank.

It should be noted that the average output hot water (HTF) temperature from desorption bed is above 50°C based on the test results from Chapter 7, which can be regarded as the useful energy for residential application. It is also assumed that the phenomenon of water stratification is obvious that the water tank output temperature can remain constant around 45°C during the charging process, which usually takes around 20 minutes. During the charging process, the loop for vapor compression heat pump is under steady state condition. After the charging process is finished, the desorption bed and condenser chamber for charging process become adsorption bed and evaporator chamber for discharging process, respectively. During discharging process, falling film coils is used as evaporator to supply heat for liquid adsorbate evaporation. The adsorbent pressure from

adsorption bed is lower and adsorbate is forced to be in adsorption phase inside adsorbent and the reaction latent heat is released, carried by the heat transfer fluid to meet the loads. The irreversibility in this process is the mass transfer driving force, i.e. finite pressure difference and the sequence is a temperature difference between stored thermal energy and released thermal energy.
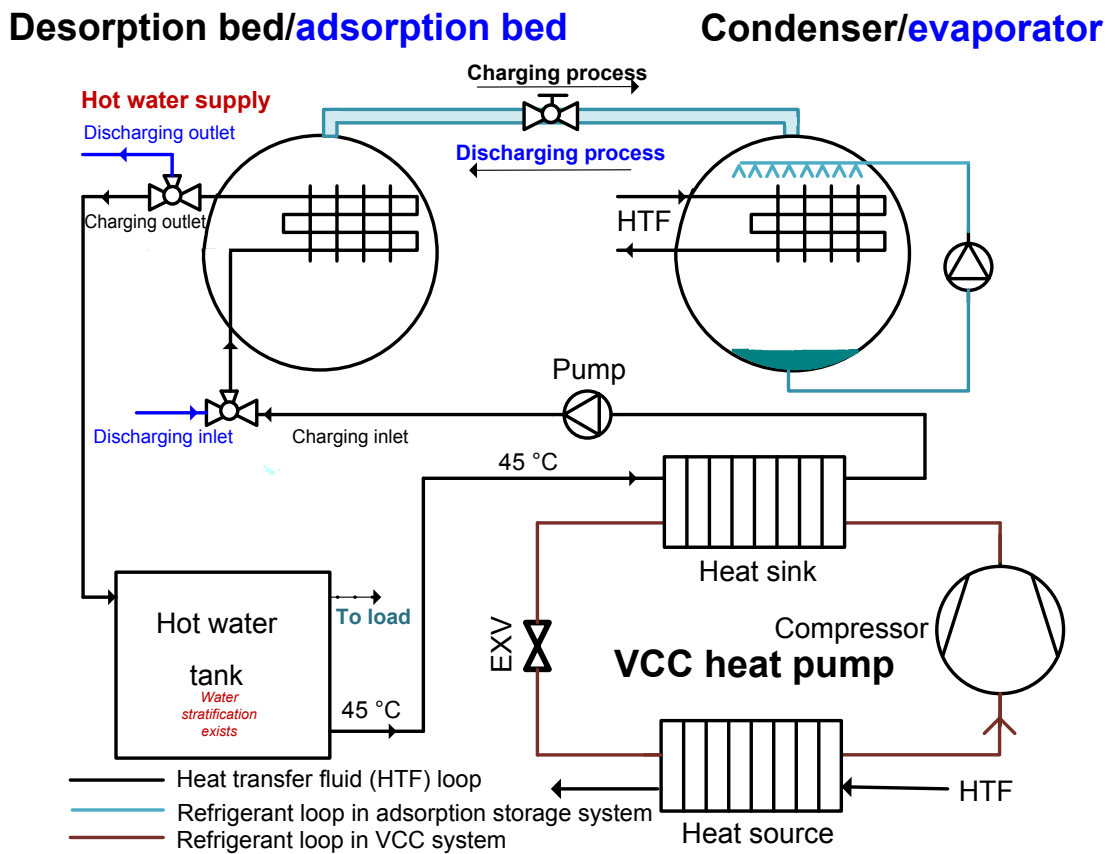
Figure 8.2: Adsorption storage system with heat pump integration in this study

To evaluate the system storage performance, several assumptions are made as follows:

- Steady state conditions are remained in all the components of compression heat pumps;

- Pressure losses in the pipeline are neglected;

- The condenser heat is assumed to be fully utilized by the desorption bed and hot water tank during charging process;

- Kinetic and potential energy and exergy destruction and loss are not considered;

- There are 5°C temperature difference between low grade heat source and evaporation temperature for the heat pump system;

- The condensation temperature of the heat pump system is set 75°C; superheat and subccooling degree of heat pump are both 4°C; ambient temperature is set 30°C;

- The compressor mechanical ($\eta_{comp,mech}$) and the compressor motor electrical ($\eta_{comp,elec}$) efficiencies are both 85%;

- The adiabatic efficiency of the compressor is taken to be 80%;

- The refrigerant used in the compression heat pump is HFC-134a, which will be discussed later;

- The HTF mass flow rate for the compression heat pump condenser side is 0.040 kg/s;

- The pump consumption for the HTF loops is not included in the energy and exergy analysis;

- The experimental data used in the sorption storage calculations are taken from Chapter 7 directly, and if the data cannot be used directly, the fitted data based on the experimental data are used;

- No leakage issues are involved both in the heat pump system and sorption storage system.

The thermodynamic properties of water and the refrigerant are found using Engineering Equation Solver (EES) software package program. The modeling for energy and exergy analysis are listed as follows:

A general expression with flow state condition for the exergy is expressed as follows:

$$\psi = (h - h_0) - T_0(s - s_0) \qquad\qquad \text{Equation 8.1}$$

ψ is the flow (specific) exergy, h is enthalpy, s is entropy, and the subscript zero indicates properties at the restricted dead state of P_0 and T_0.

- ❖ Charging process:
  - ○ Compressor of vapor compression heat pump

$$\dot{m}_{comp,in,r} = \dot{m}_{comp,out,r} = \dot{m}_r \qquad\qquad \text{Equation 8.2}$$

$$\dot{W}_{comp-HP} = \dot{m}_r(h_{comp,out,act} - h_{comp,in}) \qquad\qquad \text{Equation 8.3}$$

$$\dot{W}_{comp-HP,elec} = \sqrt{3}V_{comp}I_{comp}cos\varphi \qquad\qquad \text{Equation 8.4}$$

$$\dot{W}_{comp-HP,elec} = \frac{\dot{W}_{comp-HP}}{\eta_{comp,elec}\eta_{comp,mech}} \qquad\qquad \text{Equation 8.5}$$

$$\dot{Ex}_{dest,comp-HP} = \dot{m}_r(\psi_{comp,in} - \psi_{comp,out,act}) + \dot{W}_{comp-HP,elec} \qquad\qquad \text{Equation 8.6}$$

$$\dot{Ex}_{dest,comp-HP} = \dot{Ex}_{dest,comp-HP,mech,elec} + \dot{Ex}_{dest,comp-HP,int} \qquad\qquad \text{Equation 8.7}$$

$$\dot{Ex}_{dest,comp-HP,mech,elec} = \dot{W}_{comp-HP,elec}(1 - \eta_{comp,elec}\eta_{comp,mech}) \qquad\qquad \text{Equation 8.8}$$

where heat interactions with the environment are neglected.

- o Condenser of vapor compression heat pump

$$\dot{m}_{cond,in,r} = \dot{m}_{cond,out,r} = \dot{m}_r \qquad \text{Equation 8.9}$$

$$\dot{m}_{cond,in,w} = \dot{m}_{cond,out,w} = \dot{m}_w \qquad \text{Equation 8.10}$$

$$\dot{Q}_{cond-HP} = \dot{m}_r(h_{cond,in,act} - h_{cond,out}) \qquad \text{Equation 8.11}$$

$$\dot{Q}_{cond-HP} = \dot{m}_w C_{p,w}(T_{cond,out,w} - T_{cond,in,w}) \ (T_{cond,in,w}\text{=45°C}) \qquad \text{Equation 8.12}$$

$$\dot{Ex}_{dest,cond-HP} = \dot{m}_r(\psi_{cond,in,r} - \psi_{cond,out,r}) + \dot{m}_w(\psi_{cond,in,w} - \psi_{cond,out.w}) \qquad \text{Equation 8.13}$$

- o Expansion (throttling) valve of vapor compression heat pump

$$\dot{m}_{exp,in} = \dot{m}_{exp,out} = \dot{m}_r \qquad \text{Equation 8.14}$$

$$h_{exp,in} = h_{exp,out} \qquad \text{Equation 8.15}$$

$$\dot{Ex}_{dest,exp-HP} = \dot{m}_r(\psi_{exp,in} - \psi_{exp,out}) \qquad \text{Equation 8.16}$$

- o Evaporator of vapor compression heat pump

$$\dot{m}_{evap,in,r} = \dot{m}_{evap,out,r} = \dot{m}_r \qquad \text{Equation 8.17}$$

$$\dot{m}_{evap,in,w} = \dot{m}_{evap,out,w} = \dot{m}_w \qquad \text{Equation 8.18}$$

$$\dot{Q}_{evap-HP} = \dot{m}_r(h_{evap,out} - h_{evap,in}) \qquad \text{Equation 8.19}$$

$$\dot{Ex}_{dest,evap-HP} = \dot{m}_r(\psi_{evap,in,r} - \psi_{evap,out,r}) + \dot{Q}_{evap-HP}(1 - \frac{T_o}{T_{evap}}) \qquad \text{Equation 8.20}$$

Vapor compression heat pump unit performance

$$COP_{HP} = \frac{\dot{Q}_{cond-HP}}{\dot{W}_{comp-HP,elec}}$$
$\qquad$ Equation 8.21

$$COP_{ex,HP} = \frac{\dot{m}_w(\psi_{cond,out,w} - \psi_{cond,in.w})}{\dot{W}_{comp-HP,elec}}$$
$\qquad$ Equation 8.22

    ○ Sorption thermal storage system

$$\dot{Q}_{des} = \dot{m}_w C_{p,w}(T_{des,in,w} - T_{des,out,w})$$
$\qquad$ Equation 8.23

$$T_{des,in,w} = T_{cond,out,w}$$
$\qquad$ Equation 8.24

$$Q_{delivered} = Q_{des} = \int_0^{t_{charg}} \dot{Q}_{des}\, dt$$
$\qquad$ Equation 8.25

$$\dot{Ex}_{delivered} = \dot{m}_w(\psi_{des,in,w} - \psi_{des,out.w})$$
$\qquad$ Equation 8.26

$$Ex_{delivered} = Ex_{des} = \int_0^{t_{charg}} \dot{Ex}_{des}\, dt$$
$\qquad$ Equation 8.27

    ○ Hot water tank

$$T_{des,out,w} = T_{tank,in,w}$$
$\qquad$ Equation 8.28

$$T_{cond,in,w} = T_{tank,out,w}$$
$\qquad$ Equation 8.29

$$\dot{Q}_{tank} = \dot{m}_w C_{p,w}(T_{tank,in,w} - T_{tank,out,w})$$
$\qquad$ Equation 8.30

$$Q_{tank} = \int_0^{t_{charg}} \dot{Q}_{tank}\, dt$$
$\qquad$ Equation 8.31

$$\dot{Ex}_{tank} = \dot{m}_w(\psi_{tank,in,w} - \psi_{tank,out.w})$$
$\qquad$ Equation 8.32

$$Ex_{tank} = \int_0^{t_{charg}} \dot{Ex}_{tank}\, dt$$
$\qquad$ Equation 8.33

❖ Discharging process:

    ○ Sorption heat TES storage system

$$\dot{Q}_{ads} = \dot{m}_w C_{p,w}(T_{ads,out,w} - T_{ads,in,w})$$
$\qquad$ Equation 8.34

$$\dot{Q}_{evap} = \dot{Q}_{evap,HTF} + \dot{Q}_{evap,falling\,film}$$ Equation 8.35

$$Q_{recovered} = abs(Q_{ads}) = abs\left(\int_0^{t_{disch}} \dot{Q}_{ads}\,dt\right)$$ (Heat storage) Equation 8.36

$$\dot{Ex}_{ads} = \dot{m}_w\left(\psi_{ads,out,w} - \psi_{ads,in,w}\right)$$ (Heat storage) Equation 8.37

$$Ex_{recovered} = abs(Ex_{ads}) = abs\left(\int_0^{t_{disch}} \dot{Ex}_{ads}\,dt\right)$$ (Heat storage) Equation 8.38

❖ Overall system heat storage performance:

$$COP_{overall} = \frac{Q_{recovered} + Q_{tank}}{\int_0^{t_{charg}} \dot{W}_{comp-HP,elec}\,dt}$$ Equation 8.39

$$COP_{adsorption} = \frac{Q_{recovered}}{\int_0^{t_{charg}} \dot{W}_{comp-HP,elec}\,dt}$$ Equation 8.40

$$COP_{ex,overall} = \frac{Ex_{recovered} + Ex_{tank}}{\int_0^{t_{charg}} \dot{W}_{comp-HP,elec}\,dt}$$ Equation 8.41

$$COP_{ex,adsorption} = \frac{Ex_{recovered}}{\int_0^{t_{charg}} \dot{W}_{comp-HP,elec}\,dt}$$ Equation 8.42

8.2 Vapor compression heat pump system performance evaluation

It is well known that CFCs act as catalysts in ozone depleting reactions and contribute to the greenhouse effect. Reduction of CFCs emissions into the ambient for the HVAC produces can be achieved by substituting of the actual refrigerants with less-polluting ones that could meet the requirements of absence of toxicity, flammability and other issues from the thermodynamic points of view. Heat pumps can make good use of waste heat into a heat production process and, therefore, drastically reduce the demand of fossil energy as well as the emission of CO_2. It can enable us to utilize and recover the waste heat more efficiently. Facing the challenges of greenhouse effect, it is necessary to search the benign fluids with no or negligible ODP and GWP. In addition, it is also vitally important to improve energy efficiency for CO_2 emission reduction. HCFCs, HFCs,

natural refrigerants (NRs) and mixtures of environmentally friendly refrigerants have been proposed to replace the CFCs.

As HCFC-22 is gradually phased out, non-ozone depleting alternative refrigerants will be introduced. Various substitutes to HCFC-22 have been proposed, as shown in Table 8.1. Among these alternatives, HFC-134a is non-flammable and non-corrosive. It is a pure refrigerant with an ODP equal to zero and a GWP lower than that of HCFC-22 and other refrigerants (GWP$_{HCFC-22}$=1700; GWP$_{HFC-134a}$=1430). It should be noted that for the integration of heat pump into the adsorption storage system, the condensation temperature of the heat pump system is set 75°C. The critical temperature for HFC-134a (101°C) is higher than that of HFC-404A (72°C), HFC-410A (70°C) and HFC-407C (86°C). Therefore, the HFC-134a is selected as the refrigerant for vapor compression heat pump.

Table 8.1: Thermophysical properties of HCFC-22 and possible substitutes to HCFC-22 for heat pump

Refrigerant	HCFC-22	HFC-134a	HFC-404A	HFC-410A	HFC-407C
Composition (wt%)	–	–	HFC-125/143a/134a (44/52/4)	HFC-32/125 (50/50)	HFC-32/125/134a (23/25/52)
Molar mass (kg/kmol)	86.48	102.03	97.6	72.59	86.2
Boiling point at 1 atm (°C)	−40.80	−26.1	−46.5	−51.81	−43.7
Freezing point (°C)	−160.00	−101	−118		
Critical temperature (°C)	96	101.06	72.1	70.17	86.05
Critical pressure (bar)	49.9	40.64	37.32	47.70	46.34
Latent heal of vaporization (kJ/kg)	234.7	215.5	208.9	271.6	243.8
Saturated vapor specific volume at 20°C	0.02604	0.035	0.01809	0.01768	0.02660
Ozone depletion potential	0.055	0	0	0	0
Global warming potential	1700	1430	3700	1900	1600

The P-h diagram of HFC-134a is shown in Figure 8.3. One cyclic operation condition with evaporating temperature of 25°C and condensing temperature of 75°C is shown in the red line. As seen from Figure 8.3, if the condensation pressure is too high, more part of condensation heat is in the single phase part, which is not desirable. For actual experimental set-up, it is needed to choose the tropical compressor which can bear the high operating pressures. Also the electronic expansion valve (EEV) is highly recommended while thermal expansion valve is not recommended since the latter maybe not bear the high pressure drop.
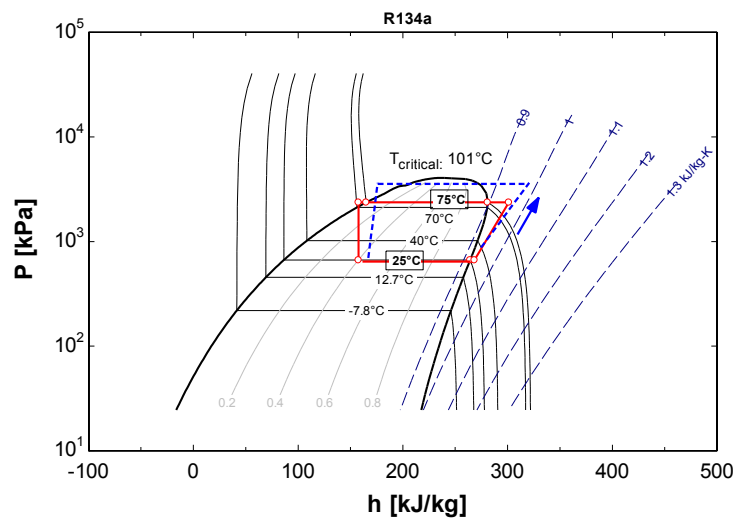
Figure 8.3: P-h diagrams for HFC-134a

Based on the modeling of heat pump, the calculated system performance are COP_{HP}=3.154, $COP_{ex,HP}$=0.26. The exergy balance diagram (also called Grassmann diagram) is shown in Figure 8.4. It can be found that the compressor exergy destruction and loss is the major part for exergy destruction in vapor compression cycle. The

following parts for exergy destruction and loss are condenser, expansive valve and evaporator.
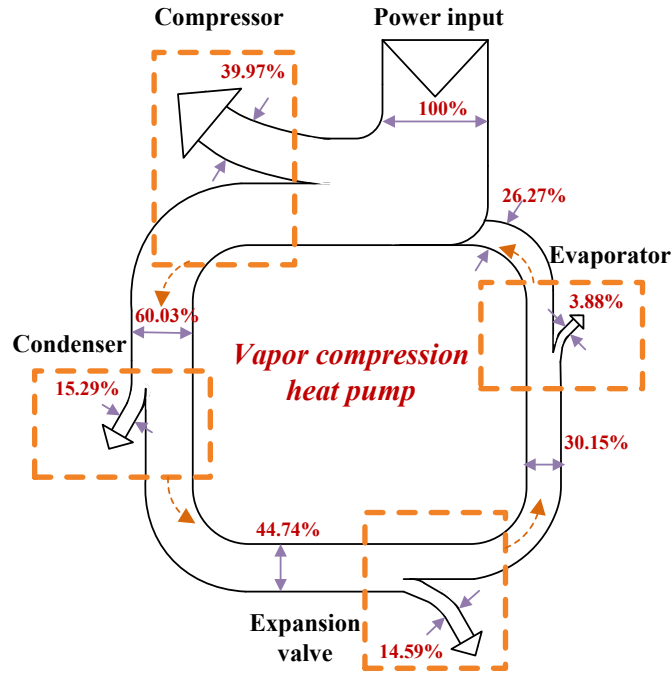
Figure 8.4: Exergy balance diagram (Grassmann diagram) for the compression heat pump system

To investigate the influencing factors for the vapor compression heat pump, the effect of low grade heat source temperature, subcooling degree and HTF mass flow rate of condenser side on system performance are shown in Figure 8.5, Figure 8.6 and Figure 8.7. It can be found that the heat source temperature has larger influence on the COP_{HP} and $COP_{ex,HP}$. With altered HTF mass flow rate, the outlet HTF temperature of condenser (regeneration temperature) is different. Small mass flow rate can lead to a higher regeneration temperature (compressor power remains constant).
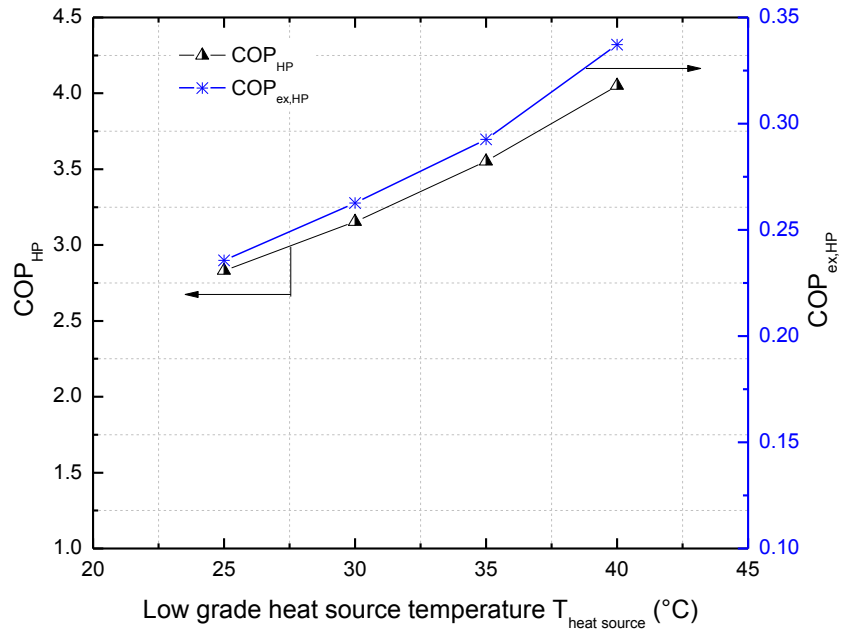
Figure 8.5: Effect of low grade heat source temperature on vapor compression heat pump performance
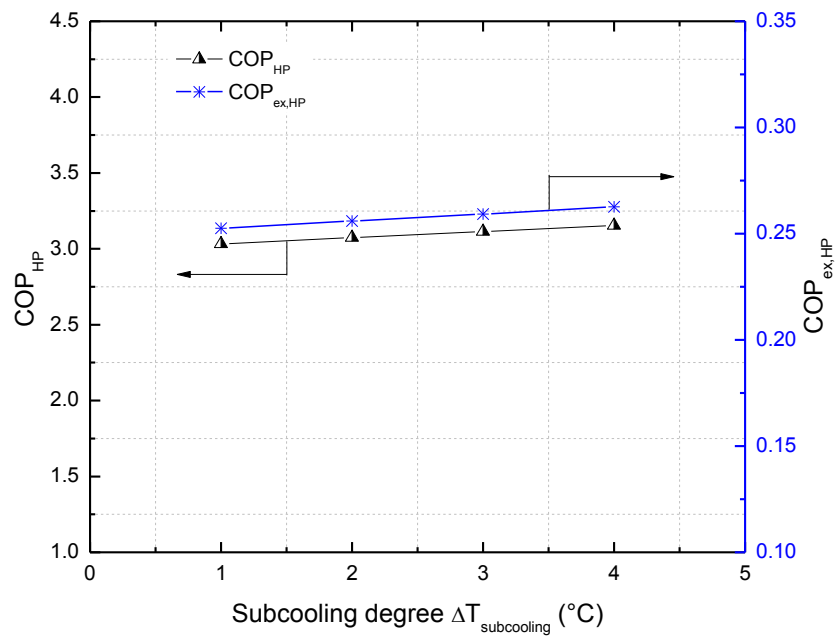
Figure 8.6: Effect of subcooling degree on vapor compression heat pump performance
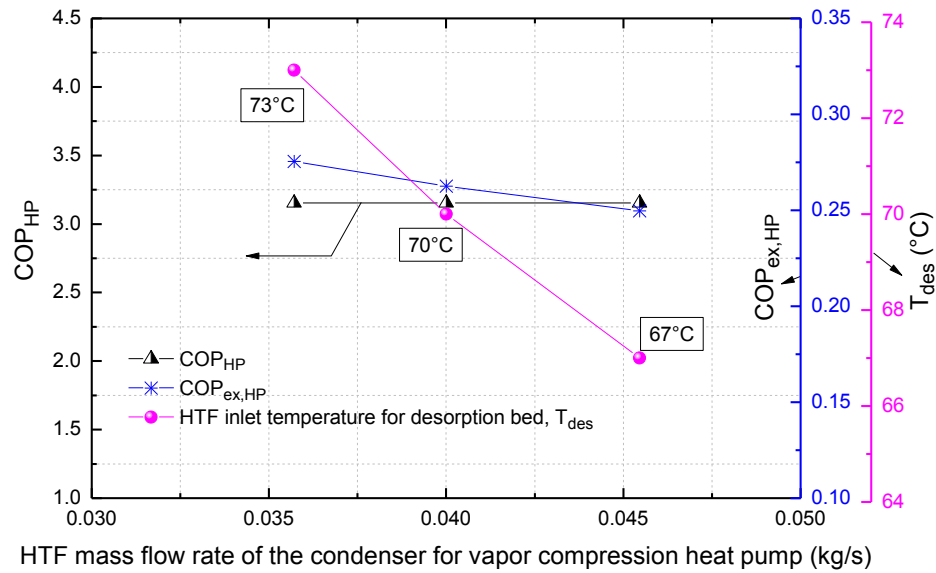
Figure 8.7: Effect of HTF mass flow rate on vapor compression heat pump performance

8.3 Performance evaluation of adsorption heat storage system integrated with heat pump

Based on the modeling for adsorption heat storage system with heat pump integration, the calculated system performance are $COP_{overall}$ =3.11, $COP_{ex,overall}$ =0.20. The exergy balance diagram (also called Grassmann diagram) is shown in Figure 8.8. Among the overall adsorption storage system, the exergy destruction and loss due to adsorption unit uses 5.8% of the total compressor power.
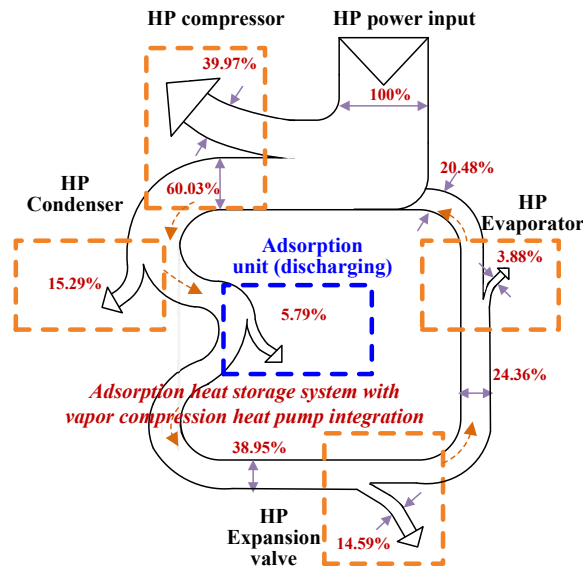
Figure 8.8: Exergy balance diagram (Grassmann diagram) for the adsorption heat TES system with vapor compression heat pump integration

Effect of HTF mass flow rate of adsorption bed is shown in Figure 8.9. With larger mass flow rate, the $COP_{overall}$ and $COP_{adsorption}$ increased while $COP_{ex,overall}$ and $COP_{ex,adsorption}$ decreased. Effect of HTF inlet temperature of adsorption bed is shown in Figure 8.10. With larger HTF inlet temperature made the $COP_{overall}$ and $COP_{adsorption}$ decreased while $COP_{ex,overall}$ and $COP_{ex,adsorption}$ increased. Effect of HTF inlet temperature of adsorption bed is shown in Figure 8.11. With larger ambient temperature, the $COP_{overall}$ and $COP_{adsorption}$ increased while $COP_{ex,overall}$ and $COP_{ex,adsorption}$ decreased. In addition, effect of low grade heat source temperature on overall sorption system performance is shown in Figure 8.12. $COP_{overall}$, $COP_{adsorption}$, $COP_{ex,overall}$ and $COP_{ex,adsorption}$ increased with higher heat source temperatures. Effect of HTF mass flow rate of desorption bed on overall sorption system performance is shown in Figure 8.13. Small mass flow rate leads to a higher regeneration temperature, thus $COP_{overall}$ is higher and exergy based system performance is also higher.

229
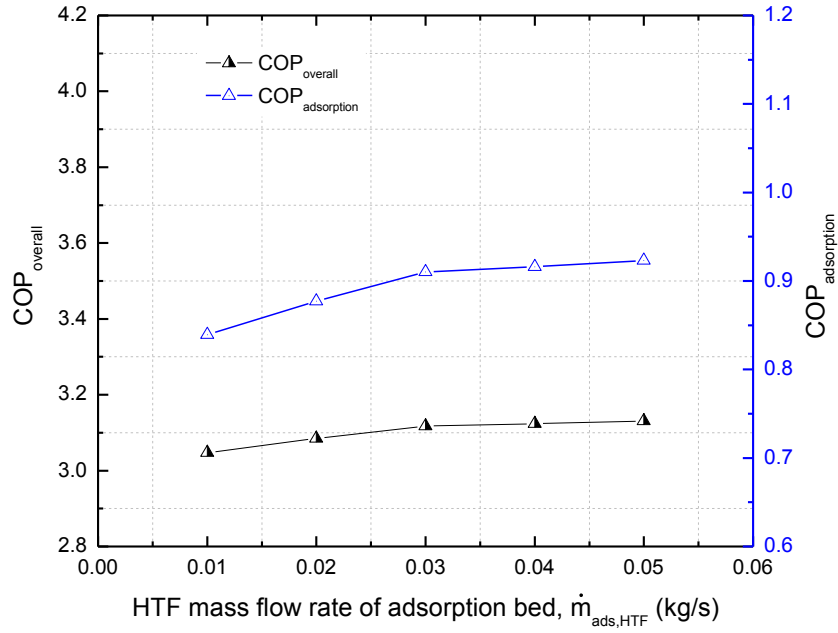
(a) COP$_{overall}$ and COP$_{adsorption}$
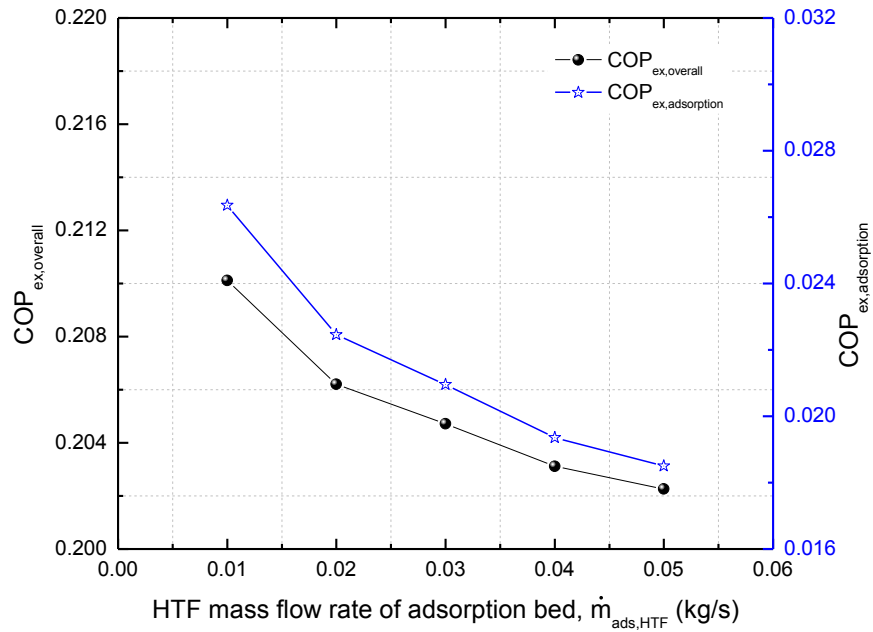
(b) COP$_{ex,overall}$ and COP$_{ex,adsorption}$

Figure 8.9: Effect of HTF mass flow rate of adsorption bed on overall sorption system performance
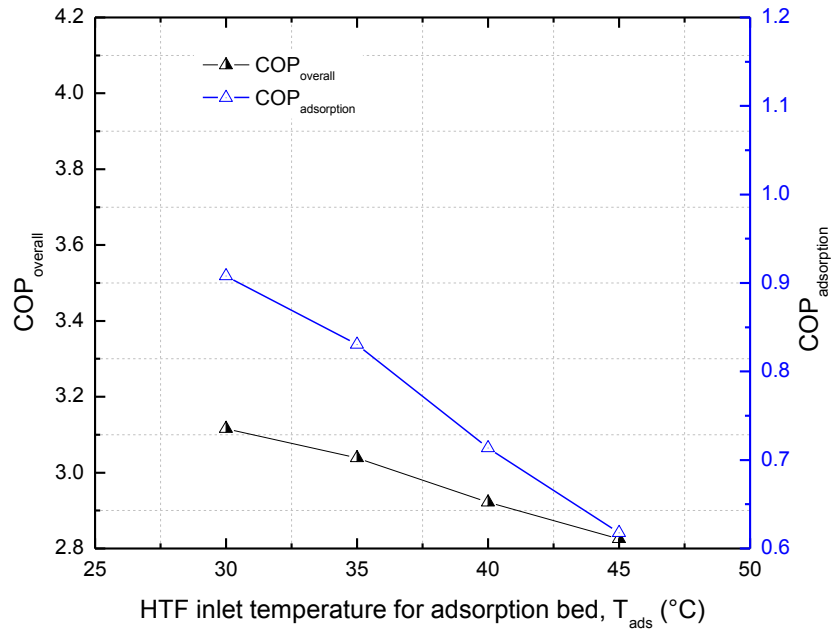
(a) $COP_{overall}$ and $COP_{adsorption}$
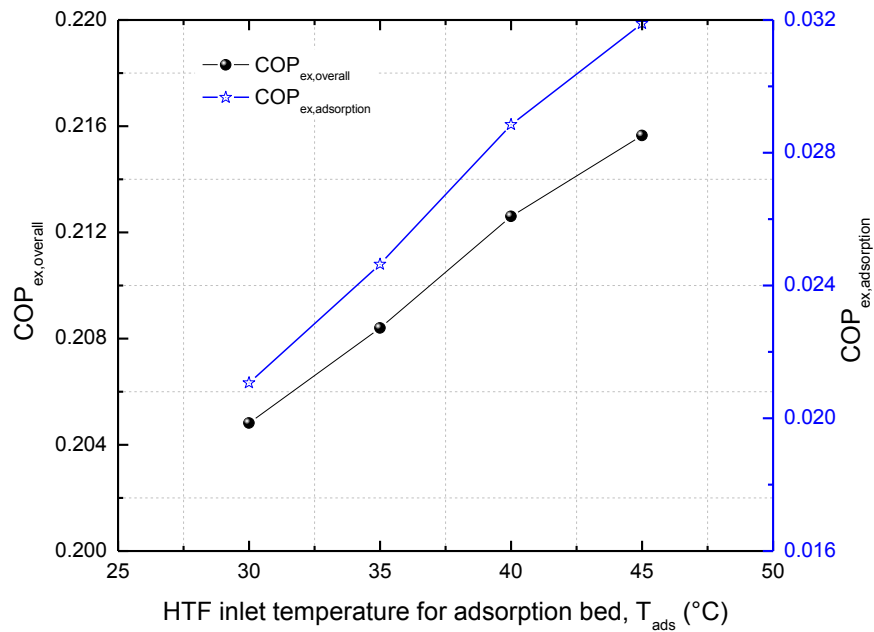
(b) $COP_{ex,overall}$ and $COP_{ex,adsorption}$

Figure 8.10: Effect of inlet temperature of adsorption bed on overall sorption system performance
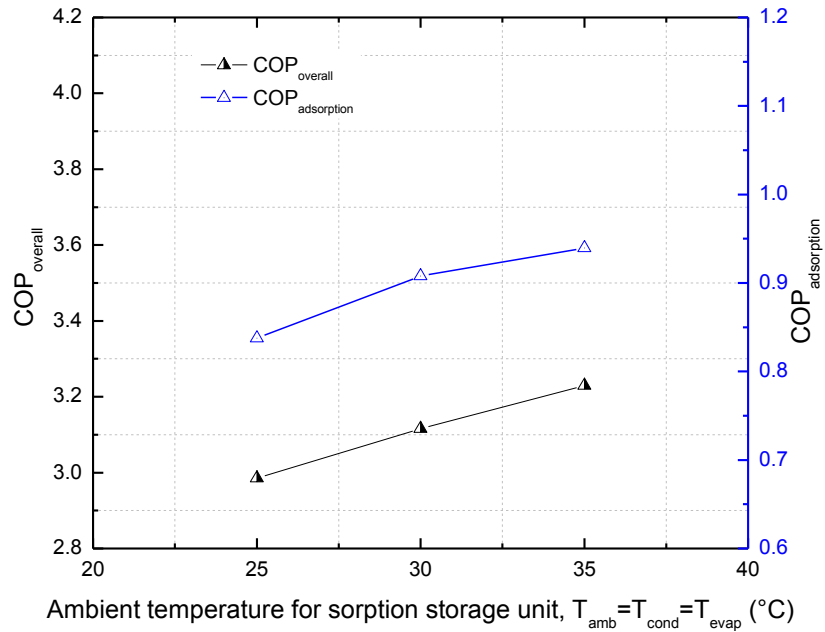
(a) $COP_{overall}$ and $COP_{adsorption}$
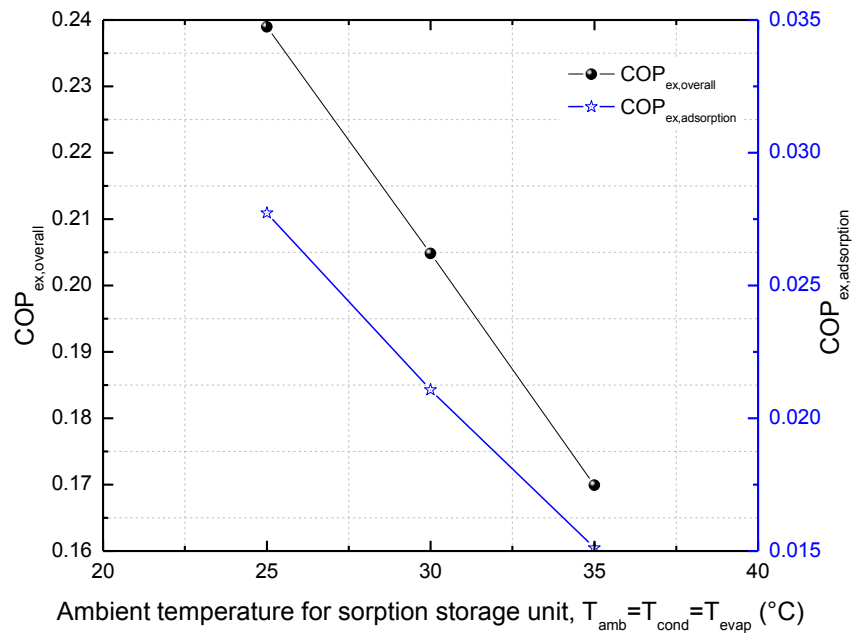
(b) $COP_{ex,overall}$ and $COP_{ex,adsorption}$

Figure 8.11: Effect of ambient temperature on overall sorption system performance
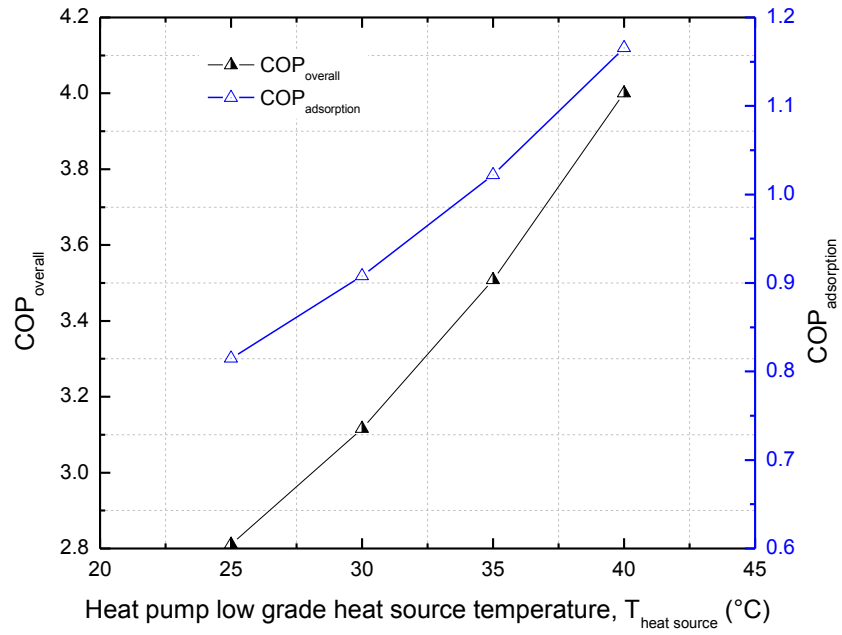
(a) COP$_\text{overall}$ and COP$_\text{adsorption}$
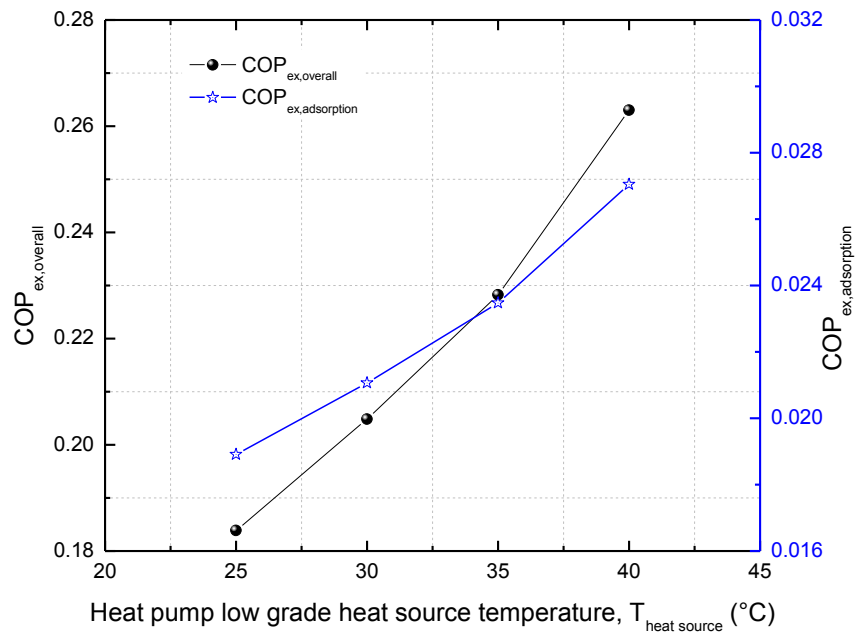
(b) COP$_\text{ex,overall}$ and COP$_\text{ex,adsorption}$

Figure 8.12: Effect of heat pump low grade heat source temperature on overall sorption system performance
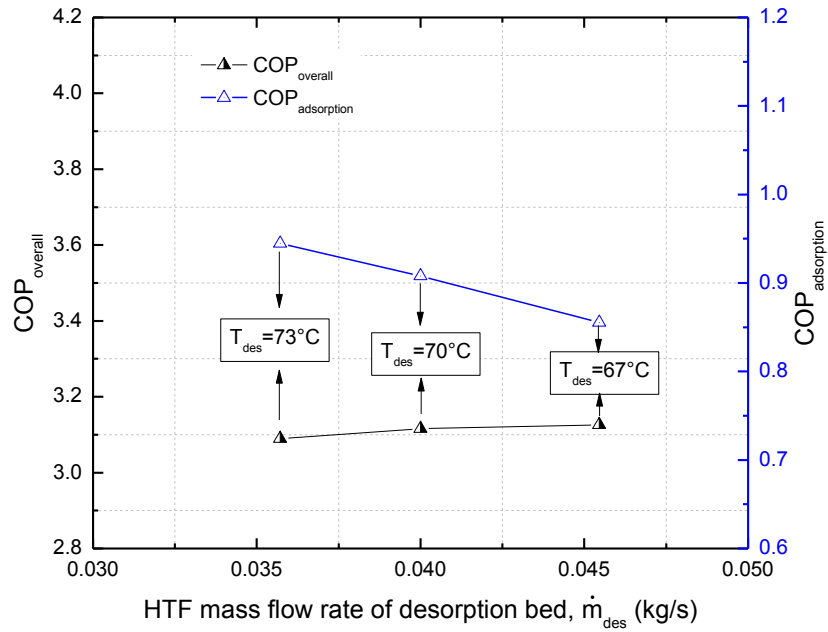
(a) $COP_{overall}$ and $COP_{adsorption}$
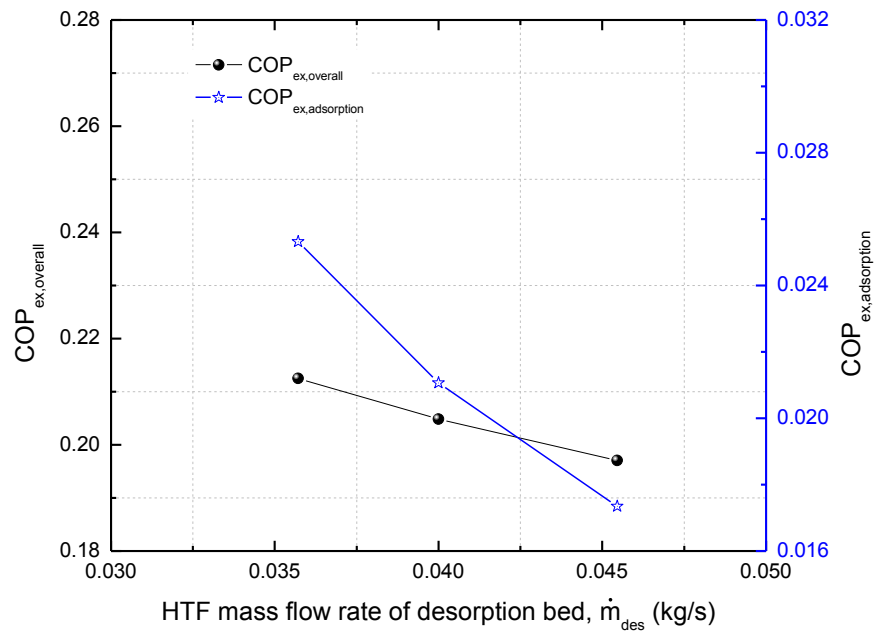
(b) $COP_{ex,overall}$ and $COP_{ex,adsorption}$

Figure 8.13: Effect of HTF mass flow rate of desorption bed on overall sorption system performance

234

8.4   System performance improvement potential

Two following solutions are discussed for improving the storage performance.

• Use more energy-efficient refrigerants

Usually the zeotropic mixtures can be regarded as alternative to pure fluids in heat pumps since they have several advantages over pure refrigerants. For applications with larger temperature glides of the heat sink and heat source, the COP can be improved in comparison with that of pure fluid. The reason can be involved that with approximating the temperature of a zeotropic mixture during evaporation or condensation to the temperature profile of the source or sink fluid, the average temperature difference is reduced. Therefore, the system performance can be improved due to the reduced irreversibilities of the components. In addition, by changing the circulating composition of the refrigerant mixture, the particular requirement for capacity can be achieved. Thus, it is more flexible than pure refrigerants. The search for zeotropic mixtures should have the requirement of environmentally safe and low cost.

• Add more adsorbents into sorption bed

It has been discussed in detail in Chapter 7. More adsorbents can be added into the fin spacing of adsorbent heat exchanger or onto heat transfer tubes to form consolidated adsorbents. The section of adsorption COP part ($COP_{adsorption}$, not $COP_{overall}$) for heat

storage mode can be evaluated with the increment of adsorbent mass, as shown in Figure 8.14.
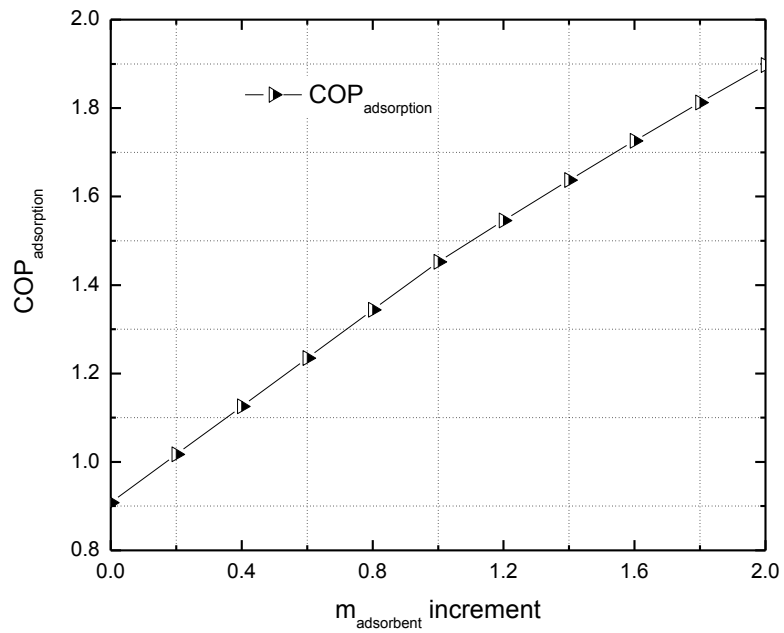
Figure 8.14: Effect of mass of adsorbents on section of adsorption COP part, $COP_{adsorption}$

In addition, for the current modeling system, the part of vapor compression heat pump is a little large for it has to supply both the heat load for hot water tank and adsorption thermal storage unit.

9   Conclusions and Future Work

9.1   Conclusions

This study mainly conducted research in two aspects: literature review for TES technologies and experimental investigation of adsorption TES for residential application. Relevant conclusions are summarized as follows:

- Cold storage technologies for air conditioning application and subzero application have been reviewed and analyzed in detail. Thermal and physicochemical properties of different phase change materials have been summarized including latent heat, thermal conductivity, phase separation, supercooling, and corrosion. Moreover, corresponding solutions for issues of different materials are also discussed. Sorption storage technologies had been also introduced. Sorption storage, especially the adsorption storage, is still at the early stage for commercialization, due to the poor heat and mass transfer of adsorbent beds, high equipment and maintenance cost, large size, and the need of an auxiliary energy system. Relevant perspectives for system performance improvement potential are discussed.

- Heat storage technologies for residential application (domestic hot water, space heating, etc.) had been reviewed and summarized. Sensible heat storage technologies were mainly introduced from liquid sensible heat and solid sensible heat, and relevant examples can be solar-assistant domestic hot water tank, aquifers, building heat storage equipment with water and stone as storage media.

Latent heat storage technologies were mainly introduced from inorganic and organic PCMs, and system performance improvement had been summarized, such as involvement of micro-encapsulated PCMs, PCMs with metal structures, and PCMs with high conductivity porous materials, nanoparticles, etc. Sorption heat storage technologies were also discussed, and currently there are only limited research works for adsorption TES technologies.

- Facing the issue of the gap between the availability and the demand in traditional energy sources, the performance assessment of TES units requires a sound and comprehensive knowledge about the thermal behavior. The energy analysis is inadequate because it does not evaluate how nearly the performance of the system approaches the ideal storage performance. The thermodynamic losses which occur within a system are often not accurately identified and assess with energy analysis. The background for energy analysis and exergy analysis was introduced and summarized.

- A previous adsorption chiller built for CHP utilization was modified to an adsorption thermal storage system for residential application. By using experimental data energy and exergy analysis were extensively investigated with different influencing factors, such as HTF mass flow rate of adsorption bed and desorption bed, regeneration temperature, adsorption temperature and ambient temperature. For the heat storage mode, results showed that mass flow rate for adsorption bed are more sensitive than that for desorption bed. With larger mass flow rate, the energy storage density and energy efficiency were larger, but the

238

exergy efficiency decreased due to the larger exergy destruction and loss caused by pressure drop. Higher regeneration temperature and lower adsorption temperature could make the energy storage density higher and energy efficiency larger, but the exergy efficiency decreased for the larger entropy generation, which is directly proportional to the finite temperature difference between regeneration/adsorption temperature and HTF temperature. With higher ambient temperature, total energy storage density and energy efficiency increased, and overall exergy efficiency decreased. For the cold storage mode, less HTF mass flow rate of the evaporator could achieve lower evaporator HTF outlet temperature for load, and the exergy efficiency increased. But the cold thermal efficiency decreased. Higher evaporator HTF inlet temperature and higher regeneration temperature could increase the cold energy storage density, and cold thermal efficiency. While the cold exergy destruction and loss or destruction would increase. Lower adsorption HTF inlet temperature lead to a higher cold energy storage density, and the exergy recovered increased for the reference temperature increased. In addition, perspective for system performance improvement potential is shown.

- To utilize the low grade energy, a vapor compression heat pump was integrated in the adsorption heat storage system to evaluate its overall performance. Modeling results showed that the overall integrated system COP is around 3.11 and exergy based COP is around 0.20. The exergy destruction and loss for different components were calculated and shown in the Grassmann diagram. In addition,

system performance evaluation was studied with different influencing factors, such as low grade heat source temperature, ambient temperature, HTF mass flow rate for desorption bed and adsorption bed. Also the solutions for system performance improvement potential are suggested.

The list of publication works from current research work either already published or under preparation is as follows:

(1) Gang Li, Yunho Hwang, Reinhard Radermacher. Review of cold storage materials for air conditioning application. International Journal of Refrigeration. 2012, 35: 2053-2077 Rank 2 for top 25 hottest articles (October to December 2012; January to March 2013)

(2) Gang Li, Yunho Hwang, Reinhard Radermacher, Ho-Hwan Chun. Review of cold storage materials for subzero applications. Energy. 2013,51:1-17

(3) Gang Li, Yunho Hwang, Reinhard Radermacher. Review of heat storage materials for residential application. Energy and Buildings. 2013 (in preparation)

(4) Gang Li, Yunho Hwang, Reinhard Radermacher. Experimental investigation of energy and exergy performance of short term adsorption heat storage for residential application. Energy. 2013 (in preparation)

(5) Gang Li, Yunho Hwang, Reinhard Radermacher. Experimental investigation of energy and exergy performance of adsorption cold storage for residential application. International Journal of Refrigeration. 2013 (in preparation)

(6) Gang Li, Yunho Hwang, Reinhard Radermacher. Energy and exergy performance evaluation of adsorption thermal energy storage with vapor compression heat pump integration. Energy. 2013 (in preparation)

(7) Gang Li, Magnus Eisele, Yunho Hwang, Reinhard Radermacher. Experimental investigation of energy and exergy performance of secondary loop automotive air-conditioning systems using low-GWP refrigerants. Energy. 2013 (in preparation)

(8) Gang Li, Magnus Eisele, Yunho Hwang, Reinhard Radermacher. Life cycle climate performance of secondary loop automotive air-conditioning systems using low-GWP refrigerants. Energy. 2013 (in preparation)

9.2   Recommendations for future work

Adsorption TES is an important aspect of available storage technologies. Several suggestions are listed for future work as follows:

- The adsorbent heat exchanger in the adsorption bed is strongly recommended for optimization. More adsorbents should be attached into the fin spacing of adsorbent heat exchanger and onto heat transfer tubes to form consolidated adsorbent. Based on the test results, the current design has the advantage that the heat transfer between adsorption bed and HTF is very good for the time of charging process (around 20 minutes). But there exists great potential to increase the storage density because fin spacing is around 15 times of fin thickness and the coating thickness is quite small. Therefore, necessary solutions need to be taken to fill more adsorbents. In addition, the storage density can be improved with

working pairs with chemical reaction effect (the current working pair is physical adsorption ones). It is also highly recommended to make the sorption chamber and condenser/evaporator chamber in one unit to make the system more compact.

- Often, a CHP system operates most efficiently at a constant load. However, the electrical and thermal energy needs of a residential building are not constant. If the heat demand by the building varies over time, this problem may be alleviated when thermal energy storage is available. Therefore, further study should be investigated in detail to size the storage capacity to balance the energy supply and demand during the whole year. It is also highly recommend to conduct some experimental tests in mid-season conditions.

- During the test, the issue of HTF temperature fluctuation due to current PID control together mixed with valves sometimes influences the storage performance assessment and evaluation greatly. Also water loop from outdoor chiller to the adsorption unit is quite long and this makes the response time for PID control long, which also affects the test results. It is highly suggested to change the control strategy to make the test more stable.

- For the adsorption heat storage tests in Chapter 7, the regeneration source is the Ecopower. For later test, it is recommended to utilize the fuel cell waste heat to drive the adsorption chamber for thermal storage. In addition, radiation-shielding materials should also be added onto the surface of chambers to reduce heat loss. In addition, further study should also be developed for economic analysis for whole storage system.

References

Abdulateef, J.M., Sopian, K., Alghoul, M.A., Sulaiman, M.Y., Zaharim, A., Ahmad, I., 2007. Solar absorption refrigeration system using new working fluid pairs. International Journal of Energy. 1 (3): 82–87.

Abhat, A., 1983.Low temperature latent heat thermal energy storage: heat storage materials. Solar Energy. 30, 313-332.

Agyenim, F., Hewitt, N., Eames, P., Smyth, M., 2010. A review of materials, heat transfer and phase change problem formulation for latent heat thermal energy storage systems (LHTESS). Renewable & Sustainable Energy Reviews.14,615-628.

Akiya,T., Tomio, S., Oowa, M., 1997. Phase equilibria of some alternative refrigerants hydrates and their mixtures using for cool storage material, Proceedings of the 32th Intersociety Energy Conversion Engineering Conference, pp. 1652-1655.

Alvarado, J.L., Sohn, C.M.C., Kessler, D., 2004. Thermophysical properties characterization of microencapsulated phase change material slurry, International Refrigeration and Air Conditioning Conference at Purdue.

Alvarado, J.L., Marsh, C., Sohn, C., Vilceus, M., Hock, V., Phetteplace, G., Newell, T., 2006. Characterization of supercooling suppression of microencapsulated phase change material by using DSC. Journal of Thermal Analysis and Calorimetry. 86, 505-509.

Alvarado, J.L., Marsh, C., Sohn, C., Phetteplace, G., Newell, T., 2007. Thermal performance of microencapsulated phase change material slurry in turbulent flow under constant heat flux. International Journal of Heat and Mass Transfer. 50(9-10), 1938-1952.

Asaoka, T., Saito, A., Okawa, S., Ito, T., Izumi, N., 2009.Vacuum freezing type ice slurry production using ethanol solution 1st report: Measurement of vapor–liquid equilibrium data of ethanol solution at 20°C and at the freezing temperature. International Journal of Refrigeration. 32 (3), 387-393.

Azzouz, K., Leducq, D., Gobin, D., 2008. Performance enhancement of a household refrigerator by addition of latent heat storage. International Journal of Refrigeration. 31, 892–901.

Azzouz, K., Leducq, D., Gobin, D., 2009. Enhancing the performance of household refrigerators with latent heat storage: an experimental investigation. International Journal of Refrigeration. 32,1634–1644.

Bahnfleth, W.P., Song, J., Cimbala, J.M., 2003. Thermal performance of single pipe diffusers in stratified chilled water storage tanks, Final report of ASHRAE, 1185-RP.

Bales, C.,Gantenbein, P.,Jaenig, D.,Kerskes, H.,Summer, K.,van Essen, M.,Weber, R., 2008. Laboratory tests of chemical reactions and prototype sorption storage units..Report no.B4-Task32.Availablefrom: http://archive.iea-shc.org/publications/downloads/task32-b4.pdf

Bansal, N.K., Blumenberg, J., Kavasch, H.J., Roettinger, T., 1997. Performance testing and evaluation of solid absorption solar cooling unit. Solar Energy. 61,127–140.

Bejan, A., 1978. Two thermodynamic optima in the design of sensible heat units for energy storage. ASME-Journal of Heat Transfer. 100, 708–712

Belton, G., Ajami, F., 1973.Thermochemistry of salt hydrates.1973.91 p. Report no.NSF/RANN/SE/GI27976/TR/73/4.

Biswas, D.R., 1977. Thermal energy storage using sodium sulfate decahydrate and water. Solar Energy. 19, 99-100.

Bogart, M., 1981. Ammonia Absorption Refrigeration in Industrial Processes, Gulf, Houston, TX.

Cabeza, L.F., Svensson, G., Hiebler, S., Mehling, H., 2003. Thermal performance of sodium acetate trihydrate thickened with different materials as phase change energy storage material. Applied Thermal Engineering. 23, 1697-1704.

Canbazoglu, S., Sahinaslan, A., Ekmekyapar, A., Aksoy, Y.G., Akarsu, F., 2005. Enhancement of solar thermal energy storage performance using sodium thiosulfate pentahydrate of a conventional solar water-heating system. Energy and Buildings. 37(3), 235-242

Cantor, S., 1978. DSC study of melting and solidification of salt hydrates. Thermochimica Acta. 26, 39–47.

Cai, L., Stewart, W.E., Sohn, C.W., 1993. Turbulent buoyant flows into a two dimensional storage tank. International Journal of Heat and Mass Transfer. 36, 4243-4256.

Cai, Y. B., Hu, Y., Song, L., Tong, Y., 2006. Flammability and thermal properties of high density polyethylene/paraffin hybrid as a form-stable phase change material. Journal of Applied Polymer Science. 99 (4), 1320-1327.

Caldwell, J.S., Bahnfleth, W.P., 1998. Identification of mixing effects in stratified chilled-water storage tanks by analysis of time series temperature data. ASHRAE Transactions, 104 (2), 366-376.

Cantor, S., 1978. DSC study of melting and solidification of salt hydrates. Thermochimica Acta. 26, 39-47.

Carbajo, J.J., 1985. A Direct-contact-charged direct-contact-discharged cool storage system using gas hydrate. ASHRAE Transactions. 91 (2A), 258-266.

Cen, H.X., Yan, Y.H., Tong, J.S., 1997. Theoretical calculation and experimental study of liquid-solid equilibrium phase diagram on cool storage materials for air conditioning system. Journal of Chemical Engineering of Chinese Universities. 11(1), 25-30. (in Chinese).

Chickos, J.S., Acree, W.E., Liebman, J.F., 2011. Students of Chem 202 (Introduction to the Literature of Chemistry), University of Missouri -- St. Louis, "Heat of Fusion data" inNIST Chemistry WebBook, NIST Standard Reference Database Number 69, Eds. Linstrom PJ and Mallard WG, National Institute of Standards and Technology, Gaithersburg MD, 20899, http://webbook.nist.gov, (retrieved December 28, 2011).

Cole, R.L., Bellinger, F.O., 1982. Thermally stratified tanks. ASHRAE Transactions. 88 (2), 1005-1017.

Costa, M., Buddhi, D., Oliva, A., 1998. Numerical simulation of a latent heat thermal energy storage system with enhanced heat conduction. Energy Conversion and Management.39, 319–330.

Darbouret, M., Cournil, M., Herri, J.M., 2005. Rheological study of TBAB hydrate slurries as secondary two-phase refrigerants. International Journal of Refrigeration.28, 663-671.

Diaconu, B.M., 2009. Transient thermal response of a PCS heat storage system. Energy and Buildings. 41(2), 212-219.

Diaconu, B.M., Varga, S., Oliveira, A.C., 2010. Experimental assessment of heat storage properties and heat transfer characteristics of a phase change material slurry for air conditioning applications. Applied Energy. 87(2), 620-628.

Dieckmann, J.H., 2006. Latent heat storage in concrete. University of Kaiserslautern, Germany, http://www.eurosolar.org. [accessed on 11.11.2011].

Dimaano, M.N.R., Escoto, A., 1998. Preliminary assessment of a mixture of capric acid and lauric acid for low-temperature thermal energy storage. Energy. 12(5), 421-427.

Dimaano, M.N.R., Watanabe, T., 2002a. The capric–lauric acid and pentadecane combination as phase change material for cooling applications. Applied Thermal Engineering. 22(4), 365-377.

Dimaano, M.N.R., Watanabe, T., 2002b.The capric and lauric mixture with chemical additives as latent heat storage materials for cooling application. Energy. 2(4), 869-888.

Dincer, I., Rosen, M.A., 2011.Thermal energy storage: Systems and applications. Wiley.

Dini, S., Saniei, N., 1992. Refrigerant hydrate as a cool storage medium. ASME Winter Annual Meeting, Anaheim, California, USA.

Domalski, E.S., Hearing, E.D., 2011."Condensed Phase Heat Capacity Data" in NIST Chemistry WebBook, NIST Standard Reference Database Number 69, Eds. Linstrom PJ and Mallard WG, National Institute of Standards and Technology, Gaithersburg MD, 20899, http://webbook.nist.gov, (retrieved December 28, 2011).

Dorgan, C.E., Elleson, J.S., 1993. Design guide for cool thermal storage. ASHRAE Inc., Atlanta, USA

Dyadin, Y.A., Udachin, K.A., 1984. Clathrate formation in water-peralkylonium salts systems. Journal of Inclusion Phenomena. 2, 61-72.

Egolf, P.W., Kitanovski, A., Ata-Caesar, D., Vuarnoz, D., Meili, F., 2008. Cold storage with ice slurries. International Journal of Energy Research. 32 (3), 187-203.

El-Dessouky, H., Al-Juwayhel ,F., 1997. Effectiveness of a thermal energy storage system using phase-change materials. Energy Conversion and Management.38,601–617.

El Qarnia, H., 2009. Numerical analysis of a coupled solar collector latent heat storage unit using phase change materials for heating the water. Energy Conversion and Management. 50,247–254.

Elgafy, A., Lafdi, K., 2005. Effect of carbon nanofiber additives on thermal behavior of phase change materials. Carbon. 43, 3067-3074.

Eltom, O.M.M., Sayigh, A.A.M., 1994. A simple method to enhance thermal conductivity of charcoal using some additives. Renewable Energy. 4(1),113–118.

Energy Information Administration, U.S. Department of Energy, 2011. Annual Energy Review 2011, Primary Energy Production by Source, Selected Years, 1949-2011.

Erek, A., Dincer, I., 2008. An approach to entropy analysis of a latent heat storage module. International Journal of Thermal Sciences. 47,1077–1085.

Erek, A., Dincer, I., 2009. A New approach to energy and exergy analyses of latent heat storage unit. Heat Transfer Engineering.30,506–515.

Eun, T.H., Song, H.K., Han, J.H., Lee, K.H., Kim, J.N., 2000. Enhancement of heat and mass transfer in silica-expanded graphite composite blocks for adsorption heat pumps. Part II. Cooling system using the composite blocks. International Journal of Refrigeration. 23, 74-81.

Ezan, M.A., Ozdogan,M., Gunerhan, H., Erek, A., Hepbasli, A., 2010.Energetic and exergetic analysis and assessment of a thermal energy storage (TES) unit for building applications. Energy and Buildings. 42(10), 1896-1901

Ezan, M.A., Erek, A., Dincer, I., 2011.Energy and exergy analyses of an ice-on-coil thermal energy storage system. Energy. 36(11),6375-6386

Fan, Y., Luo, L., Souyri, B., 2007. Review of solar sorption refrigeration technologies: Development and applications. Renewable and Sustainable Energy Reviews. 11 (8),1758–1775

Fang, J.S., 2011.Experimental research on effects of magnetic field on supercooling degree and crystallization process of low-temperature cool storage materials (Master Thesis). Shandong University.

Faninger, G., 2004. Thermal energy storage. www.etn.wsr.ac.at [accessed on 11.11.2011]

Farid, M.M., Khudhair, A.M., Razack, S.A.K., Al-Hallaj, S., 2004. A review on phase change energy storage: material and application. Energy Conversion and Management. 45, 1597-1615.

Farrell, A.J., Norton, B., Kennedy, D.M., 2006. Corrosive effects of salt hydrate phase change materials used with aluminum and copper. Journal of Materials Processing Technology. 175, 198-205.

Fournaison, L., Delahaye, A., Chatti, I., Petitet, J.P., 2004. CO_2 hydrates in refrigeration processes. Industrial & Engineering Chemistry Research. 43, 6521-6526.

Fukai, J., Morozumi ,Y., Hamada, Y., Miyatake, O.,2000. Transient response of thermal energy storage unit using carbon fibers as thermal conductivity promoter. In: Proceedings of the 3rd European Thermal Science Conference, Pisa, Italy.

Ge, Y.Q., Zhang, X.L., Liu, J.N., Zhao, L., 2007. Analysis and study of binary ice vacuum making technique. HV&AC. 37(3), 10-14. (in Chinese).

Ghajar, A.J., Zurigat, Y.H., 1991. Numerical study of the effect of inlet geometry on stratification in thermal energy storage. Numerical Heat Transfer. 19, 65-83.

Gin, B., Farid, M.M., Bansal, P.K., 2010. Effect of door opening and defrost cycle on a freezer with phase change panels. Energy Conservation and Management. 51,2698–2706.

Gin, B., Farid, M.M., 2010. The use of PCM panels to improve storage condition of frozen food. Journal of Food Engineering.100, 372–376.

Gormley, R., Walshe, T., Hussey, K., Butler, F., 2002. The effect of fluctuating vs. constant frozen storage temperature regimes on some quality parameters of selected food products. LWT - Food Science and Technology. 35 (2), 190–200.

Grandum, S., Nakagomi, K., 1997. Characteristics of ice slurry containing antifreeze protein for ice storage applications. Journal of Thermophysics and Heat Transfer. 11(3), 461-466.

Grandum, S., Yabe, A., Nakagomi, K., Tanaka, M., Takemura, F., Kobayashi, Y., Frivik, P.E., 1999. Analysis of ice crystal growth for a crystal surface containing absorbed antifreeze proteins. Journal of Crystal Growth. 205, 382-390.

Guo, K.H., Shu, B.F., Yang, W.J., 1996. Advances and applications of gas hydrate thermal energy storage technology, Proceedings of 1st Trabzon International Energy & Environment Symposium, Trabzon, Turkey.

Guo, K.H., Shu, B.F., Zhao, Y.L., 1998. Characterization of phase change and cool-storage process of mixed gas hydrate, Cryogenics and Refrigeration, Proceeding of ICCR'98, Hangzhou, China.

Guo, N.N., 2008. Thermal properties research of the multivariate organic phase change materials for cooling system (Master thesis). College of power engineering, Chongqing University, PR China.

Hackeschmidt, K., Khelifa, N., Girlich, D.,2007. Verbesserung der Nutzbaren Wärmeleitung in Latentspeichern durch offenporige Metallschäume, KI Kälte – Luft – Klimatechnik.33–36.

Hägg, C., 2005. Ice slurry as secondary fluid in refrigeration systems. School of Industrial Engineering and Management, Royal Institute of Technology (KTH), Licentiate Thesis, Stockholm.

Han, B.Q., Yuan, H.Y., Yang, D.Q., Liu, G.X., 1994. Utilization of natural zeolites for solar energy storage, Lu N, Best G, Carvalho Neto CC. Editors, Integrated energy systems in China-the cold Northeastern region experience, FAO, Rome. www.fao.org [accessed on 11.11.2011].

Han, Z.H., 2008. Nanofluids with Enhanced Thermal Transport Properties (PhD Dissertation). Department of Mechanical Engineering, University of Maryland at College Park.

Hasnain, S.M., 1998. Review on sustainable thermal energy storage Technologies, part II; Cool thermal storage. Energy Conversion and Management. 24 (11), 1139 -1153.

Hawes, D.W., Feldman, D., Banu, D., 1993. Latent heat storage in building materials. Energy and Buildings.20, 77–86.

Hawlader, M.N.A., Uddin, M.S., Khin, M.M., 2003. Microencapsulated PCM thermal-energy storage system. Applied Energy. 74 (1–2), 195-202.

Hayashi, K., Takao, S., Ogoshi, H., Matsumoto, S., 2000. Research and development on high-density cold latent-heat medium transportation technology. In: Fifth Workshop, Final Proceedings; p. 1-9 [PPIEA, Annex 10].

He, B., Gustafsson, E.M., Setteerwall, F., 1999. Tetradecane and hexadecane binary mixture as phase change materials (PCMs) for cool storage in district cooling systems. Energy. 24, 1015–1028.

He, B., Setteerwall, F., 2002. Technical grade paraffin waxes as phase change materials for cool thermal storage and cool storage systems capital cost estimation. Energy Conversion and Management. 43(9), 1709-1723.

He, Q.B.,2005. Study on Thermal Properties and Characteristics of Cool Charge and Discharge of Nanofluids. College of Power Engineering. Chongqing University. (in Chinese).

Hirata, T., Nagasaka, K., Ishikawa, M., 2000. Crystal ice formation of solution and its removal phenomena at cooled horizontal solid surface, part I: ice removal phenomena. International Journal of Heat and Mass Transfer. 43, 333-339.

Hongois, S.,Kuznik, F.,Stevens, P.,Roux, J.J., 2011. Development and characterization of a new MgSO4–zeolite composite for long-term thermal energy storage. Solar Energy Materials and Solar Cells.95,1831–1837.

Huang, L., Petermann, M., Doetsch, C., 2009. Evaluation of paraffin/water emulsion as a phase change slurry for cooling applications. Energy. 34, 1145-1155.

Inaba, H., 1996. Cold heat-release characteristics of phase change emulsion by air-emulsion direct-contact heat exchange method. International Journal of Heat and Mass Transfer. 39, 1797-1803.

Inaba, H., Lee, D.W., Horibe, A., 1998. Study on the critical conditions of ice formation for a continuous ice making system in a cooling pipe. Heat Transfer Japanese Research. 27(1), 74-83.

Inaba, H., Kim, M.J., Horibe, A., 2004. Melting heat transfer characteristics of microencapsulated phase change material slurries with plural microcapsules having different diameters. ASME Journal of Heat Transfer. 126(4), 558-565.

Inada, T., Yabe, A., Saito, T., Lu, S.S., Zhang, X., Yoshimura, K., Tanaka, M., Grandum, S., 1999. Microscale analysis of ice crystals made from aqueous solutions by scanning tunneling microscope. Proceedings of 6th International Symposium on Thermal Engineering and Sciences for Cold Regions, pp. 545-554.

Inada, T., Yabe, A., Grandum, S., Saito, T., 2000. Control of molecular-level ice crystallization using antifreeze protein and silane coupling agent. Materials Science and Engineering: A. 292(2), 149-154.

Infante Ferreira, C.A., 1984.Thermodynamic and physical property data equations for ammonia–lithium nitrate and ammonia–sodium thiocyanate solutions. Solar Energy. 32, 231–236.

International Energy Agency, 2009. World Energy Outlook 2009.

Isobe, F., Mori, Y.H., 1992. Formation of gas hydrate or ice by direct-contact evaporation of CFC alternatives. International Journal of Refrigeration. 15(3), 137-142.

Jegadheeswaran, S., Pohekar, S.D., Kousksou, T., 2010. Exergy based performance evaluation of latent heat thermal storage system: A review. Renewable and Sustainable Energy Reviews.14(9),2580-2595

Kaizawa, A., Kamano, H., Kawai, A., Jozuka, T., Senda, T., Maruoka, N., Akiyama, T., 2008. Thermal and flow behaviors in heat transportation container using phase change material. Energy Conversion and Management. 49, 698–706

Kaygusuz, K.,2003. Phase change energy storage for solar heating systems. Energy Sources. 25,791–807.

Khattab, N.M., 2004. A novel solar-powered adsorption refrigeration module. Applied Thermal Engineering. 24 (17–18), 2747–2760

Khokhar, A.A., Gudmundsson, J.S., Sloan, E.D., 1998. Gas storage in structure H hydrate. Fluid Phase Equilibria. 150-151, 383-392.

Kim, B.S., Shin, H.T., Lee, Y.P., Jurng, J., 2001. Study on ice slurry production by water spray. International Journal of Refrigeration. 24, 176-184.

Kimura, H., Kai, J., 1984. Phase change stability of $CaCl_2 \cdot 6H_2O$. Solar Energy. 33, 557-563.

Kousksou, T., Strub, F., Lasvignottes, J.S., Jamil, A., Bedecarrats, J.P., 2007. Second law analysis of latent thermal storage for solar system. Solar Energy Materials and Solar Cells. 91,1275–1281.

Kousksou, T., El Rhafiki, T., Arid, A., Schall, E., Zeraouli, Y., 2008. Power, efficiency, and irreversibility of latent energy systems. Journal of Thermophysics and Heat Transfer.22,234–239.

Kozawa, Y., Aizawa, N., Tanino, M., 2005. Study on ice storing characteristics in dynamic-type ice storage system by using supercooled water. Effects of the supplying conditions of ice-slurry at deployment to district heating and cooling system. International Journal of Refrigeration. 28(1), 73-82.

Kumano, H., Asaoka, T., Saito, A., Okaw, S., 2007. Study on latent heat of fusion of ice in aqueous solutions. International Journal of Refrigeration. 30, 267-273.

Kumano, H., Hirata, T., Izumi, Y., 2010. Study on specific enthalpy of ice including solute in aqueous solution. International Journal of Refrigeration. 33 (3), 480-486.

Lai, H.M., 2000. An enhanced adsorption cycle operated by periodic reversal forced convection. Applied Thermal Engineering. 20, 595-617.

Lane, G.A., 1980. Low temperature heat storage with phase change materials. The International Journal of Ambient Energy.1, 155–168.

Lane, G.A., 1992. Phase change materials for energy storage nucleation to prevent supercooling. Solar Energy Materials and Solar Cells. 27,135-160.

Leaist, D.G., Murray, J.J., Post, M.L., Davidson, D.W., 1982. Enthalpies of decomposition and heat capacities of ethylene oxide and tetrahydrofuran hydrates. Journal of Physical Chemistry. 86, 4175-4178.

Le-Pierrès, N., Liu, H., Luo, L., 2011.$CaCl_2/H_2O$ absorption seasonal storage of solar heat. In: Proceedings of the international conference for sustainable energy storage.

251

Li, X., Zheng, Z.H., Wang, Q.H., Guo, X.C., Chen, W.K., Zheng, C.C., 1996. The phase-change performance of cooling storage materials. Journal of Refrigeration. 5(1), 22-25. (in Chinese).

Li, Z.F., Sumathy, K., 2000. Technology development in the solar absorption air-conditioning systems. Renewable & Sustainable Energy Reviews. 4(3), 267-293.

Li, M., Wang, R.Z., 2002. A study of the effects of collector and environment parameters on the performance of a solar powered solid adsorption refrigerator. Renewable Energy.27, 369-382.

Li, X.W., Zhang, X.S., 2009. Evaporative super-cooled water method for ice-slurry producing. Journal of Southeast University (Natural Science Edition). 39(2), 269-275. (in Chinese).

Li, G., Liu, D.P., Xie, Y.M., 2010. Study on thermal properties of TBAB–THF hydrate mixture for cold storage by DSC. Journal of Thermal Analysis and Calorimetry. 102(2), 819-826.

Li, M., Wang, R.Z., Xu, Y.X., Wu, J.Y., Dieng, A.O., 2002. Experimental study on dynamic performance analysis of a flat-plate solar solid-adsorption refrigeration for ice maker. Renewable Energy. 27 (2), 211–221

Li, M., Sun, C.J., Wang, R.Z., Ca, W.D., 2004. Development of no valve solar ice maker. Applied Thermal Engineering. 24, 865–872

Lin, K., Zhang, Y., Xu, X., Di, H., Yang, R., Qin, P., 2005. Experimental study of under-floor electric heating system with shape-stabilized PCM plates. Energy and Buildings. 37, 215-220.

Lindner, F., 1996.Heat storage with salts and salt hydrates. KiLuft-und K¨altetechnik. 10, 462–467.

Liu, Y., Guo, K.H., Liang, D.Q., Fan, S.S., 2003a. Effects of magnetic fields on HCFC-141b refrigerant gas hydrate formation. Science in China Series B-Chemistry. 46(4), 407-415.

Liu, Y.H., Guo, K.H., Liang, D.Q., 2003b.Study on refrigerant hydrate crystallization process in the action of ultrasonic. Journal of Engineering Thermal Physics. 24(3), 385-387. (in Chinese).

Liu, D.Y., 2005. Preparation and thermal property study of low-temperature cool storage nanocomposite PCM (Doctoral Dissertation). Chongqing University. (in Chinese).

Liu, H., Le Pierrès, N., Luo, L., 2009. Seasonal storage of solar energy for house heating by different absorption couples.11th International Conference on Energy Storage, Effstock, Stockholm , Suède.

Lu, S.S., Inada, T., Yabe, A., Zhang, X., Grandum, S., 2002. Microscale study of poly (vinyl alcohol) as an effective additive for inhibiting recrystallization in ice slurries. International Journal of Refrigeration. 25, 562-568.

Lu, Y. Z., Wang, R. Z., Zhang, M., Jiangzhou, S., 2003. Adsorption cold storage system with zeolite–water working pair used for locomotive air conditioning. Energy Conversion and Management. 44(10):1733-1743.

Lu, Z.S., Wang, R.Z., Wu, J.Y., Chen, C.J., 2006. Performance analysis of an adsorption refrigerator using activated carbon in a compound adsorbent. Carbon. 44, 747–752

Lugo, R., 2004. Contribution à l'étude de deux méthodes de fabrication de coulis de glace par contact direct: évaporation sous vide et injection directe (PhD Thesis). Conservatoire National des Arts et métiers.

Lugo, R., Fournaison, L., Guilpart, J., 2006. Ice–liquid–vapour equilibria of ammonia and ethanol aqueoussolutions applied to the production of ice-slurries: prediction and experimental results. Chemical Engineering and Processing: Process Intensification. 45(1), 66-72.

Ma, Z.W., Zhang, P., Wang, R.Z., Furui,S., Xi, G.N., 2010. Forced flow and convective melting heat transfer of clathrate hydrate slurry in tubes. International Journal of Heat and Mass Transfer. 53(19-20), 3745-3757.

Mackie, E.I., Reeves, G., 1988. EPRI stratified chilled-water storage design guide. Electric Power Research Institute, Inc. Final report.

Marinhas, S., Delahaye, A., Fournaison, L., Dalmazzone, D., Furst, W., Petitet, J.P., 2006. Modeling of the available latent heat of a CO2 hydrate slurry in an experimental loop applied to secondary refrigeration. Chemical Engineering and Processing: Process Intensification. 45(3), 184-192.

Mauran, S.,Lahmidi, H.,Goetz, V., 2008. Solar heating and cooling by a thermo-chemical process. First experiments of a prototype storing 60kWh by a solid/gas reaction. Solar Energy. 7, 623–636.

McCormack, R.A., 1990. Use of clathrates for 'off-peak' thermal energy storage. Proceedings of the 25th Intersociety Energy Conversion Engineering Conference, pp. 300-305.

Medrano, M., Bourouis, M., Coronas, A., 2001. Double-lift absorption refrigeration cycles driven by low-temperature heat sources using organic fluid mixtures as working pairs. Applied Energy.68,173–185.

Mehling, H., Cabeza, L.F., 2008. Heat and cold storage with PCM: An up to date introduction into basics and applications (Heat and Mass Transfer). Publisher: Springer. Berlin; London.

Mehling, H., Hiebler, S., Ziegler, F., 1999. Latent heat storage using a PCM-graphite composite material: advantages and potential applications. In: Proceedings of the 4th Workshop of IEA ECES IA Annex 10, Bendiktbeuern, Germany.

Mettawee, E.B.S., Assassa, G.M.R., 2006. Experimental study of a compact PCM solar collector. Energy.31, 2958–2968.

Mettawee, E.B.S., Assassa, G.M.R., 2007. Thermal conductivity enhancement in a latent heat storage system. Solar Energy. 81, 839-845.

Michaud, F., Mondieig, D., Soubzmaigne, V., Negrier, P., Haget, Y., Tauler, E., 1996. A system with a less than 2 degree melting window in the range within −31°C and −45°C: chlorobenzene-bromobenzene. Materials Research Bulletin. 31(8), 943–950

Microtek Laboratories Inc., 2011. http://www.microteklabs.com/micropcm_products.html [accessed on 11.11.2011].

Mills, A., Farid, M., Selman, J.R., Al-Hallaj, S., 2006. Thermal conductivity enhancement of phase change materials using a graphite matrix. Applied Thermal Engineering. 26, 1652-1661.

Molina, A., Gabaldon, A., Alvarez, C., Fuentes, J.A., Gomez, E., 2003. Electrical thermal storage modeling tool to evaluate new opportunities and bids for residential users in a deregulated market. IEEE Power Tech Conference, Bologna

Morcos, V.H., 1990. Investigation of a latent heat thermal energy storage system. Solar & Wind Technology. 7, 197–202.

Mori, T., Mori, Y.H., 1989. Characterization of gas hydrate formation in direct-contact cool storage process. International Journal of Refrigeration. 12, 259-265.

Mugnier, D., Goetz, V., 2001. Energy storage comparison of sorption systems for cooling and refrigeration. Solar Energy. 71 (1), 47-55.

Musser, A., Bahnfleth, W.P., 2001a. Parametric study of charging inlet diffuser performance in stratified chilled water storage tanks with radial diffusers: part 1- model development and Validation. HVAC&R Research. 7(1), 52-65.

Musser, A., Bahnfleth, W.P., 2001b. Parametric study of charging inlet diffuser performance in stratified chilled water storage tanks with radial diffusers: part 2- dimensional analysis, parametric simulations and simplified model development. HVAC&R Research. 7(2), 205-222.

Najafi, M., Schaetzle, W.J., 1991. Cooling and heating with clathrate thermal energy storage system. ASHRAE Transactions. 97(1A), 177-183.

Nakayama, H., 1987. Hydrates of organic compounds. VI. Heats of fusion and of solution of quaternary ammonium halide clathrate hydrates. Bulletin of the Chemical Society of Japan. 55, 389-393; Hydrates of organic compounds. XI: Determination of the melting point and hydration numbers of the clathrate-like hydrate of tetrabutylammonium chloride by differential scanning calorimetry. Bulletin of the Chemical Society of Japan. 60, 839-843.

Naumann, R., Emons, H.H., 1989. Results of thermal analysis for investigation of salt hydrates as latent heat-storage materials. Journal of Thermal Analysis. 35,1009–1031.

Nielsen, K., 2003. Thermal energy storage—a state-of-the-art. A report within the research program Smart Energy-Efficient Buildings at the Norwegian University of Science and Technology and SINTEF.

N'Tsoukpoe, K.E., Le-Pierrès, N., Luo, L., 2012. Numerical dynamic simulation and analysis of a lithium bromide/water long-term solar heat storage system. Energy. 37, 346–358

Ogoshi, H., Takao, S., 2004. Air-conditioning system using clathrate hydrate slurry. JFE Technical Report.(3):1-5.

Ohkubo, H., Matsumoto, N., Fukuchi, M., Chandratillelke, R., 1999. Development of fluid latent heat storage material using ethanol water solution. Proceedings of the 20th International Congress of Refrigeration, IIR/IIF, Sydney, Vol.1, Paper No. 488.

Okawa, S., Saito, A., Harada, T., 1997. Experimental study on the effect of the electric field on the freezing of supercooled water. International Conference on Fluid and Thermal Energy Conversion'97, pp. 347-352.

Okawa, S., Saito, A., 1998. Experimental study controlling the initiation of freezing of supercooled water. Proceedings of the 11th International Heat Transfer Conference, Vol.7, pp. 229-234.

Okawa, S., Saito, A., Fukao, T., 1999. Freezing of supercooled water by applying the electric charge. Proceedings of the 5th ASME/JSME Joint Thermal Engineering Conference, pp.1-7.

Onwubiko, C., Russell, L.D., 1984. Experimental investigation of physical characteristics of Glauber's salt as a storage medium. Solar Energy. 33, 465-467.

Onyejekwe, D., 1989. Cold storage using eutectic mixture of $NaCl/H_2O$: An application to photovoltaic compressor vapours freezers. Solar & Wind Technology. 6, 11–18.

Oowa, M., Nakaiwa, M., Akiya, T., Fukuura, H., Suzuki, K., Ohsuka, M., 1990. Formation of CFC Alternative R134a Gas Hydrate, Proceedings of the 25th Intersociety Energy Conversion Engineering Conference, New York, USA, pp. 269-274.

Oró, E., Miró, L., Farid, M.M., Cabeza, L.F., 2012. Improving thermal performance of freezers using phase change materials. International Journal of Refrigeration. 35 (4), 984–991.

Oyama, H., Shimada, W., Ebinuma, T., Kamata, Y., Takeya, S., Uchida, T., Nagao, J., Narita, H., 2005. Phase diagram, latent heat, and specific heat of TBAB semiclathrate hydrate crystals. Fluid Phase Equilibria. 234(1-2), 131-135.

P. Tatsidjodoung, N. Le-Pierrès, L. Luo. 2013. A review of potential materials for thermal energy storage in building applications, Renewable and Sustainable Energy Reviews. 18, 327-349

Padmanabhan, P.V., Murthy, M.V., 1986. Outward phase change in a cylindrical annulus with axial fins on the inner tube. International Journal of Heat and Mass Transfer. 29,1855–1868.

PCM Products Ltd., 2011. http://www.pcmproducts.net [accessed on 11.11.2011].

Phase change material Products from PLUSS®.2011. http://www.thermalenergystorage.in/products.html. [accessed on 11.11.2011].

Ponec, V., Knor, Z., Cerny, S., 1974. Adsorption on solids. Butterworth Group, London, England.

Pons, M., Guilleminot, J.J., 1986. Design of an experimental solar-powered, solid-adsorption ice maker. Journal of Solar Energy Engineering-Transactions of the ASME. 108 (4),332–337

Porisini, F.C., 1988. Salt hydrates used for latent heat storage: corrosion of metals and reliability of thermal performance. Solar Energy. 41(2), 193-197.

Py, X., Olives, S., Mauran, S., 2001. Paraffin/porous graphite matrix composite as a high and constant power thermal storage material. International Journal of Heat and Mass Transfer. 44: 2727–2737.

Qiu, J., Liang, J., Chen, G.M., Du, R.X., 2009. Modeling and numerical simulation of a novel solar-powered absorption air conditioning system driven by a bubble pump with energy storage. Chinese Science Bulletin. 54, 504-515.

Qu, K.Y., 2000. Fundamental and applied study on making supercooled water (Doctoral Dissertation). Tsinghua University. (in Chinese).

Renewable alternatives products. 2011.http://www.renewablealternatives.com/pcm.htm. [accessed on 11.11.2011].

Rivera, C.O., Rivera, W., 2003. Modeling of an intermittent solar absorption refrigeration system operating with ammonia/lithium nitrate mixture. Solar Energy Materials and Solar Cells. 76,417–427.

Rizza, J.J., 1998. Ammonia-water low-temperature thermal storage system. Journal of Solar Energy Engineering. 120, 25–31

Rizza, J.J., 2003. Aqueous lithium bromide TES and R-123 chiller in series. Journal of Solar Energy Engineering. 125, 49-54.

RUBITHERM. 2011.Phase change materials from RUBITHERM® RT. www.rubitherm.de. [accessed on 11.11.2011].

Ryu, H.W., Woo, S.W., Shin, B.C., Kim, S.D., 1992. Prevention of supercooling and stabilization of inorganic salt hydrates as latent heat storage materials. Solar Energy Materials and Solar Cells. 27, 161-172.

Sadasuke, I., Naokatsu, M., 1991. Heat transfer enhancement by fins in latent heat thermal energy devices. Journal of Solar Energy Engineering-Transactions of the ASME.223–228.

Saito, A., Okawa, S., Tojiki, A., Une, H., Tanogashira, K., 1992. Fundamental research on external factors affecting the freezing of supercooled. International Journal of Heat and Mass Transfer. 35(10), 2527-2536.

Saito, A., 2002. Recent advances in research on cold thermal energy storage. International Journal of Refrigeration. 25, 177-189.

Sapienza, A.,Glaznev, I.S.,Santamaria, S.,Freni, A., Aristov, Y.I., 2012. Adsorption chilling driven by low temperature heat: new adsorbent and cycle optimization. Applied Thermal Engineering. 32,141–146.

Seeniraj, R.V., Velraj, R., Narasimhan, N.L., 2002. Thermal analysis of a finned-tube LHTS module for a solar dynamic power system. Heat and Mass Transfer. 38,409–417.

Sharma, A., Tyagi, V.V., Chen, C.R., Buddhi, D., 2009. Review on thermal energy storage with phase change materials and applications, Renewable and Sustainable Energy Reviews.13(2),318-345

Shen, H.Y., 2008.Thermal properties of compound low-temperature phase change materials and application in numeric simulation of refrigerator (Master Thesis). College of power engineering, Chongqing University. China.

Sheridan, N.R., Kaushik, S.C., 1981. A novel latent heat storage for solar space heating systems: Refrigerant storage. Applied Energy. 9(3), 165-172.

Shimada, W., Ebinuma, T., Oyama, H., Kamata, Y., Takeya S., Uchida, T., Nagao, J., Narita H., 2003. Separation of gas molecule using tetra-n-butyl ammonium bromide semi-clathrate hydrate crystals. Japanese Journal of Physics. 42, L129-L131.

Shin, H.T., Lee, Y.P., Jurng, J., 2000. Spherical-shaped ice particle production by a water in vacuum chamber. Applied Thermal Engineering. 20, 439-454.

Shu, B.F., Guo, K.H., Mong, Z.X., Zhao, J.W., 1999. New type of gas hydrate cool storage device and its performance. Journal of Engineering Thermophysics. 20(5), 542-544. (in Chinese).

Song, G.L., Ma, S.D., Tang, G.Y., Yin, Z.S., Wang, X.W., 2010. Preparation and characterization of flame retardant form-stable phase change materials composed by EPDM, paraffin and nano magnesium hydroxide. Energy. 35, 2179-2183.

Spall, R.E., 1998. A numerical study of transient mixed convection in cylindrical thermal storage tanks. International Journal of Heat and Mass Transfer. 41(13), 2003-2011.

Standard microPCM products.2011. http://www.microteklabs.com/micropcm_products.html. [accessed on 11.11.2011].

Stewart, W.E., Becker, B.R., Cai, L., 1992. Downward impinging flows for stratified chilled water storage. ASHRAE Transactions. 206(2), 131-138.

Subramaniam, P., Tulapurkar, C., Thiyagarajan, R., Thangamani, G., 2010. Phase change materials for domestic refrigerators to improve food quality and prolong compressor off time. International Refrigeration and Air Conditioning Conference at Purdue.

Sumathy, K, Yeung, K.H., Li, Y., 2003. Technology development in the solar adsorption refrigeration systems. Progress in Energy and Combustion Science. 29, 301-327.

Sun, D.W., 1996. Thermodynamic design data and optimum design maps for absorption refrigeration systems, Applied Thermal Engineering. 17(3), 211–221.

Sun, D.W., 1998. Comparison of the performance of NH_3–H_2O, NH_3–$LiNO_3$ and NH_3–NaSCN absorption refrigeration systems. Energy Conversion and Management. 39 (5/6), 357–368.

Sub-zero eutectic PCM solutions. 2012. http://www.pcmproducts.net/Eutectic_Refrigeration_PCMs.htm. [accessed on 07.04.2012].

Tamainot-Telto, Z., Critoph, R.E., 1997. Adsorption refrigerator using monolithic carbon-ammonia pair. International Journal of Refrigeration.20 (2), 146–155

Tanii, T., Minemoto, M., Nakazawa, K., 1997. Study on a cool storage system using HCFC (Hydro-chlorofluoro-carbon)-141b (CCL2FCH3) (1,1-dichloro-1-fluoro-ethane) clathrate. The Canadian Journal of Chemical Engineering. 75, 353-361.

Tatsidjodoung, P., Le-Pierrès, N., Luo, L., 2013. A review of potential materials for thermal energy storage in building applications, Renewable and Sustainable Energy Reviews. 18, 327-349

Telkcs, M., 1974. Solar energy storage. ASHRAE Journal. 16(9), 38-44.

Telkes, M., 1952. Nucleation of super saturated inorganic salt solution. Industrial and Engineering Chemistry. 44,1308-1310.

Telkes, M., 1976. Thixotropic mixture and method of making same. U.S. Pat No. 3,986,969, 19 Oct.

Ternes, M.P., 1983. Studies on the R-12 gas hydrate formation process for heat pump cool storage Application. Proceedings of DOE Physical and Chemical Energy Storage Annual Contractor's Review Meeting, CONF-830974.

The ISAAC solar icemaker.2012. http://www.energy-concepts.com/isaac/. [accessed on 07.04.2012].

Tomlinson, J.J., 1982. Heat pump cool storage in a clathrate of freon, Proceedings of the 17th Intersociety Energy Conversion Engineering Conference, pp. 2060-2064.

Tong, M.W., Lin, K., Li, J.S., 2000. Characterization of gas hydrate formation and cool storage in jet Pump. Journal of Chongqing University. 23(3), 91-93. (in Chinese).

Truman, C.R., Wildin, M.W., 1989. Finite difference model for heat transfer in a stratified thermal storage tank with through flow, Numerical heat transfer with personal computers and supercomputing. National Heat Transfer Conference. ASME/AIChE National Heat Transfer Conference, Philadelphia, PA, pp. 45-55.

Vinu, A., Mori, T., Ariga, K., 2006. New families of mesoporous materials, Science and Technology of Advanced Materials. 7(8), 753-771

Vonnegut, B., 1947. The nucleation of ice formation by silver iodide. Journal of Applied Physics. 18,593–595.

Waite, W.F., Gilbert, L.Y., Winters, W.J., Mason, D.H., 2005. Thermal property measurements in Tetrahydrofuran (THF) hydrate and hydrate-bearing sediment between -25 and +4°C, and their application to methane hydrate. Fifth International Conference on Gas Hydrates, Trondheim, Norway, Tapir Academic Press, vol.5, p1724-1733.

Wan, Z.M., Shu, S.M., Hu, X.H., 2006. Research of energy storage in novel solar with absorption air-condition system. Refrigeration and air-conditioning (China). 6, 36-39. (in Chinese).

Wang, D.C., Xia, Z.Z., Wu, J.Y., Wang, R.Z., Zhai, H., Dou, W.D., 2005a. Study of a novel silica gel–water adsorption chiller. Part I. Design and performance prediction. International Journal of Refrigeration. 28(7), 1073-1083.

Wang, D.C., Wu, J.Y., Xia, Z.Z., Zhai, H., Wang, R.Z., Dou, W.D., 2005b. Study of a novel silica gel–water adsorption chiller. Part II. Experimental study. International Journal of Refrigeration. 28(7), 1084-1091.

Wang, D.C., Li, Y.H., Li, D., Xia, Y.Z., Zhang, J.P., 2010. A review on adsorption refrigeration technology and adsorption deterioration in physical adsorption systems. Renewable and Sustainable Energy Reviews.14 (1), 344–353

Wang, K., Wu, J.Y., Wang, R.Z., Wang, L.W., 2006. Composite adsorbent of CaCl2 and expanded graphite for adsorption ice maker on fishing boats International Journal of Refrigeration. 29(2), 199–210

Wang, L.W., Wang, R.Z., Wu, J.Y., Wang, K., 2004. Compound adsorbent for adsorption ice maker on fishing boats. International Journal of Refrigeration. 27(4), 401–408.

Wang, L.W., Wang, R.Z., Oliveira, R.G., 2009. A review on adsorption working pairs for refrigeration. Renewable and Sustainable Energy Reviews. 13(3), 518-534.

Wang, R.Z., Jia, J.P., Teng, Y., Zhu, Y.H., Wu, J.Y., 1997. Study on a new solid adsorption refrigeration pair, active carbon fiber-methanol. ASME Journal of Solar Energy Engineering.119, 214–218.

Wang, R.Z., Oliveira, R.G., 2006. Adsorption refrigeration—an efficient way to make good use of waste heat and solar energy. Progress in Energy and Combustion Science. 32(4), 424–458

Wang, S.G., Wang, R.Z., 2005. Recent developments of refrigeration technology in fishing vessels. Renewable Energy. 30 (4), 589–600

Wang, X.C., Niu, J.L., Li, Y., Zhang, Y.P., Wang, X., Chen, B.J., Zeng, R.L., 2008. Heat transfer of microencapsulated PCM slurry flow in a circular tube. AIChE Journal, 54(4),1110-1120.

Weber, R., Dorer, V., 2008. Long-term heat storage with NaOH.Vacuum. 82,708–716.

Wikipedia, 2012. Gallium. Available from: http://en.wikipedia.org/wiki/Gallium

Xia, Y., Jian, X.G., Li, J. F., 2007. Synergistic effect of montmorillonite and intumescent flame retardant on flame retardance enhancement of ABS. Polymer-Plastics Technology and Engineering. 46 (3), 227-232.

Xiao, R., Wu, S.S., Tang, L.G., Huang, C., Feng, Z.P., 2006. Experimental investigation of the pressure-drop of clathrate hydrate slurry (CHS) flow of tetrabutylammonium bromide (TBAB) in straight pipe. Proceedings of 10th International Conference on Thermal Energy Storage, Richard Stockton College of New Jersey.

Xiao, R., He, S.H., Huang, C., Feng, Z.P., Fan, S.S., 2007. Convectional heat transfer of TBAB clathrate hydrate slurry flow in copper tube. Journal of Chemical Industry and Engineering . 58(9), 2205-2210. (in Chinese).

Xie, Y.M., Liang, D.Q., Guo, K.H., Fan, S.S., Gu, J.M., Chen, J.G., 2004. Advances of gas hydrate cool storage technology. HV&AC. 34(9), 1-4. (in Chinese).

Xu, H., Yang, R., Zhang, Y.P., Huang, Z., Lin, J., Wang, X., 2005a. Thermal physical properties and key influence factors of phase change emulsion. Chinese Science Bulletin. 50(1), 88-93.

Xu, S.M., Zhang, L., Li, G., Zhang, W.M., 2005b. Research on characteristics of refrigerating/heating potential storage system using H2O-LiBr as working fluid. Journal of Dalian University of Technology. 45, 194-200. (in Chinese).

Xu, S.M., Zhang, L., 2007. Theoretical research on the working characteristics of an advanced energy storage system using NH_3-H_2O as working fluid, part (1)—working principle description and modeling. Acta Energiae Solaris Sinica. 28: 457–463

Xu, S.M., Zhang, L., 2007. Theoretical research on the working characteristics of an advanced energy storage system using NH_3-H_2O as working fluid, part (2)—simulation and analysis of working process under the full-storage strategy. Acta Energiae Solaris Sinica. 28,1380–1388

Xu, S.M., Xu, C.H., Zhang, L., 2008. Numerical simulation and analysis on operation characteristics of energy storage system for air-conditioning and heating using water-LiBr solution as working fluid. Journal of Dalian University of Technology. 48, 503-508. (in Chinese).

Yamagishi, Y., Sugeno, T., Ishige, T., 1996. An evaluation of microencapsulated PCM for use in cold energy transportation medium. Proceedings of the Intersociety Energy Conversion Engineering Conference. 2077-2083.

Yamagishi, Y., Takeuchi, H., Pyatenko, A.T., Kayukawa, N., 1999. Characteristics of microencapsulated PCM slurry as a heat-transfer fluid. AIChE Journal. 45(4), 696-707.

Yang, Q.C., Zhang, X.L., Wang, X., Li, X.T., Shi, W.X., 2011. Review on absorption thermal energy storage technologies. Chinese Sci Bull (Chinese Ver). 56, 669–678 (in Chinese).

Yang, R.T., 1991. Gas separation by adsorption methods. Publishing House of Chemical Industry, Beijing, China. (in Chinese).

Yilmaz, S., Sayin, K., Gök, Ö., Yilmaz, M.Ö., Beyhan, B., Sahan, N., Paksoy, H., 2009. New binary alkane mixtures as pcms for cooling applications. 11th International Conference on Thermal Energy Storage for Energy Efficiency and Sustainability, Stockholm International Fairs. Stockholm, Sweden.

Zeolith-Technologie GmbH., 2008. Clean tech for Cooling, Heating and Drying. www.zeo-tech.de. [accessed on 11.11.2011].

Zhang, Y.P., Yu, S.S., Gao, X.N., Wang, S.P., 1999. Experimental research on gas hydrate cool storage Technique. Journal of South China University of Technology. 27(2), 110-115. (In Chinese).

Zhang, X.L., Li, R.Y., Yu, H.L., 2002. Additives and their effects on direct contact phase change heat transfer. Journal of Chemical Engineering. 53(8), 837-841. (in Chinese).

Zhang, X.L., Fan, J.B., Zhong, D.L., Sun, W.Z., 2008. Heat Transfer characteristic in direct contact binary ice-making process. Chinese Journal of Mechanical Engineering. 44(9), 188-192. (in Chinese).

Zhang, Z.G., Fang, X.M., 2006. Study on paraffin/expanded graphite composite phase change thermal energy storage material. Energy Conversion and Management. 47,303-310.

Zhang, P., Song, L., Lu, H.D., Wang, J., Hu, Y., 2010a. The thermal property and flame retardant mechanism of intumescent flame retardant paraffin system with metal. Industrial & Engineering Chemistry Research. 49, 6003-6009.

Zhang, P., Ma, Z.W., Wang, R.Z., 2010b. An overview of phase change material slurries: MPCS and CHS. Renewable and Sustainable Energy Reviews.14, 598-614.

Zhao, Z.N., Wu, T., Shi, Y.Q., Li, L.X., 2001. An investigation on rheology and heat transfer characteristics for a phase change emulsion. Journal of Engineering Thermophysics. 22, 589-592. (in Chinese)

Zhao, Z.N., Shi, Y.Q., Zhang, Y., Gai, P.Y., 2002. Flow and heat transfer characteristics of phase-change emulsion in a coiled double-tube heat exchanger. Journal of Engineering Thermophysics. 23, 730-732. (in Chinese).

Zhou, H., Fang, C. P., Sheng, H. S., Mu, C. J., 2008. Synergistic action of nanometer ZnO prepared by sol-gel method on halogen free flame-retarded polypropylene. Rare Metal Materials and Engineering. 37, 617-619.

Zhu, L., Gu, J.,2009. Thermodynamic analysis of a novel thermal driven refrigeration system. World Academy of Science, Engineering and Technology.56:351–355

Zurigat, Y.H., Liche, P.R., Ghajar, A.J., 1991. Influence of inlet geometry on mixing in thermocline thermal energy storage. International Journal of Heat and Mass Transfer. 34, 115-125.

Zheng, D.X., Wu, X.H., 2002. Comprehensive evaluation of eutectic character used as low temperature thermal energy storage. Cryogenics. (1), 37-45. (in Chinese)

Zalba, B., Marín, J.M., Cabeza, L.F., Mehling, H., 2003. Review on thermal energy storage with phase change: materials, heat transfer analysis and applications. Applied Thermal Engineering. 23,251–283.